USF Tampa Graduate Theses and Dissertations

USF Graduate Theses and Dissertations

March 2020

Polycyclic Aromatic Hydrocarbon Exposure, Hepatic Accumulation, and Associated Health Impacts in Gulf of Mexico Tilefish (Lopholatilus chamaeleonticeps)

Susan M. Snyder
University of South Florida

Follow this and additional works at: https://digitalcommons.usf.edu/etd

Part of the Other Oceanography and Atmospheric Sciences and Meteorology Commons

Polycyclic Aromatic Hydrocarbon Exposure, Hepatic Accumulation, and Associated

Health Impacts in Gulf of Mexico Tilefish (*Lopholatilus chamaeleonticeps*)

by

Susan M. Snyder

A dissertation submitted in partial fulfillment
of the requirements for the degree of
Doctor of Philosophy Marine Science
with a concentration in Marine Resource Assessment
College of Marine Science
University of South Florida

Major Professor: Steven A. Murawski, Ph.D.
David J. Hollander, Ph.D.
Ernst B. Peebles, Ph.D.
Erin L. Pulster, Ph.D.
Gina M. Ylitalo, M.S.

Date of Approval:
March 28, 2020

Keywords: *Deepwater Horizon*, marine pollution, baseline, condition factor, lipid, histology

Acknowledgments

Table of Contents

List of Tables

List of Figures

Abstract

Following the 2010 *Deepwater Horizon* oil spill, systematic demersal longline surveys were conducted throughout the Gulf of Mexico (GoM) continental shelf to evaluate polycyclic aromatic hydrocarbon (PAH) exposure, hepatic accumulation, and health indices in demersal fishes. Tilefish (*Lopholatilus chamaeleonticeps*) were chosen as a target species due to high vulnerability to environmental disturbance, commercial importance, Gulf-wide distribution, and documented high exposure to PAHs post-*Deepwater Horizon*. Over 200 Tilefish were sampled in the north central GoM at repeat stations from 2012 to 2017, and from the northwest GoM, southwest GoM, Bay of Campeche, and Yucatán Shelf over years 2015 and 2016. Tilefish were sampled for biometrics, and bile and liver for contaminant analyses. Tilefish livers were also obtained from demersal longline surveys in the northwest Atlantic Ocean for comparison.

Bile samples were analyzed via high performance liquid chromatography with fluorescence (HPLC-F) detection for PAH metabolites, a biomarker of short-term (e.g. days) exposure to PAHs. Longer-term accumulation of PAHs was assessed by analyzing liver samples for PAHs and alkylated homologs using the Quick, Easy, Cheap, Effective, Rugged, and Safe (QuEChERS) extraction method and gas chromatography tandem mass spectrometry (GC-MS/MS). Fish health indices including Fulton's condition factor and total liver lipid were evaluated. Liver samples were also analyzed for microscopic hepatic changes (MHCs) by a board-certified veterinary pathologist.

Over the six-year time series in the north central GoM, exposure to petrogenic PAHs increased by an average of 178%, correlating with an average 22% decline in Fulton's condition factor. The decline in Fulton's condition factor was positively correlated with a 53% decline in percent liver lipid. There was no accumulation of PAHs in liver tissue over time. Together, these results suggest that increasing and chronic PAH exposure and resultant elevated xenobiotic metabolism may be taxing the energy budgets of Tilefish, particularly adult females, with potentially negative effects on fitness.

Gulf-wide spatial comparisons revealed the highest PAH exposure, and concentrations in liver tissue in the north central GoM, with decreasing concentrations from the north central Gulf counterclockwise, and an increase on the Yucatán Shelf. Total hepatic PAH concentrations were similar between the GoM and the northwest Atlantic, however, Tilefish from the northwest Atlantic had higher concentrations and more frequent detection of carcinogenic high molecular weight PAHs. Overall, results demonstrate that PAH pollution was ubiquitous within the study regions, with PAH exposure and measurable hepatic PAH concentrations observed in Tilefish from both the GoM and northwest Atlantic.

Histological examinations identified 14 MHCs, ranging from mild to severe (i.e. neoplasia). Prevalence of MHCs was generally uniform throughout the GoM, except for low prevalence on the Yucatán Shelf. Inflammatory and vacuolar changes were most prevalent, while pre-neoplasia and neoplasia were rare. Ten MHCs including glycogen and lipid-type vacuolar change, biliary fibrosis, increased pigmented macrophage aggregates, granulomas, foci of cellular alteration, inflammation with lymphocytic aggregation, parasites, hepatocellular atrophy, and necrosis were associated with hepatic PAH accumulation. In the north central GoM, where Tilefish were sampled at repeat stations 2012 to 2015, inflammatory MHCs and

glycogen-type vacuolar change increased over time, while lipid-type vacuolar change decreased, potentially indicating a switch from preferential storage of hepatic lipids to hepatic glycogen. Combined with previous studies of PAH exposure and health indices in north central GoM Tilefish post-*Deepwater Horizon*, which also identified decreases in hepatic lipid storage that were correlated to increasing PAH exposure, these data indicate concerning temporal trends and changes in hepatic energy metabolism.

The results of this dissertation indicate chronic and increasing exposure of GoM Tilefish to petrogenic PAHs with significant effects on health indices. Specifically, in the north central GoM where PAH exposure and hepatic accumulation are highest Gulf-wide, the time series of PAH exposure and associated health effects indicates increasing exposure, alterations in hepatic energy storage, and decreasing Fulton's condition factor. The implications are serious for individual health, reproductive capacity, and population productivity of GoM Tilefish. Due to their economic and ecological value, and signs of chronic PAH exposure and accumulating impact, the GoM Tilefish population, particularly individuals from north central Gulf, should be closely monitored until a new, stable baseline is achieved.

Chapter 1

General Introduction

Research Motivation: *Deepwater Horizon*

The Gulf of Mexico (GoM) is one of the most ecologically and economically important

bodies of water in the world (Ward and Tunnel 2017). Ecologically, the GoM is home to diverse

habitats, communities, and organisms, including numerous endangered species, and recently

discovered species (Love et al. 2013; Sutton et al. 2020; Trustees 2016). The main economic

interests in the GoM are the oil and gas industry, commercial and recreational fisheries, shipping,

and tourism, which together generate approximately $770 billion in coastal and ocean revenues

in the United States alone (Shepard et al. 2013). Challengingly, the development of the offshore

oil and gas industry creates substantial risk to the environmental quality that fisheries, tourism,

and the other ecologically valuable resources depend upon. In order to balance productivity of

these vastly different industries, increase environmental disaster preparedness, and foremost,

conserve the GoM's natural resources, a sound understanding of the overall health of the GoM

ecosystem and its stressors is necessary.

There has been a considerable increase in research on these topics since the April 20th,

2010 explosion on the drilling rig *Deepwater Horizon* (*DWH*). The rig, located 66 km offshore

of Louisiana, USA, in 1,522 m of water, ultimately discharged 3.19 million barrels of type A

Louisiana light sweet crude oil into the GoM over the course of 87 days (United States of

America v. BP Exploration & Production 2015). In addition to the oil, 7.9 million liters of

chemical dispersant (primarily Corexit™ 9500) were used in spill response (40% subsea injection at the wellhead, 60% surface application) (Beyer et al. 2016; Kujawinski et al. 2011). After exiting the damaged wellhead the oil generated three large features: 1) a buoyant plume rising from the wellhead to the sea surface, 2) a neutrally buoyant subsurface plume located at approximately 1100 m (and a less pronounced plume at ~400 m), and 3) surface oil covering ~112,115 km^2 (Thibodeaux et al. 2011; Passow and Hetland 2016; Trustees 2016). The subsurface and deep-sea features made *DWH* unique compared to previous U.S. oil spills and greatly increased the potential to effect sensitive deep-sea and benthic communities.

Surfaced oil clean-up employed a variety of response actions (e.g. skimming, chemical dispersion, *in situ* burning), augmented by natural weathering processes (e.g. evaporation, physical dispersion, photodegradation, biodegradation). However, a portion of the oil was stranded in coastal habitats. Over 2,100 km of shoreline from Louisiana to Florida was effected by thick weathered oil, including salt marsh, estuarine, and beach habitats (Beyer et al. 2016). Oil in the water column was also acted upon by weathering processes (e.g. dissolution, biodegradation), entered the food web, and incorporated into marine oil snow sedimentation and flocculent accumulation (MOSSFA) (Passow and Hetland 2016; Chanton et al. 2012; Graham et al. 2010; Mitra et al. 2012; Beyer et al. 2016). MOSSFA, which occurred through August 2010, is a process whereby materials naturally present in the water column (e.g. clay particles, plankton, exopolymeric substances) and enhanced by *DWH* and the chemical dispersants, combine with oil droplets, generating a mechanism for petrogenic, pyrogenic, lithogenic, and biogenic material to ballast, ultimately sinking to the seafloor as "marine oil snow" (Daly et al. 2016; Passow and Ziervogel 2016; Passow et al. 2012; Ziervogel et al. 2016). MOSSFA was the primary mechanism for *DWH* oil residue to accumulate on the seafloor, with an estimated 4-14%

of total *DWH* oil released deposited over a spatial extent of 12,805-35,425km^2 of the northern

GoM seafloor (Passow and Hetland 2016; Schwing et al. 2017). Other mechanisms such as

direct impingement of subsurface plumes with the continental slope, and sinking of *in situ* burn

residues also deposited oil and oil residues on the northern GoM seafloor (Passow and Hetland

2016).

Due to the 4-dimensional and highly dynamic distribution of oil released by the

submarine blowout, the footprint of *DWH* spanned all ecozones of the GoM, from coastal to

oceanic, including both pelagic and benthic, causing ecosystem-wide injury (Beyer et al. 2016;

Trustees 2016). The massive footprint of *DWH* presented unprecedented and novel challenges to

emergency responders and oil spill researchers assessing ecological damage and recovery

potential, as critical considerations such as chemical composition of the oil, oil residence time,

biomass, diversity, toxicity, and resilience different among the unique communities of the GoM,

most of which were vastly understudied at the time of the spill.

A considerable number of studies have documented effects on natural resources related to

DWH and more will be published in the years to come as research is ongoing and effects often

manifest slowly (Trustees 2016). Surfaced and stranded oil has been associated with negative

effects on biota from microbes to mammals, including a dieback of marsh vegetation, changes in

biomass, diversity and productivity of marsh vegetation, loss of marsh invertebrates, direct

mortality to marine mammals, oysters, birds, and adult sea turtles, decreased body mass and

fledging in shorebirds, and poor health and reproductive outcomes in bottlenose dolphins

(*Tursiops truncatus*) (Beyer et al. 2016; Rabalais and Turner 2016; Trustees 2016; Tran,

Yazdanparast, and Suess 2014; Antonio, Mendes, and Thomaz 2011; Carmichael et al. 2012;

Haney, Geiger, and Short 2014a, 2014b; Schwacke et al. 2014; Zengel et al. 2016; Zengel et al.

2015; Burns et al. 2014; Silliman et al. 2012). Effects to offshore waters included sinking of oiled *Sargassum*, short-lived increases and decreases in phytoplankton abundance, mortality of larval fish, planktonic invertebrates, and juvenile sea turtles, redistribution of marine mammals, and startling declines in abundance of meso- and bathypelagic fishes (Murawski et al. 2016; Fisher, Montagna, and Sutton 2016; Trustees 2016; Sutton et al. 2018; Parsons et al. 2015; Hu et al. 2011; Powers et al. 2013; Ackleh et al. 2012). Effects on benthic organisms were expected to be extensive and severe, as sedimented oil residues are likely to persist for decades with the potential for re-exposure via bioturbation and resuspension mechanisms (e.g. hurricanes), and much of the benthos are sedentary. Sedimented oil residues following *DWH* have been associated with negative effects on benthic fauna including 80-93% declines in benthic foraminifera density, death and damage to deep-water coral colonies, changes in benthic meio-, macro-, and megafauna abundance and diversity, dietary and trophic shifts in Red Snapper (*Lutjanus campechanus*), and increased prevalence of external skin lesions and decreases in health indices in demersal fishes (Beyer et al. 2016; Fisher, Montagna, and Sutton 2016; Pulster, Gracia, Armenteros, et al. 2020; Tarnecki and Patterson 2015; Schwing et al. 2015; Montagna et al. 2013; Valentine and Benfield 2013; White et al. 2012; Etnoyer et al. 2016; Silva, Etnoyer, and MacDonald 2016; Murawski et al. 2014).

Following *DWH*, there was serious concern that the extensive oiling during peak spawning season, when sensitive and vulnerable early life stages are developing would affect the region's productive fisheries potentially triggering economic effects in the billions of dollars (Sumaila et al. 2012). Twelve days after the incident began, state and federal fisheries closures were initiated, peaking in July 2010 with over 10% of the total surface area of the GoM closed to commercial fishing (McCrea-Strub et al. 2011). Although the federal Natural Resource Damage

Assessment (NRDA) estimated trillions of larval fish died as a result of exposure to *DWH* oil, no stock collapses, nor clear population-level effects, have been reported, with many declines in fisheries landings attributed to the fishery closure and quickly rebounding to pre-*DWH* numbers (Gracia, Murawski, and Vazquez-Bader 2020). Murawski et al. (2016) explained that characteristics of many GoM fish species (e.g. prolonged spawning seasons, expansive range, high larval dispersal) led to exposure of only limited fractions of populations to toxic concentrations of oil in the environment, combined with high metabolic capacity to eliminate oil, and avoidance capacity, all contributed to resilience in early life stage and adult fishes. Fortunately, there was only minor contamination of seafood reported (Fernando et al. 2019; Fitzgerald and Gohlke 2014; Xia et al. 2012; Ylitalo et al. 2012).

Following a large-scale pollution event, the predominant concern for wildlife are effects at the population-level (e.g. altered abundance, age distribution, sex ratio) that can cascade to the ecosystem level, potentially effecting a variety of critical ecosystem services. Due to the volume of oil released and the sensitivity of certain communities effected, population and ecosystem-level injuries related to *DWH* are likely to unfold in the ensuing years and decades. Preceding *DWH*, the nation's largest oil spill had been the 1989 *Exxon Valdez* oil spill (EVOS) in Prince William Sound, that released 42 million liters (~262,000 barrels; ~8% of *DWH*) of Alaska North Slope crude oil effecting surface waters and rocky shoreline beaches (Shigenaka 2014). Before EVOS, studies of oil spill impacts and toxic effects employed short-term environmental monitoring and laboratory exposure studies of model species with a focus on organism mortality, which at the time was thought to be the direct link to population-level effects. EVOS introduced a new focus towards understand persistent oiling, chronic exposures (particularly in sediment-associated species), and sublethal effects that impact health, growth, and reproduction (not

directly mortality), and resultant delayed recovery, and long-term population impacts which may arise through indirect effects and interactions (Peterson et al. 2003). Because of this paradigm shift, post-*DWH* research emphasized sublethal effect end points that span all levels of biological organization from molecular to ecosystem. However, there has been a gap between consistent individual-level effects observed in both the field and laboratory studies, and a lack of population-level effects in *DWH*-impacted environments (Fodrie et al. 2014; Able et al. 2015; Rabalais and Turner 2016). Fodrie et al. (2014) concluded there were processes that both obscured and dampened negative population effects post-*DWH*, including natural variability in processes such as recruitment, high spatiotemporal variability in oiling, alterations to the food-web, release from fishing pressure due to fisheries closures, temporal lags associated with sublethal effects, behavioral avoidance of oiled areas and oiled food sources, compensatory (e.g. density-mediated) pathways, and poor representativeness of laboratory exposure studies using model species and short (e.g. days) exposure periods.

The mismatch between extensive individual-level effects and a general absence of population-level effects has been observed following other large oil spills; EVOS and the 1979 *Ixtoc-I* submarine oil well blowout in the Bay of Campeche, Mexico (the first large-scale submarine oil-well blowout to occur in the GoM). *Ixtoc-I* released approximately 3.4 million barrels of oil over nine months at a shallow 54 m site 80 km offshore of the state of Campeche, Mexico (Jernelov and Linden 1981; Soto et al. 2014). Research post-*Ixtoc* concluded there was minimal lasting effect on natural resources, likely due to local circulation patterns, an estuarine plume that separated oiled offshore water from coastal water, extensive weathering of the oil in the tropical environment, and life history characteristics of local fish communities, which together kept *Ixtoc* oil offshore, away from the coastal natural resources in the region, where it

6

was weathered quickly (Soto et al. 2014). Population-level effects of increased mortality and reduced population sizes were observed post-EVOS in organisms that associate with sediments via egg laying, or foraging (e.g. sea otters [*Enhydra lutris*], pink salmon [*Oncorhynchus gorbuscha*], Pacific herring [*Clupea pallasi*], Harlequin ducks [*Histrionicus histrionicus*], black oystercatchers [*Haematopus bachmani*], killer whales [*Orcinus orca*]) (Peterson et al. 2003). One of the most notable and controversial population-level effects of EVOS was a collapse of the Pacific herring stock which was attributed to the combined effects of oil toxicity, disease, predation, fisheries pressure, and shifts in primary production (Thorne and Thomas 2008). Population effects following EVOS were likely more apparent than those potentially following *DWH* in part due to the limited distribution of species and their critical habitats in Prince William Sound, for example, the fixed spawning habitats of both pink salmon and Pacific herring led to annual deposition of embryos in persistently oiled habitat, resulting in perpetual effects. Restricted spawning grounds were also implicated in increased vulnerability of penaeid shrimp following *Ixtoc-I* (Soto et al. 2014). As discussed previously, the widespread spatial distribution of spawning habitats, extended spawning periods, and high larval dispersal likely spared many GoM species from population-level effects (Murawski et al. 2016).

Post-*DWH*, a scientific consensus has emerged of the critical need that emerged from *DWH* was the need to understand the understudied GoM ecosystem, to generate broadscale baselines for future preparedness, and to reassess regulation related to oil spill prevention and response. One month after *DWH*, rig operator British Petroleum announced a commitment of $500 million over ten years to develop and fund an industry-independent research program; the Gulf of Mexico Research Initiative (GoMRI). This unique program allowed for the long-term, interdisciplinary research to study the effects of an oil spill the scale of *DWH*, be able to

distinguish the signal of the event from natural background variability, track sublethal health effects that may take decades to appear, and collect baseline data over expansive spatial and temporal scales.

Following *DWH*, one of the most pressing scientific needs was to assemble a pre-spill baseline for future incidents that will doubtlessly occur. Baseline data on species abundance, hydrocarbon concentrations in animal tissues, and indicators of animal health status was missing for many communities of the GoM pre-*DWH*. Baseline data were also missing following EVOS and *Ixtoc-I*, making ecosystem effects exceedingly difficult to assess (Shigenaka 2014; Soto et al. 2014). After the lessons learned following EVOS and the risky expansion of the GoM oil industry into deeper waters, ecological and chemical baselines should be prioritized. Especially in the GoM, where hydrocarbon pollution is chronic and there is substantial input from multiple natural and anthropogenic sources, baselines are critical to deconvolve the event signal from the polluted background. The collection of comprehensive baseline data post-*DWH* is critical as it is likely that the sublethal effects and chronic exposures to hydrocarbon pollution will shift effected communities to a new post-*DWH* baseline condition. GoMRI's resources provided this opportunity post-*DWH*, allowing for the extended time series, broad spatial scale, and interdisciplinary research efforts, some of which are presented herein.

Polycyclic Aromatic Hydrocarbons

Polycyclic aromatic hydrocarbons (PAHs) are organic pollutants found world-wide in air, water, ice, sediment, soil, and biota (Lima, Farrington, and Reddy 2005; Collier et al. 2014). PAHs, considered the most toxic component of crude oil, are the focus of toxicity studies

following oil spills (Krahn and Stein 1998). PAHs account for approximately 0.5-4% of the bulk composition of crude oils, with *DWH* oil composed of 3% PAHs by weight (Wang et al. 2016; Reddy et al. 2012).

PAHs contain two or more fused aromatic benzene rings which can be either unsubstituted (parent) or alkylated (e.g. methyl, ethyl, or isopropyl groups). Together, PAHs and their alkylated homologs can form over 19,000 isomers; however, environmental analyses typically focus on 16 priority parent PAHs selected by the U.S. Environmental Protection Agency (EPA), which range from the two-ring naphthalene up to six-ring compounds (e.g. benzo[*g,h,i,*]perylene) (Emsbo-Mattingly and Litman 2016). PAHs are regularly examined as two groups: low molecular weight (LMW; 2-3 ring; $\log(K_{ow})$<5), and high molecular weight (HMW; 4-6 ring; $\log(K_{ow})$>5) molecules. Although, molecular weight is not substantially different between the two groupings (<150 g/mol between LMW and HMW), structural differences lead to substantial discrepancies in hydrophobicity (Meador et al. 1995). The octanol-water partitioning coefficient (K_{ow}), is a numerical measure of a molecule's hydrophobicity, predicting how that molecule will thermodynamically partition between water and octanol (as representative of biological lipid membranes). As an example, $\log(K_{ow})$ of PAHs range from naphthalene (3.34) to indeno[1,2,3-*c,d*]pyrene (7.43), representing the extreme difference in hydrophobicity (~12,300 fold in this example) between LMW and HMW PAHs (Meador et al. 1995). Hydrophobicity is related to aspects of molecular structure (e.g. number of rings, degree of alkylation) and is one of the most dominant characteristics explaining behavior and fate of chemical contaminants such as PAHs in the environment through susceptibility to weathering processes, bioavailability to organisms, and toxicokinetics.

Sources of PAHs that enter aquatic environment are both natural and anthropogenic, including natural oil seeps, discharges from the oil and gas industry, coastal runoff, riverine discharge, atmospheric deposition, and transportation activities (NRC 1987; Kennicutt et al. 1988). In addition to chronic sources, oil spills release large pulses of PAHs into the aquatic environment. Once released into the environment, PAHs are degraded by weathering processes (e.g. dissolution, dispersion, evaporation, biodegradation, photooxidation) or sequestered into compartments (e.g. sediment, tissue) where they may persist or continue undergoing alteration via weathering or metabolism. Limited susceptibility to weathering processes, environmental conditions, and chemical properties can lead to the persistence of PAHs (e.g. years) in the environment (Hinga and Pilson 1987; Meador et al. 1995). Generally, HMW PAHs are more persistent in the environment than LMW PAHs.

Advanced analytical chemistry techniques allow for "fingerprinting" of PAHs, among other molecules, via hydrocarbon profile and diagnostic ratio comparisons, to identify the source of the compounds. PAH sources can broadly be grouped as petrogenic (petroleum-derived), pyrogenic (combustion-derived), or biogenic (biologically-derived), with the later making insignificant contributions in most environments. Petrogenic PAHs contain high proportions of alkylated PAHs (~85%) with low proportions of unsubstituted two- to four-ring PAHs and little to no five- and six-ring PAHs (Wang et al. 2016; Wang et al. 2003). Pyrogenic PAHs, on the other hand, are characterized by a greater relative abundance of parent HMW PAHs and minor alkylated components. Pyrogenic versus petrogenic PAH profiles can be distinguished by examining the relative abundance of a parent PAH and its alkylated homolog series, where a bell-shaped pattern indicates a petrogenic (non-weathered) source, and a sloping "skewed" shape indicates a pyrogenic source (Emsbo-Mattingly and Litman 2016). More complex analysis of

petroleum biomarkers (e.g. hopanes, steranes, terpanes), ancestral biogenic precursors to petroleum resistant to weathering, allows for positive identification of petroleum hydrocarbons against candidate sources (Wang et al. 2016). Fingerprinting techniques work well on skimmed oil, water, or sediment samples; however, they have limited application for exposed wildlife. While some studies have fingerprinted *DWH* oil from external samples on bird feathers or sea turtle skin, the processes of bioavailability and xenobiotic metabolism alter the PAH profile leading to difficulty definitely interpreting results (Ylitalo et al. 2017; Bonisoli-Alquati et al. 2016). However, Murawski et al. (2014) reported a high correlation between the composition of PAHs measured in GoM red snapper livers and *DWH* source oil, perhaps indicating recent and significant oil exposure.

Essential controls governing PAH body burden and toxicity to organisms include uptake, metabolic capacity, and elimination. PAH uptake is regulated externally by bioavailability, and internally by organism behavior and physiology (Meador et al. 1995). Chemical partitioning of PAHs between matrices, controlled by hydrophobicity, is the main factor regulating bioavailability. As hydrophobicity increases, thermodynamics favors partitioning of the PAH molecule into a nonpolar matrix, for example via sorption to organic carbon in sediments or uptake and incorporation into tissue (Meador et al. 1995). Other physical factors, for example water temperature and salinity, can also modulate PAH bioavailability by altering solubility, although their influence is minor compared to hydrophobicity (McElroy, Farrington, and Teal 1989; Meador et al. 1995). Organism behavior influences route of exposures, and physiological parameters including membrane permeability, lipid content, ventilation rate, gut residence time, and extraction efficiency all impact uptake, and lead to complex species-specific differences in PAH accumulation.

Routes of exposure of aquatic organisms to PAHs are 1) respiration of dissolved molecules, 2) ingestion of contaminated prey, sediment, and porewater, and 3) transdermal absorption (Varanasi, Stein, and Nishimoto 1989; Meador et al. 1995). Water-based exposure is the main route of exposure to LMW PAHs, as their lower hydrophobicity allows for dissolution in water. Both LMW and HMW are bioavailable by ingestion (the main route of exposure for HMW PAHs) where PAHs bound to organic molecules can be desorbed at biological membranes of the gastrointestinal tract, skin, or gill and ultimately absorbed. Waterborne exposures typically occur on short time scales, while exposure to contaminated sediment and benthic prey can provide long-term chronic exposures (Meador et al. 1995).

Once absorbed, PAHs are transported via the circulatory system to the hepatobiliary system for metabolism and eventual elimination. Xenobiotic metabolism is an enzymatic process that increases the polarity and water solubility of a molecule in preparation for excretion. Metabolism of PAHs increases in speed and efficiency at higher levels of biological organization, with limited capacity in low-level invertebrates (e.g. protozoa, cnidaria, mollusks), slow and inefficient capacity in higher-level invertebrates (e.g. arthropods, echinoderms, annelids), and rapid and efficient metabolism in vertebrates (e.g. teleosts) (James 1989; Varanasi, Stein, and Nishimoto 1989). Due to limited ability to metabolize and eliminate PAHs, invertebrates are prone to bioaccumulation of these compounds, at higher levels than those measured in vertebrates (Meador et al. 1995). Although prey are a considerable source of PAHs to their predators, PAHs do not biomagnify as metabolic capacity increases with increasing trophic level (Meador et al. 1995). There are also known species-specific differences in PAH metabolism capacities and pathways (e.g. English Sole [*Parophyrys vetulus*] vs. Starry Flounder

[*Platichthys stellatus*]) that can lead to differential body burdens, metabolites, and susceptibility to resultant toxic effects (Varanasi et al. 1986).

Metabolism of PAHs in vertebrates occurs in two general steps, both of which have an energetic cost. Phase I metabolism is most commonly a series of oxidation reactions catalyzed by enzymes of the family cytochrome P450 (CYP450) and epoxide hydrolase, first adding an epoxide functional group, which is then converted to a phenol or dihydrodiol. Phase II metabolism further increases the polarity of the molecule by adding a bulky, polar, endogenous molecule (e.g. glutathione, sulfonate, glucuronide). The resultant highly polar metabolite can then be excreted via the urine or bile. In teleosts, the most common route of elimination is via the bile which is stored in the gallbladder and emptied into the gastrointestinal tract during digestion. Although this is typically an efficient route of xenobiotic elimination, there is the possibility of reabsorption and return to the liver via enterohepatic circulation, leading to a second metabolic pass of the molecule, increased residence time in the organism, and increased chance for toxic action (Hinton et al. 2008). The process of xenobiotic metabolism serves a main purpose of elimination, however, in the case of PAHs it also creates a more reactive molecule capable of binding to cellular macromolecules, which is known to be a main mechanism of PAH toxicity (Myers, Johnson, and Collier 2003).

As PAHs are rapidly metabolized and eliminated by teleosts, concentrations in tissues are poor indicators of exposure. Analytical methods have been developed to quantify biliary PAH metabolites as they are the best biomarker of short-term exposure (e.g. days) to PAHs (Krahn et al. 1984; Beyer et al. 2010). Hepatic PAHs are also often quantified to represent any longer-term accumulation which may occur if the metabolic capacity of the individual is overwhelmed (Meador et al. 1995). PAH concentrations in teleost muscle tissue are normally low due to

13

relatively low lipid composition and role of the hepatobiliary system in PAH disposition, leading

to low risk of seafood contamination.

Even with efficient elimination mechanisms of fishes, PAH exposure is known to have

negative health effects on these organisms. Acute exposure to high concentrations of PAHs can

cause direct mortality via narcosis, however, sublethal effects, which can result from low

exposure concentrations (<10 μg/L PAHs) and chronic exposures, are more important for impact

assessment (Pasparakis et al. 2019; Barron et al. 2004; Meador et al. 1995). Sublethal health

effects of PAH exposures in fishes include neoplasia (i.e. cancer), pre-neoplastic and non-

neoplastic microscopic hepatic changes, reproductive impairment, endocrine disruption, reduced

growth and condition, cardiotoxicity, immunotoxicity, and transgenerational changes (Collier et

al. 2014). Sensitivity to PAH toxicity is partly dependent on life stage, with younger life stages

most vulnerable due to their large surface-area-to-volume ratio, transparency, limited mobility,

and developing detoxification systems. Exposure studies have identified that petrogenic PAHs,

specifically tricyclic PAHs (e.g. phenanthrene, fluorene, dibenzothiophene), as having the most

severe effects on early-life stages of fish via cardiotoxicity. Exposure to *DWH* oil caused

pericardial and yolk sac edema in early life stage fishes and resulted in functional failure of the

cardiac system later in life, as well as alterations to other downstream systems that depend upon

proper cardiac function, likely decreasing survivorship (Incardona, Collier, and Scholz 2011;

Incardona et al. 2014; Incardona et al. 2013; Pasparakis et al. 2019). In addition to life stage,

other factors including species, route and duration of exposure, exposure mixture, and other

synergistic stressors can impact sensitivity to PAH exposure. Species-specific differences in

PAH toxicity can be substantial, leading to difficulties in extrapolating results of individual

studies to draw broad conclusions (Pasparakis et al. 2019; Stein et al. 1990)

Tilefish (*Lopholatilus chamaeleonticeps*)

Lopholatilus chamaeleonticeps are a large, shelter-seeking, demersal teleost belonging to the family Malacanthidae (Goode and Bean 1880). Common names include Tilefish (used herein), Golden Tilefish, and Great Northern Tilefish. As the largest of the Malacanthidae, Tilefish can grow up to 120cm in total length, 30kg in total weight, and live up to 45 years (Steimle et al. 1999). Tilefish have an expansive range, from Nova Scotia down the east coast of the USA, and throughout the GoM. The majority of Tilefish research has been on the northern stock, centered around the Mid-Atlantic Bight, however the life history, habitat, and behavior of the southern stock which ranges from south of Cape Hatteras and throughout the GoM is similar (Katz, Grimes, and Able 1983). Commercial fishing on the northern and southern stocks began in 1879 and the 1980s, respectively, and the latest stock assessment reports indicate the northern stock is overfished and undergoing overfishing, while the GoM population is not overfished nor is overfishing occurring (SEDAR 2011, 2004; NEFSC 2005; Steimle et al. 1999).

Reproductive biology of Tilefish is complex and not completely understood. The reproductive strategy of the northern stock has been identified as gonochoristic, while extensive histological evaluation of Tilefish from the GoM and east coast of Florida has provided strong evidence for a protogynous hermaphroditic strategy (Lombardi-Carlson 2012; Grimes et al. 1988). Tilefish exhibit sexual dimorphism, with males exhibiting faster growth rates, reaching larger sizes, and mature males developing an enlarged dorsal adipose flap (Katz, Grimes, and Able 1983; Grimes and Turner 1999; Grimes et al. 1988). Females and males reach sexually maturity at 60-65 cm and 65-70 cm total length, respectively, and between five to seven years of age (Steimle et al. 1999). Tilefish have been described as serial or fractional spawners, spawning from March to November, with a peak between May and September in the Atlantic, and January

to June, with a peak in April in the GoM (Erickson, Harris, and Grossman 1985; Grimes et al. 1988; Lombardi-Carlson 2012). Little is known about the early life stages of Tilefish. Tilefish diet is dominated by crabs, and includes demersal teleosts (including other Tilefish), chondrichthyes, bivalve mollusks, brittlestars, polychaetes, holothurians, sea anemones, salps, squid, amphipods, mesopelagic fishes, and human trash (Steimle et al. 1999).

The most well-studied aspect of Tilefish biology is their habitat, which is restricted by two physical factors, malleable sediments and stable relatively warm bottom temperatures, and focused around submarine canyons (e.g. Hudson Canyon, De Soto Canyon). Tilefish require fine-grained silt/clay sediments to support their main form of shelter: vertical burrows (Grimes, Able, and Jones 1986; Able et al. 1982). Adult Tilefish build characteristic, large (meters x meters) funnel-shaped burrows in the seafloor which they use as long-term habitat and protection from predators (Able et al. 1982). These burrows are believed to be constructed over the course of a lifetime of an individual, who gradually deepens and widens the burrow over time (Twichell et al. 1985). Juvenile Tilefish have been observed occupying simple vertical shafts, invading abandoned burrows, or using other forms of shelter until they are able to construct their own larger burrow (Able et al. 1982). Tilefish burrows are formed and maintained by frequent oral excavation of sediment, flushing of sediment through movement, and secondary bioerosion by other benthic species (e.g. crabs, isopods) associated with the burrow communities, which are also presumed to be Tilefish prey (Grimes, Able, and Jones 1986; Able et al. 1982). Removal experiments have indicated that burrows fill in rapidly, leading to frequent excavation and maintenance by Tilefish (Grimes, Able, and Jones 1986). Burrows have also been observed cutting horizontally into the walls of submarine canyons, described as intricate, interconnected "pueblo" habitat similar to that of the ancient Puebloans of the American Southwest (Grimes,

Able, and Jones 1986). In addition to burrows, Tilefish have also been observed using boulders, rock slabs, lobster pots, crab traps, shipwrecks, and marine debris as shelter (Freeman and Turner 1977; Steimle et al. 1999; Grimes, Able, and Jones 1986). The southern stock of Tilefish appears to have identical habitat requirements and burrowing behavior as the northern stock (Able et al. 1993; Grossman, Harris, and Hightower 1985; Jones et al. 1989). Tilefish burrows form dense communities of up to 2,500-13,000 burrows/km^2 in the Atlantic, but likely lower (~1600 burrows/km^2) in the GoM (Grimes, Able, and Jones 1986; Steimle et al. 1999; Matlock et al. 1991). Tilefish are described as sedentary and non-migratory, foraging close to their burrow communities. Mark-recapture studies in the North Atlantic and stable isotopes studies in the north central GoM both indicated that adult Tilefish have high site fidelity (Grimes, Able, and Jones 1986; Ostroff 2017 personal communication).

The second habitat constraint of Tilefish is the narrow offshore "warm belt" found at the interface of continental shelf and slope water masses. Tilefish are restricted to bottom water temperatures between 8-17°C at depths of approximately 80-540 meters (Steimle et al. 1999). In the GoM specifically, Tilefish have been caught at depths of 150-400 meters, with water temperatures between 9-18°C (Murawski et al. 2018; Nelson and Carpenter 1968).

Many characteristics of Tilefish (habitat-restricted, burrow-forming, dense aggregation, non-migratory, long-lived, slow-growing, late-maturing, hermaphroditic) make the species particularly vulnerable to environmental change, anthropogenic disturbance, and exploitation (Grimes and Turner 1999). Due to their specific habitat requirements and sedentary nature, Tilefish are unable to alter their distribution in response to an environmental disturbance. This was exhibited in one of the largest recorded die-offs of vertebrates, the 1882 Tilefish kill, which resulted in the death of an estimated 1.5 billion individuals between Nantucket Shoals and

17

Maryland from thermal shock due to an intrusion of lethally cold water from the Labrador Current as a result of a strong negative in the North Atlantic Oscillation (Fisher et al. 2014; Steimle et al. 1999). Dense aggregation in limited habitat leaves them vulnerable to spatially concentrated disturbances, such as oil spills, that can heavily impact small areas. Life history characteristics of relatively slow growth rate, complex reproductive strategy, and delayed sexual maturity lead to lower resilience following disturbance (Couillard, Courtenay, and Macdonald 2008; Koslow et al. 2000). Lastly, due to their strong association with the sediments, Tilefish have multiple co-occurring routes of exposure to environmental pollutants, including incidental sediment ingestion and transdermal exposure from burrowing, dietary uptake from contaminated benthic prey, and respiration of dissolved chemicals which may occur frequently as Tilefish bioturbate and re-suspend any sedimented contaminants. Although studies of contaminants in Tilefish tissues are limited, GoM Tilefish are known to have some of the highest mercury levels in the U.S. commercial seafood market (Hall, Zook, and Meaburn 1978; FDA 2019).

Tilefish were selected as the study species of this dissertation due to relatively high and persistent levels of PAH exposure compared to other GoM demersal fishes, Gulf-wide distribution, commercial importance, and ability to use the north Atlantic population as an outgroup spatially removed from the GoM. Initial studies on demersal fishes post-*DWH* identified Tilefish as a key species for extensive study due to findings that a biomarker of petrogenic PAH exposure, biliary naphthalene metabolites, was four to six times higher than Red Snapper and King Snake Eel (*Ophichthus rex*) respectively, likely due to their burrowing lifestyle and diet of benthic prey (Snyder et al. 2015). This discovery prompted further investigation into PAH exposure, hepatic accumulation, and health indices in both the region of *DWH*, and Gulf-wide.

Dissertation Objectives

This research was initiated in the aftermath of *DWH* to determine exposure to PAHs, hepatic accumulation of PAHs, and associated negative health effects in Tilefish. The first research chapter presents a time series of these variables in Tilefish from nine stations sampled annually in the north central GoM, 2012 to 2017. After the initial *DWH*-focused studies, the scope of the research expanded to generate a Gulf-wide baseline in anticipation of future oil spills. The second research chapter is a broad-scale spatial analysis of the same variables in Tilefish sampled at 49 stations throughout the GoM from the north central, northwest, and southwest GoM, the Bay of Campeche, and Yucatán Shelf. Additionally, Tilefish samples were obtained from the northwest Atlantic Ocean to be used as a non-GoM "outgroup". Last, the third research chapter is both a spatial and temporal synthesis of traditional biomarkers of PAHs, microscopic hepatic changes (MHCs; commonly referred to as hepatic lesions), and associations with PAH exposure and hepatic accumulation in Tilefish from five stations sampled annually in the north central GoM, 2012 to 2015, and from 19 additional stations Gulf-wide

Overall, this dissertation is a synthetic body of research on PAH exposure, hepatic accumulation, and associated negative health effects in one species of commercially important GoM fish over an unprecedented Gulf-wide spatial scale, and a time series of six years. It is the first description of spatiotemporal patterns in these variables in Tilefish, as well as the first description of the microscopic hepatic anatomy of Tilefish. Results indicate significant, chronic, and increasing exposure to PAH pollution, and significant associations with negative health effects, with implications on individual health, reproductive capacity, and ultimately fitness.

References

Able, K. W., C. B. Grimes, R. A. Cooper, and J. R. Uzmann. 1982. 'Burrow construction and behavior of Tilefish, Lopholatilus chamaeleonticeps, in Hudson submarine canyon', *Environmental Biology of Fishes*, 7: 199-205.

Able, K. W., C. B. Grimes, R. S. Jones, and D. C. Twichell. 1993. 'Temporal and spatial variation in habitat characteristics of Tilefish (Lopholatilus chamaeleonticeps) off the East coast of Florida', *Bulletin of Marine Science*, 53: 1013-26.

Able, K. W., P. C. Lopez-Duarte, F. J. Fodrie, O. P. Jensen, C. W. Martin, B. J. Roberts, J. Valenti, K. O'Connor, and S. C. Halbert. 2015. 'Fish Assemblages in Louisiana Salt Marshes: Effects of the Macondo Oil Spill', *Estuaries and Coasts*, 38: 1385-98.

Ackleh, A. S., G. E. Ioup, J. W. Ioup, B. L. Ma, J. J. Newcomb, N. Pal, N. A. Sidorovskaia, and C. Tiemann. 2012. 'Assessing the Deepwater Horizon oil spill impact on marine mammal population through acoustics: Endangered sperm whales', *Journal of the Acoustical Society of America*, 131: 2306-14.

Antonio, F. J., R. S. Mendes, and S. M. Thomaz. 2011. 'Identifying and modeling patterns of tetrapod vertebrate mortality rates in the Gulf of Mexico oil spill', *Aquatic Toxicology*, 105: 177-79.

Barron, M. G., M. G. Carls, R. Heintz, and S. D. Rice. 2004. 'Evaluation of fish early life-stage toxicity models of chronic embryonic exposures to complex polycyclic aromatic hydrocarbon mixtures', *Toxicological Sciences*, 78: 60-67.

Beyer, J., G. Jonsson, C. Porte, M. M. Krahn, and F. Ariese. 2010. 'Analytical methods for determining metabolites of polycyclic aromatic hydrocarbon (PAH) pollutants in fish bile: A review', *Environmental Toxicology and Pharmacology*, 30: 224-44.

Beyer, J., H. C. Trannum, T. Bakke, P. V. Hodson, and T. K. Collier. 2016. 'Environmental effects of the Deepwater Horizon oil spill: A review', *Marine Pollution Bulletin*, 110: 28-51.

Bonisoli-Alquati, A., P. C. Stouffer, R. E. Turner, S. Woltmann, and S. S. Taylor. 2016. 'Incorporation of Deepwater Horizon oil in a terrestrial bird', *Environmental Research Letters*, 11.

Burns, C. M. B., J. A. Olin, S. Woltmann, P. C. Stouffer, and S. S. Taylor. 2014. 'Effects of Oil on Terrestrial Vertebrates: Predicting Impacts of the Macondo Blowout', *Bioscience*, 64: 820-28.

Chanton, J. P., J. Cherrier, R. M. Wilson, J. Sarkodee-Adoo, S. Bosman, A. Mickle, and W. M. Graham. 2012. 'Radiocarbon evidence that carbon from the Deepwater Horizon spill entered the planktonic food web of the Gulf of Mexico', *Environmental Research Letters*, 7.

Carmichael, R. H., W. M. Graham, A. Aven, G. Worthy, and S. Howden. 2012. 'Were Multiple Stressors a 'Perfect Storm' for Northern Gulf of Mexico Bottlenose Dolphins (Tursiops truncatus) in 2011?', *Plos One*, 7.

Collier, T. K., B. F. Anulacion, M. R. Arkoosh, J.P. Dietrich, J. P. Incardona, L. L. Johnson, G. M. Ylitalo, and M. S. Myers. 2014. 'Effects on fish of polycyclic aromatic hydrocarbons (PAHS) and naphthenic acid exposures.' in K. B. Tierney, A. P. Farrell and C.L. Brauner (eds.), *Fish Physiology: Organic Chemical Toxicology of Fishes* (Elsevier Inc.).

Couillard, C. M., S. C. Courtenay, and R. W. Macdonald. 2008. 'Chemical-environment interactions affecting the risk of impacts on aquatic organisms: A review with a Canadian perspective - interactions affecting vulnerability', *Environmental Reviews*, 16: 19-44.

Daly, K. L., U. Passow, J. Chanton, and D. Hollander. 2016. 'Assessing the impacts of oil-associated marine snow formation and sedimentation during and after the Deepwater Horizon oil spill', *Anthropocene*, 13: 18-33.

Emsbo-Mattingly, S. D., and E. Litman. 2016. 'Polycyclic aromatic hydrocarbon homolog and isomer fingerprinting.' in S. A. Stout and Z. Wang (eds.), *Standard Handbook Oil Spill Environmental Forensics: Fingerprinting and Source Identification* (Elsevier Inc.).

Erickson, D. L., M. J. Harris, and G. D. Grossman. 1985. 'Ovarian cycling of Tilefish, Lopholatilus chamaeleonticeps Goode and Bean, from the South Atlantic Bight, USA', *Journal of Fish Biology*, 27: 131-46.

Etnoyer, P. J., L. N. Wickes, M. Silva, J. D. Dubick, L. Balthis, E. Salgado, and I. R. MacDonald. 2016. 'Decline in condition of gorgonian octocorals on mesophotic reefs in the northern Gulf of Mexico: before and after the Deepwater Horizon oil spill', *Coral Reefs*, 35: 77-90.

FDA, U.S. 2019. 'Advice about eating fish: For women who are or might become pregnant, breastfeeding mothers, and young children', Accessed 12/23/19. https://www.fda.gov/food/consumers/advice-about-eating-fish.

Fernando, H., H. Ju, R. Kakumanu, K. K. Bhopale, S. Croisant, C. Elferink, B. S. Kaphalia, and G. A. S. Ansari. 2019. 'Distribution of petrogenic polycyclic aromatic hydrocarbons (PAHs) in seafood following Deepwater Horizon oil spill', *Marine Pollution Bulletin*, 145: 200-07.

Fisher, C. R., P. A. Montagna, and T. T. Sutton. 2016. 'How Did the Deepwater Horizon Oil Spill Impact Deep-Sea Ecosystems?', *Oceanography*, 29: 182-95.

Fisher, J. A. D., K. T. Frank, B. Petrie, and W. C. Leggett. 2014. 'Life on the edge: environmental determinants of tilefish (Lopholatilus chamaeleonticeps) abundance since its virtual extinction in 1882', *Ices Journal of Marine Science*, 71: 2371-78.

Fitzgerald, T. P., and J. M. Gohlke. 2014. 'Contaminant Levels in Gulf of Mexico Reef Fish after the Deepwater Horizon Oil Spill As Measured by a Fishermen-Led Testing Program', *Environmental Science & Technology*, 48: 1993-2000.

Fodrie, F. J., K. W. Able, F. Galvez, K. L. Heck, O. P. Jensen, P. C. Lopez-Duarte, C. W. Martin, R. E. Turner, and A. Whitehead. 2014. 'Integrating Organismal and Population Responses of Estuarine Fishes in Macondo Spill Research', *Bioscience*, 64: 778-88.

Freeman, B.L., and S. C. Turner. 1977. "Biological and fisheries data on Tilefish, Lopholatilus chamaeleonticeps Goode and Bean." In, edited by U.S. National Marine Fisheries Service Northeast Fisheries Center Sand Hook Laboratory, 1-41. Highlands, New Jersey: NOAA.

Goode, G.B., and T.H. Bean. 1880. "Description of a new genus and species of fish, Lopholatilus chamaeleonticeps, from the south coast of New England." In *Nineteenth Proceedings of the United States National Museum*, 205-09.

Gracia, A., S.A. Murawski, and A.R. Vazquez-Bader. 2020. 'Impacts of deep oil spills on fish and fisheries.' in S.A. Murawski, C.H. Ainsworth, S. Gilbert, D.J. Hollander, C.B. Paris, M. Schluter and D.L. Wetzel (eds.), *Deep Oil Spills: Facts, Fate, and Effects* (Springer Nature Switzerland AG: Cham, Switzerland).

Graham, W. M., R. H. Condon, R. H. Carmichael, I. D'Ambra, H. K. Patterson, L. J. Linn, and F. J. Hernandez. 2010. 'Oil carbon entered the coastal planktonic food web during the Deepwater Horizon oil spill', *Environmental Research Letters*, 5.

Grimes, C. B., K. W. Able, and R. S. Jones. 1986. 'Tilefish, Lopholatilus chamaeleonticeps, habitat, behavior and community structure in Mid-Atlantic and Southern New England waters', *Environmental Biology of Fishes*, 15: 273-92.

Grimes, C. B., C. F. Idelberger, K. W. Able, and S. C. Turner. 1988. 'The reproductive biology of Tilefish, Lopholatilus chamaeleonticeps Goode and Bean, from the United States Mid-Atlantic Bight, and the effects of fishing on the breeding system', *Fishery Bulletin*, 86: 745-62.

Grimes, C. B., and S. C. Turner. 1999. 'The complex life history of tilefish Lopholatilus chamaeleonticeps and vulnerability to exploitation.' in J. A. Musick (ed.), *Life in the Slow Lane: Ecology and Conservation of Long-Lived Marine Animals*.

Grossman, G. D., M. J. Harris, and J. E. Hightower. 1985. 'The relationship between Tilefish, Lopholatilus chamaeleonticeps, abundance and sediment composition off Georgia', *Fishery Bulletin*, 83: 443-47.

Hall, R.A., E.G. Zook, and G.M. Meaburn. 1978. "National Marine Fisheries Serivice survey of trace elements in the fishery resource." In, edited by U.S. Department of Commerce. NOAA Technical Report NMFS SSRF-721.

Haney, J. C., H. J. Geiger, and J. W. Short. 2014a. 'Bird mortality from the Deepwater Horizon oil spill. I. Exposure probability in the offshore Gulf of Mexico', *Marine Ecology Progress Series*, 513: 225-37.

———. 2014b. 'Bird mortality from the Deepwater Horizon oil spill. II. Carcass sampling and exposure probability in the coastal Gulf of Mexico', *Marine Ecology Progress Series*, 513: 239-52.

Hinga, K. R., and M. E. Q. Pilson. 1987. 'Persistence of benz[a]anthracene degradation products in an enclosed marine ecosytem', *Environmental Science & Technology*, 21: 648-53.

Hu, C. M., R. H. Weisberg, Y. G. Liu, L. Y. Zheng, K. L. Daly, D. C. English, J. Zhao, and G. A. Vargo. 2011. 'Did the northeastern Gulf of Mexico become greener after the Deepwater Horizon oil spill?', *Geophysical Research Letters*, 38.

Incardona, J. P., T. K. Collier, and N. L. Scholz. 2011. 'Oil spills and fish health: exposing the heart of the matter', *Journal of Exposure Science and Environmental Epidemiology*, 21: 3-4.

Incardona, J. P., L. D. Gardner, T. L. Linbo, T. L. Brown, A. J. Esbaugh, E. M. Mager, J. D. Stieglitz, B. L. French, J. S. Labenia, C. A. Laetz, M. Tagal, C. A. Sloan, A. Elizur, D. D. Benetti, M. Grosell, B. A. Block, and N. L. Scholz. 2014. 'Deepwater Horizon crude oil impacts the developing hearts of large predatory pelagic fish', *Proceedings of the National Academy of Sciences of the United States of America*, 111: E1510-E18.

Incardona, J. P., T. L. Swarts, R. C. Edmunds, T. L. Linbo, A. Aquilina-Beck, C. A. Sloan, L. D. Gardner, B. A. Block, and N. L. Scholz. 2013. 'Exxon Valdez to Deepwater Horizon: Comparable toxicity of both crude oils to fish early life stages', *Aquatic Toxicology*, 142: 303-16.

James, M. O. 1989. 'Biotransformation of disposition of PAH in aquatic invertebrates.' in U. Varanasi (ed.), *Metabolism of Polycyclic Aromatic Hydrocarbons in the Aquatic Environment* (CRC Press, Inc.: Boca Raton, FL).

Jernelov, A., and O. Linden. 1981. 'Ixtoc I: A case study of the world's largest oil spill', *Ambio*, 10: 299-306.

Jones, R. S., E. J. Gutherz, W. R. Nelson, and G. C. Matlock. 1989. 'Burrow utilization by yellowedge grouper, Epinephelus flavolimbatus, in the northwestern Gulf of Mexico', *Environmental Biology of Fishes*, 26: 277-84.

Katz, S. J., C. B. Grimes, and K. W. Able. 1983. 'Delineation of Tilefish, Lopholatilus chamaeleonticeps, stocks along the United States East coast and in the Gulf of Mexico', *Fishery Bulletin*, 81: 41-50.

Kennicutt, M. C., J. M. Brooks, E. L. Atlas, and C. S. Giam. 1988. 'Organic compounds of environmental concern in the Gulf of Mexico: a review', *Aquatic Toxicology*, 11: 191-212.

Koslow, J. A., G. W. Boehlert, J. D. M. Gordon, R. L. Haedrich, P. Lorance, and N. Parin. 2000. 'Continental slope and deep-sea fisheries: implications for a fragile ecosystem', *Ices Journal of Marine Science*, 57: 548-57.

Krahn, M. M., M. S. Myers, D. G. Burrows, and D. C. Malins. 1984. 'Determination of metabolites of xenobiotics in the bile of fish from polluted waterways', *Xenobiotica*, 14: 633-46.

Krahn, M. M., and J. E. Stein. 1998. 'Assessing exposure of marine biota and habitats to petroleum compounds', *Analytical Chemistry*, 70: 186A-92A.

Kujawinski, E. B., M. C. K. Soule, D. L. Valentine, A. K. Boysen, K. Longnecker, and M. C. Redmond. 2011. 'Fate of Dispersants Associated with the Deepwater Horizon Oil Spill', *Environmental Science & Technology*, 45: 1298-306.

Lima, A. L. C., J. W. Farrington, and C. M. Reddy. 2005. 'Combustion-derived polycyclic aromatic hydrocarbons in the environment - A review', *Environmental Forensics*, 6: 109-31.

Lombardi-Carlson, L.A. 2012. 'Life history, population dynamics, and fishery management of the Golden Tilefish, *Lopholatilus chamaeleonticeps*, from the Southest Atlantic and Gulf of Mexico', University of Florida.

Love, M., A. Baldera, C. Yeung, and C. Robbins. 2013. "The Gulf of Mexico Ecosystem: A Coastal and Marine Atlas." In. New Orleans, LA: Ocean Conservancy, Gulf Restoration Center.

Lubchenco, J., M. K. McNutt, G. Dreyfus, S. A. Murawski, D. M. Kennedy, P. T. Anastas, S.

Matlock, G. C., W. R. Nelson, R. S. Jones, A. W. Green, T. J. Cody, E. Gutherz, and J. Doerzbacher. 1991. 'Comparison of 2 techniques for estimating Tilefish, Yellowedge grouper, and other deepwater fish populations', *Fishery Bulletin*, 89: 91-99.

McCrea-Strub, A., K. Kleisner, U. R. Sumaila, W. Swartz, R. Watson, D. Zeller, and D. Pauly. 2011. 'Potential Impact of the Deepwater Horizon Oil Spill on Commercial Fisheries in the Gulf of Mexico', *Fisheries*, 36: 332-36.

McElroy, A.E., J. W. Farrington, and J.M. Teal. 1989. 'Bioavailability of polycyclic aromatic hydrocarbons in the aquatic environment.' in U. Varanasi (ed.), *Metabolism of Polycyclic Aromatic Hydrocarbons in the Aquatic Environment* (CRC Press, Inc.: Boca Raton, FL).

Meador, J. P., J. E. Stein, W. L. Reichert, and U. Varanasi. 1995. 'Bioaccumulation of Polycyclic Aromatic Hydrocarbons by Marine Organisms', *Reviews of Environmental Contamination and Toxicology <D>*, 143: 79-165.

Mitra, S., D. G. Kimmel, J. Snyder, K. Scalise, B. D. McGlaughon, M. R. Roman, G. L. Jahn, J. J. Pierson, S. B. Brandt, J. P. Montoya, R. J. Rosenbauer, T. D. Lorenson, F. L. Wong,

and P. L. Campbell. 2012. 'Macondo-1 well oil-derived polycyclic aromatic hydrocarbons in mesozooplankton from the northern Gulf of Mexico', *Geophysical Research Letters*, 39.

Montagna, P. A., J. G. Baguley, C. Cooksey, I. Hartwell, L. J. Hyde, J. L. Hyland, R. D. Kalke, L. M. Kracker, M. Reuscher, and A. C. E. Rhodes. 2013. 'Deep-Sea Benthic Footprint of the Deepwater Horizon Blowout', *Plos One*, 8.

Murawski, S. A., J. W. Fleeger, W. F. Patterson, C. M. Hu, K. Daly, I. Romero, and G. A. Toro-Farmer. 2016. 'How Did the Deepwater Horizon Oil Spill Affect Coastal and Continental Shelf Ecosystems of the Gulf of Mexico?', *Oceanography*, 29: 160-73.

Murawski, S. A., W. T. Hogarth, E. B. Peebles, and L. Barbeiri. 2014. 'Prevalence of External Skin Lesions and Polycyclic Aromatic Hydrocarbon Concentrations in Gulf of Mexico Fishes, Post-Deepwater Horizon', *Transactions of the American Fisheries Society*, 143: 1084-97.

Murawski, S. A., E. B. Peebles, A. Gracia, J. W. Tunnell, and M. Armenteros. 2018. 'Comparative Abundance, Species Composition, and Demographics of Continental Shelf Fish Assemblages throughout the Gulf of Mexico', *Marine and Coastal Fisheries*, 10: 325-46.

Myers, M. S., L. L. Johnson, and T. K. Collier. 2003. 'Establishing the causal relationship between polycyclic aromatic hydrocarbon (PAH) exposure and hepatic neoplasms and neoplasia-related liver lesions in English sole (Pleuronectes vetulus)', *Human and Ecological Risk Assessment*, 9: 67-94.

NEFSC. 2005. "A report of the 41st Northeast regional stock assessment workshop (41st SAW)." In, edited by Northeast Fisheries Science Center Reference Document 09-15. Woods Hole, Massachusetts.

Nelson, W. R., and J.S. Carpenter. 1968. 'Bottom longline explorations in the Gulf of Mexico- A report on "Oregon. II's" first cruise', *Commercial Fisheries Review*, 30: 57-62.

National Research Council. 1987. 'Biological markers in environmental health research. Committee on Biological Markers of the National Research Council', *Environmental Health Perspectives*, 74: 3-9.

Parsons, M. L., W. Morrison, N. N. Rabalais, R. E. Turner, and K. N. Tyre. 2015. 'Phytoplankton and the Macondo oil spill: A comparison of the 2010 phytoplankton assemblage to baseline conditions on the Louisiana shelf', *Environmental Pollution*, 207: 152-60.

Pasparakis, Christina, Andrew J. Esbaugh, Warren Burggren, and Martin Grosell. 2019. 'Physiological impacts of Deepwater Horizon oil on fish', *Comparative Biochemistry and Physiology Part C: Toxicology & Pharmacology*, 224: 108558.

Passow, U., and K. Ziervogel. 2016. 'Marine Snow Sedimented Oil Released During the Deepwater Horizon Spill', *Oceanography*, 29: 118-25.

Passow, U., K. Ziervogel, V. Asper, and A. Diercks. 2012. 'Marine snow formation in the aftermath of the Deepwater Horizon oil spill in the Gulf of Mexico', *Environmental Research Letters*, 7.

Passow, Uta, and Robert Hetland. 2016. 'What Happened to All of the Oil?', *Oceanography*, 29: 88-95.

Peterson, C. H., S. D. Rice, J. W. Short, D. Esler, J. L. Bodkin, B. E. Ballachey, and D. B. Irons. 2003. 'Long-term ecosystem response to the Exxon Valdez oil spill', *Science*, 302: 2082-86.

Powers, S. P., F. J. Hernandez, R. H. Condon, J. M. Drymon, and C. M. Free. 2013. 'Novel Pathways for Injury from Offshore Oil Spills: Direct, Sublethal and Indirect Effects of the Deepwater Horizon Oil Spill on Pelagic Sargassum Communities', *Plos One*, 8.

Pulster, E. L., A. Gracia, S. M. Snyder, K. Deak, S Fogelson, and S.A. Murawski. 2020. 'Chronic Sub-lethal Effects Observed in Wild-Caught Fishes Following Two Major Oil Spills in the Gulf of Mexico: Deepwater Horizon and Ixtoc 1.' in S.A. Murawski, C.H. Ainsworth, S. Gilbert, D.J. Hollander, C.B. Paris, M. Schluter and D. L. Wetzel (eds.), *Deep Oil Spills: Facts, Fate, and Effects* (Springer Nature Switzerland AG).

Rabalais, N. N., and R. E. Turner. 2016. 'Effects of the Deepwater Horizon Oil Spill on Coastal Marshes and Associated Organisms', *Oceanography*, 29: 150-59.

Reddy, Christopher M., J. Samuel Arey, Jeffrey S. Seewald, Sean P. Sylva, Karin L. Lemkau, Robert K. Nelson, Catherine A. Carmichael, Cameron P. McIntyre, Judith Fenwick, G. Todd Ventura, Benjamin A. S. Van Mooy, and Richard Camilli. 2012. 'Composition and fate of gas and oil released to the water column during the Deepwater Horizon oil spill', *Proceedings of the National Academy of Sciences*, 109: 20229-34.

Schwacke, L. H., C. R. Smith, F. I. Townsend, R. S. Wells, L. B. Hart, B. C. Balmer, T. K. Collier, S. De Guise, M. M. Fry, L. J. Guillette, S. V. Lamb, S. M. Lane, W. E. McFee, N. J. Place, M. C. Tumlin, G. M. Ylitalo, E. S. Zolman, and T. K. Rowles. 2014. 'Health of Common Bottlenose Dolphins (Tursiops truncatus) in Barataria Bay, Louisiana Following the Deepwater Horizon Oil Spill (vol 48, pg 93, 2014)', *Environmental Science & Technology*, 48: 10528-28.

Schwing, P. T., G. R. Brooks, R. K. Larson, C. W. Holmes, B. J. O'Malley, and D. J. Hollander. 2017. 'Constraining the Spatial Extent of Marine Oil Snow Sedimentation and Flocculent Accumulation Following the Deepwater Horizon Event Using an Excess Pb-210 Flux Approach', *Environmental Science & Technology*, 51: 5962-68.

SEDAR. 2004. "SEDAR 4 stock assessment of the deep-water snapper-group complex in the South Atlantic." In, 594. Charleston, South Carolina: SEDAR.

———. 2011. "SEDAR 22 stock assessment report Gulf of Mexico Tilefish." In, 330. North Charleston, South Carolina: SEDAR.

Shepard, Andrew, John Valentine, Christopher D'Elia, David W. Yoskowitz, and David Dismukes. 2013. *Economic Impact of Gulf of Mexico Ecosystem Goods and Services and Integration Into Restoration Decision-Making*.

Shigenaka, G. 2014. "Twenty-five years after the Exxon Valdez oil spill: NOAA's scientific support, monitoring, and research." In, edited by NOAA Office of Response and Restoration, 78. Seattle, WA.

Silliman, B. R., J. van de Koppel, M. W. McCoy, J. Diller, G. N. Kasozi, K. Earl, P. N. Adams, and A. R. Zimmerman. 2012. 'Degradation and resilience in Louisiana salt marshes after the BP-Deepwater Horizon oil spill', *Proceedings of the National Academy of Sciences of the United States of America*, 109: 11234-39.

Silva, M., P. J. Etnoyer, and I. R. MacDonald. 2016. 'Coral injuries observed at Mesophotic Reefs after the Deepwater Horizon oil discharge', *Deep-Sea Research Part Ii-Topical Studies in Oceanography*, 129: 96-107.

Snyder, S. M., E. L. Pulster, D. L. Wetzel, and S. A. Murawski. 2015. 'PAH Exposure in Gulf of Mexico Demersal Fishes, Post-Deepwater Horizon', *Environmental Science & Technology*, 49: 8786-95.

Soto, L.A., A. V. Botello, S. Licea-Durán, M.L. Lizárraga-Partida, and A. Yáñez-Arancibia. 2014. 'The environmental legacy of the Ixtoc-I oil spill in Campeche Sound, southwestern Gulf of Mexico', *Frontiers in Marine Science*, 1.

Steimle, F. W., C.A. Zetlin, P.L. Berrien, D.L. Johnson, and S. Chang. 1999. "Tilefish, Lopholatilus chamaeleonticpes, life history and habitat characteristics." In, edited by U.S. Department of Commerce.

Stein, J. E., W. L. Reichert, M. Nishimoto, and U. Varanasi. 1990. 'Overview of studies on liver carcinogenesis in English sole from Puget Sound; Evidence for a xenobiotic chemical etiology II: biochemical studies', *Science of the Total Environment*, 94: 51-69.

Sumaila, U. R., A. M. Cisneros-Montemayor, A. Dyck, L. Huang, W. Cheung, J. Jacquet, K. Kleisner, V. Lam, A. McCrea-Strub, W. Swartz, R. Watson, D. Zeller, and D. Pauly. 2012. 'Impact of the Deepwater Horizon well blowout on the economics of US Gulf fisheries', *Canadian Journal of Fisheries and Aquatic Sciences*, 69: 499-510.

Sutton, T.T., T. Frank, H. Judkins, and I.C. Romero. 2020. 'As Gulf oil extraction goes deeper, who is at risk? Community structure, distribution, and connectivity of the deep-pelagic fauna.' in S.A. Murawski, C.H. Ainsworth, S. Gilbert, D.J. Hollander, C.B. Paris, M. Schluter and D.L. Wetzel (eds.), *Scenarios and responses to future deep oil spills: Fighting the next war* (Springer Nature Switzerland AG: Cham, Switzerland).

Sutton, T.T., R. Milligan, A.B. Cook, J. Moore, and K.B. Boswell. 2018. "Evidence of dramatic and persistent declines in meso- and bathypelagic fishes in the Gulf of Mexico after the Deepwater Horizon oil spill." In *Ocean Sciences*. Portland, OR.

Tarnecki, J. H., and W. F. Patterson. 2015. 'Changes in Red Snapper Diet and Trophic Ecology Following the Deepwater Horizon Oil Spill', *Marine and Coastal Fisheries*, 7: 135-47.

Thibodeaux, L. J., K. T. Valsaraj, V. T. John, K. D. Papadopoulos, L. R. Pratt, and N. S. Pesika. 2011. 'Marine Oil Fate: Knowledge Gaps, Basic Research, and Development Needs; A Perspective Based on the Deepwater Horizon Spill', *Environmental Engineering Science*, 28: 87-93.

Tran, T., A. Yazdanparast, and E. A. Suess. 2014. 'Effect of Oil Spill on Birds: A Graphical Assay of the Deepwater Horizon Oil Spill's Impact on Birds', *Computational Statistics*, 29: 133-40.

Trustees, Deepwater Horizon Natural Resource Damage Assesssment. 2016. "Deepwater Horizon Oil Spill: Final Programmatic Damage Assessment and Restoration Plan and Final Programmatic Environmental Impact Statement." In. Silver Spring, MD: National Oceanic and Atmospheric Administration.

Twichell, D. C., C. B. Grimes, R. S. Jones, and K. W. Able. 1985. 'The role of erosion by fish in shaping topography around Hudson Submarine Canyon', *Journal of Sedimentary Petrology*, 55: 712-19.

United States of America v. BP Exploration & Production, Inc., et al. 2015. "Findings of fact and conclusions of law: Phase two trial. RE: Oil spill by the oil rig "Deepwater Horizon" in the Gulf of Mexico, on April 20, 2010." In, edited by U.S. District Court from the Eastern District of Louisiana.

Valentine, M. M., and M. C. Benfield. 2013. 'Characterization of epibenthic and demersal megafauna at Mississippi Canyon 252 shortly after the Deepwater Horizon Oil Spill', *Marine Pollution Bulletin*, 77: 196-209.

Varanasi, U., M. Nishimoto, W.L. Reichert, and B. Le Eberhart. 1986. 'Comparative Metabolism of Benzo(a)pyrene and Covalent Binding to Hepatic DNA in English Sole, Starry Flounder, and Rat', *Cancer Research*, 46: 3817-24.

Varanasi, U., J. E. Stein, and M. Nishimoto. 1989. 'Biotransformation and disposition of polycyclic aromatic hydrocarbons (PAH) in fish.' in U. Varanasi (ed.), *Metabolism of polycyclic aromatic hydrocarbons in the aquatic environment* (CRC Press, Inc.: Boca Raton, Florida).

Wang, Z., C. Yang, Z. Yang, C.E. Brown, B.P. Hollebone, and S. A. Stout. 2016. 'Petroleum biomarker fingerprinting for oil spill characterization and source identification.' in S. A. Stout and Z. Wang (eds.), *Standard Handbook Oil Spill Environmental Forsensics: Fingerprinting and Source Identification* (Elsevier Inc.).

Wang, Zhendi, B. Hollebone, Merv Fingas, Ben Fieldhouse, L. Sigouin, M. Landriault, P. Smith, J. Noonan, G. Thouin, and James Weaver. 2003. 'Characteristics of Spilled Oils, Fuels, and Petroleum Products: 1. Composition and Properties of Selected Oils'.

Ward, C.H., and J. W. Tunnel. 2017. 'Habitats and biota of the Gulf of Mexico: An overview.' in C.H. Ward (ed.), *Habitats and Biota of the Gulf of Mexico: Before the Deepwater Horizon Oil Spill* (Springer Nature).

White, H. K., P. Y. Hsing, W. Cho, T. M. Shank, E. E. Cordes, A. M. Quattrini, R. K. Nelson, R. Camilli, A. W. J. Demopoulos, C. R. German, J. M. Brooks, H. H. Roberts, W. Shedd, C. M. Reddy, and C. R. Fisher. 2012. 'Impact of the Deepwater Horizon oil spill on a deep-water coral community in the Gulf of Mexico', *Proceedings of the National Academy of Sciences of the United States of America*, 109: 20303-08.

Xia, K., G. Hagood, C. Childers, J. Atkins, B. Rogers, L. Ware, K. Armbrust, J. Jewell, D. Diaz, N. Gatian, and H. Folmer. 2012. 'Polycyclic Aromatic Hydrocarbons (PAHs) in Mississippi Seafood from Areas Affected by the Deepwater Horizon Oil Spill', *Environmental Science & Technology*, 46: 5310-18.

Ylitalo, G. M., T. K. Collier, B. F. Anulacion, K. Juaire, R. H. Boyer, D. A. M. da Silva, J. L. Keene, and B. A. Stacy. 2017. 'Determining oil and dispersant exposure in sea turtles from the northern Gulf of Mexico resulting from the Deepwater Horizon oil spill', *Endangered Species Research*, 33: 9-24.

Ylitalo, G. M., M. M. Krahn, W. W. Dickhoff, J. E. Stein, C. C. Walker, C. L. Lassitter, E. S. Garrett, L. L. Desfosse, K. M. Mitchell, B. T. Noble, S. Wilson, N. B. Beck, R. A. Benner, P. N. Koufopoulos, and R. W. Dickey. 2012. 'Federal seafood safety response to the Deepwater Horizon oil spill', *Proceedings of the National Academy of Sciences of the United States of America*, 109: 20274-79.

Zengel, S., B. M. Bernik, N. Rutherford, Z. Nixon, and J. Michel. 2015. 'Heavily Oiled Salt Marsh following the Deepwater Horizon Oil Spill, Ecological Comparisons of Shoreline Cleanup Treatments and Recovery', *Plos One*, 10.

Zengel, S., C. L. Montague, S. C. Pennings, S. P. Powers, M. Steinhoff, G. Fricano, C. Schlemme, M. N. Zhang, J. Oehrig, Z. Nixon, S. Rouhani, and J. Michel. 2016. 'Impacts of the Deepwater Horizon Oil Spill on Salt Marsh Periwinkles (Littoraria irrorata)', *Environmental Science & Technology*, 50: 643-52.

Ziervogel, K., C. Dike, V. Asper, J. Montoya, J. Battles, N. D'Souza, U. Passow, A. Diercks, M. Esch, S. Joye, C. Dewald, and C. Arnosti. 2016. 'Enhanced particle fluxes and heterotrophic bacterial activities in Gulf of Mexico bottom waters following storm-induced sediment resuspension', *Deep-Sea Research Part Ii-Topical Studies in Oceanography*, 129: 77-88.

Chapter 2

Associations Between Chronic Exposure to Polycyclic Aromatic Hydrocarbons and Health Indices in Gulf of Mexico Tilefish (*Lopholatilus chamaeleonticeps*) post-*Deepwater Horizon*

Note to Reader

Portions of this chapter have been previously published in Snyder, S.M., Pulster, E.L., Murawski S., 2019. Associations Between Chronic Exposure to Polycyclic Aromatic Hydrocarbons and Health Indices in Gulf of Mexico Tilefish (*Lopholatilus chamaeleonticeps*) post-*Deepwater Horizon*. Environmental Toxicology and Chemistry 38, 2659-2671, and have been reproduced with permission from Wiley Periodicals, Inc. on behalf of SETAC under the terms of the Creative Commons Attribution Non-Commercial License CC BY-NC (which may be updated from time to time) and permits non-commercial use, distribution and reproduction in any medium, provided the original work is properly cited.

Introduction

The *Deepwater Horizon* (*DWH*) blowout began on April 20th, 2010, lasted for 87 days, and ultimately released four million barrels of oil into the Gulf of Mexico (GoM), becoming the largest accidental marine oil spill in global history (United States of America v. BP Exploration & Production 2015). Early in the response efforts, scientists realized there was a critical lack of pre-spill data on oil contamination levels in GoM fishes, and how concentrations varied over space and time. The lack of comprehensive pre-spill data is not unique to *DWH*, as similar

29

circumstances occurred in the case of the 1989 *Exxon Valdez* oil spill in Alaska's Prince William Sound and the 1979 *Ixtoc I* blowout in the southern GoM (Pulster, Gracia, Snyder, Romero, et al. 2020).

Due to the four-dimensional and highly dynamic distribution of the oil, the effects of *DWH* spanned almost all ecozones of the GoM, from coastal to oceanic, including both pelagic and benthic (Beyer et al. 2016). Petroleum hydrocarbons at the ocean surface and mid-water depths weather rapidly but once sequestered in deep sea sediments oil residues may persist for decades (Mackay and McAuliffe 1989). An estimated $21 \pm 10\%$ of the total *DWH* oil not recovered (3.19 million barrels) was deposited on the seafloor (Romero et al. 2017). Multiple mechanisms, including a sedimentation pulse of oiled marine snow, sinking of *in situ* burn resides and impingement of deep hydrocarbon plumes were responsible for oil sequestration. Sedimented oil residue is bioavailable to demersal fish through inhalation of re-suspended and re-dissolved hydrocarbons, dermal uptake, consumption of contaminated benthic prey and direct ingestion of contaminated sediment (Meador et al. 1995). Sedimented oil has been linked with negative impacts on GoM benthic fauna following *DWH*, including 80 to 93% declines in foraminifera density, changes in meio- and macrofauna diversity and abundance, oil-damaged corals, dietary and trophic shifts in Red Snapper (*Lutjanus campechanus*), and elevated frequency of external skin lesions in demersal fishes (Beyer et al. 2016).

Polycyclic aromatic hydrocarbons (PAHs) are the most toxic component of crude oil, although they made up only about 3% of the total hydrocarbons released from *DWH* by weight (Reddy et al. 2012). Negative effects of PAHs on fish health include reproductive impairment, cardiotoxicity, developmental defects, reduced growth, decreased condition, immunotoxicity, and hepatic lesions (Collier et al. 2014). PAHs are efficiently metabolized in the teleost liver by

30

a series of oxidation and conjugation reactions, which increase the solubility of parent PAHs for easy elimination via bile and gastrointestinal tract (Meador et al. 1995). Due to this efficient biotransformation, PAHs rarely accumulate to high levels in fish tissue, making tissue concentrations a poor indicator of previous or current PAH exposure. A more suitable biomarker of exposure to PAHs is measurement of biliary PAH metabolites (Beyer et al. 2010). Concentrations of PAHs in tissue reflect any bioaccumulation that may occur over and above metabolism and excretion.

An initial study of PAH exposure in GoM demersal fishes following *DWH* found Tilefish (*Lopholatilus chamaeleonticeps*) to have significantly higher concentrations of low molecular weight (LMW), often considered petrogenic, biliary PAH metabolites compared to two other demersal fishes, King Snake Eel (*Ophichthus rex*) and Red Snapper (Snyder et al. 2015). When contrasted with biliary PAH metabolite levels from published studies using similar quantification methods globally, Tilefish ranked as the third highest fish species for LMW PAH exposure. That study also documented a decline in LMW PAH exposure for King Snake Eel (2012-2013) and Red Snapper (2011-2013), but no change over time (2012-2013) for Tilefish, with levels of LMW biliary PAH metabolites remaining consistently high. Tilefish habitat, physiology and diet most likely accounted for their high levels of petrogenic PAH exposure (Snyder et al. 2015).

Tilefish are highly susceptible to exposure to sedimented contaminants because of their burrow-forming lifestyle. Remotely operated vehicle observations have recorded their primary habitat as large (meters x meters), funnel-shaped vertical burrows constructed in silt-clay sediments, which an individual Tilefish inhabits throughout its lifetime (Able et al. 1982; Grimes, Able, and Jones 1986; Jones et al. 1989). Fine grained silt-clay sediments tend to retain hydrophobic contaminants, such as PAHs, due to their high surface area and generally high

31

organic matter content. In a depositional environment, burrows rapidly accumulate sediment and

considerable burrow maintenance and enlargement has been observed via frequent oral

excavation (Grimes, Able, and Jones 1986). Secondary burrowing by other species in the

community, such as crustaceans and small fishes, also helps shape and maintain the burrows.

Tilefish have been observed preying on these associated species, which are likely to be highly

contaminated prey due to their benthic nature and inability to metabolize these compounds.

Strong association with sediments, via burrow maintenance and diet high in benthic prey, is

hypothesized to be why Tilefish have some of the highest levels of PAH exposure ever

measured, and highest skin lesion frequency following *DWH* (Murawski et al. 2014; Snyder et

al. 2015).

As a follow up to Snyder et al. (2015) findings on Tilefish, a lengthier time series of PAH

exposure and hepatic accumulation, and biometric data in the northern GoM was completed

during 2012 to 2017. We monitored nine sampling locations in the northern GoM around the

DeSoto Canyon, aiming to track a "return to baseline" following *DWH*, and provide data on the

variability of that baseline over a six-year period. Tilefish are fished commercially and

recreationally in the GoM, and their life history characteristics (long lived, slow growing, late

maturing, complex reproductive strategy, nonmigratory) make them especially sensitive to the

negative individual and population-level impacts of chronic contaminant exposure.

Materials and Methods

Field Sampling

Fisheries-independent demersal longline surveys were conducted at repeat stations in the northern GoM 2012 to 2015, and 2017. Tilefish were caught consistently at nine stations in the northern GoM, which ranged from west of the Mississippi River, around the DeSoto Canyon, and onto the northern West Florida Shelf (Figure 2.1). Sampling occurred in the months of July (2017) and August (2012, 2013, 2014, 2015) aboard the *R/V Weatherbird II*. At each station an average of 474 size 13/0 circle hooks, baited with cut Atlantic Mackerel (*Scomber scombus*) or various squid (mainly Humbolt squid [*Dosidicus gigas*] wings) were attached to 2.4m 136-kg-test leaders and a 3.2mm galvanized steel (2012) or 544-kg-test monofilament (2013-2017) main line for an average soak time of two hours. Temperature/depth/time recorders (Star:Oddi CDST Centi-TD) were attached to the main line of each longline set to record bottom time, bottom temperature, and fished depth. More detailed methods for longlining and sampling have been previously described in Murawski et al. (2014), Snyder et al. (2015), and Murawski et al. (2018).

Tilefish were caught at depths of 147 to 438m, with a mean depth of 265m. Once landed, fish were sampled immediately, or placed on ice prior to processing. Standard and total lengths, total body weight, sex, and organ weights (liver, gastrointestinal and gonad) were determined. Sexes were identified visually as male, female, or unknown. If present in sufficient volume, bile was collected by draining the contents of the gall bladder into an 8mL precleaned (fired in a 400°C muffle furnace to remove contaminants) amber vial. Livers were collected in either a precleaned glass jar, or precleaned aluminum foil and inserted into Whirl-Paks[TM] if jars were not available. Samples were frozen immediately and stored at -20°C until analysis.

Chemicals and Reagents

Analytical standards were purchased from Absolute Standards, Inc. Surrogate MC252 crude oil was provided by British Petroleum (BP). All solvents were Fisher Chemical Optima® grade, except for HPLC grade methyl tert-butyl ether (MTBE). All glassware was washed with Alconox®, combusted for a minimum of four hours, and solvent rinsed with acetone and hexane prior to use.

Analysis of Biliary PAH Metabolites Using HPLC-F

Two separate laboratories, Mote Marine Lab (MML) and the University of South Florida (USF) analyzed the bile samples, however, the analyst remained the same. At each facility, an inter-laboratory comparison was performed in conjunction with the NOAA Northwest Fisheries Science Center (NWFSC), Seattle, WA, whose quality assurance plan regularly monitors accuracy through a fish bile control sample from Atlantic Salmon (*Salmo salar*) exposed to 25 µg/mL of Monterey Crude oil for 48 hours. As described in Snyder et al. (2015) the inter-laboratory comparison used bile samples from three fish species and measured biliary PAH metabolite equivalents of naphthalene (NPH), phenanthrene (PHN), and benzo[*a*]pyrene (B*a*P) over a wide range of concentrations. The comparison agreed, with a coefficient of variation (*CV*) of <15% for biliary PAH metabolite equivalents among all three analytical facilities for each of the three quality control samples.

A semi-quantitative high performance liquid chromatography with fluorescence detection (HPLC-F) bile screening method developed by the NWFSC was used to analyze all bile samples (Krahn et al. 1984; Krahn, Moore, and Macleod 1986; Snyder et al. 2015). In summary, 3µL of

untreated bile was injected directly onto the HPLC-F system (MML: Agilent Technologies, 1100 Series; USF: Hitachi High-Technologies, Elite LaChrom L-2000 Series). Throughout the study the same model of C-18 reverse-phase column (Phenomenex Synergi™ 4μm Hydro-RP 80$\mathring{A}$) was used. With the column oven held at 50°C, fluorescent aromatic compounds (FACs) were eluted at a flow rate of 1mL/min using a linear gradient from 100% solvent A (water containing 5μL/L acetic acid) to 100% solvent B (methanol). Chromatograms were recorded at representative wavelength pairs of 292/335nm for two to three ring FACs (e.g. NPH metabolite equivalents), and 380/430nm for four to five ring FACs (e.g. BaP metabolite equivalents). All peaks within a time window of six to 19 minutes on the chromatogram were integrated, summed, and FACs were calculated for each wavelength pair using an external standard of the representative parent PAH (NPH or BaP) to quantify FACs from fluorescence response. Biliary PAH data are reported to two significant figures as μgFACs/g of bile.

Quality assurance was initially evaluated through the inter-laboratory comparison, and continuously monitored via methanol blanks between samples, sample analysis in duplicate (2012-2013) or triplicate (2014-2017), and a continuing calibration of PAH standards (NPH 2.5μg/mL, BaP 250ng/mL) with each batch of 12 field samples.

Analysis of Livers for PAHs and Alkylated Homologs Using GC-MS/MS

Liver tissue was extracted using a modified QuEChERS method (Lucas and Zhao 2015). The entire tissue sample was homogenized, and a 2g aliquot was spiked with a surrogate standard solution containing the deuterated form of each of the 19 parent PAH analytes (Table B2; 16 EPA PAHs plus dibenzothiophene, benzo[*e*]pyrene and perylene). After a ten-minute

35

marination of the surrogate standard solution in the homogenized sample, acetonitrile (ACN) was added and samples were shaken with two cleaned steel beads using a 1600 MiniG® automated tissue homogenizer and cell lyser (SPEX SamplePrep). Acetonitrile extracts were transferred to a Bond Elut Enhanced Matrix Removal-Lipid (EMR-Lipid) dispersive solid phase extraction tube (Agilent Technologies) and shaken in the MiniG®. The extract was decanted and mixed with Bond Elut EMR-Lipid polish pouch (Agilent Technologies), containing anhydrous magnesium sulfate for water removal, and agitated. Final extracts were spiked with a post-extraction standard of *p*-Terphenyl-d14 and brought to a volume of 1mL. The QuEChERS extraction method was optimized for this species and matrix by varying duration of marination and extraction in the MiniG® for maximum recovery of matrix spikes.

Extracts were injected in splitless mode as a two-layer sandwich comprised of 2µL of sample extract and 0.2µL of analyte protectant (20mg/mL L-gulonolactone and 10mg/mL D-sorbitol composite solution in ACN). Analytes were separated by gas chromatography (Agilent Technologies, 7890B) on a 30m Rxi-5Sil fused silica capillary column (Restek) and analyzed by a triple quadrupole mass spectrometer (Agilent Technologies, 7010) operating in multiple reaction monitoring and full scan modes. Operating and acquisition parameters for GC-MS/MS analysis can be found in the Supplemental Information (Tables B1 and B2).

A matrix-matched standard containing all analytes (both deuterated and non-deuterated forms) was made and analyzed with each batch of samples to quantify surrogate recoveries as well as relative response factors for each analyte within each sample. Target analyte concentrations were quantified using the relative response factors from the matrix-matched standard, and identities were confirmed by matching spectra, retention times, and relative intensity ratios of the selected ions with matrix-matched standard. Liver PAH concentrations for

36

all analytes above the lower limit of quantitation (1 ng/g) were reported to three significant

figures as ng/g wet weight (w.w.). Liver PAH concentrations for all analytes quantified below

the lower limit of quantitation were adjusted to have the lower limit of quantitation (i.e. 0.5 ng/g

w.w.). Target analytes (n = 46) include 19 parent PAHs and selected alkylated homologs (Table

B2). Sum total of the analytes are reported as $TPAH_{46}$. The sum of LMW PAHs consisted of

two to three ring PAHs and their alkylated homologs. The sum of high molecular weight

(HMW) PAHs consisted of four to six ring PAHs and their alkylated homologs. Commercial

standards in both solvent and matrix, as well as BP surrogate crude oil were used to optimize

instrument parameters initially and as needed throughout the study.

Quality assurance measures followed NOAA's MC252 Analytical Quality Assurance

Plan's method performance criteria (NOAA 2012). Prior to sample analysis, linearity of all

analytes within an appropriate concentration range (1 – 1000ng/mL) was verified via seven-point

matrix-matched and solvent calibration curves. In addition, a standard reference material (NIST

SRM 1974c, organics in mussel tissue) was analyzed at the beginning of the project to verify

accurate quantification of all analytes. A series of matrix spikes using the appropriate species

and tissue was performed to optimize extraction methods and assess precision. Procedural

blanks were extracted and analyzed with every batch, and ACN solvent blanks were analyzed in

between samples to monitor for background contamination. The post-extraction standard in each

sample was monitored for changes in instrument stability. Recoveries of surrogate standards in

sample extracts (LMW: 82 ± 12%; HMW: 78 ± 15%), SRM (82 ± 9%), and matrix spikes (84 ±

5%), procedural blanks, solvent blanks, and post-extraction standard monitoring all met

acceptable QA criteria established in NOAA (2012).

Analysis of Livers for Total Lipid

Total lipid in liver tissue was extracted using a modified Folch method (Matyash et al. 2008). A 200mg aliquot of homogenized liver was extracted in a two-series extraction, first using MTBE, and second using a mixture of MTBE/methanol/water (10/3/2.5 v/v/v). Extracts were evaporated to dryness and total lipid was determined gravimetrically and reported as % liver lipid (based on wet weight).

Statistical Analyses

All statistics were performed in MATLAB R2017a using the Fathom Toolbox for Matlab (Jones 2017). All hypothesis tests used permutation-based *p*-values (1000 iterations) assessed at $\alpha = 0.05$. Pearson's correlations or regressions were used to determine the concordance in variation between continuous data. A modified permutational multivariate analysis of variance (PERMANOVA) was used to assess the difference in mean between groups, allowing for accuracy of *p*-values when between-group dispersions were heterogenous (Anderson et al. 2017). If modified PERMANOVAs were significant, they were followed by a pair-wise modified PERMANOVA. Analysis of covariance (ANCOVA) was run to test the difference in the mean of specific variables that were found to vary by another continuous variable, such as collection year. A Chi-square test of independence was used to test the difference in sex ratio by year.

Fulton's condition factor (K) was calculated as $\frac{total\ body\ weight}{total\ length^3}$ x 100, where weight is expressed in kg and length in cm. Hepatosomatic index (HSI) was calculated as

$$\frac{liver\ weight\ (kg)}{total\ body\ weight\ (kg)}$$ x 100. Percent change was calculated between the first and last year

sampled for each variable in the time series.

Results

Biometric and Liver Lipid Data

A total of 286 Tilefish were sampled at nine repeat stations via 38 longline sets during

2012 to 2015, and 2017 (Table 2.1). The sex ratio of sampled fish was dominated by females

and did not significantly change over time (Table 2.1, $X^2 = 28.9$, $p = 0.162$). There was no

significant difference in mean total length (TL) of Tilefish over time for all stations combined (F

$= 1.61$, $p = 0.164$), nor at any individual station except for 7-150 (Table 2.1, $F = 4.83$, $p = 0.006$).

There was a significant decrease in mean total body weight of Tilefish over time for all stations

combined (Table 2.1, $F = 2.87$, $p = 0.023$), and for two out of nine individual stations (Table

2.1): 7-150 ($F = 4.99$, $p = 0.004$), and 8-100 ($F = 3.14$, $p = 0.032$). At station 7-150 the decrease

in total body weight was significantly correlated with the decrease in TL over time ($r = 0.935$, p

$= 0.001$).

A significant 22% decrease in the mean of Fulton's condition factor (K) occurred over

the study period for all stations combined (Figure 2.2, $F = 29.6$, $p = 0.001$), and for six out of

nine individual stations (Figure 2.3): 7-150 (↓17%, $F = 3.45$, $p = 0.018$), 8-100 (↓28%, $F = 13.1$,

$p = 0.001$), 9-150 (↓21%, $F = 8.77$, $p = 0.001$), 14-60 (↓27%, $F = 12.9$, $p = 0.001$), 11-150

(↓10%, $F = 3.34$, $p = 0.039$), and MC04 (↓26%, $F = 28.9$, $p = 0.001$). Mean K for all stations

combined was 1.26 ± 0.165 in 2012 and 0.986 ± 0.089 in 2017.

Mean K varied significantly by sex ($F = 5.57$, $p = 0.007$) with males having higher K than females ($t = 2.78$, $p = 0.012$), and unknowns ($t = 3.25$, $p = 0.003$). There was no significant difference in mean K between females and unknowns ($F = 1.35$, $p = 0.197$). Mean K was 1.17 ± 0.163 for males, 1.10 ± 0.175 for females, and 1.06 ± 0.173 for unknowns. Since mean K was found to vary over time, an ANCOVA was also used to evaluate differences in mean K by sex, with year as a covariate. Both sex and year effects on K were significant, with year having a larger impact as seen in the F-ratio which is ~22x higher ($F_{Sex*Year} = 0.615$, $p_{Sex*Year} = 0.526$; $F_{Sex} = 4.75$, $p_{Sex} = 0.010$; $F_{Year} = 104$, $p_{Year} = 0.001$). For males, mean K varied significantly between years (Figure 2.2, $F = 10.7$, $p = 0.001$), with year 2012 removed since n = 1 for males in 2012. Male K increased 2013 to 2014, followed by a significant decrease in 2015, followed by a significant increase in 2017. For females, K significantly decreased 22% from 2012 to 2017 (Figure 2.2, $F = 23.8$, $p = 0.001$), from a mean of 1.27 ± 0.181 in 2012 to 0.981 ± 0.076 in 2017. Since the sex ratio of sampled fish was dominated by females, the overall trend in K is mirrored in the trend in females alone. There was no significant change in mean K over time for Tilefish of unknown sex (Figure 2.2, $F = 2.11$, $p = 0.121$), however, the dominant trend was a decrease over time, which was not detected by statistical testing due to low sample size.

There was a significant change in mean hepatosomatic index (HSI) over time for all stations combined ($F = 17.8$, $p = 0.001$), and at six out of nine individual stations (Figure B1): 7-150 ($F = 15.5$, $p = 0.001$), 8-100 ($F = 3.80$, $p = 0.01$), 9-150 ($F = 4.55$, $p = 0.01$), 14-60 ($F = 2.80$, $p = 0.03$), 14-100 ($F = 4.94$, $p = 0.026$), and MC04 ($F = 26.0$, $p = 0.001$). For all stations combined, mean HSI was significantly higher in 2014 (1.86 ± 1.02) than all other years (1.03 ± 0.51), which were statistically similar. For the individual stations with significant differences in

mean HSI, the predominant pattern over time was similar to the region as a whole, with HSI typically highest in 2014 and lower in other years (Figure B1).

There was a significant 53% decrease in mean % liver lipid over time for all stations combined (Figure 2.4, $F = 17.4$, $p = 0.001$), and at five out of nine individual stations: 7-150 ($\downarrow$6%, $F = 23.2$, $p = 0.001$), 8-100 ($\downarrow$65%, $F = 14.3$, $p = 0.001$), 9-150 ($\downarrow$56%, $F = 12.6$, $p = 0.001$), 14-60 ($\downarrow$15%, $F = 43.2$, $p = 0.001$), and 11-150 ($\downarrow$2%, $F = 2.97$, $p = 0.036$). For all stations combined, the mean % liver lipid was $12.8 \pm 4.9\%$ in 2012 and $6.0 \pm 2.9\%$ in 2017. There was no significant difference in mean % liver lipid by sex with year as a covariate ($F_{Sex*Year} = 1.31$, $p_{Sex*Year} = 0.334$; $F_{Sex} = 1.79$, $p_{Sex} = 0.182$; $F_{Year} = 24.3$, $p_{Year} = 0.001$). Percent liver lipid was significantly correlated with K ($r = 0.2967$, $p = 0.001$).

Relationship Between Total Lipid and PAHs in Liver Tissue

There was no relationship between the % liver lipid and liver $TPAH_{46}$ concentration ($R^2 = 0.009$, $p = 0.266$). Regressions were insignificant for all stations combined and individually. Without a direct relationship between % liver lipid and liver $TPAH_{46}$ concentration, $TPAH_{46}$ concentrations were thus not lipid-normalized for data analysis (Hebert and Keenleyside 1995).

PAHs and Alkylated Homologs in Liver Tissue

A total of 230 Tilefish livers were analyzed for PAHs and alkylated homologs (Table 2.1). For all stations combined, there was no significant change in mean liver $TPAH_{46}$ concentration over the study period (Figure 2.5, $F = 0.351$, $p = 0.876$). Mean concentration for

all stations and all years combined was 956 ± 773 ng/g w.w., ranging from 288 to 8110 ng/g w.w.. For individual stations, only one station (14-60) had a significant change in liver $TPAH_{46}$ concentration over the study period ($F = 4.60$, $p = 0.004$), which was a significant increase 2012 to 2013, and a decline until 2017.

The composition of the 46 PAHs and alkylated homologs measured in liver tissue did not change over the study period ($F = 1.04$, $p = 0.396$). Liver PAH profiles were consistently dominated by LMW PAHs and homologs, which constituted >99% of the $TPAH_{46}$ concentration. The mean sum of LMW PAHs in liver tissue was 953 ± 773 ng/g w.w., while mean sum of HMW PAHs in liver tissue was 4.49 ± 8.24 ng/g w.w.. It was common that all HMW PAHs identified were less than the method detection limit (MDL; 1 ng/g). Analytes identified at <MDL were reported at ½ MDL. Therefore, frequently the total HMW PAH concentration in liver tissue was solely comprised of analytes identified at <MDL, and quantities should thus be interpreted with caution.

There was a significant difference in mean liver $TPAH_{46}$ concentration by sex ($F = 3.46$, $p = 0.044$), with individuals of unknown sex having significantly lower concentrations compared to males ($t = 2.38$, $p = 0.023$), and females ($t = 2.71$, $p = 0.007$). Mean liver $TPAH_{46}$ concentrations were not different between males and females ($t = 0.017$, $p = 0.992$). The mean liver $TPAH_{46}$ concentration was 739 ± 417 ng/g w.w. for unknown, 998 ± 534 ng/g w.w. for male, and 1000 ± 884 ng/g w.w. for female Tilefish. Liver $TPAH_{46}$ concentrations did not vary significantly with TL ($r = 0.100$, $p = 0.064$). However, mean TL did vary by sex ($F = 31.8$, $p = 0.001$) with males being significantly larger than females ($t = 6.29$, $p = 0.001$), and both males ($t = 7.75$, $p = 0.001$), and females ($t = 3.35$, $p = 0.001$) being significantly larger than unknowns. Mean TL was 56.9cm for unknowns, 63.5cm for females, and 77.0cm for males. An ANCOVA

with TL as the covariate could not assess the relationship between sex and mean liver $TPAH_{46}$

concentration, since the relationship between $TPAH_{46}$ and TL was not homogenous by year

($F_{Sex*TL} = 3.47$, $p_{Sex*TL} = 0.005$).

Biliary PAH Metabolites

A total of 256 Tilefish bile samples were analyzed for PAH metabolites (Table 2.1).

There was a significant increase in mean total biliary PAH metabolite equivalents (NPH + BaP)

over time for all stations combined (Figure 2.6, ↑178%, $F = 21.8$, $p = 0.001$), and at six out of

nine individual stations (Figure 2.7): 7-150 (↑166%, $F = 2.92$, $p = 0.043$), 8-100 (↑153%, $F =$

4.33, $p = 0.009$), 9-150 (↑155%, $F = 3.75$, $p = 0.009$), 11-150 (↑235%, $F = 5.45$, $p = 0.018$), 14-

60 (↑317%, $F = 7.65$, $p = 0.001$), and 14-100 (↑181%, $F = 7.34$, $p = 0.001$). The three stations

(9-80, MC04 and GP03) that did not have a significant increase in total biliary PAH metabolite

equivalents each had one year where $n = 1$ for bile samples (Table 2.1), therefore, the modified

PERMANOVA would not assess significance, although the dominant trend was an increase in

concentration over time (215%, 8.38%, 72.5% increases respectively). For all stations combined

mean total biliary PAH metabolite equivalents increased by a factor of 2.8, from 230 ± 68

µgFACs/g in 2012 to 640 ± 410 µgFACs/g in 2017 (Figure 2.6).

Concentrations of NPH metabolite equivalents were consistently three orders of

magnitude higher than concentrations of BaP metabolite equivalents, making total biliary PAH

metabolite equivalents dominated by NPH metabolite equivalents. Therefore, trends in biliary

NPH metabolite equivalents mirrored those of total biliary PAH metabolite equivalents. There

was no difference in mean biliary BaP metabolite equivalents over time for all stations combined

43

($F = 1.46$, $p = 0.207$). There was also no significant difference in mean total biliary PAH metabolite equivalents by sex, with year as a covariate ($F_{Sex*Year} = 1.87$, $p_{Sex*Year} = 0.168$; $F_{Sex} = 0.347$, $p_{Sex} = 0.706$; $F_{Year} = 71.1$, $p_{Year} = 0.001$).

Relationship Between PAH Exposure and Fish Condition

There was a significant negative correlation between K and total biliary PAH metabolite equivalents for all stations, all sexes, and all years combined (Figure 2.8, $r = -0.150$, $p = 0.021$), and at two out of nine individual stations: 8-100 (Figure 2.8, $r = -0.330$, $p = 0.033$), and 14-60 (Figure 2.8, $r = -0.273$, $p = 0.050$). The significant negative correlation between K and total biliary PAH metabolite equivalents occurred for females ($r = -0.166$, $p = 0.014$), but not males. The correlation between K and total biliary PAH metabolite equivalents was significant, but positive for males ($r = 0.311$, $p = 0.029$). The correlation was insignificant for Tilefish of unknown sex ($r = -0.195$, $p = 0.115$). There were no significant correlations between liver TPAH$_{46}$ concentrations and K for all data combined ($r = -0.032$, $p = 0.329$), males ($r = 0.060$, $p = 0.344$), females ($r = -0.054$, $p = 0.258$), or unknowns ($r = -0.1323$, $p = 0.202$).

Discussion

Tilefish were selected as a target species for this extended time series study due to their high levels of biliary PAH metabolites, a biomarker of exposure to PAHs, compared to other demersal fish species in the GoM, and their proximity to the *DWH*. Snyder et al. (2015) found Tilefish sampled in 2012 and 2013 had higher mean concentrations of biliary NPH metabolite equivalents compared to King Snake Eel and Red Snapper sampled in the same region, assorted

44

demersal fish sampled offshore of Texas in the early 1990's, and Atlantic Croaker (*Micropogonias undulatus*) sampled in Louisiana waters pre- and post-Hurricane *Katrina* (Hom et al. 2008; McDonald et al. 1996). Since the study was published, we sampled an additional 186 Tilefish and extended the time series by three years (2014, 2015 and 2017). Since 2012 there has been a significant 178% increase in mean total biliary PAH metabolite equivalents (dominated by NPH metabolite equivalents) from 230 ± 68 µgFACs/g to 640 ± 410 µgFACs/g in 2017.

Tilefish sampled in 2017 now have the highest levels of biliary NPH metabolite equivalents measured in comparable studies (Snyder et al. 2015). Contrasted against additional biliary PAH metabolite data from twelve GoM demersal fishes sampled in the same region in the same time window (2012-2015) Tilefish have higher mean total biliary PAH metabolite equivalents compared to all species, which ranged from ~10 to 180 µgFACs/g bile (Pulster, Gracia, Snyder, Romero, et al. 2020). Other demersal fishes sampled from the northern GoM post-*DWH*, Gulf Hake (*Urophycis cirrata*), Snowy Grouper (*Epinephelus niveatus*), Yellowedge Grouper (*Hyporthodus flavolimbatus*), Red Snapper, and Red Grouper (*Epinephelus morio*), also had increased total biliary PAH metabolites over time (Pulster, Gracia, Snyder, Romero, et al. 2020).

The exceptionally high exposure of Tilefish to PAHs may be attributed to their burrow-forming lifestyle and limited movement. Tilefish excavate large vertical funnel-shaped burrows into silt-clay sediments, which they use for protection over their lifetime. Direct observations of Tilefish have noted frequent maintenance of burrows, with their mouths and bodies, in order to keep burrows from filling in (Grimes, Able, and Jones 1986). The hypothesis for high PAH exposure in Tilefish is that maintaining their burrows exposes them to sedimented pollution at

significantly higher levels than other demersal fishes. Tilefish diet consists primarily of benthic organisms living amongst the burrows, which also perform secondary burrowing. Benthic invertebrate prey, especially infaunal or burrowing organisms, are prone to high tissue pollutant accumulation due to their limited ability to metabolize these compounds and are likely another source of high exposure for Tilefish.

Following *DWH*, numerous studies described marine oil snow sedimentation and flocculent accumulation (MOSSFA) as a mechanism for transferring oil and its residues from the sea surface and the water column to the seafloor (Beyer et al. 2016). Over time, deposited oil residues may become resuspended by physical oceanographic processes (e.g. bottom currents, internal waves, and storms) and redistributed to new locations via transport of the benthic nepheloid layer downslope to be redeposited onto the sediments at other locations (Ziervogel et al. 2016; Diercks et al. 2018). This resuspension and secondary deposition is likely a mechanism of impact on benthic communities that were marginally affected by the initial MOSSFA or *DWH* event, possibly explaining why PAH exposure is increasing over time for Tilefish and other GoM demersal fishes. Resuspension events will result in the renewed bioavailability of oil residues that were previously sequestered in sediments to both Tilefish and their prey.

Other time series studies following *DWH* note varied patterns of PAH exposure over time in which re-suspension events are implicated. Cytochrome P4501A expression in Seaside Sparrows (*Ammodramus maritmus*) decreased post-*DWH*, but then abruptly increased in 2013 at sites that had, and had not been directly oiled by *DWH* (Perez-Umphrey et al. 2018). The authors concluded that weather, storms and hurricanes, such as 2012's *Hurricane Isaac*, influenced spatial and temporal exposure to oil in their post-*DWH* time series by resuspending and redistributing contaminated sediments. Gulf Menhaden (*Brevoortia patronus*) exhibited

increases in BaP concentrations 2012 to 2013, which Olson, Meyer, and Portier (2016) concluded was not due to a new source, but to re-suspension of *DWH* oil. In addition, blood PAH concentrations in Common Loons (*Gavia immer*) increased significantly post-*DWH* to a maximum in 2013, which was also hypothesized to be related to sediment resuspension following *Issac* (Paruk et al. 2016).

In contrast to biliary PAH metabolites, mean concentrations of liver TPAH$_{46}$ in Tilefish did not vary significantly over the study period. Liver TPAH$_{46}$ concentration did not vary with TL or % liver lipid but did vary by fish sex. Tilefish gonads were difficult to sex macroscopically in the field, in part due to their protogynous hermaphrodite reproductive strategy, and due to sampling of the fish post-spawning season, therefore, sex data should be interpreted cautiously. Tilefish of unknown sex, which were also significantly smaller in TL, had lower liver TPAH$_{46}$ concentrations compared to those identified as males or females. Although the relationship between Tilefish TL and liver TPAH$_{46}$ was not significant, it is possible that the smaller Tilefish, more commonly identified as unknown sex, consume different prey items, possibly leading to differences in exposure. Limited information on Tilefish food habits indicate that juveniles consume more echinoderms and mollusks as compared to larger individuals (Freeman and Turner 1977). Burrowing behavior of smaller Tilefish may also be different, since juveniles have been observed in simple vertical shafts, instead of the larger funnel-shaped burrows (Able et al. 1982).

Compared to other demersal fishes sampled in the same northern GoM region and time period, Tilefish have comparable concentrations of liver TPAH$_{46}$ (288-8110 ng/g w.w.). Liver TPAH$_{46}$ concentrations ranged from 7.7 to 407 ng/g w.w. for Hakes (*Urophycis* sp.), and 67.6 to 17,300 ng/g w.w. for Groupers (*Epinephelus* sp.) (Pulster, Gracia, Snyder, Romero, et al. 2020).

Although the data were highly variable year-to-year, these other demersal fishes exhibited a general increasing trend in liver $TPAH_{46}$ concentrations over time, in contrast to stable concentrations as exhibited in Tilefish.

The significant increase in biliary PAH metabolite equivalents over time, concurrent with no change in $TPAH_{46}$ concentrations in liver tissue, suggests that exposure of Tilefish to PAHs is increasing; however, metabolism continues to efficiently eliminate compounds, thus limiting accumulation in liver tissue. After exposure, liver enzymes (e.g. cytochrome P450) metabolize PAHs to more water-soluble metabolites for elimination via the bile. If the level of exposure to PAHs overwhelms enzymatic capacity to metabolize and eliminate, the compounds will accumulate in the liver and other lipid-rich extrahepatic tissues (Meador et al. 1995). The lack of a clear increasing trend in $TPAH_{46}$ concentration in liver tissue implies that Tilefish have heretofore been able to efficiently metabolize and eliminate PAHs. However, although Tilefish appear to be keeping up with this metabolic demand, the energetic cost to the individual may result in other negative health impacts, perhaps as manifested in decreased condition or other health indices (Figures 2.2-2.4).

Fulton's condition factor (K) is length-weight based metric commonly used as a proxy for fish health at individual and population-levels, with higher values (heavier fish at a specific length) signifying more robust fish (Blackwell, Brown, and Willis 2000). Higher K values thus imply favorable environmental conditions, including suitable water quality, habitat, and prey availability. Condition factor can be used as a measure of a fish's energy reserves, and a basic biomarker of effect of contaminants (Chellappa et al. 1995; Lambert and Dutil 1997; van der Oost, Beyer, and Vermeulen 2003).

Fish condition may vary by sex due to differences in sex-specific physiology and energy allocation (Blackwell, Brown, and Willis 2000). For Tilefish, K varied by sex, with males having significantly higher mean K values compared to females, and fish of unknown sex. This result is logical in post-spawning fishes, since females will lose greater mass from spawning due to both higher biomass of eggs compared to sperm, and the substantially higher energetic burden of reproduction on females compared to males (Blackwell, Brown, and Willis 2000; Hayward and Gillooly 2011). The energetic cost of gamete biomass production is estimated to be roughly 3.5 orders of magnitude higher in females as compared to males (300% vs. 0.1% of energy for basal metabolism used for to gamete biomass production) (Hayward and Gillooly 2011).

For all individuals combined, there was a statistically significant 22% decrease in K and a 38% decrease in total body weight in GoM Tilefish between 2012 and 2017 (Figure 2.2, Table 2.1). With no significant change in TL over time, the decrease in K is due to a decrease in fish total weight at a given length. A log-transformed regression of TL vs. total weight by year calculated that an average-sized Tilefish caught on our survey (TL = 65 cm) weighs 21% less in 2017 (2.709 kg) than in 2012 (3.427 kg). Condition varied significantly over time for both male and female Tilefish (Figure 2.2). The mean K for males exhibited an initial increase 2013 to 2014, decreased 2014 to 2015, and rebounded to 2013 values in 2017. In contrast, female Tilefish exhibited a strong decline (22%) in K over the entire study period. Variation in K over time may be related to reproductive state, season, water temperature, nutritional status/prey availability and or poor environmental conditions, such as exposure to contaminants (Blackwell, Brown, and Willis 2000; Ratz and Lloret 2003).

Although reproductive state in these fish was not specifically assessed, all fish were sampled in late July to August. The spawning season for Tilefish in this region is generally

January to June, based on histological determination of spawning-capable females, therefore, all fish caught in this study are likely to be in post-spawning state (Lombardi-Carlson 2012). Female fish typically exhibit a drop in condition immediately post-spawning, with condition increasing steadily thereafter (Blackwell, Brown, and Willis 2000). Thus, condition should be recovering by our sampling dates in late July to August. As our sampling periods were in a tight window it is unlikely that the significant decrease in K over the study period is due to sampling the spawning cycle at different times.

Average bottom temperature at each station, as recorded by sensors on each longline set, was not associated with mean K ($R^2 = 0.032$, $p = 0.306$). Bottom temperature at occupied stations remained relatively stable over the time series, with a mean temperature of 12.4 ± 1.86°C.

Nutritional status of the sampled fish was not evaluated and is unknown. However, % liver lipid (measured in this study) is generally indicative of nutrition status and energy reserves. Percent liver lipid and K both declined significantly 2012 to 2017 (53% and 22% respectively). Condition factor and % liver lipid were significantly correlated ($r = 0.297$, $p = 0.001$). The significant and concordant decreases over time in K and % liver lipid indicates a simultaneous decrease in overall condition and energy reserves of theses GoM Tilefish.

The 22% declines in K were significantly negatively correlated with total biliary PAH metabolite concentrations for all individuals combined and females (Figure 2.8). The increasing and chronic exposure to PAHs and the energetic burden of their biotransformation are likely related to the significant decrease in condition of Tilefish, specifically adult females. Numerous studies reviewed in Collier et al. (2014) found reduced K (9-21%) in fishes exposed to PAHs and other environmental contaminants in both field and lab-based studies. Conversely, a variety of

other studies reviewed in van der Oost, Beyer, and Vermeulen (2003) found no significant change in K with exposure to contaminants, however, the majority of these studies were short-duration exposure studies, with either single injections, or short exposure periods (days) compared to our study over six years of adult fish chronically exposed to PAHs. For adult fish, it's expected that a significant change in K would occur over a time period longer than the standard time of laboratory exposure experiments.

Multiple studies have shown a significant energetic cost of biotransformation of xenobiotics, although the physiological link between xenobiotic exposure and K is currently unknown. Exposure to and detoxification of PAHs is associated with increased metabolic demand in fish, with studies concluding the increased demand was due to the associated significant energetic costs of xenobiotic metabolism (Bains and Kennedy 2004; Alves dos Santos et al. 2006; Klinger et al. 2015). Bains and Kennedy (2004) note the energetic cost of PAH metabolism may be even higher than that of other xenobiotics, since most PAHs undergo both phase I and phase II metabolism, which require separate enzyme molecules and reactions. Quantitative research on the cost of xenobiotic metabolism has more frequently been performed with terrestrial organisms and plant secondary metabolites, although, studies often fail to differentiate the direct cost of xenobiotic detoxification from the cost of toxicological impact of the xenobiotic, such as feeding inhibition or reduced digestive efficiency, which together limit total energy assimilation. The energetic costs to Ruffed Grouse (*Bonasa umbellus)* to detoxify plant secondary metabolites in quaking aspen tree buds was found to be 10 to 14% of metabolizable energy intake, which was enough to alter foraging behavior (Guglielmo, Karasov, and Jakubas 1996).

Previous studies and our data indicate that xenobiotic metabolism, particularly PAHs, significantly increases energetic costs to fishes, which often results in decreased body condition and energy reserves. Energy that would otherwise be used for fitness (growth and reproduction) is likely being diverted to enzyme induction and function, and to repair cellular damage caused by xenobiotics. Studies have shown this reallocation of energy occurs within a hierarchy, where the costs of physiological maintenance are paid first, followed by those of growth and reproduction (Beyers et al. 1999).

It is likely that the declines in both condition factor and stored lipids occurring for GoM Tilefish chronically exposed to PAHs may impact reproductive capacity. Stored energy is required for quality gamete production. Female fish in lower condition generally have lower fecundity, lower egg quality, atresia of oocytes, lower larval quality and survivorship, may mature at a later age, and possibly even skip spawning (Hislop, Robb, and Gauld 1978; Demartini 1991; Solemdal et al. 1993; Koslow et al. 1995; Chambers and Waiwood 1996; Kjesbu et al. 1998; Marteinsdottir and Steinarsson 1998; Rideout, Burton, and Rose 2000; Morgan 2004). Reduced condition of Tilefish may also have implications at the population level. Fish stocks in poorer condition generally have slower growth, lower recruitment, and thus lower production, and natural mortality may be higher (Marshall and Frank 1999; Dutil and Lambert 2000; Ratz and Lloret 2003). An analysis of ten Atlantic Cod (*Gadus morhua*) stocks in the north Atlantic revealed that individuals in poorer condition had lower mean weight at age, lower recruitment potential at low spawning stock biomass (SSB), and were less likely to be able to sustain long-term fishery exploitation (Ratz and Lloret 2002). The weight of an average length Tilefish from our survey decreased 21% from 2012 (3.427kg) to 2017 (2.709kg). This

translates in lower interannual production of the mass of the population and lower overall egg production.

Conclusions

Our six-year of study of GoM Tilefish post-*DWH* indicated chronic and relatively high PAH exposure and associated negative health effects that may have serious consequences for long-term population viability. Exposure to LMW (often deemed "petrogenic") PAHs increased 2.8-fold from 2012 to 2017. Fulton's condition factor (K) of Tilefish, predominately adult females, declined by 22%. The decline in condition was correlated with the 178% increase in PAH exposure and the 53% decrease in % liver lipid over the study period. Tilefish appear to be efficiently metabolizing and eliminating PAHs due to lack of increase in hepatic PAH concentrations, however, the energetic cost of chronic PAH metabolism may be related to the decrease in condition and liver lipid reserves. Chronic pollution, particularly exposure to PAHs, is having ongoing effects on health indices in Tilefish, and ultimately, effects on fecundity, stock productivity, and fitness may occur. This time series confirms the need for continued monitoring of the health of GoM organisms chronically exposed to contaminants. Additional analyses on temporal and spatial variability in species-specific physiology (e.g. xenobiotic metabolism capability), nutritional status, and other baseline health indices will aid in interpretation of these studies and future evaluations of GoM fish health as it relates to chronic pollution.

Tables

Table 2.1. Sample collection and biometric data for Tilefish sampled 2012 to 2015, and 2017 in the northern Gulf of Mexico.

Sampling station	Collection year	n (fish sampled)	n (bile)	n (liver)	Total length (cm)[a]	Total weight (kg)[a]	Liver weight (g)[a]	Sex ratio (M:F:U)[b]
All stations	2012	27	25	24	68 ± 15	4.44 ± 2.7	43 ± 26	1:21:5
	2013	73	66	38	65 ± 13	3.71 ± 2.5	39 ± 20	20:33:17
	2014	62	55	45	62 ± 13	3.32 ± 2.2	60 ± 62	13:46:2
	2015	53	46	53	67 ± 15	3.56 ± 2.5	40 ± 59	6:35:11
	2017	71	64	70	62 ± 14	2.76 ± 2.1	25 ± 16	6:53:12
7-150	2012	6	6	5	76 ± 14	5.54 ± 2.2	54 ± 29	0:6:0
	2013	6	2	5	52 ± 14	1.46 ± 0.45	15 ± 4.8	6:6:0
	2014	12	10	10	59 ± 4	2.84 ± 2.7	82 ± 120	2:10:0
	2015	12	10	12	69 ± 13	3.69 ± 2.0	43 ± 19	3:8:1
	2017	12	12	11	58 ± 11	2.07 ± 1.0	25 ± 11	0:11:1
8-100	2012	3	3	2	54 ± 4	2.12 ± 0.57	45 ± 6.1	0:1:2
	2013	12	12	7	65 ± 13	3.49 ± 1.8	33 ± 14	4:2:6
	2014	10	10	5	69 ± 15	4.51 ± 2.3	47 ± 42	5:5:0
	2015	10	10	10	64 ± 11	2.93 ± 1.5	21 ± 8.2	0:9:1
	2017	10	9	10	58 ± 13	2.09 ± 1.8	19 ± 12	1:9:0
9-150	2012	9	8	8	73 ± 16	5.69 ± 3.2	45 ± 27	0:7:2
	2013	11	11	5	66 ± 12	3.69 ± 1.9	35 ± 13	6:1:4
	2014	6	6	5	58 ± 12	2.49 ± 1.4	52 ± 13	1:5:0
	2015	9	9	9	71 ± 20	4.58 ± 4.1	71 ± 140	0:5:4
	2017	6	6	6	68 ± 7	3.25 ± 1.3	37 ± 13	0:4:2
14-60	2012	9	8	9	61 ± 11	3.23 ± 2.0	35 ± 29	1:7:1
	2013	17	17	5	67 ± 15	4.09 ± 3.0	50 ± 14	3:11:3
	2014	10	8	5	66 ± 10	3.67 ± 2.3	49 ± 34	1:8:1
	2015	10	7	10	57 ± 18	2.35 ± 2.2	24 ± 12	1:5:4
	2017	11	10	11	56 ± 17	2.17 ± 2.5	15 ± 17	0:5:6
9-80	2013	9	8	6	65 ± 14	3.80 ± 2.4	31 ± 12	2:5:1
	2014	4	3	4	62 ± 15	3.11 ± 2.6	35 ± 24	1:2:1
	2015	1	1	1	82	6.20	40	0:1:0
	2017	4	4	4	73 ± 14	4.57 ± 3.0	28 ± 15	2:2:0
11-150	2013	10	8	5	67 ± 11	3.99 ± 2.0	45 ± 15	2:8:0
	2014	5	4	5	67 ± 9	3.78 ± 1.6	62 ± 52	1:4:0
	2015	4	4	4	68 ± 11	3.65 ± 1.5	35 ± 21	0:4:0
	2017	10	9	10	66 ± 15	3.69 ± 2.9	31 ± 20	2:8:0
14-100	2013	8	8	5	70 ± 17	4.60 ± 3.8	67 ± 22	3:0:3
	2014	6	5	5	53 ± 14	1.79 ± 1.2	32 ± 19	1:5:0
	2015	2	2	2	60 ± 3	2.03 ± 0.14	24 ± 2.8	0:1:1
	2017	8	5	8	68 ± 12	3.22 ± 2.1	24 ± 13	0:5:3
GP03	2014	1	1	1	60	2.93	34	0:1:0
	2015	2	2	2	81 ± 16	5.7 ± 3.3	60 ± 31	0:2:0
	2017	2	2	2	54 ± 0	1.56 ± 0.11	13 ± 1.4	1:1:0
MC04	2014	8	8	5	65 ± 9	3.77 ± 2.1	86 ± 41	1:7:0
	2015	3	1	3	79 ± 15	6.0 ± 2.5	67 ± 26	2:1:0
	2017	8	7	8	64 ± 3	2.81 ± 2.0	30 ± 20	0:8:0

[a]Data are mean ± one standard deviation
[b]M = male; F = female; U = unknown

Figures
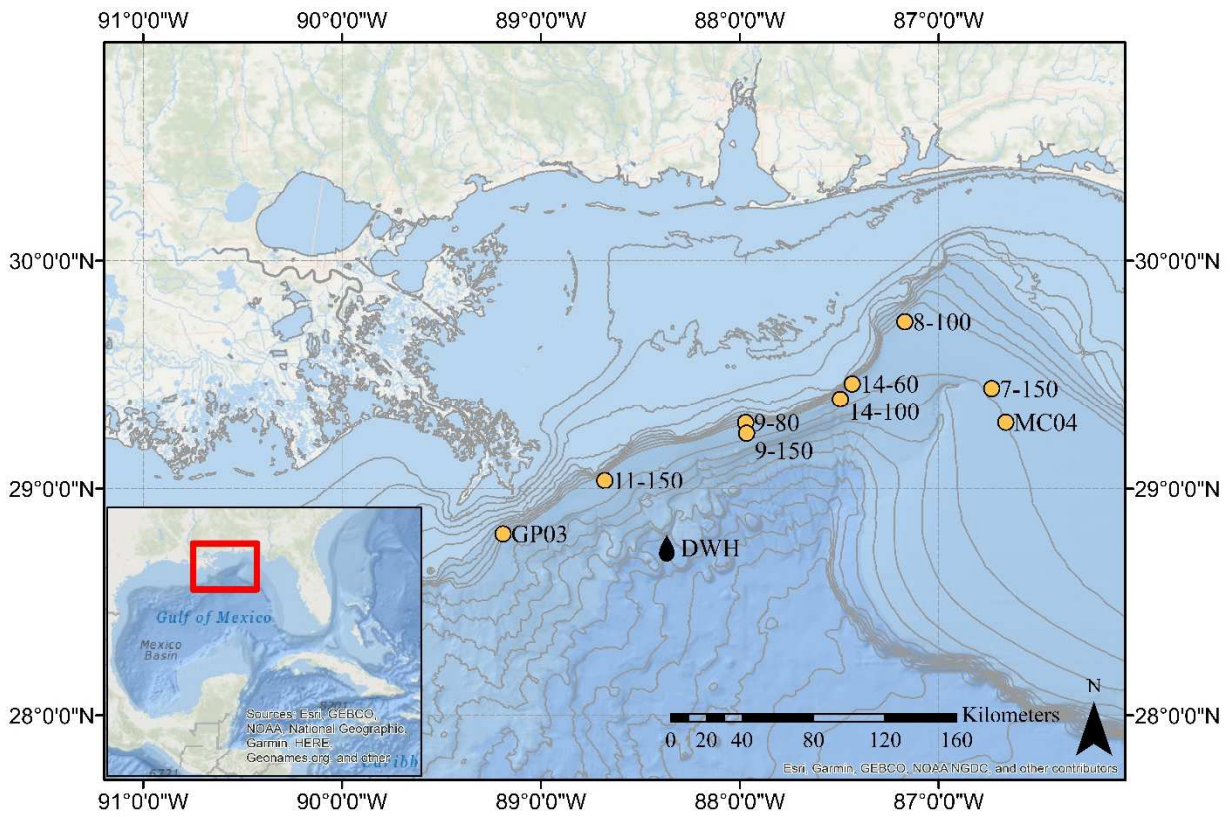
Figure 2.1. Location of the nine time series sampling stations in the northern Gulf of Mexico where Tilefish were sampled and *Deepwater Horizon* (DWH) blowout. Bathymetric isolines are in 20m increments.
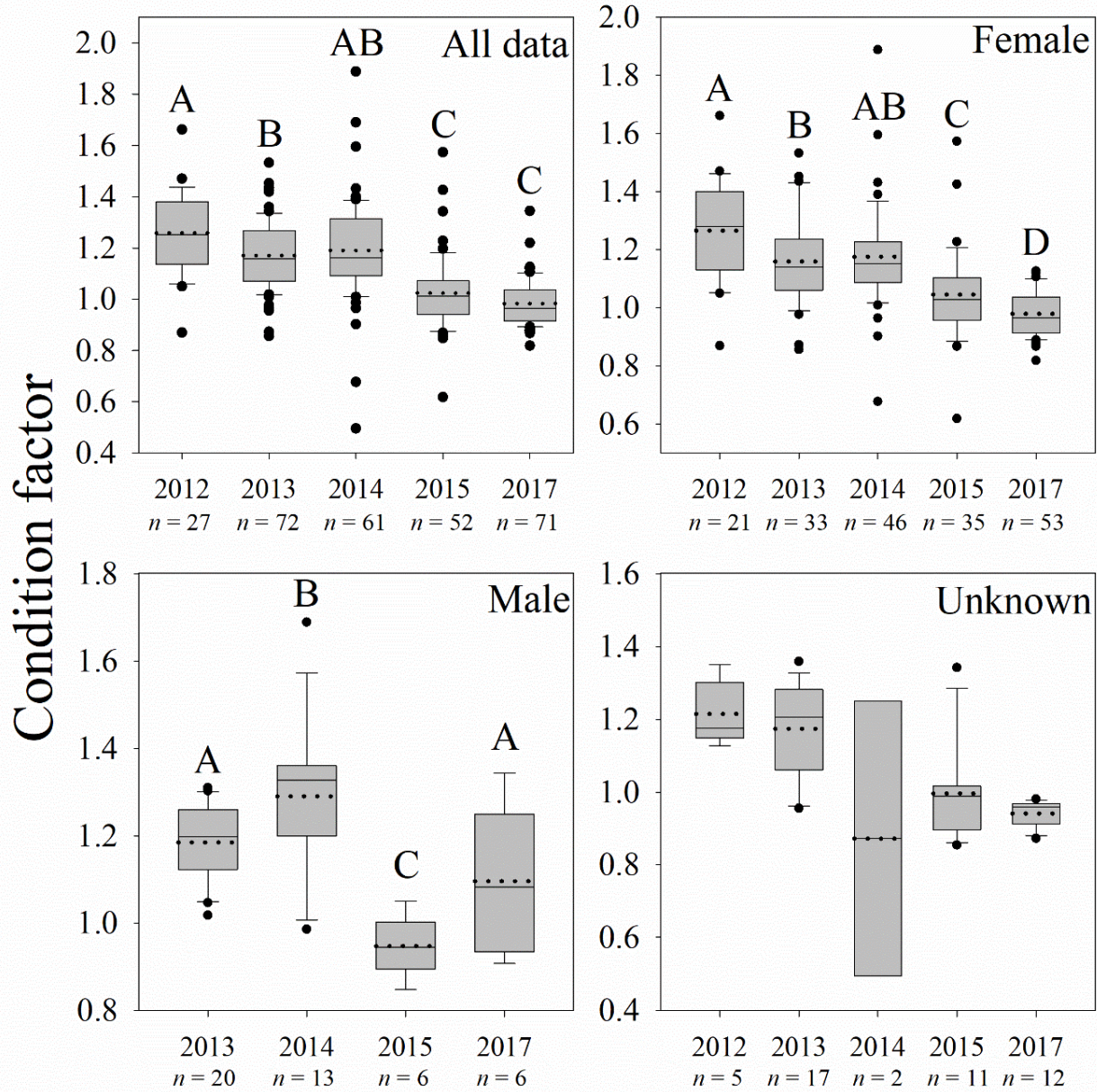
Figure 2.2. Fulton's condition factor (K) for Tilefish sampled 2012 to 2015, and 2017 in the northern Gulf of Mexico. Data are combined for all stations and sexes (top left), then by sex (female, male and unknown sex). Sample size (n) noted by year. Letters (ABC) denote significantly different years. Solid line = median; dotted line = mean.
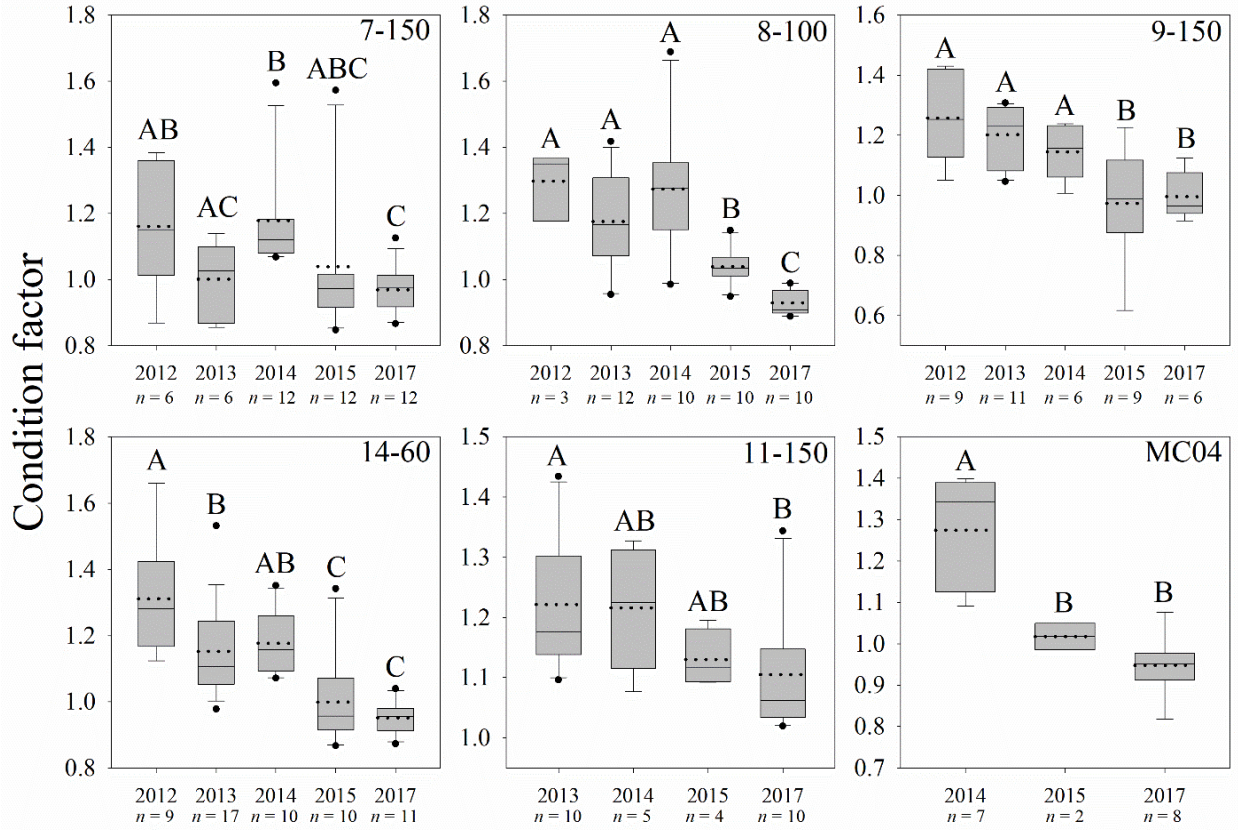
Figure 2.3. Fulton's condition factor (K) over time for Tilefish sampled 2012 to 2015, and 2017 at individual stations (station number designated on plot) in the northern Gulf of Mexico. Sample size (n) noted by year. Letters (ABC) denote significantly different years. Solid line = median; dotted line = mean.
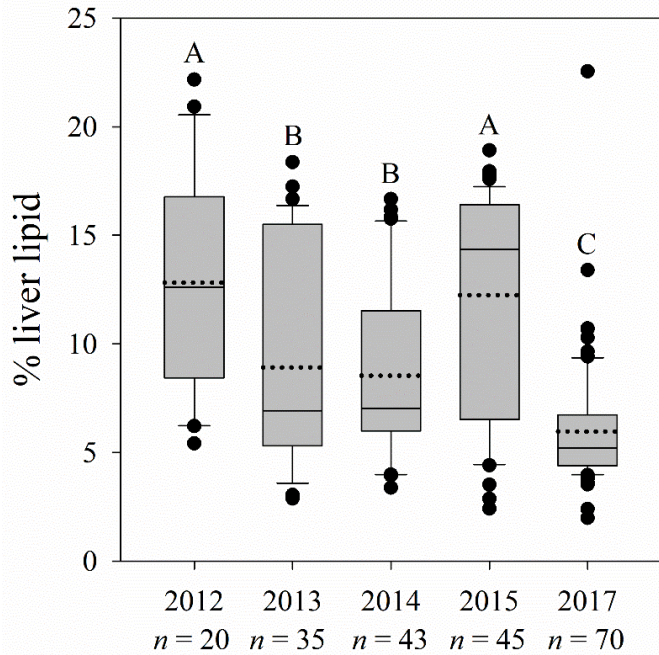
Figure 2.4. Percent liver lipid over time for Tilefish sampled 2012 to 2015, and 2017 in the northern Gulf of Mexico. Data are combined for all stations. Sample size (n) noted by year. Letters (ABC) denote significantly different years. Solid line = median; dotted line = mean.
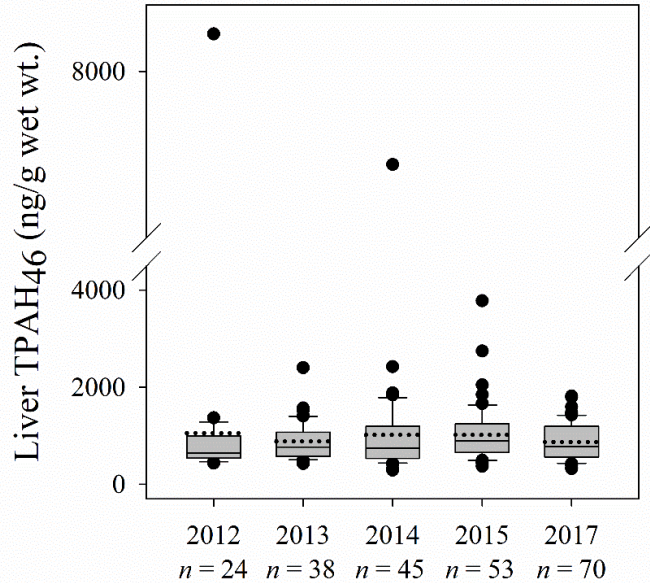
Figure 2.5. Total liver PAH concentration (TPAH$_{46}$) for Tilefish sampled 2012 to 2015, and 2017 in the northern Gulf of Mexico. Data are combined for all stations. Sample size (n) noted by year. Solid line = median; dotted line = mean.
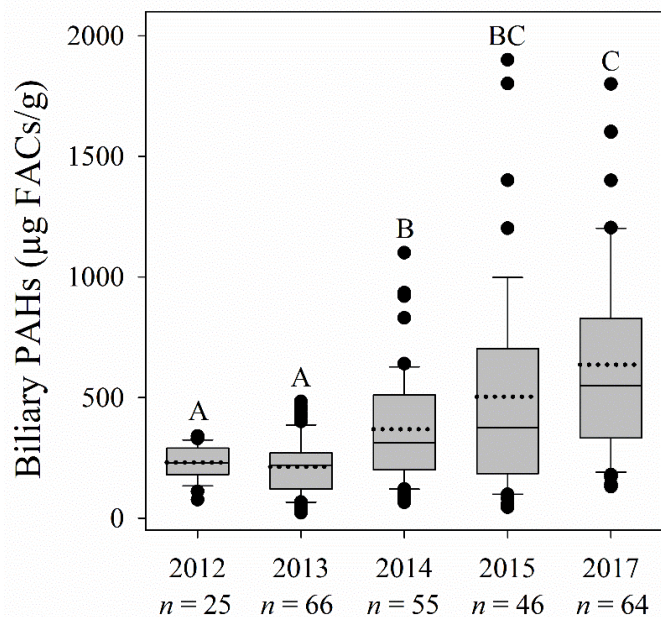
Figure 2.6. Total biliary PAH metabolite equivalents for Tilefish sampled 2012 to 2015, and 2017 in the northern Gulf of Mexico. Data are combined for all stations. Sample size (n) noted by year. Letters (ABC) denote significantly different years. Solid line = median; dotted line = mean.
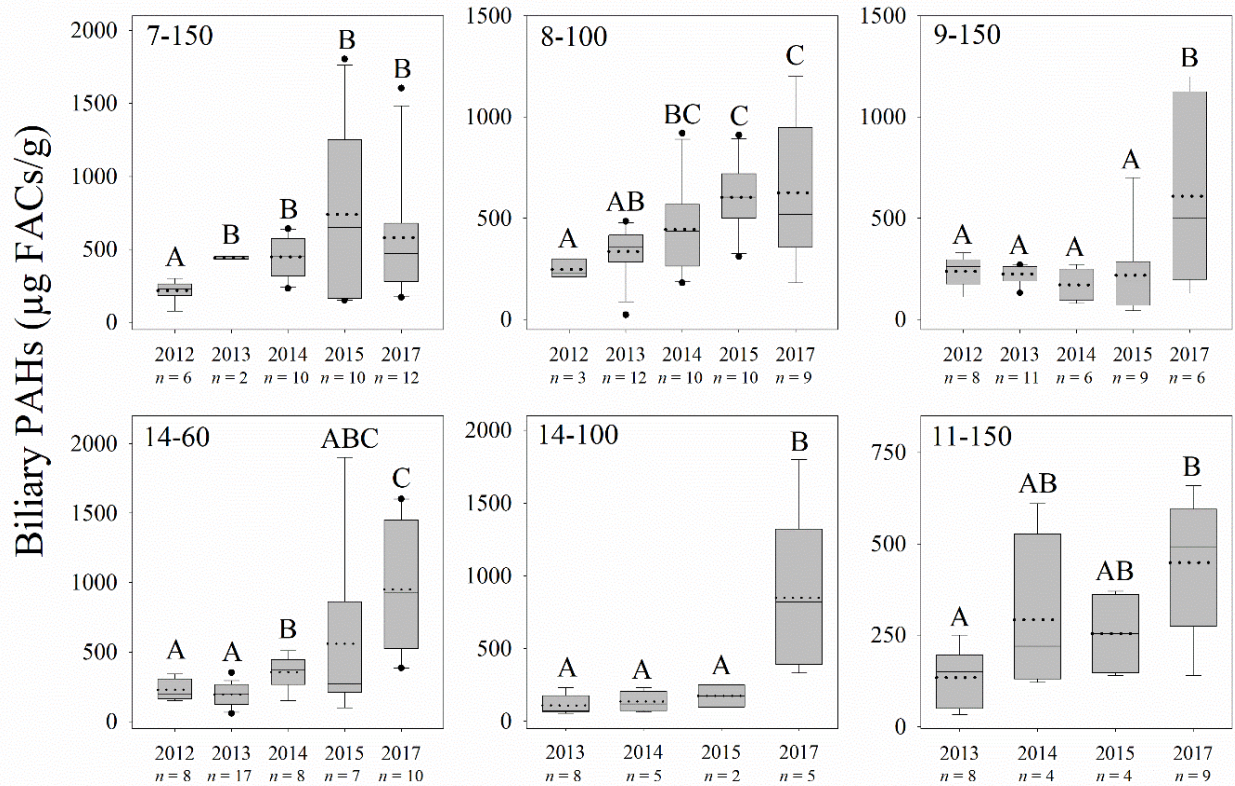
Figure 2.7. Total biliary PAH metabolite equivalents over time for Tilefish sampled 2012 to 2015, and 2017 at individual stations (station number designated on plot) in the northern Gulf of Mexico. Sample size (n) noted by year. Letters (ABC) denote significantly different years. Solid line = median; dotted line = mean.
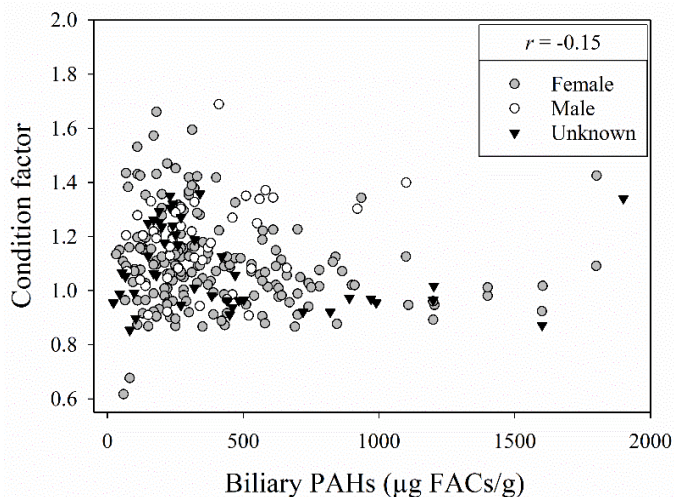
Figure 2.8. Fulton's condition factor (K) vs. total biliary PAH metabolite equivalents for Tilefish sampled 2012 to 2015, and 2017 in the northern Gulf of Mexico. Data are combined for all years and separated by sex.

References

Able, K. W., C. B. Grimes, R. A. Cooper, and J. R. Uzmann. 1982. 'Burrow construction and behavior of Tilefish, Lopholatilus chamaeleonticeps, in Hudson submarine canyon', *Environmental Biology of Fishes*, 7: 199-205.

Alves dos Santos, T. D., P. Van Ngan, M. J. D. Campos Rocha Passos, and V. Gomes. 2006. 'Effects of naphthalene on metabolic rate and ammonia excretion of juvenile Florida pompano, Trachinotus carolinus', *Journal of Experimental Marine Biology and Ecology*, 335: 82-90.

Anderson, M. J., D. C. I. Walsh, K. R. Clarke, R. N. Gorley, and E. Guerra-Castro. 2017. 'Some solutions to the multivariate Behrens-Fisher problem for dissimilarity-based analyses', *Australian & New Zealand Journal of Statistics*, 59: 57-79.

Bains, O. S., and C. J. Kennedy. 2004. 'Energetic costs of pyrene metabolism in isolated hepatocytes of rainbow trout, Oncorhynchus mykiss', *Aquatic Toxicology*, 67: 217-26.

Beyer, J., G. Jonsson, C. Porte, M. M. Krahn, and F. Ariese. 2010. 'Analytical methods for determining metabolites of polycyclic aromatic hydrocarbon (PAH) pollutants in fish bile: A review', *Environmental Toxicology and Pharmacology*, 30: 224-44.

Beyer, J., H. C. Trannum, T. Bakke, P. V. Hodson, and T. K. Collier. 2016. 'Environmental effects of the Deepwater Horizon oil spill: A review', *Marine Pollution Bulletin*, 110: 28-51.

Beyers, D. W., J. A. Rice, W. H. Clements, and C. J. Henry. 1999. 'Estimating physiological cost of chemical exposure: integrating energetics and stress to quantify toxic effects in fish', *Canadian Journal of Fisheries and Aquatic Sciences*, 56: 814-22.

Blackwell, Brian G, Michael L Brown, and David W Willis. 2000. 'Relative weight (Wr) status and current use in fisheries assessment and management', *Reviews in Fisheries Science*, 8: 1-44.

Chambers, R. C., and K. G. Waiwood. 1996. 'Maternal and seasonal differences in egg sizes and spawning characteristics of captive Atlantic cod, Gadus morhua', *Canadian Journal of Fisheries and Aquatic Sciences*, 53: 1986-2003.

Chellappa, S., F. A. Huntingford, R. H. C. Strang, and R. Y. Thomson. 1995. 'Condition factor and hepatosomatic index as estimates of energy status in male 3-Spined Stickleback', *Journal of Fish Biology*, 47: 775-87.

Collier, T. K., B. F. Anulacion, M. R. Arkoosh, J.P. Dietrich, J. P. Incardona, L. L. Johnson, G. M. Ylitalo, and M. S. Myers. 2014. 'Effects on fish of polycyclic aromatic hydrocarbons (PAHS) and naphthenic acid exposures.' in K. B. Tierney, A. P. Farrell and C.L. Brauner (eds.), *Fish Physiology: Organic Chemical Toxicology of Fishes* (Elsevier Inc.).

Demartini, E. E. 1991. 'Anuual variations in fecundity, egg size, and the gonadal and somatic conditions of Queenfish Seriphus polutus (Sciaenidae)', *Fishery Bulletin*, 89: 9-18.

Diercks, A. R., C. Dike, V. L. Asper, S. F. DiMarco, J. P. Chanton, and U. Passow. 2018. 'Scales of seafloor sediment resuspension in the northern Gulf of Mexico', *Elementa-Science of the Anthropocene*, 6.

Dutil, J. D., and Y. Lambert. 2000. 'Natural mortality from poor condition in Atlantic cod (Gadus morhua)', *Canadian Journal of Fisheries and Aquatic Sciences*, 57: 826-36.

Freeman, B.L., and S. C. Turner. 1977. "Biological and fisheries data on Tilefish, Lopholatilus chamaeleonticeps Goode and Bean." In, edited by U.S. National Marine Fisheries Service Northeast Fisheries Center Sand Hook Laboratory, 1-41. Highlands, New Jersey: NOAA.

Grimes, C. B., K. W. Able, and R. S. Jones. 1986. 'Tilefish, Lopholatilus chamaeleonticeps, habitat, behavior and community structure in Mid-Atlantic and Southern New England waters', *Environmental Biology of Fishes*, 15: 273-92.

Guglielmo, C. G., W. H. Karasov, and W. J. Jakubas. 1996. 'Nutritional costs of a plant secondary metabolite explain selective foraging by ruffed grouse', *Ecology*, 77: 1103-15.

Hayward, A., and J. F. Gillooly. 2011. 'The Cost of Sex: Quantifying Energetic Investment in Gamete Production by Males and Females', *Plos One*, 6.

Hebert, Craig E., and Karen A. Keenleyside. 1995. 'To normalize or not to normalize? Fat is the question', *Environmental Toxicology and Chemistry*, 14: 801-07.

Hislop, J. R. G., A. P. Robb, and J. A. Gauld. 1978. 'Observations on effects of feeding level on growth and reproduction in Haddock, Melenogrammus aeglefinus (L.) in captivity', *Journal of Fish Biology*, 13: 85-98.

Hom, T., T. K. Collier, M. M. Krahn, M. S. Strom, G. M. Ylitalo, W. B. Nilsson, R. N. Papunjpye, and U. Varanasi. 2008. 'Assessing seafood safety, in the aftermath of Hurricane Katrina.' in K. D. McLaughlin (ed.), *Mitigating Impacts of Natural Hazards on Fishery Ecosystems*.

Jones, D.L. 2017. 'Fathom Toolbox for MATLAB: software for multivariate ecological and oceanographic data analysis'. https://www.marine.usf.edu/research/matlab-resources/.

Jones, R. S., E. J. Gutherz, W. R. Nelson, and G. C. Matlock. 1989. 'Burrow utilization by yellowedge grouper, Epinephelus flavolimbatus, in the northwestern Gulf of Mexico', *Environmental Biology of Fishes*, 26: 277-84.

Kjesbu, O. S., P. R. Witthames, P. Solemdal, and M. G. Walker. 1998. 'Temporal variations in the fecundity of Arcto-Norwegian cod (Gadus morhua) in response to natural changes in food and temperature', *Journal of Sea Research*, 40: 303-21.

Klinger, D. H., J. J. Dale, B. E. Machado, J. P. Incardona, C. J. Farwell, and B. A. Block. 2015. 'Exposure to Deepwater Horizon weathered crude oil increases routine metabolic demand in Chub mackerel, Scomber japonicus', *Marine Pollution Bulletin*, 98: 259-66.

Koslow, J. A., J. Bell, P. Virtue, and D. C. Smith. 1995. 'Fecundity and its variability in orange roughy: Effects of population density, condition, egg size, and senescence', *Journal of Fish Biology*, 47: 1063-80.

Krahn, M. M., L. K. Moore, and W. D. Macleod. 1986. "Standard Analytical Procedures of the NOAA National Analytical Facility, 1986: Metabolites of Aromatic Compounds in Fish Bile." In, edited by U.S. Department of Commerce, 1-29.

Krahn, M. M., M. S. Myers, D. G. Burrows, and D. C. Malins. 1984. 'Determination of metabolites of xenobiotics in the bile of fish from polluted waterways', *Xenobiotica*, 14: 633-46.

Lambert, Y., and J. D. Dutil. 1997. 'Can simple condition indices be used to monitor and quantify seasonal changes in the energy reserves of cod (Gadus morhua)?', *Canadian Journal of Fisheries and Aquatic Sciences*, 54: 104-12.

Lombardi-Carlson, L.A. 2012. 'Life history, population dynamics, and fishery management of the Golden Tilefish, *Lopholatilus chamaeleonticeps*, from the Southest Atlantic and Gulf of Mexico', University of Florida.

Lucas, D., and L. Zhao. 2015. 'PAH analysis in salmon with enhanced matrix removal', *Agilent Tech Memo*.

Mackay, Donald, and Clayton D. McAuliffe. 1989. 'Fate of hydrocarbons discharged at sea', *Oil and Chemical Pollution*, 5: 1-20.

Marshall, C. T., and K. T. Frank. 1999. 'The effect of interannual variation in growth and condition on haddock recruitment', *Canadian Journal of Fisheries and Aquatic Sciences*, 56: 347-55.

Marteinsdottir, G., and A. Steinarsson. 1998. 'Maternal influence on the size and viability of Iceland cod Gadus morhua eggs and larvae', *Journal of Fish Biology*, 52: 1241-58.

Matyash, V., G. Liebisch, T. V. Kurzchalia, A. Shevchenko, and D. Schwudke. 2008. 'Lipid extraction by methyl-tert-butyl ether for high-throughput lipidomics', *Journal of Lipid Research*, 49: 1137-46.

McDonald, S. J., K. L. Willett, J. Thomsen, K. B. Beatty, K. Connor, T. R. Narasimhan, C. M. Erickson, and S. H. Safe. 1996. 'Sublethal detoxification responses to contaminant exposure associated with offshore production platforms', *Canadian Journal of Fisheries and Aquatic Sciences*, 53: 2606-17.

Meador, J. P., J. E. Stein, W. L. Reichert, and U. Varanasi. 1995. 'Bioaccumulation of Polycyclic Aromatic Hydrocarbons by Marine Organisms', *Reviews of Environmental Contamination and Toxicology <D>*, 143: 79-165.

Morgan, M. J. 2004. 'The relationship between fish condition and the probability of being mature in American plaice (Hippoglossoides platessoides)', *Ices Journal of Marine Science*, 61: 64-70.

Murawski, S. A., W. T. Hogarth, E. B. Peebles, and L. Barbeiri. 2014. 'Prevalence of External Skin Lesions and Polycyclic Aromatic Hydrocarbon Concentrations in Gulf of Mexico Fishes, Post-Deepwater Horizon', *Transactions of the American Fisheries Society*, 143: 1084-97.

Murawski, S. A., E. B. Peebles, A. Gracia, J. W. Tunnell, and M. Armenteros. 2018. 'Comparative Abundance, Species Composition, and Demographics of Continental Shelf Fish Assemblages throughout the Gulf of Mexico', *Marine and Coastal Fisheries*, 10: 325-46.

NOAA. 2012. "Analytical Quality Assurance Plan: Mississippi Canyon 252 (Deepwater Horizon) Natural Resource Damange Assessment V3.1." In, edited by U.S. Department of Commerce NOAA.

Olson, G. M., B. M. Meyer, and R. J. Portier. 2016. 'Assessment of the toxic potential of polycyclic aromatic hydrocarbons (PAHs) affecting Gulf menhaden (Brevoortia patronus) harvested from waters impacted by the BP Deepwater Horizon Spill', *Chemosphere*, 145: 322-28.

Paruk, James D., Evan M. Adams, Hannah Uher-Koch, Kristin A. Kovach, Darwin Long, Christopher Perkins, Nina Schoch, and David C. Evers. 2016. 'Polycyclic aromatic hydrocarbons in blood related to lower body mass in common loons', *Science of the Total Environment*, 565: 360-68.

Perez-Umphrey, Anna A., Christine M. Bergeon Burns, Philip C. Stouffer, Stefan Woltmann, and Sabrina S. Taylor. 2018. 'Polycyclic aromatic hydrocarbon exposure in seaside sparrows (Ammodramus maritimus) following the 2010 Deepwater Horizon oil spill', *Science of the Total Environment*, 630: 1086-94.

Pulster, E. L., A. Gracia, S. M. Snyder, I.C. Romero, B. Carr, G. Toro-Farmer, and S.A. Murawski. 2020. 'Polycyclic Aromatic Hydrocarbon Baselines in Gulf of Mexico Fishes.' in S.A. Murawski, C.H. Ainsworth, S. Gilbert, D.J. Hollander, C.B. Paris, M. Schluter and D. L. Wetzel (eds.), *Scenarios and responses to future deep oil spills: Fighting the next war* (Springer Nature Switzerland AG).

Ratz, H. J., and J. Lloret. 2003. 'Variation in fish condition between Atlantic cod (Gadus morhua) stocks, the effect on their productivity and management implications', *Fisheries Research*, 60: 369-80.

Reddy, Christopher M., J. Samuel Arey, Jeffrey S. Seewald, Sean P. Sylva, Karin L. Lemkau, Robert K. Nelson, Catherine A. Carmichael, Cameron P. McIntyre, Judith Fenwick, G. Todd Ventura, Benjamin A. S. Van Mooy, and Richard Camilli. 2012. 'Composition and fate of gas and oil released to the water column during the Deepwater Horizon oil spill', *Proceedings of the National Academy of Sciences*, 109: 20229-34.

Rideout, R. M., M. P. M. Burton, and G. A. Rose. 2000. 'Observations on mass atresia and skipped spawning in northern Atlantic cod, from Smith Sound, Newfoundland', *Journal of Fish Biology*, 57: 1429-40.

Romero, I. C., G. Toro-Farmer, A. R. Diercks, P. Schwing, F. Muller-Karger, S. Murawski, and D. J. Hollander. 2017. 'Large-scale deposition of weathered oil in the Gulf of Mexico following a deep-water oil spill', *Environmental Pollution*, 228: 179-89.

Snyder, S. M., E. L. Pulster, D. L. Wetzel, and S. A. Murawski. 2015. 'PAH Exposure in Gulf of Mexico Demersal Fishes, Post-Deepwater Horizon', *Environmental Science & Technology*, 49: 8786-95.

Solemdal, P., O. Bergh, G. Dahle, I. B. Falk-Petersen, H.J. Fyhn, O. Grahlnielsen, J.M. Haaland, O. S. Kjesbu, E. Kjorsvik, S. Loken, I. Opstad, Pederson T., A.B. Skiftesvik, and A. Thorsen. 1993. "Size of spawning Arcto-Norwegian cod (Gadus morhua L.) and the effects on their eggs and early larvae." In *ICES Statutory Meeting*.

United States of America v. BP Exploration & Production, Inc., et al. 2015. "Findings of fact and conclusions of law: Phase two trial. RE: Oil spill by the oil rig "Deepwater Horizon" in the Gulf of Mexico, on April 20, 2010." In, edited by U.S. District Court from the Eastern District of Louisiana.

van der Oost, R., J. Beyer, and N. P. E. Vermeulen. 2003. 'Fish bioaccumulation and biomarkers in environmental risk assessment: a review', *Environmental Toxicology and Pharmacology*, 13: 57-149.

Ziervogel, K., C. Dike, V. Asper, J. Montoya, J. Battles, N. D'Souza, U. Passow, A. Diercks, M. Esch, S. Joye, C. Dewald, and C. Arnosti. 2016. 'Enhanced particle fluxes and heterotrophic bacterial activities in Gulf of Mexico bottom waters following storm-induced sediment resuspension', *Deep-Sea Research Part Ii-Topical Studies in Oceanography*, 129: 77-88.

Chapter 3

Spatial Contrasts in Hepatic and Biliary PAHs in Tilefish Throughout the Gulf of Mexico, with Comparison to the Northwest Atlantic

Note to Reader

Portions of this chapter have been previously published in Snyder, S.M., Pulster, E.L., Murawski S., 2020. Spatial contrasts in hepatic and biliary PAHs in Tilefish (*Lopholatilus chamaeleonticeps*) throughout the Gulf of Mexico, with comparison to the Northwest Atlantic. Environmental Pollution 2588, 113775, and have been reproduced with permission from Elsevier Ltd. under the terms of the Creative Commons Attribution Non-Commercial No-Derivatives License CC BY-NC-ND and permits non-commercial use provided the original work is properly cited.

Introduction

The Gulf of Mexico (GoM) is the ninth largest and one of the most economically and ecologically important semi-enclosed seas in the world (Ward and Tunnel 2017). The natural resources in this region support coastal and ocean economies worth billions of dollars in total economic productivity annually, primarily from oil and gas revenues, commercial and recreational fisheries, shipping, and tourism (Shepard et al. 2013). In order to sustain the productivity of the GoM's natural resources, and to be better prepared for the next major

submarine oil well blowout, many studies have emphasized the criticality of periodic, broad-scale studies of environmental baselines for pollution, and its impacts on biota.

Hydrocarbon pollution (e.g. polycyclic aromatic hydrocarbons, PAHs) is of significant interest in the GoM due to numerous and substantial anthropogenic and natural sources, including the oil and gas industry, coastal runoff, riverine discharge, atmospheric deposition, transportation activities, and natural oil seeps (Kennicutt et al. 1988; National Research Council 2003). PAHs are the class of hydrocarbon pollutants with the greatest concern to fishes, due to their bioavailability, toxicity, and persistence in the environment. The hepatobiliary system in fishes efficiently metabolizes PAHs into more polar molecules for elimination via the gastrointestinal tract, therefore, PAHs rarely accumulate to high levels in tissue and exposure is best quantified by biliary PAH metabolites (Collier et al. 2014). Accumulation of PAHs in tissues can occur if exposure is high or chronic, and the individual's biotransformation capacity is overwhelmed.

In addition to the aforementioned chronic sources of hydrocarbon pollution, the GoM experienced two major pulse events in the past 40 years, which were two of the three largest marine oil spills in the world by volume, the 2010 *Deepwater Horizon* (*DWH*) and the 1979 *Ixtoc I* (Powers et al. 2017). The *DWH* occurred in deep water (~1500 m) in the northern GoM offshore of Louisiana, USA (Figure 3.1), and released an estimated 4.0 million barrels of crude oil over 87 days (Lubchenco et al. 2012; United States of America v. BP Exploration & Production 2015). The *Ixtoc I* occurred in shallow water (54 m) in the southern GoM Bay of Campeche, Mexico (Figure 3.1), and released an estimated 3.4 million barrels of crude oil over nine months (Jernelov and Linden 1981; Soto et al. 2014). Signals from these massive pulses of hydrocarbon pollution can still be seen in sediment cores today (Lincoln et al. 2020; Schwing et

al. 2020). As both events were submarine blowouts, the full spectrum of marine ecosystems were impacted, from the deep-sea benthos, through the water column, surface waters and shorelines (Beyer et al. 2016).

Assessments of impacts of pollution on fishes are facilitated greatly with the collection of periodic, broad spatial-scale baselines on levels and health indices. However, as was the case for the *Exxon Valdez* and *Ixtoc I* oil spills that proceeded *DWH*, scientists lacked necessary baseline data to assess impacts, leading to considerable challenges and limited ability to discern incremental changes in pollution uptake and effect post-*DWH* (Soto et al. 2014; Lewis and Ricker 2020; Pulster, Gracia, Snyder, Romero, et al. 2020).

Initiated in the aftermath of *DWH*, a multinational Gulf-wide survey of continental shelf demersal fishes was conducted to acquire baseline information on species composition and abundance, population dynamics, health indices, and contaminant levels (Murawski et al. 2018; Pulster, Gracia, Snyder, Romero, et al. 2020). Herein, we report spatial contrasts in PAH exposure and hepatic accumulation in one GoM demersal fish, Tilefish (*Lopholatilus chamaeleonticeps*), caught from five large regions of the GoM, with a comparison to Tilefish caught as an "outgroup" from the northwest Atlantic Ocean (Figure 3.1). Tilefish were used as a target species for this study due to their Gulf-wide distribution and relatively high levels of exposure to PAHs, which we hypothesize to be due to their burrow-forming lifestyle and diet comprised of benthic organisms (Snyder et al. 2015; Snyder, Pulster, and Murawski 2019). In addition, Snyder, Pulster, and Murawski (2019) identified substantial increases in PAH exposure coincident with declines in health indices in Tilefish from the north central GoM over years 2012 to 2017, therefore, continued monitoring of this species is necessary as it is commercially and ecologically important.

Materials and Methods

Fish Collection- Gulf of Mexico

We undertook a series of multinational fisheries-independent demersal longline surveys on the GoM continental shelf 2011 to 2017 onboard the *R/V Weatherbird II*. Herein, we selected samples from the years of 2015 and 2016 to best make spatial comparisons and minimize the confounding effect of temporal variation.

Tilefish were caught in five regions in the GoM (Figure 3.1, Table 3.1) from three surveys in the summers of 2015 and 2016. At each station, five miles of monofilament main line with an average of 459 evenly spaced #13/0 circle hooks were set for an average soak time of two hours. Bait alternated between Atlantic Mackerel (*Scomber scombus*) and Humbolt squid (*Dosidicus gigas*) wings. Detailed longline survey methods are provided in Murawski et al. (2018).

Tilefish were caught at consistent depths between regions, ranging from 163 to 591 meters, with a mean of 280 meters. Once landed, Tilefish were processed immediately or placed on ice briefly until sampling. Tilefish were measured for lengths (standard, fork, total), and total weight. A subset of Tilefish were sacrificed and subsampled for tissues (Table 3.1). Organ (liver, gastrointestinal, gonad) weights were recorded. Sex was determined visually (macroscopically) during dissection as male, female, or unknown as described in McBride, Vidal, and Cadrin (2013). Bile, if present, was collected by draining the contents of the gallbladder into a combusted amber vial. The liver was collected in a combusted amber jar. Bile and liver samples were frozen immediately and stored at -20 °C until analysis.

Fish Collection- Northwest Atlantic Ocean

Tilefish were collected from two fisheries-independent surveys onboard the *F/V Sea Capture* between July and August 2017 in the mid-Atlantic Bight, from Georges Bank to Cape Hatteras (Figure 3.1), from depths ranging between 80 and 303 meters (Frisk et al. 2018). Demersal longlines consisted of a one-nautical mile 417-kg-test steel cable main line equipped with 150 evenly spaced hooks baited with squid. Hook size alternated between 8/0, 12/0, and 14/0 circle hooks in a 20:60:20 ratio.

Tilefish were measured for total length and weight, and sex was identified visually (macroscopically) during dissection as male, female, or unknown according to McBride, Vidal, and Cadrin (2013). Liver samples were collected from a subset of individuals (Table 3.1), stored in cryovials at -20 °C, and transferred to the University of South Florida for analysis.

Analysis of Biliary PAH Metabolites via HPLC-F

Tilefish bile samples were analyzed using a standard semi-quantitative high performance liquid chromatography with fluorescence detection (HPLC-F) method (Krahn et al. 1984; Krahn, Moore, and Macleod 1986). Detailed analytical and quality assurance methods can be found in Snyder et al. (2015). Biliary PAHs were quantified for naphthalene (NPH) and benzo[*a*]pyrene (B*a*P) metabolite equivalents and reported to two significant figures in units of µg FACs g^{-1} bile. Total biliary PAH metabolites is the sum of NPH and B*a*P metabolite equivalents.

Analysis of Hepatic PAHs and Alkylated Homologs via GC-MS/MS

A modified QuEChERS method was used to extract PAHs and alkylated homologs ($n =$ 46 analytes) from Tilefish liver tissue. Detailed information on QuEChERS methods, gas chromatography tandem mass spectrometry (GC-MS/MS) operating parameters, target analytes, and quality assurance protocols are provided in Snyder, Pulster, and Murawski (2019). Performance of procedural and solvent blanks, post-extraction standard, and surrogate standard recoveries in the certified reference material (NIST SRM 1974c; $82 \pm 9\%$), matrix spikes ($84 \pm 5\%$), and samples ($81 \pm 11\%$) all met the QA criteria established in NOAA (2012).

Analyte concentrations were reported to three significant figures in units of ng g^{-1} wet weight (w.w.). Sum total of the 46 analytes is reported as $TPAH_{46}$. Sum of low molecular weight (LMW) PAHs is comprised of two and three ring analytes. Sum of high molecular weight (HMW) PAHs is comprised of four to six ring analytes.

Analysis of % Liver Lipid

Lipid extractions were performed following PAH extractions if the liver sample had sufficient mass for both. Total lipid was extracted from liver tissue with a modified Folch method described in Snyder, Pulster, and Murawski (2019). Total lipid was quantified gravimetrically and reported as % liver lipid.

Statistical Analyses

Data were binned *a priori* into regions of the north central, northwest, and southwest GoM, Bay of Campeche, Yucatán Shelf, and northwest Atlantic (Figure 3.1). Hypothesis testing focused on regional differences between variables. Associations between variables both within each region, and for all regions combined, were also examined.

Statistical analyses were performed using MATLAB R2017a and the Fathom Toolbox for Matlab (Jones 2017). All hypothesis tests generated permutation-based p-values from 1000 iterations, and test statistics were evaluated at $\alpha = 0.05$. Permutation-based or randomization methods were chosen as a solution to the statistical problems often encountered in biological studies (e.g. small sample size, unbalanced data, non-normal distribution) (Potvin and Roff 1993; Manly 1997). Relationships between continuous data were evaluated with a Pearson's correlation, or a regression. Differences in mean between groups were evaluated using a modified permutational multivariate analysis of variance (PERMANOVA), which allows for accurate quantification of p-values when between-group dispersions are heterogeneous (Anderson et al. 2017). Post-hoc pairwise tests followed a significant modified PERMANOVA. A Holms-adjusted p-value was used if more than ten pair-wise comparisons were tested to reduce type-I error from multiple comparisons, otherwise the unadjusted p-value was assessed. Canonical analysis of principal coordinates (CAP) was used to visualize the significant difference in PAH concentration and composition by region. The difference in sex ratio by region was evaluated with a Chi-square test of independence.

Proxy fish health indices of Fulton's condition factor (K) and hepatosomatic index (HSI) were calculated as follows:

$$K = \frac{total\ body\ weight\ (kg)}{total\ length\ (cm)^3} \text{x}100 \text{ and HSI} = \frac{liver\ weight\ (kg)}{total\ body\ weight\ (kg)} \text{x}100.$$

Graduated symbols maps were created in ArcMap 10.5.1 using the Jenks Natural Breaks method to create concentration groupings specific to each mapped dataset.

Results

Biometric Data and Health Indices

Over 300 Tilefish from 49 stations between the six geographic regions 2015 to 2017 were assessed in this study (Table 3.1). The sex ratio was not significantly different between regions. Mean total length (TL) differed significantly by region (Table 3.1, $F = 11.4$, $p = 0.001$) and sex ($F = 27.3$, $p = 0.001$). GoM Tilefish (64 cm) were significantly larger compared to northwest Atlantic Tilefish (51 cm). Male Tilefish (71 cm) were significantly larger than females (59 cm), and unknowns (55 cm). Females were also significantly larger than unknowns. Mean total weight (2.91 kg) was not significantly different by region.

Mean Fulton's condition factor (K) differed significantly by region (Figure C1, $F = 29.2$, $p = 0.001$) and sex ($F = 4.48$, $p = 0.008$). Within the GoM, mean K was highest on the Yucatán Shelf and north central regions. Tilefish from the GoM (1.01) had significantly lower mean K compared to the northwest Atlantic (1.23). Males (1.09), and females (1.06) had significantly higher K compared to Tilefish of unknown sex (1.01). Mean K was not significantly different between male and female Tilefish.

72

A total of 228 GoM Tilefish sampled had sufficient liver tissue mass for lipid extraction. Mean % liver lipid differed significantly by region (Figure C2; $F = 21.5$, $p = 0.001$) with north central Tilefish having significantly lower % liver lipid (10.7) compared to all other GoM regions (15.8). Mean % liver lipid was not significantly different by sex, nor correlated with TL.

Hepatic PAHs and Alkylated Homologs

A total of 305 Tilefish liver samples from the six regions were analyzed for PAHs and alkylated homologs (Table 3.1). No association between % liver lipid and liver $TPAH_{46}$ was observed; therefore, $TPAH_{46}$ data were not lipid normalized for data analysis (Hebert and Keenleyside 1995).

Mean liver $TPAH_{46}$ concentrations differed significantly by region (Figure C2, $F = 2.86$, $p = 0.016$). Within the GoM, liver $TPAH_{46}$ concentrations (ng g^{-1} w.w.; mean ± SD) were: north central (1020 ± 564), northwest (901 ± 434), Yucatán Shelf (847 ± 716), southwest (631 ± 369), and Bay of Campeche (718 ± 428). Within the GoM, a general pattern in liver $TPAH_{46}$ concentrations was apparent- highest concentrations were observed in the north central region, with decreasing concentrations counterclockwise around the GoM, followed by an increase from the Bay of Campeche eastward on to the Yucatán Shelf (Figure 3.3). Mean liver $TPAH_{46}$ concentrations were not significantly different between Tilefish from the GoM and the northwestern Atlantic (1020 ± 1080).

In all regions, liver PAH composition was dominated (>99% of $TPAH_{46}$) by LMW PAHs. Liver PAH concentration and composition differed significantly by region as identified by a modified PERMANOVA ($F = 15.8$, $p = 0.001$), and CAP (trace statistic = 1.99, $p = 0.001$).

CAP ordination (Figure C3) revealed three groups: (1) north central, northwest, and southwest GoM, (2) Bay of Campeche, and Yucatán Shelf, (3) northwest Atlantic. CAP results indicate minor differences in the concentration and composition of LMW PAHs by group, but noteworthy differences in HMW PAHs, with the northwest Atlantic Tilefish being defined by 10/12 HMW PAHs analyzed (benzo[*a*]anthracene, chrysene, benzo[*b*]fluoranthene, benzo[*k*]fluoranthene, benzo[*e*]pyrene, benzo[*a*]pyrene, indeno[1,2,3-*c*,*d*]pyrene, dibenzo[*a*,*h*]anthracene, benzo[*g*,*h*,*i*]perylene), which is also seen in liver PAH profile comparisons (Figure 3.4).

The ΣHMW liver PAHs differed significantly by region (Table C1, $F = 6.13$, $p = 0.001$) with northwest Atlantic Tilefish (13.4 ± 31.5 ng g^{-1} w.w.) having 31% higher concentrations compared to all GoM regions (8.44 ± 8.10 ng g^{-1} w.w.). HMW PAHs were detected in 63% of Tilefish from the northwest Atlantic, compared to only 5.6% of individuals from the GoM (Table C1).

Liver TPAH$_{46}$ correlated with TL for the northwest GoM ($r = 0.278$, $p = 0.031$), and Bay of Campeche ($r = 0.343$, $p = 0.016$), but not for the other regions nor all data combined. Liver TPAH$_{46}$ concentration (ng g^{-1} w.w.) differed significantly by sex for all regions combined ($F = 6.48$, $p = 0.002$), with both males (857 ± 576), and females (980 ± 805) having higher concentrations compared to Tilefish of unknown sex (666 ± 398). Liver TPAH$_{46}$ correlated negatively with HSI for all regions combined (Figure C4, $r = -0.226$, $p = 0.002$), and for the northwest ($r = -0.308$, $p = 0.012$), and Yucatán Shelf ($r = -0.3917$, $p = 0.031$). No correlation between liver TPAH$_{46}$ and K was observed.

Biliary PAH Metabolites

A total of 225 Tilefish bile samples from the five regions of the GoM were analyzed for PAH metabolites of NPH and B*a*P (Table 3.1). Total biliary PAH metabolites were dominated by NPH metabolites (~99.9%) which were consistently three orders of magnitude higher in concentration than B*a*P metabolite equivalents.

Mean total biliary PAH metabolite concentration differed significantly by region (Figure 3.5, $F = 19.5$, $p = 0.001$). Total biliary PAH metabolite concentrations (μg FACs g^{-1}; mean $\pm$ SD) were significantly higher in the north central GoM (470 ± 400) compared to all other regions of the GoM: northwest (270 ± 160), Yucatán Shelf (260 ± 180), southwest (160 ± 130), and Bay of Campeche (140 ± 110). Within the GoM, a general pattern in total biliary PAH metabolite concentrations was apparent- highest concentrations were observed in the north central region, with decreasing concentrations counterclockwise around the GoM, followed by an increase from the Bay of Campeche eastward on to the Yucatán Shelf (Figure 3.6). Results for mean biliary NPH metabolites mirrored those for total biliary PAH metabolites. Mean biliary B*a*P metabolite concentration was not significantly different by region (210 ± 430 ng FACs g^{-1}).

Total biliary PAH metabolites correlated with TL for all data combined ($r = 0.214$, $p = 0.001$), and in the Bay of Campeche ($r = 0.604$, $p = 0.001$). Total biliary PAH metabolites correlated with K for all regions combined (Figure C5, $r = 0.272$, $p = 0.001$), the north central ($r = 0.432$, $p = 0.003$), and the Bay of Campeche ($r = 0.301$, $p = 0.035$). No significant association between total biliary PAH metabolites and sex, % liver lipid, nor HSI was observed.

Total biliary PAH metabolites correlated with liver $TPAH_{46}$ for all regions combined (Figure 3.7, $R^2 = 3.72\%$, $p = 0.025$), the southwest ($R^2 = 45.9\%$, $p = 0.001$), and the Bay of Campeche ($R^2 = 25.7\%$, $p = 0.001$).

Discussion

Spatial Patterns in GoM Tilefish Biometrics and Health Indices

Within the GoM, significant regional differences in Fulton's condition factor (K), and % liver lipid were observed. Fulton's condition factor (K), is a common metric used as a proxy of relative fish health, with higher values indicating a healthier individual and/or population (Blackwell, Brown, and Willis 2000). Fish condition may be affected by numerous variables including sex, reproductive state, season, prey availability, water temperature, and stressors (Blackwell, Brown, and Willis 2000). Sex and reproductive state of Tilefish is difficult to determine by visual inspection due to their sequential protogynous hermaphrodite reproductive strategy and prolonged spawning season, and data should thus be interpreted with caution. There was no difference in sex ratio between regions, therefore, sex should not be driving any regional variability. Mean bottom temperature ($13.2 \pm 2.04 \,°C$) also did not differ between GoM regions. Spawning season of GoM Tilefish is January through June, therefore all GoM Tilefish sampled herein are presumed to be in a post-spawning state (Lombardi-Carlson 2012). There appears to be a positive relationship between Tilefish K and regional primary productivity, where the regions with the highest K (north central GoM, Yucatán Shelf) have higher primary production compared to the regions with lower K (northwest, southwest, Bay of Campeche) (Benway and Coble 2014).

Snyder, Pulster, and Murawski (2019) studied Tilefish from the north central region of the GoM from 2012 to 2017 and found a significant negative correlation between biliary PAH metabolites and K, accompanied by a 178% increase in biliary PAH metabolites and a 22% decrease in K over the study period. Their results are independent of the results herein as the two studies are examining different datasets (e.g. individuals and regions), and hypotheses.

Tilefish from the north central had 32% less liver lipid compared to all other regions of the GoM. Snyder, Pulster, and Murawski (2019) found a 53% decrease in % liver lipid in north central GoM Tilefish over the years 2012 to 2017. Although unexplained by the other variables measured herein, the significantly lower % liver lipid in north central GoM Tilefish is important as the main role of lipids in fish is storage and supply of energy for growth, reproduction, and daily activities (Tocher 2003). Together, these results demonstrate a need for further research into GoM Tilefish health.

Spatial Patterns in GoM Tilefish PAH Exposure and Hepatic Accumulation

Within the GoM, both PAH exposure and hepatic accumulation were dominated by LMW PAHs and corresponding alkylated homologs, indicating the primary source of hydrocarbon pollution is petrogenic. The distribution of PAHs in a sample can be used to distinguish petrogenic from pyrogenic sources, with petrogenic PAHs characterized by a dominance of LMW PAHs and a bell-shaped distribution profile of the unsubstituted PAH and its corresponding alkylated homologs. In contrast, pyrogenic PAHs are characterized by a dominance of HMW PAHs and a dominance of unsubstituted (parent) PAHs over their corresponding alkylated homologs. Both characteristics of a petrogenic source were seen in

samples from GoM Tilefish, suggesting the predominant source of hydrocarbon pollution in the GoM that demersal fishes are exposed to is petrogenic, with minimal pyrogenic inputs. However, LMW PAHs have higher bioavailability compared to HMW compounds, due to lower hydrophobicity, thus less sorption to environmental organic carbon, potentially contributing to the dominance of LMW PAHs measured in Tilefish tissues (Meador et al. 1995).

Within the GoM, there were similar spatial patterns in PAH exposure and hepatic accumulation. Total biliary PAH metabolites and liver $TPAH_{46}$ concentrations were significantly correlated, which is consistent with the model that elevated exposure leads to increased accumulation in target tissues if biotransformation capacity is exceeded (Meador et al. 1995).

Spatial patterns in PAH exposure and hepatic accumulation likely reflect the magnitude and number of sources of PAHs by region as associations with regional biometrics were insignificant or weak. The north central and northwest regions of the GoM both have significant sources of PAH pollution emanating from large coastal cities, seaports and shipping traffic, dense offshore oil infrastructure, associated refineries petrochemical plants, oil supply and services bases, transportation traffic, and pipelines, natural oil seeps, large riverine inputs, and coastal erosion (Botello, Villanueva, and Diaz 1997; Santschi et al. 2001; Mitra and Bianchi 2003; National Research Council 2003; Yanez-Arancibia and Day 2004; MacDonald et al. 2015; Murawski et al. 2020). The Bay of Campeche region also has numerous sources of PAH pollution, including most of Mexico's offshore oil industry, major petrochemical complexes and refineries, ship traffic, natural oil seeps, and riverine inputs (e.g. Usumacinta/Grijalva River system) (Botello, Villanueva, and Diaz 1997; Yanez-Arancibia and Day 2004; Scholz-Bottcher et al. 2008; Soto et al. 2014; MacDonald et al. 2015; Ruiz-Fernandez et al. 2016). The

Coatzacoalcos River, Mexico's third largest river discharge, also empties into the Bay of Campeche, supporting Mexico's oldest refinery, several petrochemical complexes, and has been polluted with PAHs since the 1950s (Ruiz-Fernandez et al. 2016). It is noteworthy that PAH exposure and hepatic accumulation in Tilefish is significantly lower in the Bay of Campeche compared to the north central, and northwest GoM, even though all three regions have extensive sources of PAHs. However, within the Bay of Campeche liver $TPAH_{46}$ concentrations are higher in the eastern sites closer to mature oil fields. Gold-Bouchot et al. (1997) reported a similar spatial pattern in PAH concentrations in oysters (*Crassostrea virginica*) from the Bay of Campeche compared to the northern GoM. Both PAH exposure and hepatic accumulation correlated with Tilefish total length in the Bay of Campeche, therefore, it is possible that physiological mechanisms may be a controlling factor in the region.

Relatively low PAH exposure and hepatic accumulation in the southwest region of the GoM was anticipated, as this region has minimal natural oil seepage and offshore oil infrastructure, and the regional river systems are not noted for hydrocarbon pollution (Yanez-Arancibia et al. 2008; MacDonald et al. 2015; Murawski et al. 2020). The increase in PAH exposure and hepatic accumulation in Tilefish on the Yucatán Shelf was surprising as this region is a carbonate shelf spatially removed from the Mexican oil industry, major river discharges, and most natural oil seeps. Potential sources of PAH pollution to the Yucatán Shelf include discharges from seaports, shipping traffic, urban runoff, submarine groundwater discharges, atmospheric deposition, and deep-water seeps (Metcalfe et al. 2011; Kuk-Dzul, Gold-Bouchot, and Ardisson 2012; MacDonald et al. 2015). Due to the distance from shore of our Yucatán Shelf sampling stations, it is likely the PAH pollution is introduced from the Caribbean by the Yucatán Current, and by oil tanker traffic via the Yucatán Channel as trade lanes trace the outer

Yucatán Shelf (Botello, Villanueva, and Diaz 1997; Yanez-Arancibia et al. 2008). In addition, MacDonald et al. (2015) identified a small number of natural seep zones in deep water (>3500 m) offshore of the Yucatán Shelf. However, fingerprinting studies on GoM seep-derived oil determined that their signature is highly localized and GoM Tilefish studied herein are not in close proximity (>10 km) to known natural seeps (Stout et al. 2016).

Gulf-wide surveys of PAHs in other demersal continental shelf species (e.g. snappers, groupers, hakes) show similar spatial patterns as Tilefish, noting "hot spots" near major shipping ports and lanes, and rivers (Pulster, Gracia, Snyder, Romero, et al. 2020; Pulster, Gracia, Armenteros, et al. 2020). Comparisons of levels of biliary NPH metabolites indicate GoM Tilefish as having the highest levels compared to all studies with comparable methods, which is notable as Tilefish are sampled offshore on the continental shelf, edge, and slope, and most previous studies are of inshore, or coastal species (Snyder et al. 2015; Snyder, Pulster, and Murawski 2019; Pulster, Gracia, Snyder, Romero, et al. 2020; Pulster, Gracia, Armenteros, et al. 2020). While biliary NPH metabolite levels are relatively high in GoM Tilefish, liver $TPAH_{46}$ concentrations are similar in magnitude to other GoM demersal fishes.

Comparison of GoM and Northwest Atlantic Tilefish

There were significant biometric differences between Tilefish caught in the GoM and the northwest Atlantic Ocean. Tilefish caught in the northwest Atlantic had a significantly smaller mean TL compared to Tilefish caught in the GoM, possibly related to smaller hook sizes used in the north Atlantic surveys (see *methods 2.1 and 2.2*).

Fulton's condition factor (K) was significantly higher in Tilefish from the northwestern Atlantic compared to Tilefish from the GoM. Mean bottom temperature was not different between the GoM and northwest Atlantic stations. Primary productivity is also comparable between the two regions (Gregg et al. 2003). North Atlantic spawning season is similar or longer than in the GoM, potentially extending into November, therefore, the K of northwest Atlantic Tilefish sampled herein may be impacted by individual spawning state, confounding the comparison in Tilefish K between the north Atlantic and GoM.

There was not a significant difference in mean liver $TPAH_{46}$ concentrations between Tilefish from the GoM and the northwest Atlantic. However, northwest Atlantic Tilefish had 31% higher hepatic HMW PAHs concentrations compared to GoM Tilefish, and HMW PAHs were detected in 63% of individuals compared to ~5% in the GoM. This is an important result as it is the HMW PAHs that are known carcinogens to fish (Myers, Johnson, and Collier 2003). Elevated hepatic accumulation of HMW PAHs in northwest Atlantic Tilefish is consistent with higher levels of pyrogenic inputs in the region. Sources of PAHs to the northwest Atlantic region are mainly from consumption of petroleum (e.g. land-based and river runoff, atmospheric deposition) and transportation activities, which would input a combination of both HMW pyrogenic and LMW petrogenic PAHs. In contrast to the main sources to the GoM, where extraction activities and natural seeps are more significant players inputting mainly LMW petrogenic PAHs (National Research Council 2003).

Steimle, Zdanowicz, and Gadbois (1990) reports substantially lower liver PAH concentrations in Tilefish sampled in 1980 and 1981 from Hudson and Lydonia Canyons in the northwest Atlantic (12.8 and 26.0 ng g^{-1} dry weight respectively), with fluoranthene being the highest PAH detected. However, these studies report concentrations in different units (dry vs.

wet weight). Using a rough unit conversion factor (3x) generated by their study, liver PAH concentrations from Tilefish sampled in the northwest Atlantic in 2017 remain substantially higher, however, it is best that conversion factors for tissues be calculated on an individual level. Either way, this result may be indicative of substantial increases in PAH exposure to northwest Atlantic Tilefish over time. Herein, the northwest Atlantic Tilefish were used as a non-GoM outgroup, however, further analysis should be undertaken to understand spatial variability, environmental drivers, and health impacts of PAH accumulation in the region.

Conclusions

The results reported herein represent an extensive dataset on Gulf-wide PAH levels in a commercially, and ecologically important demersal fish. PAH pollution was found to be ubiquitous, with exposure and hepatic accumulation in demersal fishes from both the GoM and northwest Atlantic, however, concentrations varied significantly by region. Within the GoM, the highest levels of PAH exposure and accumulation in Tilefish were in the north central region, and the lowest were in the southwest and Bay of Campeche regions. The high concentrations in the north central GoM are likely related to the numerous and substantial sources in the region, including the 2010 *Deepwater Horizon* blowout. The GoM and northwest Atlantic Tilefish had similar levels of hepatic PAH accumulation, though Tilefish from the northwest Atlantic had significantly higher concentrations and detection frequency of carcinogenic HMW PAHs compared to Tilefish from the GoM, warranting further evaluation of northwest Atlantic populations.

As the GoM supports both productive offshore oil and fishing industries, there is a critical need for large-scale baselines of PAH pollution and the impacts on marine resources. These baselines have been largely absent following major oil spills hindering assessments of impact and recovery. The expansive baseline data provided herein will serve as a reference for future GoM oil development activities particularly for undeveloped areas and areas under current moratorium.

Tables

Table 3.1. Collection and sample data for Tilefish from the six geographic regions of the study.

Region	Collection year	Collection month	n (stations)	n (bile)	n (liver)	Total length (cm)[1]	Sex ratio (M:F:U)[2]
North central	2015	August	10	56	63	67 ± 15	6:44:13
Northwest	2016	September	6	50	60	64 ± 15	21:28:12
Southwest	2016	August	4	38	33	62 ± 11	10:19:13
Bay of Campeche	2015 2016 Comb.[3]	September August	7	26 26 52	26 21 47	61 ± 15 58 ± 15 60 ± 15	4:14:8 5:16:6 9:30:14
Yucatán shelf	2015 2016 Comb.[3]	September August	6	15 14 29	17 15 32	67 ± 13 67 ± 11 67 ± 12	3:11:3 5:9:2 8:20:5
Northwest Atlantic	2017	July-August	16	0	70	51 ± 15	28:36:6

[1]Mean ± one standard deviation
[2]M:F:U = Male:Female:Unknown sex
[3]Comb. = combined years

Figures
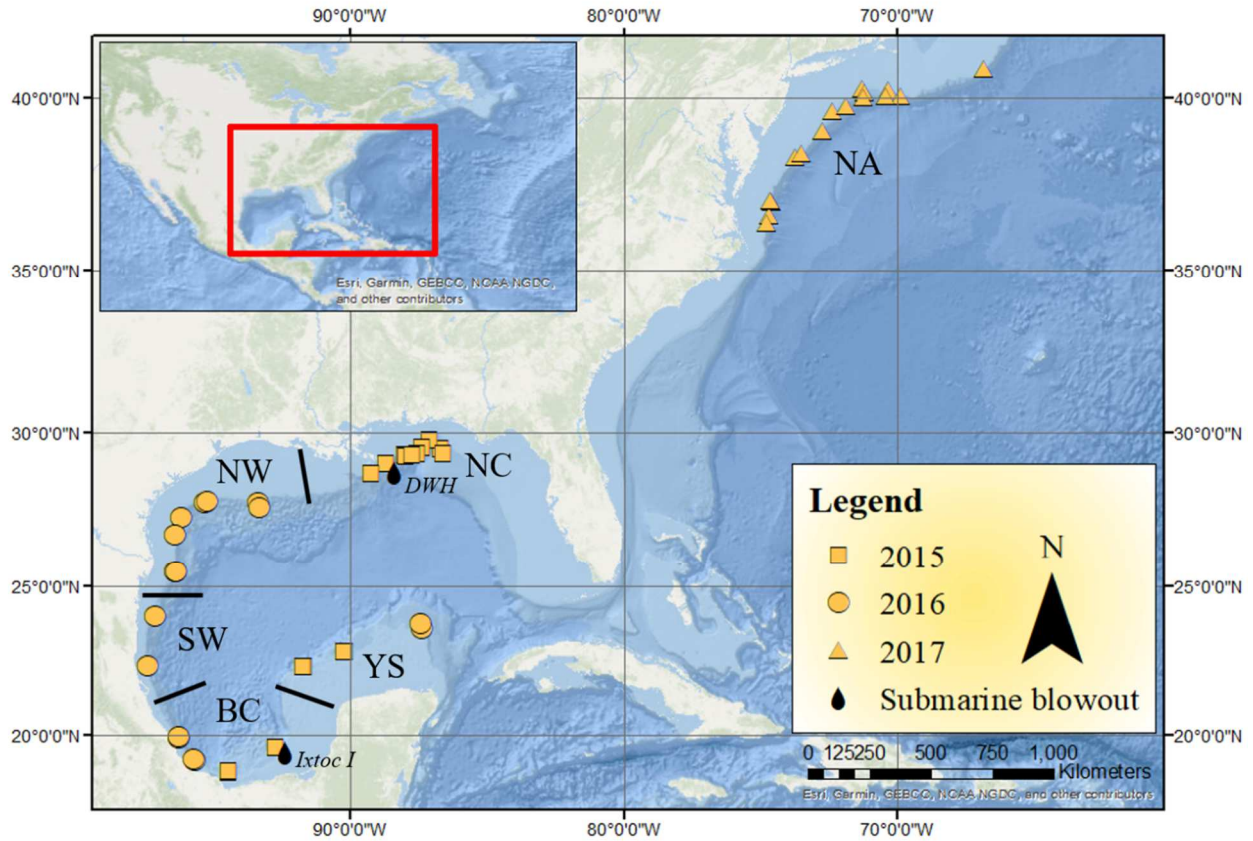
Figure 3.1. Map of the 49 stations where Tilefish were sampled in the Gulf of Mexico (GoM), and northwest Atlantic Ocean. Sampling area is divided into six regions: NA = northwest Atlantic; NC = north central GoM; NW = northwest GoM; SW = southwest GoM; BC = Bay of Campeche; YS = Yucatán Shelf. Legend denotes sampling year.
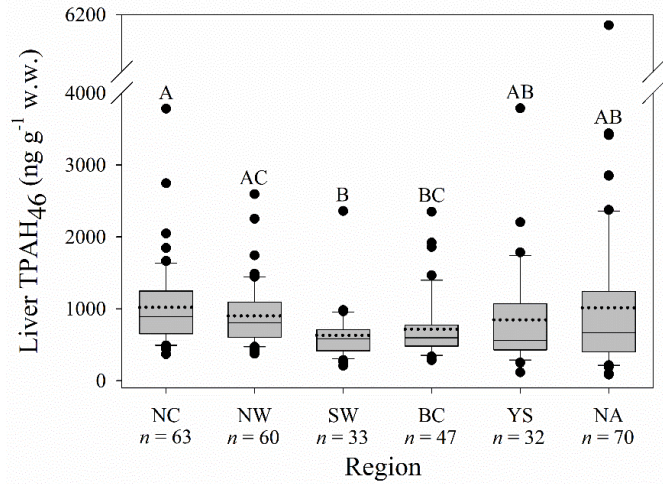
Figure 3.2. Total liver PAH (TPAH$_{46}$) concentrations for Tilefish by region (NC = north central; NW = northwest; SW = southwest; BC = Bay of Campeche; YS = Yucatán Shelf; NA = northwest Atlantic). Sample size (*n*) noted by region. Letters (ABC) denote significantly different regions at α = 0.05. Solid line = median; dotted line = mean.
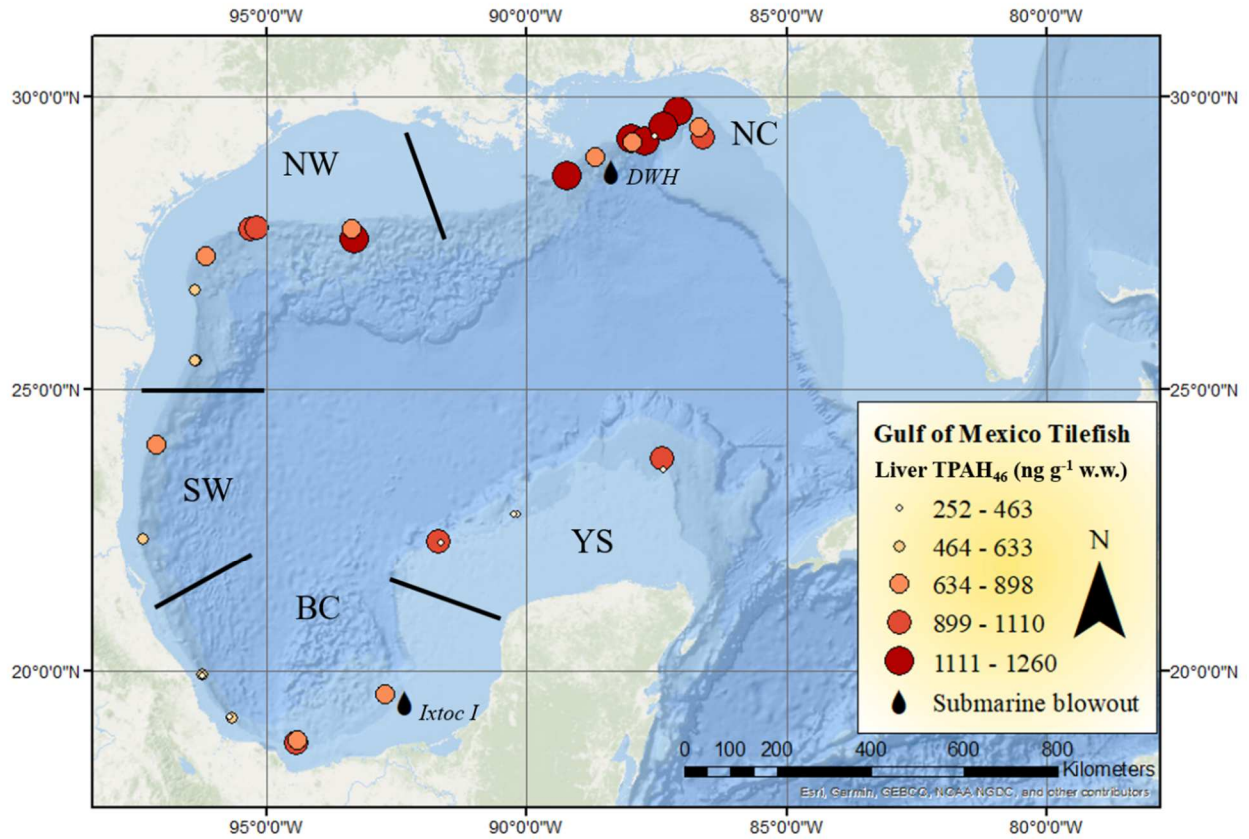
Figure 3.3. Graduated symbols map of total liver PAH (TPAH$_{46}$) for Gulf of Mexico Tilefish sampled 2015 to 2016 by region (NC = north central; NW = northwest; SW = southwest; BC = Bay of Campeche; YS = Yucatán Shelf).
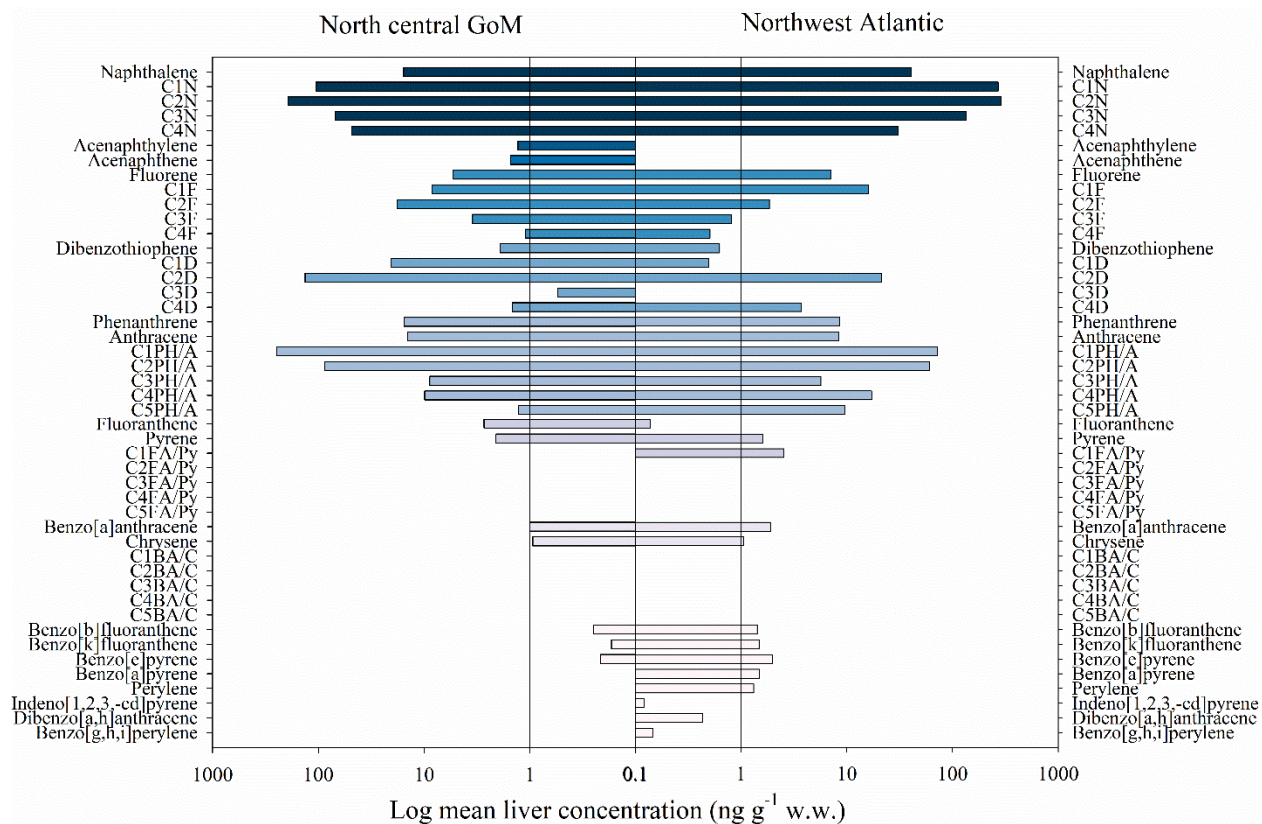
Figure 3.4. Liver PAH profiles for Tilefish sampled in the north central Gulf of Mexico (GoM; *n* = 63), and the northwest Atlantic (*n* = 70). Alkylated homologs are plotted underneath their respective parent PAH.
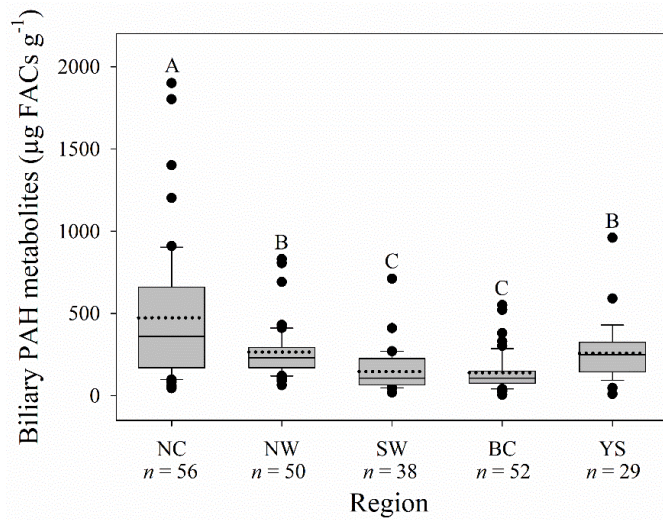
Figure 3.5. Total biliary PAH metabolites for Gulf of Mexico Tilefish sampled 2015 to 2016 by region (NC = north central; NW = northwest; SW = southwest; BC = Bay of Campeche; YS = Yucatán Shelf). Sample size (*n*) noted by region. Letters (ABC) denote significantly different regions at α = 0.05. Solid line = median; dotted line = mean.
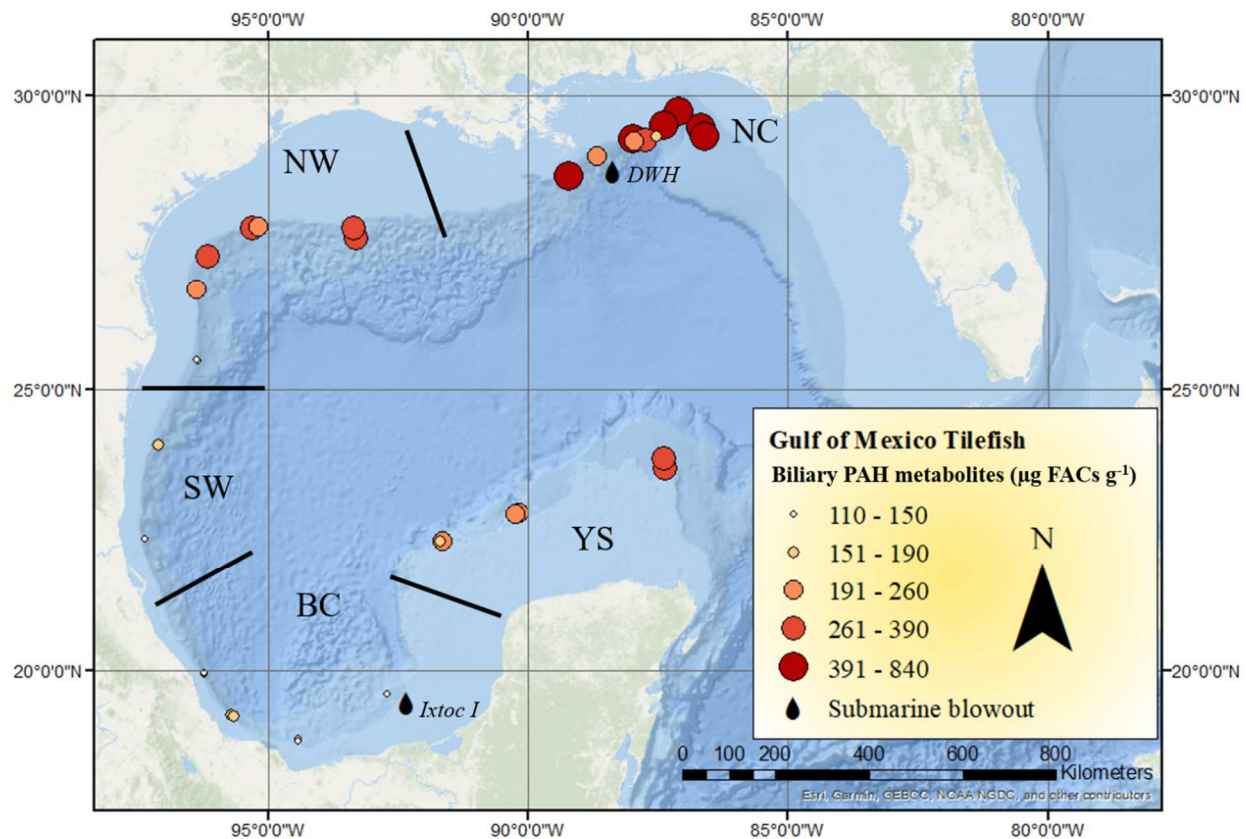
Figure 3.6. Graduated symbols map of mean total biliary PAH metabolites for Gulf of Mexico Tilefish sampled 2015 to 2016 by region (NC = north central; NW = northwest; SW = southwest; BC = Bay of Campeche; YS = Yucatán Shelf).
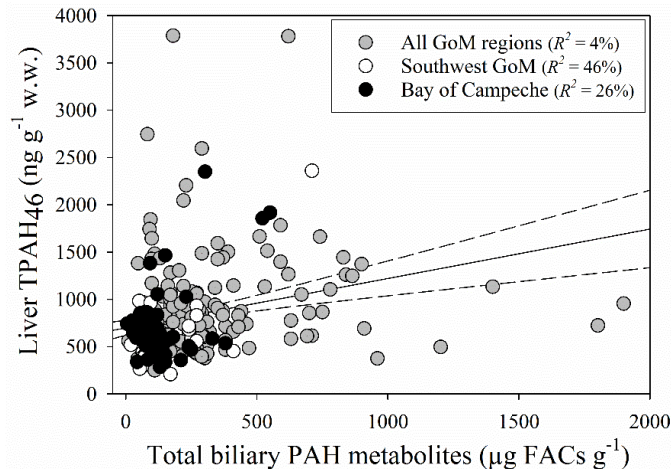
Figure 3.7. Total liver PAHs (TPAH$_{46}$) versus total biliary PAH metabolite equivalents for Tilefish sampled in the Gulf of Mexico (GoM) 2015 to 2016. Regressions are significant at α = 0.05. Dotted lines represent the 95% confidence intervals on the solid regression line.

References

Anderson, M. J., D. C. I. Walsh, K. R. Clarke, R. N. Gorley, and E. Guerra-Castro. 2017. 'Some solutions to the multivariate Behrens-Fisher problem for dissimilarity-based analyses', *Australian & New Zealand Journal of Statistics*, 59: 57-79.

Benway, H.M., and P.G. Coble. 2014. "Report of the Gulf of Mexico Coastal Carbon Synthesis Workshop." In, 67. Ocean Carbon and Biogeochemistry Program and North American Carbon Program.

Beyer, J., H. C. Trannum, T. Bakke, P. V. Hodson, and T. K. Collier. 2016. 'Environmental effects of the Deepwater Horizon oil spill: A review', *Marine Pollution Bulletin*, 110: 28-51.

Blackwell, Brian G, Michael L Brown, and David W Willis. 2000. 'Relative weight (Wr) status and current use in fisheries assessment and management', *Reviews in Fisheries Science*, 8: 1-44.

Botello, A. V., S. Villanueva, and G. Diaz. 1997. 'Petroleum Pollution in the Gulf of Mexico and Caribbean Sea.' in G.W. Ware (ed.), *Reviews of Environmental Contamination and Toxicology* (Springer).

Collier, T. K., B. F. Anulacion, M. R. Arkoosh, J.P. Dietrich, J. P. Incardona, L. L. Johnson, G. M. Ylitalo, and M. S. Myers. 2014. 'Effects on fish of polycyclic aromatic hydrocarbons (PAHS) and naphthenic acid exposures.' in K. B. Tierney, A. P. Farrell and C.L. Brauner (eds.), *Fish Physiology: Organic Chemical Toxicology of Fishes* (Elsevier Inc.).

Council, National Research. 2003. *Oil in the sea III: Inputs, fates, and effects* (The National Academies Press).

Frisk, M.G., J.A. Olin, R.M. Cerrato, P. Nitschke, and L. Nolan. 2018. "Fisheries-independent pilot survey for Golden (Lopholatilus chamaelonticeps) & Blueline (Caulolatilus microps) Tilefish throughout the range from Georges Bank to Cape Hatteras." In *Fisheries Report, Mid-Atlantic Fishery Management Council, Dover, Delaware*, 1-37.

Gold-Bouchot, G., M. ZavalaCoral, O. ZapataPerez, and V. CejaMoreno. 1997. 'Hydrocarbon concentrations in oysters (Crassostrea virginica) and recent sediments from three coastal lagoons in Tabasco, Mexico', *Bulletin of Environmental Contamination and Toxicology*, 59: 430-37.

Gregg, Watson W., Margarita E. Conkright, Paul Ginoux, John E. O'Reilly, and Nancy W. Casey. 2003. 'Ocean primary production and climate: Global decadal changes', *Geophysical Research Letters*, 30.

Hebert, Craig E., and Karen A. Keenleyside. 1995. 'To normalize or not to normalize? Fat is the question', *Environmental Toxicology and Chemistry*, 14: 801-07.

Jernelov, A., and O. Linden. 1981. 'Ixtoc I: A case study of the world's largest oil spill', *Ambio*, 10: 299-306.

Jones, D.L. 2017. 'Fathom Toolbox for MATLAB: software for multivariate ecological and oceanographic data analysis'. https://www.marine.usf.edu/research/matlab-resources/.

Kennicutt, M. C., J. M. Brooks, E. L. Atlas, and C. S. Giam. 1988. 'Organic compounds of environmental concern in the Gulf of Mexico: a review', *Aquatic Toxicology*, 11: 191-212.

Krahn, M. M., L. K. Moore, and W. D. Macleod. 1986. "Standard Analytical Procedures of the NOAA National Analytical Facility, 1986: Metabolites of Aromatic Compounds in Fish Bile." In, edited by U.S. Department of Commerce, 1-29.

Krahn, M. M., M. S. Myers, D. G. Burrows, and D. C. Malins. 1984. 'Determination of metabolites of xenobiotics in the bile of fish from polluted waterways', *Xenobiotica*, 14: 633-46.

Kuk-Dzul, J. G., G. Gold-Bouchot, and P. L. Ardisson. 2012. 'Benthic infauna variability in relation to environmental factors and organic pollutants in tropical coastal lagoons from the northern Yucatan Peninsula', *Marine Pollution Bulletin*, 64: 2725-33.

Lewis, C.G., and R. W. Ricker. 2020. 'Overview of Ecological Impacts of Deep Spills: Deepwater Horizon.' in S.A. Murawski, C.H. Ainsworth, S. Gilbert, D.J. Hollander, C.B. Paris, M. Schluter and D.L. Wetzel (eds.), *Deep Oil Spills: Facts, Fate, and Effects* (Springer Nature Switzerland AG).

Lincoln, S.A., J. R. Radovic, A. Gracia, A. Jaggi, T. B. P. Oldenburg, S.R. Larter, and K.H. Freeman. 2020. 'Molecular Legacy of the 1979 Ixtoc 1 Oil Spill in Deep-Sea Sediments of the Southern Gulf of Mexico.' in S.A. Murawski, C.H. Ainsworth, S. Gilbert, D.J. Hollander, C.B. Paris, M. Schluter and D.L. Wetzel (eds.), *Deep Oil Spills: Facts, Fate, and Effects* (Springer International Publishing).

Lombardi-Carlson, L.A. 2012. 'Life history, population dynamics, and fishery management of the Golden Tilefish, *Lopholatilus chamaeleonticeps*, from the Southest Atlantic and Gulf of Mexico', University of Florida.

Lubchenco, J., M. K. McNutt, G. Dreyfus, S. A. Murawski, D. M. Kennedy, P. T. Anastas, S. Chu, and T. Hunter. 2012. 'Science in support of the Deepwater Horizon response', *Proceedings of the National Academy of Sciences of the United States of America*, 109: 20212-21.

MacDonald, I. R., O. Garcia-Pineda, A. Beet, S. D. Asl, L. Feng, G. Graettinger, D. French-McCay, J. Holmes, C. Hu, F. Huffer, I. Leifer, F. Muller-Karger, A. Solow, M. Silva, and G. Swayze. 2015. 'Natural and unnatural oil slicks in the Gulf of Mexico', *Journal of Geophysical Research-Oceans*, 120: 8364-80.

Manly, B.F. 1997. *Randomization, bootstrap and Monte Carlo methods in biology* (Chapman and Hall: London, New York).

McBride, R. S., T. E. Vidal, and S. X. Cadrin. 2013. 'Changes in size and age at maturity of the northern stock of Tilefish (Lopholatilus chamaeleonticeps) after a period of overfishing', *Fishery Bulletin*, 111: 161-74.

Meador, J. P., J. E. Stein, W. L. Reichert, and U. Varanasi. 1995. 'Bioaccumulation of Polycyclic Aromatic Hydrocarbons by Marine Organisms', *Reviews of Environmental Contamination and Toxicology <D>*, 143: 79-165.

Metcalfe, C. D., P. A. Beddows, G. G. Bouchot, T. L. Metcalfe, H. X. Li, and H. Van Lavieren. 2011. 'Contaminants in the coastal karst aquifer system along the Caribbean coast of the Yucatan Peninsula, Mexico', *Environmental Pollution*, 159: 991-97.

Mitra, S., and T. S. Bianchi. 2003. 'A preliminary assessment of polycyclic aromatic hydrocarbon distributions in the lower Mississippi River and Gulf of Mexico', *Marine Chemistry*, 82: 273-88.

Murawski, S. A., E. B. Peebles, A. Gracia, J. W. Tunnell, and M. Armenteros. 2018. 'Comparative Abundance, Species Composition, and Demographics of Continental Shelf Fish Assemblages throughout the Gulf of Mexico', *Marine and Coastal Fisheries*, 10: 325-46.

Murawski, S.A., D.J. Hollander, S. Gilbert, and A. Gracia. 2020. 'Deepwater oil and gas production in the Gulf of Mexico and related global trends.' in S.A. Murawski, C.H. Ainsworth, S. Gilbert, D.J. Hollander, C.B. Paris, M. Schluter and D.L. Wetzel (eds.), *Scenarios and Responses to Future Deep Oil Spills: Fighting the Next War* (Springer International Publishing).

Myers, M. S., L. L. Johnson, and T. K. Collier. 2003. 'Establishing the causal relationship between polycyclic aromatic hydrocarbon (PAH) exposure and hepatic neoplasms and neoplasia-related liver lesions in English sole (Pleuronectes vetulus)', *Human and Ecological Risk Assessment*, 9: 67-94.

NOAA. 2012. "Analytical Quality Assurance Plan: Mississippi Canyon 252 (Deepwater Horizon) Natural Resource Damange Assessment V3.1." In, edited by U.S. Department of Commerce NOAA.

Potvin, C., and D. A. Roff. 1993. 'Distribution-free and robust statistical methods: viable alternatives to parametric statistics', *Ecology*, 74: 1617-28.

Powers, S. P., C. H. Peterson, J. Cebrian, and K. L. Heck. 2017. 'Response of nearshore ecosystems to the Deepwater Horizon oil spill', *Marine Ecology Progress Series*, 576: 107-10.

Pulster, E. L., A. Gracia, S. M. Snyder, I.C. Romero, B. Carr, G. Toro-Farmer, and S.A. Murawski. 2020. 'Polycyclic Aromatic Hydrocarbon Baselines in Gulf of Mexico Fishes.' in S.A. Murawski, C.H. Ainsworth, S. Gilbert, D.J. Hollander, C.B. Paris, M. Schluter and D. L. Wetzel (eds.), *Scenarios and responses to future deep oil spills: Fighting the next war* (Springer Nature Switzerland AG).

Pulster, Erin L., Adolfo Gracia, Maickel Armenteros, Brigid E. Carr, Justin Mrowicki, and Steven A. Murawski. 2019. 'Chronic PAH exposures and associated declines in fish health indices observed for ten grouper species in the Gulf of Mexico', *Science of the Total Environment*: 135551.

Ruiz-Fernandez, A. C., J. M. B. Portela, J. L. Sericano, J. A. Sanchez-Cabeza, L. F. Espinosa, J. G. Cardoso-Mohedano, L. H. Perez-Bernal, and J. A. G. Tinoco. 2016. 'Coexisting sea-

based and land-based sources of contamination by PAHs in the continental shelf sediments of Coatzacoalcos River discharge area (Gulf of Mexico)', *Chemosphere*, 144: 591-98.

Santschi, P. H., B. J. Presley, T. L. Wade, B. Garcia-Romero, and M. Baskaran. 2001. 'Historical contamination of PAHs, PCBs, DDTs, and heavy metals in Mississippi River Delta, Galveston Bay and Tampa Bay sediment cores', *Marine Environmental Research*, 52: 51-79.

Scholz-Bottcher, B. M., S. Ahlf, F. Vazquez-Gutierrez, and J. Rullkotter. 2008. 'Sources of hydrocarbon pollution in surface sediments of the Campeche Sound, Gulf of Mexico, revealed by biomarker analysis', *Organic Geochemistry*, 39: 1104-08.

Schwing, P.T., D.J. Hollander, G. R. Brooks, R. A. Larson, D. W. Hastings, J.P. Chanton, S.A. Lincoln, J. R. Radovic, and A. Langenhoff. 2020. 'The Sedimentary Record MOSSFA Events in the Gulf of Mexico: A Comparison of the Deepwater Horizon (2010) and Ixtoc 1 (1979) Oil Spills.' in S.A. Murawski, C.H. Ainsworth, S. Gilbert, D.J. Hollander, C.B. Paris, M. Schluter and D.L. Wetzel (eds.), *Deep Oil Spills: Facts, Fate, and Effects* (Springer International Publishing).

Shepard, Andrew, John Valentine, Christopher D'Elia, David W. Yoskowitz, and David Dismukes. 2013. *Economic Impact of Gulf of Mexico Ecosystem Goods and Services and Integration Into Restoration Decision-Making*.

Snyder, S. M., E. L. Pulster, and S. Murawski. 2019. 'Associations between chronic exposure to polycyclic aromatic hydrocarbons and health indices in Gulf of Mexico Tilefish (Lopholatilus chamaeleonticeps) post-Deepwater Horizon', *Environmental Toxicology and Chemistry*, 38: 2659-71.

Snyder, S. M., E. L. Pulster, D. L. Wetzel, and S. A. Murawski. 2015. 'PAH Exposure in Gulf of Mexico Demersal Fishes, Post-Deepwater Horizon', *Environmental Science & Technology*, 49: 8786-95.

Soto, L.A., A. V. Botello, S. Licea-Durán, M.L. Lizárraga-Partida, and A. Yáñez-Arancibia. 2014. 'The environmental legacy of the Ixtoc-I oil spill in Campeche Sound, southwestern Gulf of Mexico', *Frontiers in Marine Science*, 1.

Steimle, F. W., V. S. Zdanowicz, and D. F. Gadbois. 1990. 'Metals and organic contaminants in Northwest Atlantic deep-sea Tilefish tissues', *Marine Pollution Bulletin*, 21: 530-35.

Stout, S. A., J. R. Payne, R. W. Ricker, G. Baker, and C. Lewis. 2016. 'Macondo oil in deep-sea sediments: Part 2-Distribution and distinction from background and natural oil seeps', *Marine Pollution Bulletin*, 111: 381-401.

Tocher, D. R. 2003. 'Metabolism and functions of lipids and fatty acids in teleost fish', *Reviews in Fisheries Science*, 11: 107-84.

United States of America v. BP Exploration & Production, Inc., et al. 2015. "Findings of fact and conclusions of law: Phase two trial. RE: Oil spill by the oil rig "Deepwater Horizon" in the Gulf of Mexico, on April 20, 2010." In, edited by U.S. District Court from the Eastern District of Louisiana.

Ward, C.H., and J. W. Tunnel. 2017. 'Habitats and biota of the Gulf of Mexico: An overview.' in C.H. Ward (ed.), *Habitats and Biota of the Gulf of Mexico: Before the Deepwater Horizon Oil Spill* (Springer Nature).

Yanez-Arancibia, A., and J. W. Day. 2004. 'Environmental sub-regions in the Gulf of Mexico coastal zone: the ecosystem approach as an integrated management tool', *Ocean & Coastal Management*, 47: 727-57.

Yanez-Arancibia, A., J.J. Ramirez-Gordillo, J. W. Day, and D.W. Yoskowitz. 2008.
'Environmental sustainability of economic trends in the Gulf of Mexico: What is the limit
for Mexican coastal development?' in J.C. Cato (ed.), *Gulf of Mexico Origin, Waters, and
Biota: Volume 2, Ocean and Coastal Economy* (Texas A&M University Press).

Chapter 4

Spatiotemporal Patterns in the Prevalence of Microscopic Hepatic Changes in Gulf of Mexico Tilefish (*Lopholatilus chamaeleonticeps*) and Associations with PAH Exposure and Hepatic Accumulation

Introduction

Polycyclic aromatic hydrocarbons (PAHs) belong to a class of organic pollutants known to be persistent in the marine environment, bioavailable, and associated with numerous negative health effects in aquatic organisms (Hylland 2006). Chronic sources of PAH pollution are of considerable concern in the Gulf of Mexico (GoM) where the main inputs are from the extensive oil and gas industry, riverine discharge (e.g. Mississippi River), transportation activities, and natural oil seeps (National Research Council 2003; Kennicutt et al. 1988). Additionally, two large submarine oil well blowouts, the 1979 *Ixtoc I* and the 2010 *Deepwater Horizon* (*DWH*) have provided large pulses of PAHs to the GoM ecosystem (National Research Council 2003; Kennicutt et al. 1988; Soto et al. 2014; Lubchenco et al. 2012). Valuable natural resources, including the GoM's productive fisheries are at risk as a result of chronic exposure to PAH-polluted environments. Numerous field studies have documented the chronic exposure of GoM fishes to PAHs and raised concerns regarding potential health effects at the individual and population level (Murawski et al. 2014; Snyder et al. 2015; Snyder, Pulster, and Murawski 2019; Pulster, Gracia, Armenteros, et al. 2020; Quintanilla-Mena et al. 2019; Gold-Bouchot et al. 2014; Struch et al. 2019; Romero et al. 2018). Negative health effects in teleosts associated with PAH

exposure include effects on the reproductive, immune, cardiovascular, endocrine, and hepatobiliary systems (Collier et al. 2014).

The hepatobiliary system is a target of PAHs and other toxicants due to its large blood supply and involvement in xenobiotic metabolism (Hinton, Segner, and Braunbeck 2001). Once exposed, teleosts can efficiently metabolize PAHs with hepatic enzymes (e.g. cytochrome P450) into more hydrophilic (water soluble) molecules for easier elimination via the bile (Varanasi, Stein, and Nishimoto 1989). The teleost hepatobiliary system also performs critical metabolic functions including uptake, processing, storage, and distribution of endogenous molecules and nutrients (e.g. glucose, lipids, proteins, hormones) (Hinton, Segner, and Braunbeck 2001). Furthermore, bile formation and excretion is handled by the functional hepatic structures (Hinton, Segner, and Braunbeck 2001). As these processes support other organ systems, deterioration of the structure or function of the hepatobiliary system may negatively affect whole organism health and fitness.

Alterations to the structure of the hepatobiliary system are commonly assessed via histology, a technique which evaluates the anatomical structures of the liver for the presence of microscopic hepatic changes (MHCs). Often referred to as hepatic lesions in the literature, many MHCs are not actually associated with disease but are related to ancillary factors including age and dietary status. MHCs encompass a wide range of cellular change, including neoplasia (cancer), pre-neoplasia (e.g. foci of cellular alteration [FCA]), and non-neoplastic MHCs (e.g. cytoplasmic vacuolation, degeneration, regeneration, inflammation, alteration in cell size or number) (Wolf and Wheeler 2018). MHCs are the most well-studied effect of PAH exposure in fishes and are often used as biomarkers in studies of contaminated environments or large-scale pollution monitoring programs (e.g. NOAA's National Status and Trends Program) as MHCs are known

96

indicators of environmental degradation that can respond on both acute and chronic timescales (Au 2004; van der Oost, Beyer, and Vermeulen 2003). However, MHCs are not specific to PAH exposure alone, therefore, it is necessary to measure both MHCs and pollutants simultaneously in order to understand associations between them.

Through decades of studies on demersal fishes living in grossly polluted bays and estuaries, a large body of research has consistently documented PAH exposure as a highly significant, major risk factor for neoplasia and associated MHCs in species including Killifish (*Fundulus heteroclitus*), and Brown Bullhead (*Ameirus nebulosus*). A cause and effect relationship has been established for English Sole (Collier et al. 2014; Myers, Johnson, and Collier 2003). The conceptual model for the sequence of histogenesis of hepatic neoplasia is defined by variables of PAH exposure (sediment PAHs, biliary PAH metabolites, hepatic PAHs, stomach PAHs), biochemical markers of early response (cytochrome P4501A induction, hepatic PAH-DNA adducts), and chronic effects (MHCs and neoplasia) (Myers, Johnson, and Collier 2003). Carcinogenesis requires the metabolism of PAHs into more reactive metabolites (e.g. benzo[*a*]pyrene-7,8-dihydrodiol-9,10-epoxide) which can directly interact with cellular macromolecules leading to PAH-DNA adducts, cellular damage, FCA, and, potentially, neoplasia (Myers, Johnson, and Collier 2003). This mutagenic process can induce proliferation of new hepatocytes that have altered (reduced) enzymatic ability to metabolize PAHs, thus, rendering new hepatocytes resistant to the mechanism of toxicity of PAHs, and ultimately protecting them from the effects of additional exposure (Collier et al. 2014). Multiple studies on Killifish from habitats heavily contaminated with persistent organic pollutants, and PAHs, have documented a heritable resistance to MHCs. However, this heritable resistance to PAH toxicity can come with the tradeoffs and potential fitness costs of increased vulnerability to other

stressors such as PAH-induced phototoxicity and hypoxia, and reductions in genetic diversity (Meyer and Di Giuliuo 2003).

Interpretations of tissue changes in relation to environmental quality is difficult since MHCs are present in healthy fish, related to age, or other confounding factors (e.g. nutritional state, underlying disease) (Wolf and Wolfe 2005). To aid in meaningful interpretation, an interdisciplinary approach measuring contaminants in conjunction with histopathological analysis is ideal. In the GoM where hydrocarbon pollution is chronic and there is persistent risk of another major oil spill, large-scale studies of biomarkers such as MHCs and their association with PAHs are imperative. Studies of MHCs in GoM fishes have been performed, however, few studies have concurrently evaluated MHCs with measured environmental pollutants in the organisms (Couch 1985; Grizzle 1986; Adams and Sonne 2013; Bentivegna et al. 2015; Mora et al. 2001; Quintanilla-Mena et al. 2019; Pulster, Gracia, Snyder, Deak, et al. 2020). Furthermore, sample size and spatial scale are often limited.

Initiated in the aftermath of *DWH*, we performed a series of demersal longline surveys on the GoM continental shelf collecting fishes to evaluate PAH contamination and associated health effects, including MHCs. Surveys were designed to assess temporal trends in the region affected by *DWH* (north central GoM), and to contrast with spatial patterns Gulf-wide. Tilefish (*Lopholatilus chamaeleonticeps*) were chosen as the study species due to consistent temporal and spatial sampling, commercial importance, and documented high exposure to PAHs (Snyder et al. 2015; Snyder, Pulster, and Murawski 2019; Snyder et al. 2020). In the present study, histological evaluation of Tilefish livers was used to describe: 1) normal microscopic anatomy, 2) MHCs and their prevalence over time and space, and 3) associations between MHCs, PAH exposure, and hepatic accumulation. Following the design of the classic English Sole studies

referenced above, biliary PAH metabolites and hepatic PAHs were used as variables of PAH exposure and accumulation, respectively, to predict prevalence of MHCs in Tilefish.

Materials and Methods

Field Sampling

From 2011 to 2017 a series of multinational fisheries-independent demersal longline surveys were conducted on the GoM continental shelf. Herein, selected samples collected from 24 stations from four large regions of the GoM, the north central, northwest, Bay of Campeche, and Yucatán Shelf, were selected to evaluate spatial patterns (Table 4.1, Figure 4.1). Samples from five stations in the north central GoM sampled annually from 2012 to 2015 were selected to evaluate temporal trends.

Tilefish were collected via demersal longline surveys onboard the *R/V Weatherbird II* in the summers of 2012 to 2016. Comprehensive longlining methods are described in Murawski et al. (2018). Briefly, at each sampling station, five miles of monofilament main line was set with an average of 460 evenly spaced #13/0 circle hooks baited with cut Humbolt squid (*Dosidicus gigas*) wings and Atlantic Mackerel (*Scomber scombus*) for a soak time of approximately two hours. Tilefish were landed from water depths ranging from 163 to 581 m with a mean depth of 274 m.

Tilefish were sampled immediately upon capture or placed on ice briefly until processing could occur. All fish were measured for lengths (standard, total, fork) and total body weight. A subsample of individuals was sacrificed to collect tissues and organ weights (liver, gastrointestinal, gonad). Sex was determined visually (macroscopically) during dissection as male, female, or unknown according to criteria of McBride, Vidal, and Cadrin (2013). Segments

of the liver were excised for histological and PAH analyses. First, the liver was sectioned for

histological analyses by excising three thin slices of tissue from three separate areas of the liver,

which were stored in 10% neutral buffered formalin (NBF) solution. Histology samples were

stored in solution at room temperature until processing. All remaining liver tissue was placed in

precleaned aluminum foil and inserted into Whirl-Paks[TM] (2012) or combusted glass jars (2013-

2016). If bile was present, the contents of the gallbladder were drained into a precleaned amber

vial. Liver and bile samples for PAH analysis were frozen immediately and stored at -20 °C

until analysis.

Histopathology

Tilefish liver samples underwent gross examination, processing, and histological

evaluation at Fishhead Labs, LLC, by a board-certified veterinary pathologist. An arbitrary

accession number was assigned to each sample for processing and to ensure evaluation of the

slides was unbiased with respect to location and date of collection. Representative sections of all

tissues in the sample container were made and placed into cassettes for routine histological

processing. All sections were stained with Hematoxylin and Eosin (H&E). After preliminary

evaluation, several fish were chosen to characterize specific MHCs with special stains, including

Periodic Acid-Schiff (PAS) with and without diastase, Masson's trichrome, Gram-stain, Perl's

Iron (PI), Von Kossa (VK), Gimori methenamine silver stain (GMS), and Oil red O.

Microscopic examination was performed using a Nikon Eclipse 80i and photomicrographs were

taken with an Accu-scope Excelis HD. MHCs were scored as zero (absent) or one (present), and

prevalence of each MHC was calculated as the percentage of individuals in a group with an

MHC present.

Hepatic PAH Accumulation

Liver samples were analyzed for PAHs and alkylated homologs using a modified QuEChERS extraction followed by separation and quantification via gas chromatography tandem mass spectrometry. Detailed extraction, analytical, and quality assurance methods followed those in Snyder, Pulster, and Murawski (2019). Analyte concentrations were reported to three significant figures in units of ng/g wet weight (w.w.). The sum of all PAH analytes ($n = 46$) is reported as $TPAH_{46}$. The sum of low molecular weight (LMW) PAHs was quantified as the sum of all two to three ring PAHs. The sum of high molecular weight (HMW) PAHs was quantified as the sum of all four to six ring PAHs. Procedural and solvent blanks, post-extraction standard, and surrogate standard recoveries in samples ($82 \pm 5\%$), matrix spikes ($84 \pm 5\%$), and the NIST SRM 1974c (organics in mussel tissue) certified reference material ($82 \pm 9\%$) all met QA standards reported in NOAA (2012).

Liver samples were also analyzed for total lipid via methods of Snyder, Pulster, and Murawski (2019), however, hepatic PAH data were not lipid-normalized as there was no relationship between $TPAH_{46}$ and total lipid (Hebert and Keenleyside 1995).

Biliary PAH Metabolites

Bile samples were analyzed for naphthalene (NPH) and benzo[*a*]pyrene (B*a*P) metabolite equivalents (fluorescent aromatic compounds [FACs]) using a standard semi-quantitative high performance liquid chromatography with fluorescence detection method (Krahn et al. 1986; Krahn et al. 1984). Biliary PAH metabolite equivalents were reported to two significant figures in units of μg FACs/g of bile. Sum total of NPH and B*a*P metabolite equivalents is reported as

total biliary PAH metabolite equivalents. Comprehensive analytical methods and quality

assurance practices followed those of Snyder et al. (2015).

Statistical Analyses

Data were binned into regional groups *a priori* (Figure 4.1, north central, northwest, Bay

of Campeche, Yucatán Shelf). Statistics were performed on all regions combined, as well as

each region individually. All statistical analyses were performed in Matlab R2017a using the

Fathom Toolbox for Matlab (Jones 2017). All statistical tests generated permutation-based *p*-

values (*n* = 1000 iterations) which were evaluated at α = 0.05. A redundancy analysis was used

to evaluate the association between biometrics and MHC prevalence. Likelihood ratio chi-

square tests of independence were used to evaluate differences in MHC prevalence and sex ratio

by region. Linear regressions were used to evaluate associations between MHCs and PAH

variables.

Results

Gross Evaluation of Tilefish Livers

Gross evaluation of Tilefish livers (*n* = 239) revealed a spectrum of morphologic

variations. In general, hepatic tissues were comprised of numerous irregular lobules separated

by variable amounts of thin, clear connective tissue (Figure D1). Level of lobulation varied

between individuals. Randomly interspersed throughout the parenchyma were small and large

blood vessels, as well as biliary ducts. The coloration of the parenchyma ranged from light to

dark tan, and many samples had dark brown mottling on the serosal surface that extended in

between lobules, consistent with fixed blood. Lighter colored livers were prone to fragmentation during handling.

Histological Evaluation of Tilefish Livers for MHCs

The normal microscopic anatomy of Tilefish liver was characterized by a muralium configuration of double-layered cords arranged in branching tubules (Figure D2). Cords of hepatocytes were arranged in large islands, or lobules, separated by thin layers of fibrous connective tissue and exocrine pancreatic acini. Hepatocytes were polygonal with moderate amounts of granular cytoplasm. Exocrine pancreatic acini were interspersed throughout the hepatic parenchyma. Exocrine pancreatic epithelial cells surrounded vessels and were filled with eosinophilic intracytoplasmic zymogen granules. Bile ducts were sporadically distributed in portal areas or randomly throughout the parenchyma. Bile ducts were lined by cuboidal epithelium supported by concentric layers of collagenous tissue of variable thickness (Figure D3).

Histological evaluation of Tilefish livers ($n = 239$) revealed a spectrum of MHCs described below (Table 4.2). Overall, 99% of Tilefish examined exhibited at least one MHC. There was no relationship between the prevalence of MHCs and biometric predictor variables of sex, total length, and age, as evaluated by a distance-based redundancy analysis. Age data were provided by Helmueller (2019).

Glycogen-type vacuolar change was the most prevalent MHC, identified in 78% of Tilefish. Glycogen-type vacuolar change was characterized by mild to moderate cellular swelling and diffuse expansion of the hepatocytes by wispy, vacuolated eosinophilic cytoplasm

(Figure D4). Individuals with vacuolization frequently had increased fragmentation of lobules and mild to moderate hemorrhage in between lobules.

Biliary fibrosis was the second most prevalent MHC, identified in 55% of Tilefish. Biliary fibrosis was characterized by inflammation and fibrosis around the bile ducts (Figure D5) and was confirmed with Masson's trichrome stain. Biliary duplication was identified in 3% of Tilefish, and present in cases of prominent biliary fibrosis (Figure D6).

Increased incidence of pigmented macrophage aggregates (PMA) was the third most prevalent MHC, observed in 53% of Tilefish. Two different pigments were present as established by special staining techniques. The first, PAS positive, diastase negative material, was suspected to be ceroid or lipofuscin (indistinguishable via light microscopy) and identified in 76% of individuals with PMA (Figure D7A). The second, hemosiderin, was positive with PI and identified in 34% of individuals with PMA (Figure D7B).

Lipid-type vacuolar change was identified in 28% of Tilefish and characterized by intracytoplasmic, discrete micro- or macrovesicles with distinct rounded borders (Figure D8).

Granulomas were identified in 25% of Tilefish. Some individual sections contained > five granulomas. Granulomas were composed of a central degenerate nematode larvae, cellular debris, or mineralized debris surrounded by concentric layers of flattened macrophages or fibrous connective tissue (Figure D9). Some granulomas had lymphocytes and plasma cells at the periphery. Lymphocytes and plasma cells admixed with rare eosinophilic granular cells occasionally expanded the connective tissues within the pancreas, surrounded bile ducts, or scattered throughout the hepatic cords. This inflammatory component was attributed to the presence of migrating metazoan larvae. Three individuals had granulomas containing presumptive mesomycetozoans.

Two different FCA were identified in Tilefish: basophilic (Figure D10A) and clear-cell (Figure D10B). Basophilic foci were identified in 8% of Tilefish, while a clear-cell focus was found in only one individual, for a combined FCA prevalence of 8%. Basophilic foci were characterized by a focal irregular area of hepatocytes, often adjacent to a vein, that were mildly disorganized and had darker basophilic cytoplasmic contents with less vacuolization than surrounding hepatocytes (Figure D10A). FCA were identified in Tilefish ages 3 to 14.

Inflammation and lymphocytic aggregation were present in 8% of Tilefish, often associated with the presence of migrating parasite larvae (Figures D11A&B). Larvae were either present randomly within the hepatic cords (Figure D11C) or encapsulated within a granuloma. Loose parasitic larvae (i.e. not encapsulated in granulomas), identified in 4% of Tilefish, were commonly metazoans consistent with larval nematodes.

Hepatocellular atrophy was identified in 7% of Tilefish and was characterized by cellular shrinkage, decreased cytoplasm, and crowding of nuclei (Figure D12). Hepatocellular necrosis (Figure D13) occurred in 1% of Tilefish. Necrosis of the bile ducts and vascular structures was rare.

Only one Tilefish, an eight-year-old female from the north central GoM sampled in 2012, had a neoplasm. The neoplasm was consistent with a hepatocellular adenoma, described as a non-encapsulated, poorly circumscribed, moderately cellular, neoplasm composed of hepatocytes arranged in nodular islands supported by fine fibrovascular stroma (Figure D14). Neoplastic cells had variably distinct cell borders, moderate amounts of eosinophilic granular cytoplasm, round nuclei with finely stippled chromatin, and one distinct basophilic nucleolus. Mitoses were rare, at less than 1 per 40x high powered field. Anisocytosis and anisokaryosis were mild. Low

numbers of lymphocytes were present around small vessels at the periphery of the mass. The neoplastic nodules compressed the adjacent pancreas and neighboring normal hepatocytes.

One Tilefish had pseudocystic areas, characterized by hepatocyte loss and the presence of a cyst-like structure within the parenchyma (Figure D15). The pseudocyst contained cellular debris, rare eosinophilic granular cells, and eosinophilic homogenous fluid lined by attenuated epithelial cells. One Tilefish had ito cell hyperplasia, characterized by an increase in the number of ito cells, also called stellate cells, or lipocytes.

Artefactual Changes Observed via Histology

Bacteria were observed in the livers of six Tilefish. Bacteria were characterized as Gram-negative short rods that were present within the vascular spaces (Figure D16). Autolysis was prominent in some of the sections, but not all. Radiating basophilic material, which stained positive with VK, was observed within vessels, adjacent to vessels, in areas of hepatocellular loss, and within peripancreatic tissues (Figure D17). Lastly, fragmentation and hemorrhage between lobules was common, especially in fish with moderate to severe glycogen-type vacuolar change. Acid formaldehyde hematin was observed in several sections.

Spatial Patterns in MHC Prevalence

Prevalence of increased PMA ($X^2 = 8.17$, $p = 0.043$), biliary fibrosis ($X^2 = 33.2$, $p < 0.001$), and hepatocellular atrophy ($X^2 = 10.7$, $p = 0.014$) were significantly different by region (Table 4.2). Prevalence of increased PMA and biliary fibrosis were highest in the Bay of Campeche. Hepatocellular atrophy was most prevalent in the north central GoM. The Yucatán Shelf had a distinctly low prevalence of MHCs compared to the other regions of the GoM. Two

MHCs, glycogen-type vacuolar change and biliary fibrosis, were identified in Tilefish from all 24 stations sampled around the GoM.

Temporal Trends in MHC Prevalence

Time series data were analyzed from five stations in the north central GoM sampled annually from 2012 to 2015. The prevalence of five MHCs increased over time (Figure 4.2). Prevalence over time increased by 30% for glycogen-type vacuolar change, 70% for inflammation with lymphocytic aggregation, 75% for granulomas, and 92% for both increased PMAs and biliary fibrosis. Prevalence of FCA was variable over time, decreasing from 10% of individuals in 2012 to 0% in 2014, and then increasing to 15% in 2015. Prevalence of one MHC, lipid-type vacuolar change, decreased by 47% from 2012 to 2015 (Figure 4.3).

Associations Between MHCs and Hepatobiliary PAHs

Of the 239 Tilefish examined for MHCs, 231 liver samples were also analyzed for PAHs and alkylated homologs, and 213 bile samples were analyzed for PAH metabolites. For all regions combined, there were statistically significant linear relationships between mean liver $TPAH_{46}$ and prevalence of parasites, lipid-type vacuolar change, increased PMA, hepatocellular atrophy, and necrosis by station (Figure 4.4). There was also a significant linear relationship between mean total biliary PAH metabolites and prevalence of hepatocellular atrophy by station ($R^2 = 11.6\%$, $p = 0.001$).

For the north central GoM stations, there were significant linear relationships between mean liver $TPAH_{46}$ and prevalence of glycogen-type vacuolar change, biliary fibrosis, necrosis, parasites, FCA, and hepatocellular atrophy (Figure 4.5A). For the northwest GoM stations, there

were significant linear relationships between mean liver $TPAH_{46}$ and prevalence of hepatocellular atrophy, parasites, inflammation, and lipid-type vacuolar change (Figure 4.5B). For the Bay of Campeche stations, there were significant linear relationships between mean liver $TPAH_{46}$ and parasites, necrosis, increased PMA, lipid-type vacuolar change, and granulomas (Figure 4.5C). For the Yucatán Shelf stations, there were significant linear relationships between mean liver $TPAH_{46}$ and glycogen-type vacuolar change, lipid-type vacuolar change, and biliary fibrosis (Figure 4.5D). Regressions with biliary fibrosis and glycogen-type vacuolar change had negative slopes for the Yucatán Shelf. Although the linear relationships may be statistically significant, interpretations should consider the small sample sizes of the northwest GoM, the Bay of Campeche, and the Yucatán Shelf.

Discussion

MHC Prevalence

This study is the first to report microscopic hepatic anatomy and changes in Tilefish. Normal anatomy was described and a total of 14 MHCs were identified in GoM Tilefish, ranging from mild to severe (e.g. cancerous) changes. Prevalence of MHCs was unrelated to biometrics of age, sex, and total length. The most prevalent MHCs (>25% individuals) observed were glycogen-type vacuolar change, biliary fibrosis, increased PMA, lipid-type vacuolar change, and granulomas. More minor MHCs (<25% individuals) observed were bile duct duplication, FCA, inflammation with lymphocytic aggregation, parasites, hepatocellular atrophy, necrosis, neoplasia, pseudocystic areas, and ito cell hyperplasia.

All 14 MHCs observed in GoM Tilefish have been described in the teleost literature, whether or not in association with exposure to environmental pollutants or other toxicants

(Couch 1991; Boorman et al. 1997; Reddy et al. 1999; Hinton, Segner, and Braunbeck 2001; Pacheco and Santos 2002; Agius and Roberts 2003; Wolf and Wolfe 2005; Miranda et al. 2008; Wolf and Wheeler 2018; Adams and Sonne 2013; Feist et al. 2015; Fricke et al. 2012; Schlacher, Mondon, and Connolly 2007; Pal et al. 2011; Marty et al. 2003; Marigómez et al. 2006; Mora et al. 2001; Pinkney et al. 2004; Ranasingha and Pathiratne 2015). Compared to prevalence in other wild-caught teleosts from the aforementioned studies, GoM Tilefish have a higher prevalence of biliary fibrosis, lower prevalence of necrosis and neoplasia, and similar prevalence of vacuolation, increased PMA, granulomas, and FCA. The majority of these studies have been in estuarine or coastal environments where anthropogenic pollution is typically higher but in different composition compared to offshore Tilefish habitat in the GoM. Therefore, it is striking that Tilefish, an offshore continental shelf edge species, generally have similar prevalence of MHCs. Feist et al. (2015) also reported similar prevalence of MHCs in teleosts sampled offshore on the continual shelf/slope (100-1500 m) of the northeast Atlantic Ocean. These results may indicate that offshore environments are becoming more polluted and inhabitants are exhibiting health effects similar to nearshore species.

In the GoM specifically, histological analyses have been performed on a variety of teleosts and in relation to oil exposure. Bentivegna et al. (2015) found MHCs in 40% of Menhaden (*Brevoortia sp.)* sampled post-*DWH* and concluded the prevalence of tissue damage was higher and more extensive in GoM Menhaden compared to Menhaden from an unoiled, urban site in New Jersey. Grizzle (1986) found significantly higher prevalence of hepatic fatty change, likely akin to lipid-type vacuolar change, in Southern Hake (*Urophycis floridana*) sampled near active oil platforms vs. control locations. Granulomas were present and associated with parasitic infections, though, unassociated with platforms. Mora et al. (2001) associated

increased ceroid/lipofuscin PMA, identified in 40 to 100% of fishes, with tissue levels of insecticides, such as DDE. Lastly, Adams and Sonne (2013) identified glycogen accumulation as the most prevalent MHC in Goliath Grouper (*Epinephelus itajara*; 100%), along with necrosis (87%), portal fibrosis (47%), increased PMA (53%), and granulomas, and ultimately concluded the MHCs were likely related to mercury accumulation, oxidative or energetic (e.g. starvation) stress, pathogenic infection, and/or temperature stress from a recent cold event.

Rightfully so, the wild-caught teleost MHC literature has focused on formation and prevalence of pre-neoplasia and neoplasia in relation to high levels of chronic pollution in urban and industrialized estuaries (Myers, Johnson, and Collier 2003; Collier et al. 2014). In English Sole from Puget Sound, Washington and Killifish from the Elizabeth River, Virginia, prevalence of FCA can top 80% and prevalence of neoplasia can reach 40% (Krahn et al. 1986; Malins et al. 1985; Malins et al. 1987; Myers, Rhodes, and McCain 1987; Vogelbein, Unger, and Gauthier 2008). Comparatively, FCA and neoplasia prevalence in GoM Tilefish was substantially lower (8% and <1%, respectively). As GoM Tilefish were collected at offshore depths far removed from urban and coastal point sources of pollution, the concentrations of PAHs in sediment (discussed below) are lower than concentrations reported in Puget Sound (5900-120,000 ng/g dry wt.) and the Elizabeth River (730-37,751 ng/g dry wt.), which, on average, can be greater than 80% HMW (carcinogenic) PAHs in both locations (Myers et al. 1994; Vogelbein, Unger, and Gauthier 2008; Malins et al. 1985). Horness et al. (1998) used a two-segment hockey stick regression and ten years of data from the National Benthic Surveillance Project to identify thresholds of 54 ppb and 2,800 ppb for sediment aromatic hydrocarbon concentrations needed to induce pre-neoplasia and neoplasia in English Sole. Post-*DWH* PAH concentrations in sediments in the De Soto Canyon region of the GoM (1000-1500 m depth) were 70 to 524 ng/g

dry weight and LMW PAHs were dominant over HMW PAHs (Romero et al. 2015). At

shallower sites in the De Soto Canyon closer to where Tilefish were sampled, total sediment

PAH concentrations did not exceed 500 ng/g dry weight, and LMW PAHs were also primarily

dominant (I.C. Romero unpublished data). As a result, Tilefish from the GoM have lower

exposure to PAHs, particularly HMW PAHs, as measured by BaP metabolite equivalents (320 $\pm$

300 ng FAC/g; mean $\pm$ one standard deviation), compared to English Sole from Puget Sound

(1,000-3,600 ng/g) (Krahn et al. 1986; Malins et al. 1987; Myers et al. 1994). A series of studies

on GoM Tilefish identified ~99% of PAH exposure and hepatic accumulation is LMW

(petrogenic) PAHs, with hepatic HMW (pyrogenic) PAH accumulation rarely identified above

instrument detection limits (Snyder et al. 2015; Snyder, Pulster, and Murawski 2019; Snyder et

al. 2020). This difference in PAH exposure (LMW vs. HMW) may be contributing to the low

FCA and neoplasia prevalence in GoM Tilefish, as models have consistently identified HMW

PAHs as more of a significant risk factor for hepatic neoplasia (Myers, Johnson, and Collier

2003; Collier et al. 2014; Horness et al. 1998). However, in the north central GoM there was a

significant association between pre-neoplastic FCA prevalence and hepatic PAH accumulation.

Artefacts

In addition to MHCs, three tissue preservation artifacts were observed in samples.

Bacteria within the vasculature is a common post-mortem finding due to movement of bacteria

throughout the body after death. Bacteria seen herein were not eliciting a pathologic response in

the tissues and were considered an incidental finding. Radiating basophilic mineral deposits

were observed in numerous samples, likely due to prolonged fixation in neutral buffered

formalin. Prolonged fixation can lead to alteration of 10% NBF pH, allowing for precipitation of

material in the tissues. In the present case, VK staining indicates the precipitate is presumably phosphate-based. Lastly, fragmentation and hemorrhage were observed in several samples, likely as a result of tissue sampling technique.

Temporal Trends and Spatial Patterns in MHCs

The prevalence of glycogen-type vacuolar change, biliary fibrosis, inflammation with lymphocytic aggregation, granulomas, increased PMA, biliary fibrosis, and FCA increased over the study period in the north central GoM where repeat stations were sampled between 2012 to 2016. The majority of these MHCs were inflammatory responses and their increases over time were considerable (>70%). Glycogen-type vacuolar change, biliary fibrosis, and FCA prevalence were also associated with hepatic accumulation of PAHs in this region. A time series analysis of PAH exposure and hepatic accumulation in Tilefish from these same GoM locations indicated a 178% increase in PAH exposure over the same time period, possibly related to the increase in prevalence of inflammatory MHCs (Snyder, Pulster, and Murawski 2019).

In addition, prevalence of lipid-type vacuolar change decreased by 47% over the study period, Snyder, Pulster, and Murawski (2019) also reported a 53% decrease in total liver lipid in northern GoM Tilefish 2012 to 2017, as measured by a modified Folch extraction. These two independent measures of liver lipid content indicate decreased storage of liver lipids in northern GoM Tilefish, which may result in serious health consequences, as teleosts use lipids as main energy sources for growth and reproduction (Tocher 2003). Paired with the increase in glycogen-type vacuolization, this suggests that Tilefish from the north central GoM may be switching from hepatic storage of lipid to glycogen (Figure 4.3), possibly as a response to chronic and relatively high levels of PAH exposure and hepatic PAH concentrations in the

region. Together, the time series of PAH exposure, hepatic PAH concentrations, associated

health indices in the north central GoM suggest increasing liver damage, changing physiology,

and decreasing condition factor, in conjunction with increasing PAH exposure. In order to fully

investigate the alterations to energy storage, additional studies on glycogen, lipid, and fatty acids

in Tilefish are needed.

Spatial patterns in MHC prevalence were difficult to interpret as MHCs were observed in

similar magnitude throughout three out of four GoM regions: north central, northwest, and the

Bay of Campeche. Prevalence of MHCs was typically low on the Yucatán Shelf, where three out

of four Yucatán Shelf stations had below average prevalence of MHCs. Overall, spatial patterns

in MHC prevalence did not precisely align with PAH exposure, and hepatic PAH concentrations

as assessed in Snyder et al. (2020), suggesting there may be regional differences in physiology in

response and adaptation to chemical insult. Quintanilla-Mena et al. (2019) hypothesized low

levels of pollutants and associated biomarkers in Shoal Flounder (*Syacium gunteri*) sampled on

the Yucatán Shelf compared to the rest of the Mexican continental shelf. However, their study

found the highest histopathological lesions index, a cumulative index of pathologies, on the

Yucatán Shelf, and the lowest index in the Bay of Campeche. Their results are inconsistent with

spatial patterns in MHCs in GoM Tilefish, which may be due to difference in species, sampling

location, and histopathological technique. Red Snapper (*Lutjanus campechanus*) sampled on the

Yucatán Shelf also had high proportion of individuals affected by MHCs (Pulster, Gracia,

Snyder, Deak, et al. 2020). As both Shoal Flounder and Red Snapper occupy shallower waters

than Tilefish, sampling location/depth may be causing the difference in prevalence of MHCs

seen in different teleosts sampled on the Yucatán Shelf.

Hepatic accumulation of PAHs in GoM Tilefish was significantly associated with the following ten MHCs for all data combined or within a region: glycogen and lipid-type vacuolar change, biliary fibrosis, increased PMA, granulomas, FCA, inflammation with lymphocytic aggregation, parasites, hepatocellular atrophy, and hepatocellular necrosis. Sample size was lower in certain regions (e.g. Yucatán Shelf), therefore, interpretations of significant regressions in certain regains should utilize caution. The north central GoM had the highest number of significant associations between hepatic PAH accumulation and MHC prevalence, and the highest levels of PAH exposure and hepatic accumulation (Snyder et al. 2020). Herein, PAH data were used as predictor variables for MHC prevalence. In-depth analysis of temporal and spatial patterns of PAH exposure and hepatic accumulation in GoM Tilefish are discussed elsewhere (Snyder, Pulster, and Murawski 2019; Snyder et al. 2020).

Hepatic glycogen and lipid-type vacuolar change in teleosts is well-described in the literature and often characterized as a toxicological response. However, inconsistent information (both increases and decreases) is published on the relationship between vacuolization and contaminant exposure, and can be commonly observed in control fishes (Boorman et al. 1997). Contaminant exposure may affect the hormonally-controlled production and/or storage of glucose and lipid in the liver, leading to changes vacuolization. Changes in vacuolation have been observed in fishes as a response to *DWH* oil, organochlorine pesticides, diethylnitrosamine (DEN), and dehydroabietic acid (DHAA) exposure (Boorman et al. 1997; Pacheco and Santos 2002; Miranda et al. 2008; Brown-Peterson et al. 2015; Wolf and Wolfe 2005). Southern Flounder (*Paralichthys lethostigma*) exposed to weathered *DWH* oil via sediment for 32 days exhibited increases in both glycogen and lipid-type vacuolation, which was not observed in

114

control fishes; which the authors concluded this was due to an observed decrease in feeding, malabsorption of nutrients, and a negative energy balance in exposed individuals (Brown-Peterson et al. 2015). While counterintuitive, malnourished fishes are known to protect hepatic glycogen stores (Hinton, Segner, and Braunbeck 2001). In addition to contaminant exposure, vacuolization may also be a response to an energy rich diet (particularly in captive fishes), stress, underlying disease or starvation (Hinton, Segner, and Braunbeck 2001; Gambardella et al. 2012). Healthy fishes, both wild and captive, may also store large amounts of hepatic lipid which fluctuate with nutritional state, season, temperature, sex, reproductive state, etc. (Hinton, Segner, and Braunbeck 2001). As all Tilefish examined herein were captured in summer and beyond the known spawning window for GoM Tilefish (January-June), season and reproductive state should not be influencing observations of vacuolization. Bottom temperature at sampling stations between regions was determined to be statistically similar (Snyder et al. 2020). The consistency of association between hepatic PAH accumulation and vacuolization in Tilefish indicates that PAHs are affecting Tilefish liver metabolism, leading to alterations in storage of hepatic glycogen or lipid. In the north central GoM specifically, temporal trends in declines of hepatic lipid storage in association with increasing PAH exposure and decreasing condition factor suggest chronic and increasing PAH exposure effecting energy storage, which has serious implications for individual health, reproductive success, recruitment, and ultimately population health.

Atrophy, or cellular shrinkage, may be a response to starvation, decreased blood supply, pressure from an adjacent MHC, or toxicant exposure, and may indicate compromised organ function. Hepatocellular atrophy has been observed in fishes exposed to DHAA (Pacheco and Santos 2002). Hepatocellular atrophy was rare in GoM Tilefish but had significant associations

with both PAH exposure and hepatic accumulation. Atrophy was the only MHC with a significant association with the short-term biomarker of PAH exposure, biliary PAH metabolites, suggesting quick onset post-exposure.

Necrosis, or premature cell death, is a clearly pathogenic MHC in response to toxin exposure (Wolf and Wolfe 2005). Hepatocellular necrosis in fish has been associated with numerous toxicants, including acetaminophen, allyl formate, carbon tetrachloride, organochlorine pesticides, BaP, bleached kraft pulp mill effluent, DEN, and DHAA (Boorman et al. 1997; Hinton, Segner, and Braunbeck 2001; Pacheco and Santos 2002; Miranda et al. 2008). Induction of necrosis by allyl formate, a model hepatotoxin, is due to binding of metabolites to cellular macromolecules (Hinton, Segner, and Braunbeck 2001). PAH metabolites are also known to bind to cellular macromolecules; therefore, it is possible the mechanism between PAH exposure and hepatocellular necrosis may be similar to that of allyl formate. Although rare in GoM Tilefish, necrosis was significantly associated with hepatic accumulation of PAHs in all regions combined, the north central GoM and the Bay of Campeche.

Increased PMA was common in GoM Tilefish and associated with hepatic accumulation of PAHs in all regions combined and the Bay of Campeche. PMA are distinctive groups of pigment-containing phagocytic cells that are constitutively present in the liver, spleen, and kidney of most teleost species, and increases in density have been frequently recommended as biomarkers of environmental quality (Agius and Roberts 2003; Wolf and Wolfe 2005). As phagocytic and immune cells, PMA functions include sequestration and detoxification of both exogenous and endogenous materials, including iron, free radicals, products of erythrocyte and cell membrane breakdown, and bacteria, as well as antigen presentation to lymphocytes (Wolf and Wolfe 2005). Contaminants associated with increases in PMA in fish include BaP, crude

116

oil, bleached kraft pulp mill effluent, and DHAA (Pacheco and Santos 2002; Ali et al. 2014).

Increases in PMA in fish have also been associated with age, stress, infectious disease, parasites, starvation, tissue catabolism, nutritional deficiencies, toxicant-induced hemolytic anemia, and degenerative necrotic conditions (Myers, Rhodes, and McCain 1987; Agius and Roberts 2003; Pacheco and Santos 2002). Ceroid and lipofuscin pigments are often called "wear and tear" pigments, as they accumulate with tissue destruction and age, and may also accumulate with dietary deficiencies, wasting syndrome, bacterial or viral infections, or toxin exposure (Agius and Roberts 2003). Hemosiderin, derived from the breakdown of hemoglobin, accumulates with increased destruction of damaged erythrocytes (e.g. hemolytic anemia), starvation, and when there are increases in iron storage as a protective mechanism (Agius and Roberts 2003). Hemosiderin and ceroid/lipofuscin are often observed together, as they were in GoM Tilefish. The presence of hemosiderin laden macrophages appeared to be closely associated with metazoan infections, or sections with inflammation. The intracellular accumulation of ceroid/lipofuscin was more closely associated with moderate to severe glycogen-type vacuolation.

Inflammatory MHCs were frequently observed together and had significant associations with hepatic PAH accumulation. Parasites are common findings in wild-caught fishes where prevalence and parasite load can be extremely high, and presence may effect organ function and nutritional state (Dezfuli et al. 2016; Buchmann and Mehrdana 2016; Marigómez et al. 2006). Granulomas are one host response to parasitic infection: walling off and degrading the organism. Granulomas may also be associated with bacterial or fungal infections, foreign body reaction, exogenous compounds, water quality, and dietary quality (Good et al. 2016). Hepatocellular inflammation has been described in fishes exposed to organochlorine pesticides, BaP, bleached

kraft pulp mill effluent, and DHAA (Pacheco and Santos 2002; Miranda et al. 2008). The presence of these inflammatory MHCs may serve as an indicator of underlying disease, possibly related to PAHs, as exposure has been linked to altered immune parameters, which may lead to a decreases in ability respond to and fight off pathogenic threats in fishes (Reynaud and Deschaux 2006; Bayha et al. 2017; Rodgers, Takeshita, and Griffitt 2018; Murawski et al. 2014).

Biliary fibrosis was associated with hepatic PAH accumulation in Tilefish from the north central GoM. Biliary fibrosis is an inflammatory process that is a manifestation of chronic biliary injury. It may be related to toxicant exposure or idiopathic (Wolf and Wolfe 2005). Biliary fibrosis may lead to structural damage of the bile ducts (Pinzani and Luong 2018). As the biliary system is critical for organism health, due to its role in secretion and elimination of bile acids, endogenous metabolic byproducts, and xenobiotic metabolites, any impairment of function may lead to more serious injury.

FCA were associated with hepatic PAH accumulation in Tilefish from the north central GoM, where in combination with other declining health indices, there is concern over significant effects on Tilefish health and fitness in relation to chronic PAH exposure.

Difficulties in Interpretation of MHCs as a Biomarker

Even in conjunction with contaminant analyses, interpretation of histopathological findings in field studies is challenging. Most large-scale field studies of teleost liver histopathology have focused on species from highly polluted coastal environments and the formation, prevalence and modeling of cancerous hepatic neoplasia (Stehr et al. 2003; Myers et al. 1994; Myers, Rhodes, and McCain 1987; Myers et al. 1990; Myers, Johnson, and Collier 2003; Malins et al. 1987; Malins et al. 1985; Johnson et al. 1993; Johnson et al. 1998; Horness et

al. 1998). Studies discussing the more subtle MHCs are less common, typically from exposure studies on small laboratory-reared or ornamental fish, and the mechanism of toxic injury in fishes is largely unknown. Studies that link MHCs to contaminants quantified in fish tissues or the environment, particularly in offshore species, are rare. Another pitfall in the literature often highlighted by reviews is the publication of studies with questionable accuracy and conclusions, due to novice pathologists, range of structural and functional diversity in fishes leading to difficulties differentiating between normal anatomic features and histopathologic changes, confounding factors (e.g. underlying disease, dietary deficiencies) and frequency of incidental and artefactual changes (Wolf and Wolfe 2005; Wolf et al. 2015). Presence of MHCs can be difficult to observe as their distribution in teleosts livers is random due to lack of zonal architecture and tissue samples evaluated are often a tiny fraction of the total organ (Hinton, Segner, and Braunbeck 2001). Histological evaluation by a highly experienced pathologist and accurate contaminant quantification are both expensive and require substantial training. Lastly, MHCs are not specific to one class of pollutants or pollutants alone. Fishes are exposed to complex mixtures of contaminants and influenced by other stressors (e.g. hypoxia, temperature stress) in the environment, all of which have the ability to alter hepatic structure and function, leading to observed MHCs. Together, these complexities make the interpretation of results challenging beyond simple associations between MHCs and pollutants quantified. Nevertheless, studies like ours are valuable in yielding Gulf-wide baseline data on MHCs in an offshore, commercially important fish with a reputation of high PAH exposure.

Conclusions

This study of MHCs in GoM Tilefish, covering both an expansive spatial scale and a four-year time series, is the first assessment of liver anatomy and microscopic changes in Tilefish. Analysis revealed a broad spectrum of cellular-level changes, ranging from mild to severe. Fourteen MHCs were identified, ten of which (glycogen and lipid-type vacuolar change, biliary fibrosis, increased PMA, granulomas, FCA, inflammation with lymphocytic aggregation, parasites, hepatocellular atrophy, and necrosis) were found to be associated with hepatic PAH accumulation. Hepatocellular atrophy was the only MHC associated with short-term exposure to PAHs. MHC prevalence was generally uniform across the GoM, with the exception of lower prevalence on the Yucatán Shelf. Prevalence of multiple MHCs was similar to studies of fish from estuarine and coastal environments, suggesting that pollution and its health effects are moving further offshore to the continental shelf edge where Tilefish reside. The most prevalent MHCs were inflammatory and vacuolar changes. Pre-neoplastic FCA and neoplasia were rare, however, FCA prevalence was associated with hepatic PAH accumulation in Tilefish from the north central GoM, and prevalence increased in 2015. Inflammatory MHCs and glycogen-type vacuolar change also increased significantly over this time period, while lipid-type vacuolar change decreased, indicating a potential switch in the molecular form of energy storage from lipid to glycogen. While the implications of this switch are unknown, liver metabolism and energy storage should be evaluated further in GoM Tilefish as hepatic lipids are known to be critical energy stores for teleosts. Together with results from a more extensive time series of PAH exposure and health indices in Tilefish from the north central GoM, PAH exposure and inflammatory MHCs are increasing, and health indices of Fulton's condition factor and two independent measures of hepatic lipid storage are decreasing. Continued monitoring of Tilefish

in the north central GoM is necessary in order to fully understand the impacts of living in a

chronically polluted environment.

Overall, MHCs identified in Tilefish are less severe and concerning than high prevalence

of neoplasia commonly observed in demersal fishes from polluted estuaries. However, results

suggest Tilefish liver function may be affected by chronic PAH exposure, specifically, changes

in hepatic lipid storage, which has the potential to significantly impact health, reproductive

capacity, and ultimately fitness.

Tables

Table 4.1. Collection information, sample size, and biometric data for microscopic hepatic
changes (MHC), liver polycyclic aromatic hydrocarbons (PAHs), and biliary PAH metabolites in
Tilefish from four regions of the Gulf of Mexico. Regions are depicted in Figure 4.1.

Region	Collection year	Collection month	n (stations)	n (MHC)	n (liver PAHs)	n (bile)	Total length[1] (cm)	Sex ratio (M:F:U)[2]
North Central	2012	August	4	31	23	23	63 ± 17	1:22:8
	2013	August	5	20	20	17	74 ± 13	10:3:6
	2014	August	5	27	27	22	62 ± 14	5:21:1
	2015	August	5	41	41	38	66 ± 15	3:28:10
	comb.[3]		5	119	111	100	66 ± 16	19:74:25
Northwest	2016	September	8	58	58	55	68 ± 14	24:24:10
Bay of Campeche	2015	September	3	24	24	24	63 ± 14	4:14:6
	2016	August	4	14	14	14	66 ± 12	4:7:3
	comb.[3]		7	38	38	38	64 ± 13	8:21:9
Yucatán Shelf	2015	September	3	15	15	13	68 ± 13	3:10:2
	2016	August	1	9	9	7	65 ± 8	3:5:1
	comb.[3]		4	24	24	20	67 ± 11	6:15:3

[1]Mean ± one standard deviation
[2]M:F:U = Male:Female:Unknown sex
[3]comb. = combined

Table 4.2. Prevalence of the 14 microscopic hepatic changes identified in Gulf of Mexico Tilefish by region (NC = north central; NW = northwest; BC = Bay of Campeche; YS = Yucatán Shelf). The region with the highest prevalence for each microscopic hepatic change is bolded. Sample size (*n*) noted by region.

Microscopic hepatic change	NC *n* = 119	NW *n* = 58	BC *n* = 38	YS *n* = 24
Glycogen-type vacuolar change	72%	81%	**89%**	83%
Bile duct fibrosis	38%	72%	**76%**	63%
↑ Pigmented macrophage aggregates	50%	57%	**68%**	33%
Lipid-type vacuolar change	**35%**	22%	21%	21%
Granuloma(s)	24%	**33%**	18%	21%
Foci of cellular alteration	8.4%	**16%**	7.9%	4.2%
Inflammation + lymphocytic aggregation	**9%**	7%	8%	0%
Hepatocellular atrophy	**12%**	2%	5%	0%
Loose parasitic larvae	2%	**9%**	5%	4%
Bile duct duplication	**4%**	3%	3%	0%
Hepatocellular necrosis	1%	0%	**3%**	0%
Cysts and pseudocysts	0%	0%	**3%**	0%
Ito cell hyperplasia	0%	0%	0%	**4%**
Neoplasia	**1%**	0%	0%	0%

Figures
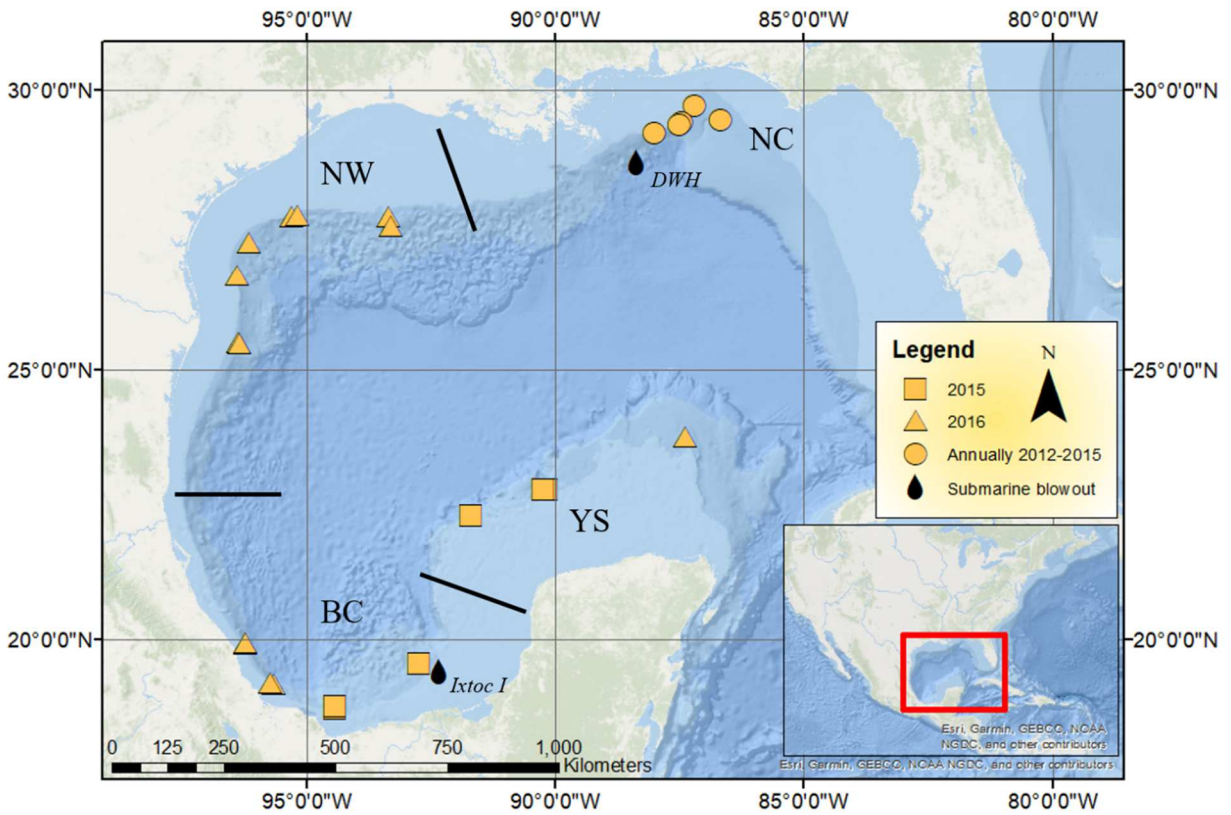
Figure 4.1. Map of the 24 stations where Tilefish were sampled in the Gulf of Mexico (2012-2016). Sampling area is divided into four regions: NC = north central; NW = northwest; BC = Bay of Campeche; YS = Yucatán Shelf. Legend denotes sampling year for each station.
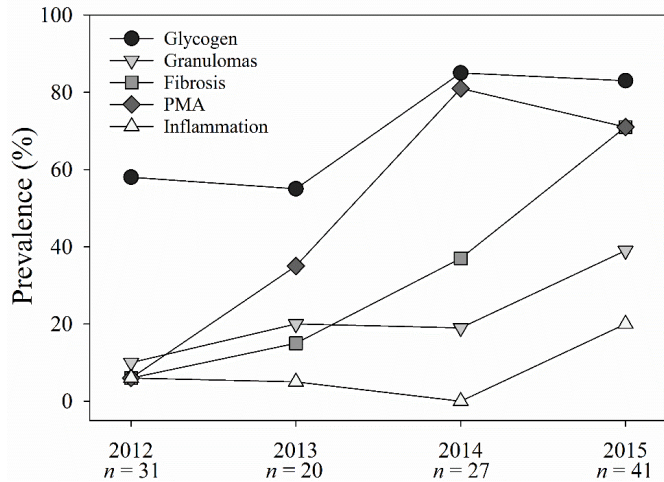
Figure 4.2. Prevalence of five microscopic hepatic changes (glycogen-type vacuolar change, granulomas, biliary fibrosis, increased pigmented macrophage aggregates (PMA), inflammation with lymphocytic aggregation) over years 2012 to 2015 in Tilefish from the north central Gulf of Mexico. Sample size (n) noted by year.
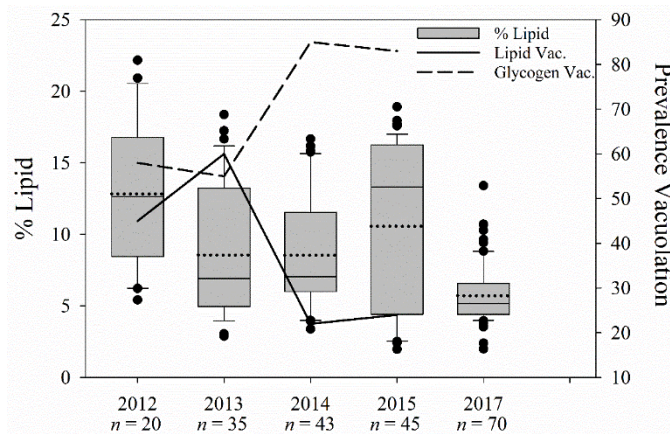
Figure 4.3. Two independent measures of hepatic lipid, percent liver lipid from Folch-extractions, and prevalence of lipid-type vacuolation via histology, and glycogen-type vacuolization over years 2012 to 2017 in Tilefish from the north central Gulf of Mexico. Sample size (n) for Folch extractions noted by year. Sample sizes for histological evaluation are in Table 1.
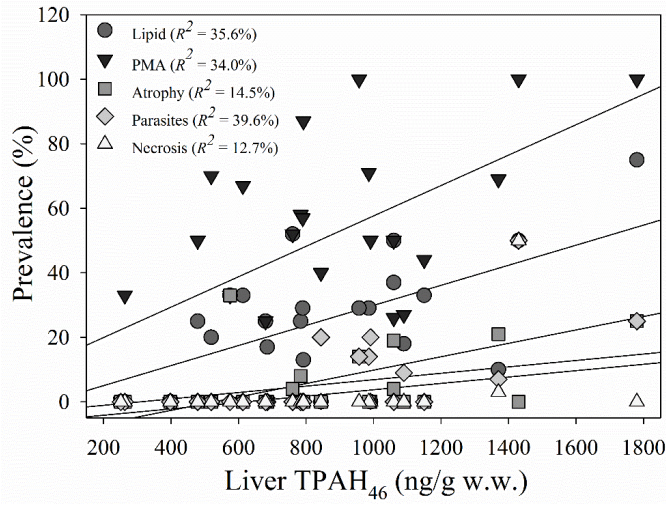
Figure 4.4. Prevalence of microscopic hepatic changes (lipid-type vacuolar change, increased pigmented macrophage aggregates (PMA), hepatocellular atrophy, parasites, necrosis) versus mean liver total PAH_{46} for Tilefish for all regions combined. Regressions are significant at $\alpha = 0.05$.
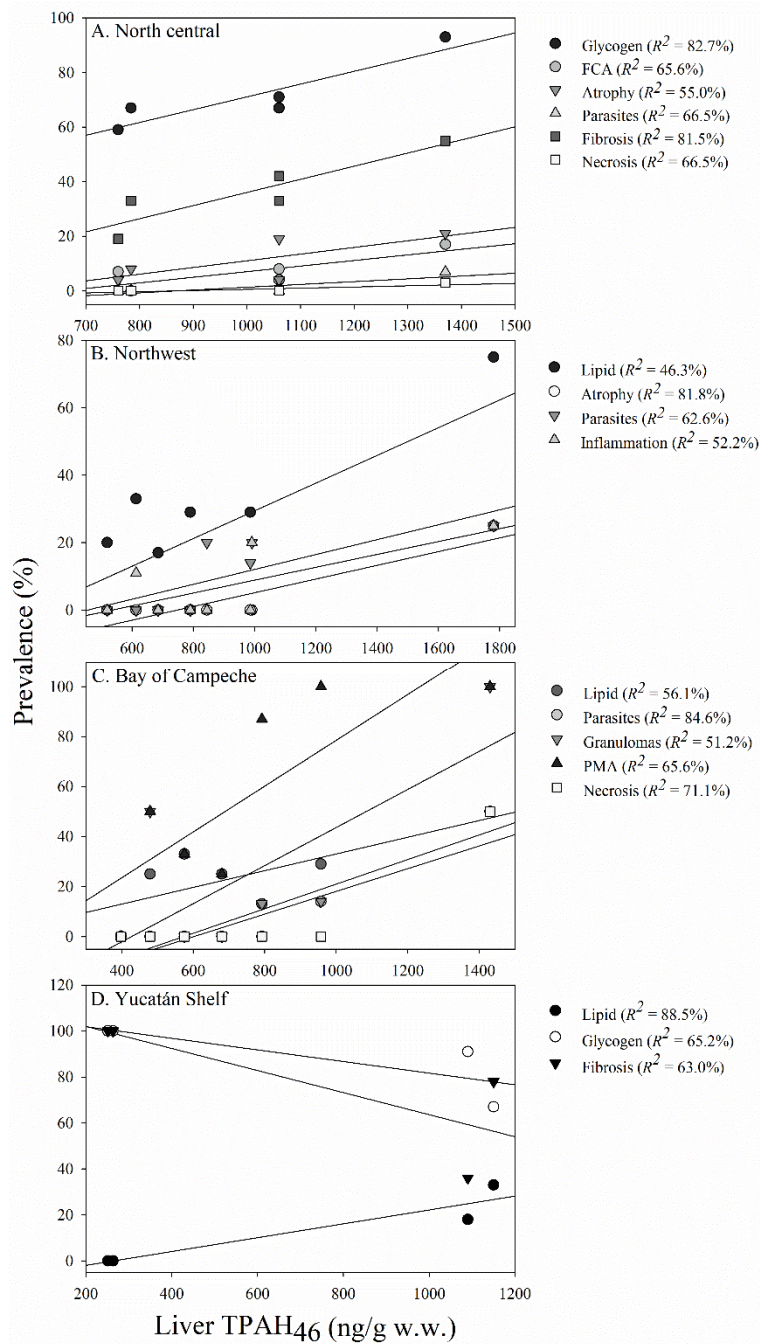
Figure 4.5. Prevalence of microscopic hepatic changes versus mean liver total PAH$_{46}$ for Tilefish by region of the Gulf of Mexico. Regressions are significant at $\alpha = 0.05$.

References

Adams, D. H., and C. Sonne. 2013. 'Mercury and histopathology of the vulnerable goliath grouper, Epinephelus itajara, in U.S. waters: A multi-tissue approach', *Environmental Research*, 126: 254-63.

Agius, C., and R. J. Roberts. 2003. 'Melano-macrophage centres and their role in fish pathology', *Journal of Fish Diseases*, 26: 499-509.

Ali, A. O., C. Hohn, P. J. Allen, L. Ford, M. B. Dail, S. Pruett, and L. Petrie-Hanson. 2014. 'The effects of oil exposure on peripheral blood leukocytes and splenic melano-macrophage centers of Gulf of Mexico fishes', *Marine Pollution Bulletin*, 79: 87-93.

Au, D. W. T. 2004. 'The application of histo-cytopathological biomarkers in marine pollution monitoring: a review', *Marine Pollution Bulletin*, 48: 817-34.

Bayha, K. M., N. Ortell, C. N. Ryan, K. J. Griffitt, M. Krasnec, J. Sena, T. Ramaraj, R. Takeshita, G. D. Mayer, F. Schilkey, and R. J. Griffitt. 2017. 'Crude oil impairs immune function and increases susceptibility to pathogenic bacteria in southern flounder', *Plos One*, 12.

Bentivegna, C. S., K. R. Cooper, G. Olson, E. A. Pena, D. R. Millemann, and R. J. Portier. 2015. 'Chemical and histological comparisons between Brevoortia sp (menhaden) collected in fall 2010 from Barataria Bay, LA and Delaware Bay, NJ following the DeepWater Horizon (DWH) oil spill', *Marine Environmental Research*, 112: 21-34.

Boorman, G. A., S. Botts, T. E. Bunton, J. W. Fournie, J. C. Harshbarger, W. E. Hawkins, D. E. Hinton, M. P. Jokinen, M. S. Okihiro, and M. J. Wolfe. 1997. 'Diagnostic criteria for degenerative, inflammatory, proliferative nonneoplastic and neoplastic liver lesions in medaka (Oryzias latipes): Consensus of a national toxicology program pathology working group', *Toxicologic Pathology*, 25: 202-10.

Brown-Peterson, N. J., M. Krasnec, R. Takeshita, C. N. Ryan, K. J. Griffitt, C. Lay, G. D. Mayer, K. M. Bayha, W. E. Hawkins, I. Lipton, J. Morris, and R. J. Griffitt. 2015. 'A multiple endpoint analysis of the effects of chronic exposure to sediment contaminated with Deepwater Horizon oil on juvenile Southern flounder and their associated microbiomes', *Aquatic Toxicology*, 165: 197-209.

Buchmann, K., and F. Mehrdana. 2016. 'Effects of anisakid nematodes Anisakis simplex (s.l.), Pseudoterranova decipiens (s.l.) and Contracaecum osculatum (s.l.) on fish and consumer health', *Food and Waterborne Parasitology*, 4: 13-22.

Collier, T. K., B. F. Anulacion, M. R. Arkoosh, J.P. Dietrich, J. P. Incardona, L. L. Johnson, G. M. Ylitalo, and M. S. Myers. 2014. 'Effects on fish of polycyclic aromatic hydrocarbons (PAHS) and naphthenic acid exposures.' in K. B. Tierney, A. P. Farrell and C.L. Brauner (eds.), *Fish Physiology: Organic Chemical Toxicology of Fishes* (Elsevier Inc.).

Couch, J. A. 1985. 'Prospective study of infectious and noninfectious diseases in oysters and fishes in 3 Gulf of Mexico estuaries', *Diseases of Aquatic Organisms*, 1: 59-82.

———. 1991. 'Spongiosis hepatis- Chemical induction, pathogenesis, and possible neoplastic fate in a teleost model', *Toxicologic Pathology*, 19: 237-50.

Council, National Research. 2003. *Oil in the sea III: Inputs, fates, and effects* (The National Academies Press).

Dezfuli, B. S., C. E. Fernandes, G. M. Galindo, G. Castaldelli, M. Manera, J. A. DePasquale, M. Lorenzoni, S. Bertin, and L. Giari. 2016. 'Nematode infection in liver of the fish

Gymnotus inaequilabiatus (Gymnotiformes: Gymnotidae) from the Pantanal Region in Brazil: pathobiology and inflammatory response', *Parasites & Vectors*, 9.

Feist, S. W., G. D. Stentiford, M. L. Kent, A. R. Santos, and P. Lorance. 2015. 'Histopathological assessment of liver and gonad pathology in continental slope fish from the northeast Atlantic Ocean', *Marine Environmental Research*, 106: 42-50.

Fricke, N. F., G. D. Stentiford, S. W. Feist, and T. Lang. 2012. 'Liver histopathology in Baltic eelpout (Zoarces viviparus) - A baseline study for use in marine environmental monitoring', *Marine Environmental Research*, 82: 1-14.

Gambardella, C., L. Gallus, A. Amaroli, G. Terova, M. A. Masini, and S. Ferrando. 2012. 'Fasting and re-feeding impact on leptin and aquaglyceroporin 9 in the liver of European sea bass (Dicentrarchus labrax)', *Aquaculture*, 354: 1-6.

Gold-Bouchot, G., V. Ceja-Moreno, E. Chan-Cocom, and O. Zapata-Perez. 2014. 'Petroleum hydrocarbons, fluorescent aromatic compounds in fish bile and organochlorine pesticides from areas surrounding the spill of the Kab121 well, in the Southern Gulf of Mexico: A case study', *Journal of Environmental Biology*, 35: 147-56.

Good, C., D. P. Marancik, T. J. Welch, T. May, J. Davidson, and S. Summerfelt. 2016. 'Systemic granuloma observed in Atlantic salmon Salmo salar raised to market size in a freshwater recirculation aquaculture system', *Aquaculture Research*, 47: 3679-83.

Grizzle, J. M. 1986. 'Lesions in fishes captured near drilling platforms in the Gulf of Mexico', *Marine Environmental Research*, 18: 267-76.

Hebert, Craig E., and Karen A. Keenleyside. 1995. 'To normalize or not to normalize? Fat is the question', *Environmental Toxicology and Chemistry*, 14: 801-07.

Helmueller, G.J. 2019. 'Population demographics of Golen Tilefish (Lopholatilus chamaeleonticepts) in the Gulf of Mexico', University of South Florida.

Hinton, D.E., H. Segner, and T. Braunbeck. 2001. 'Toxic responses of the liver.' in D. Schlenk and W.H. Benson (eds.), *Target Organ Toxicity in Marine and Freshwater Teleosts* (Taylor & Francis).

Horness, B. H., D. P. Lomax, L. L. Johnson, M. S. Myers, S. M. Pierce, and T. K. Collier. 1998. 'Sediment quality thresholds: Estimates from hockey stick regression of liver lesion prevalence in English sole (Pleuronectes vetulus)', *Environmental Toxicology and Chemistry*, 17: 872-82.

Hylland, K. 2006. 'Polycyclic aromatic hydrocarbon (PAH) ecotoxicology in marine ecosystems', *Journal of Toxicology and Environmental Health-Part a-Current Issues*, 69: 109-23.

Johnson, L. L., D. Misitano, S. Y. Sol, G. M. Nelson, B. French, G. M. Ylitalo, and T. Hom. 1998. 'Contaminant effects on ovarian development and spawning success in rock sole from Puget Sound, Washington', *Transactions of the American Fisheries Society*, 127: 375-92.

Johnson, L. L., C. M. Stehr, O. P. Olson, M. S. Myers, S. M. Pierce, C. A. Wigren, B. B. McCain, and U. Varanasi. 1993. 'Chemical contaminants and hepatic lesions in Winter Flounder (Pleuronectes americanus) from the Northeast coast of the United States', *Environmental Science & Technology*, 27: 2759-71.

Jones, D.L. 2017. 'Fathom Toolbox for MATLAB: software for multivariate ecological and oceanographic data analysis'. https://www.marine.usf.edu/research/matlab-resources/.

Kennicutt, M. C., J. M. Brooks, E. L. Atlas, and C. S. Giam. 1988. 'Organic compounds of environmental concern in the Gulf of Mexico: a review', *Aquatic Toxicology*, 11: 191-212.

Krahn, M. M., M. S. Myers, D. G. Burrows, and D. C. Malins. 1984. 'Determination of metabolites of xenobiotics in the bile of fish from polluted waterways', *Xenobiotica*, 14: 633-46.

Krahn, M. M., L. D. Rhodes, M. S. Myers, L. K. Moore, W. D. Macleod, and D. C. Malins. 1986. 'Associations between metabolites of aromatic compounds in bile and the occurrence of hepatic lesions in English sole (Parophrys vetulus) from Puget Sound, Washington', *Archives of Environmental Contamination and Toxicology*, 15: 61-67.

Lubchenco, J., M. K. McNutt, G. Dreyfus, S. A. Murawski, D. M. Kennedy, P. T. Anastas, S. Chu, and T. Hunter. 2012. 'Science in support of the Deepwater Horizon response', *Proceedings of the National Academy of Sciences of the United States of America*, 109: 20212-21.

Malins, D. C., M. M. Krahn, M. S. Myers, L. D. Rhodes, D. W. Brown, C. A. Krone, B. B. McCain, and S. L. Chan. 1985. 'Toxic chemicals in sediments and biota from a creosote-polluted harbor: Relationships with hepatic neoplasms and other hepatic lesions in English sole (Parophrys vetulus)', *Carcinogenesis*, 6: 1463-69.

Malins, D. C., B. B. McCain, D. W. Brown, U. Varanasi, M. M. Krahn, M. S. Myers, and S. L. Chan. 1987. 'Sediment-associated contaminants and liver diseases in bottom-dwelling fish', *Hydrobiologia*, 149: 67-74.

Marigómez, Ionan, Manu Soto, Ibon Cancio, Amaia Orbea, Larraitz Garmendia, and Miren P. Cajaraville. 2006. 'Cell and tissue biomarkers in mussel, and histopathology in hake and anchovy from Bay of Biscay after the Prestige oil spill (Monitoring Campaign 2003)', *Marine Pollution Bulletin*, 53: 287-304.

Marty, G. D., A. Hoffmann, M. S. Okihiro, K. Hepler, and D. Hanes. 2003. 'Retrospective analysis: bile hydrocarbons and histopathology of demersal rockfish in Prince William Sound, Alaska, after the Exxon Valdez oil spill', *Marine Environmental Research*, 56: 569-84.

McBride, R. S., T. E. Vidal, and S. X. Cadrin. 2013. 'Changes in size and age at maturity of the northern stock of Tilefish (Lopholatilus chamaeleonticeps) after a period of overfishing', *Fishery Bulletin*, 111: 161-74.

Meyer, J. N., and R. T. Di Giuliuo. 2003. 'Heritable adaptation and fitness costs in killifish (Fundulus beteroclitus) inhabiting a polluted estuary', *Ecological Applications*, 13: 490-503.

Miranda, A. L., H. Roche, M. A. F. Randi, M. L. Menezes, and C. A. O. Ribeiro. 2008. 'Bioaccumulation of chlorinated pesticides and PCBs in the tropical freshwater fish Hoplias malabaricus: Histopathological, physiological, and immunological findings', *Environment International*, 34: 939-49.

Mora, M. A., D. Papoulias, I. Nava, and D. R. Buckler. 2001. 'A comparative assessment of contaminants in fish from four resacas of the Texas, USA-Tamaulipas, Mexico border region', *Environment International*, 27: 15-20.

Murawski, S. A., W. T. Hogarth, E. B. Peebles, and L. Barbeiri. 2014. 'Prevalence of External Skin Lesions and Polycyclic Aromatic Hydrocarbon Concentrations in Gulf of Mexico Fishes, Post-Deepwater Horizon', *Transactions of the American Fisheries Society*, 143: 1084-97.

Murawski, S. A., E. B. Peebles, A. Gracia, J. W. Tunnell, and M. Armenteros. 2018. 'Comparative Abundance, Species Composition, and Demographics of Continental Shelf Fish Assemblages throughout the Gulf of Mexico', *Marine and Coastal Fisheries*, 10: 325-46.

Myers, M. S., L. L. Johnson, and T. K. Collier. 2003. 'Establishing the causal relationship between polycyclic aromatic hydrocarbon (PAH) exposure and hepatic neoplasms and neoplasia-related liver lesions in English sole (Pleuronectes vetulus)', *Human and Ecological Risk Assessment*, 9: 67-94.

Myers, M. S., C. M. Stehr, O. P. Olson, L. L. Johnson, B. B. McCain, S. L. Chan, and U. Varanasi. 1994. 'Relationships between toxicopathic hepatic lesions and exposure to chemical contaminants in English sole (Pleuronectes vetulus), Starry flounder (Platichthys stellatus), and White croaker (Genyonemus lineatus) from selected marine sites on the Pacific coast, USA', *Environmental Health Perspectives*, 102: 200-15.

Myers, M. S., J. T. Landahl, M. M. Krahn, L. L. Johnson, and B. B. McCain. 1990. 'Overview of studies on liver carcinogensis in English sole from Puget Sound; Evidence for a xenobiotic chemical etiology I: Pathology and epizootiology', *Science of the Total Environment*, 94: 33-50.

Myers, Mark S., Linda D. Rhodes, and Bruce B. McCain. 1987. 'Pathologic Anatomy and Patterns of Occurrence of Hepatic Neoplasms, Putative Preneoplastic Lesions, and Other Idiopathic Hepatic Conditions in English Sole (Parophrys vetulus) From Puget Sound, Washington23', *JNCI: Journal of the National Cancer Institute*, 78: 333-63.

NOAA. 2012. "Analytical Quality Assurance Plan: Mississippi Canyon 252 (Deepwater Horizon) Natural Resource Damange Assessment V3.1." In, edited by U.S. Department of Commerce NOAA.

Pacheco, M., and M. A. Santos. 2002. 'Biotransformation, genotoxic, and histopathological effects of environmental contaminants in European eel (Anguilla anguilla L.)', *Ecotoxicology and Environmental Safety*, 53: 331-47.

Pal, S., E. Kokushi, J. O. Cheikyula, J. Koyama, and S. Uno. 2011. 'Histopathological effects and EROD induction in common carp exposed to dietary heavy oil', *Ecotoxicology and Environmental Safety*, 74: 307-14.

Pinkney, A. E., J. C. Harshbarger, E. B. May, and M. J. Melancon. 2004. 'Tumor prevalence and biomarkers of exposure in Brown bullhead (Ameiurus nebulosus) from Back River, Furnace Creek, and Tuckahoe River, Maryland', *Archives of Environmental Contamination and Toxicology*, 46: 492-501.

Pinzani, M., and T. V. Luong. 2018. 'Pathogenesis of biliary fibrosis', *Biochimica Et Biophysica Acta-Molecular Basis of Disease*, 1864: 1279-83.

Pulster, E. L., A. Gracia, S. M. Snyder, K. Deak, S Fogelson, and S.A. Murawski. 2020. 'Chronic Sub-lethal Effects Observed in Wild-Caught Fishes Following Two Major Oil Spills in the Gulf of Mexico: Deepwater Horizon and Ixtoc 1.' in S.A. Murawski, C.H. Ainsworth, S. Gilbert, D.J. Hollander, C.B. Paris, M. Schluter and D. L. Wetzel (eds.), *Deep Oil Spills: Facts, Fate, and Effects* (Springer Nature Switzerland AG).

Pulster, Erin L., Adolfo Gracia, Maickel Armenteros, Brigid E. Carr, Justin Mrowicki, and Steven A. Murawski. 2019. 'Chronic PAH exposures and associated declines in fish health indices observed for ten grouper species in the Gulf of Mexico', *Science of the Total Environment*: 135551.

Quintanilla-Mena, Mercedes, Gerardo Gold-Bouchot, Omar Zapata-Pérez, Jorge Rubio-Piña, Adriana Quiroz-Moreno, Víctor Manuel Vidal-Martínez, Ma Leopoldina Aguirre-Macedo, and Carlos Puch-Hau. 2019. 'Biological responses of shoal flounder (Syacium gunteri) to toxic environmental pollutants from the southern Gulf of Mexico', *Environmental Pollution*: 113669.

Ranasingha, Ratcs, and A. Pathiratne. 2015. 'Histological alterations and polycyclic aromatic hydrocarbon exposure indicative bile fluorescence patterns in fishes from Koggala lagoon, Sri Lanka', *Journal of the National Science Foundation of Sri Lanka*, 43: 65-73.

Reddy, A.P., J. M. Spitsbergen, C. Mathews, J. D. Hendricks, and G. S. Bailey. 1999. 'Experimental hepatic tumorigenicity by environmental hydrocarbon dibenzo[a,l]pyrene', *Journal of Environmental Pathology Toxicology and Oncology*, 18: 261-69.

Reynaud, S., and P. Deschaux. 2006. 'The effects of polycyclic aromatic hydrocarbons on the immune system of fish: A review', *Aquatic Toxicology*, 77: 229-38.

Rodgers, M. L., R. Takeshita, and R. J. Griffitt. 2018. 'Deepwater Horizon oil alone and in conjunction with Vibrio anguillarum exposure modulates immune response and growth in red snapper (Lutjanus campechanus)', *Aquatic Toxicology*, 204: 91-99.

Romero, I. C., P. T. Schwing, G. R. Brooks, R. A. Larson, D. W. Hastings, G. Ellis, E. A. Goddard, and D. J. Hollander. 2015. 'Hydrocarbons in Deep-Sea Sediments following the 2010 Deepwater Horizon Blowout in the Northeast Gulf of Mexico', *Plos One*, 10.

Romero, I. C., T. Sutton, B. Carr, E. Quintana-Rizzo, S. W. Ross, D. J. Hollander, and J. J. Torres. 2018. 'Decadal Assessment of Polycyclic Aromatic Hydrocarbons in Mesopelagic Fishes from the Gulf of Mexico Reveals Exposure to Oil-Derived Sources', *Environmental Science & Technology*, 52: 10985-96.

Schlacher, T. A., J. A. Mondon, and R. M. Connolly. 2007. 'Estuarine fish health assessment: Evidence of wastewater impacts based on nitrogen isotopes and histopathology', *Marine Pollution Bulletin*, 54: 1762-76.

Snyder, S. M., J.A. Olin, E. L. Pulster, and S.A. Murawski. 2020. 'Spatial contrasts in hepatic and biliary PAHs in Tilefish (Lopholatilus chamaeleonticeps) throughout the Gulf of Mexico, with comparison to the Northwest Atlantic', *Environmental Pollution*.

Snyder, S. M., E. L. Pulster, and S. Murawski. 2019. 'Associations between chronic exposure to polycyclic aromatic hydrocarbons and health indices in Gulf of Mexico Tilefish (Lopholatilus chamaeleonticeps) post-Deepwater Horizon', *Environmental Toxicology and Chemistry*, 38: 2659-71.

Snyder, S. M., E. L. Pulster, D. L. Wetzel, and S. A. Murawski. 2015. 'PAH Exposure in Gulf of Mexico Demersal Fishes, Post-Deepwater Horizon', *Environmental Science & Technology*, 49: 8786-95.

Soto, L.A., A. V. Botello, S. Licea-Durán, M.L. Lizárraga-Partida, and A. Yáñez-Arancibia. 2014. 'The environmental legacy of the Ixtoc-I oil spill in Campeche Sound, southwestern Gulf of Mexico', *Frontiers in Marine Science*, 1.

Stehr, C. M., M. S. Myers, L. L. Johnson, S. Spencer, and J. E. Stein. 2003. 'Toxicopathic liver lesions in English sole and chemical contaminant exposure in Vancouver Harbour, Canada', *Marine Environmental Research*, 57: 55-74.

Struch, R. E., E. L. Pulster, A. D. Schreier, and S. A. Murawski. 2019. 'Hepatobiliary Analyses Suggest Chronic PAH Exposure in Hakes (Urophycis spp.) Following the Deepwater Horizon Oil Spill', *Environmental Toxicology and Chemistry*, 38: 2740-49.

Tocher, D. R. 2003. 'Metabolism and functions of lipids and fatty acids in teleost fish', *Reviews in Fisheries Science*, 11: 107-84.

van der Oost, R., J. Beyer, and N. P. E. Vermeulen. 2003. 'Fish bioaccumulation and biomarkers in environmental risk assessment: a review', *Environmental Toxicology and Pharmacology*, 13: 57-149.

Varanasi, U., J. E. Stein, and M. Nishimoto. 1989. 'Biotransformation and disposition of polycyclic aromatic hydrocarbons (PAH) in fish.' in U. Varanasi (ed.), *Metabolism of polycyclic aromatic hydrocarbons in the aquatic environment* (CRC Press, Inc.: Boca Raton, Florida).

Vogelbein, W.K., M. Unger, and D. Gauthier. 2008. "The Elizabeth River monitoring program 2006-2007: Association between Mummichog liver histopathology and sediment chemical contamination." In, edited by The Virginia Department of Environmental Quality.

Wolf, J. C., W. A. Baumgartner, V. S. Blazer, A. C. Camus, J. A. Engelhardt, J. W. Fournie, S. Frasca, D. B. Groman, M. L. Kent, L. H. Khoo, J. M. Law, E. D. Lombardini, C. Ruehl-Fehlert, H. E. Segner, S. A. Smith, J. M. Spitsbergen, K. Weber, and M. J. Wolfe. 2015. 'Nonlesions, Misdiagnoses, Missed Diagnoses, and Other Interpretive Challenges in Fish Histopathology Studies: A Guide for Investigators, Authors, Reviewers, and Readers', *Toxicologic Pathology*, 43: 297-325.

Wolf, J. C., and J. R. Wheeler. 2018. 'A critical review of histopathological findings associated with endocrine and non-endocrine hepatic toxicity in fish models', *Aquatic Toxicology*, 197: 60-78.

Wolf, J. C., and M. J. Wolfe. 2005. 'A brief overview of nonneoplastic hepatic toxicity in fish', *Toxicologic Pathology*, 33: 75-85.

Chapter 5

Conclusions

Research Conclusions

Research presented herein is unique as it covers a broad, international (Gulf-wide) spatial scale and a six-year time series of PAH exposure, hepatic accumulation, and associated health effects in the commercially and ecologically important Tilefish. Results indicate chronic and increasing exposure of GoM Tilefish to PAHs, likely from a petrogenic source, with effects on health indices, and potential consequences for fecundity, recruitment, and ultimately population-level effects. The conclusions herein highlight the need for continued monitoring of GoM Tilefish contaminant levels, health, and abundance.

Results of chapter two indicate that in Tilefish from the north central GoM, a region heavily impacted by the U.S. oil industry and the 2010 *DWH* oil spill, there was a 178% increase in PAH exposure, a 22% decline in Fulton's condition factor, and a 53% decline in hepatic lipids between 2012 and 2017. Hepatic accumulation of PAHs over this time period was not observed, suggesting xenobiotic metabolism mechanisms are efficiently eliminating PAHs. However, the energetic cost of continuous multi-step PAH metabolism due to chronic exposure may be taxing the energy budget of Tilefish leading to declines in stored energy, and decreased condition, with potential implications for decreased fecundity, larval survivorship, growth rate, and recruitment, all of which have potential longer-term population-level effects. A parallel study of north central GoM Tilefish population dynamics pre- and post-*DWH* found no difference in length

133

distribution, age frequency, growth rate, or instantaneous mortality, concluding no detectable effect of *DWH* at the population-level, possibly due to the longevity of Tilefish (Helmueller 2019). However, that study did not assess interannual temporal trends, which were found to be significant herein. Also, many of the fish aged by Helmueller (2019) were alive prior to *DWH*, thus no systematic evaluation of generational effects on growth were possible.

Chapter three determined that Tilefish from the north central region of the GoM have the highest levels of PAH exposure and hepatic PAH concentrations in demersal fishes Gulf-wide, likely reflecting the magnitude and number of sources in the region, and further exemplifying the need for continued long-term monitoring of contamination and the health of biota in this region. Hepatic PAH concentrations for Tilefish from the north central GoM were similar to Tilefish from the northwestern Atlantic Ocean, however, samples from the later had high concentrations and more frequent detection of carcinogenic HMW PAHs, indicating higher pyrogenic PAH inputs in the northwestern Atlantic. Remarkably, PAH exposure and hepatic accumulation was relatively low in the Bay of Campeche, the region containing Mexico's Cantarell oil fields and dense offshore infrastructure. Only speculation on the significance of variables driving these regional differences can be made without the ability to definitively fingerprint PAH sources in internal biotic samples, and additional research. Geochemical and/or biological mechanisms altering bioavailability may be driving low biotic uptake of contaminants in the Bay of Campeche. Quantifying biota-sediment accumulation factors (BSAFs) would aid in interpretation of Gulf-wide data due to the strong association between Tilefish and sediment, if comprehensive data on sediment PAHs and organic carbon content were available. Ongoing Gulf-wide studies of Tilefish population genetics and transcriptomics would also aid in

interpretation, possibly illuminating regional differences in physiology that may affect toxicokinetics of PAHs.

Chapter four provides the first description of the microscopic hepatic anatomy of Tilefish, along with prevalence of 14 identified MHCs, ten of which were significantly associated with hepatic PAH accumulation. Prevalence of MHCs was generally uniform Gulf-wide, with an exception of relatively low prevalence on the Yucatán Shelf. Hepatic neoplasia, a classic effect of chronic PAH exposure, were rare ($n = 1$) in GoM Tilefish, most likely due to to low HMW PAH exposure, as HMW PAHs are implicated in the mechanism of formation of neoplasia. Temporal analysis of MHC prevalence in the northern GoM indicated that prevalence of inflammatory MHCs and hepatic glycogen storage is increasing, while hepatic lipid storage is decreasing over time.

One of the most intriguing results of this dissertation is that two independent measures of hepatic lipid storage, total liver lipid as measured by a modified Folch-extraction and lipid vacuolation measured by histopathology, both measured respective declines of 53% and 47% in northern GoM Tilefish over the same time period. Concurrently, glycogen vacuolation increased by 30%, and Fulton's condition factor declined by 22%. These measurements provide strong evidence for a significant effect on energy storage of north central GoM Tilefish, a process with population-level implications. Research on energy metabolism in teleosts identifies a species-specific process rendering any conclusions drawn herein speculative without further investigation into the biochemical processes specific to Tilefish. However, hepatic lipids have an important role in teleosts of providing energy for essential functions of swimming, growth, and especially reproduction (Tocher 2003, 2010; Parma et al. 2015; Furuita et al. 2002). While fish are capable of lipogenesis, the main source of lipids and fatty acids, especially in higher

trophic level teleosts, is dietary (Tocher 2003, 2010). Although some teleost species store excess carbohydrates as hepatic glycogen, it is believed that carbohydrates have reduced importance in teleosts, and especially in carnivores that cannot efficiently utilize dietary carbohydrates due to poor regulation of glucose homeostasis (Enes et al. 2009; De Pedro et al. 2001; Song et al. 2018; Hinton, Segner, and Braunbeck 2001). Certain species build a reserve of hepatic glycogen for use as an energy source during periods of starvation; however, the importance of this mechanism is species-specific with some teleosts relying on lipid stores during starvation (Enes et al. 2009; Hinton, Segner, and Braunbeck 2001).

The alteration of hepatic energy storage may be explained by a few hypotheses directly and indirectly related to living in a chronically polluted environment, and all of which may be inherently harmful to the organism. First, decreased prey abundance or prey quality may be resulting in decreased dietary lipid intake, dietary deficiencies, and increased hepatic glycogen storage, a known response to starvation. This theory aligns with the observed decrease in Fulton's condition factor, representing a 21% decrease in the total body weight of a Tilefish at a given length. In addition, a significant 19% decrease in Tilefish gastrointestinal tract weight, which may be used as a proxy for feeding status, was observed for individuals sampled in the north central GoM from 2012 to 2017. Losses of benthic megafauna were documented post-*DWH*, mainly in the immediate vicinity of the wellhead, however, MOSSFA deposited oil residues over a vast expanse of the northern GoM including our study region, leading to chronic sediment contamination and persistent effects on the benthic community, suggesting the theory of decreased benthic prey availability or quality is viable. This conclusion was also reached in the *DWH* Final Programmatic Damage Assessment and Restoration Plan, where the Trustees concluded sedimented oil residues contaminated benthic invertebrates (e.g. red crabs) in zones

hundreds of miles away from *DWH*, leading to a degradation of food quality for organisms that prey on crabs, which include Tilefish (Trustees 2016). Second, factors such as feeding inhibition, reduced foraging success, feeding rate, or dietary assimilation efficiency, which are known indirect effects of xenobiotic exposure, could be causing decreased uptake and storage of lipids. Third, chronic exposure to PAHs could lead to endocrine disruption of lipid and carbohydrate metabolism by impeding hormonally-controlled homeostasis (Enes et al. 2009; Tocher 2003). Fourth, the significant energetic cost of chronic xenobiotic metabolism and/or cellular repair is utilizing energy that would otherwise be stored. This hypothesis was discussed extensively in chapter two and is supported by the results of both chapters two and four, which describe increasing PAH metabolite concentrations and MHCs in Tilefish from the north central GoM from 2012 to 2017.

Whatever the cause, the implications of reduced hepatic lipid storage are grave. Dietary deficiencies in teleosts can result in reduced growth, negative impacts on reproduction, and increased mortality (Tocher 2010). Teleosts mobilize hepatic lipid stores in times of high energy demand, for example, during migration or gonadal development for spawning. Lipid and fatty acid composition of eggs is directly related to egg quality, as embryonic and larval development is dependent on the nutrition provided, with known influences on fertilization rate, hatching, survival, and growth rate of larvae (Parma et al. 2015; Tocher 2010; Furuita et al. 2002). Without adequate nutrition, survivorship of larvae will decrease, leading to a corresponding decrease in recruitment. This has been observed in Atlantic Cod (*Gadus morhua*) where total lipid energy in mature females correlated directly with fecundity and thus recruitment (Marshall et al. 1999). Also in Atlantic Cod, loss of high energy prey items (i.e. Capelin [*Mallotus villosus*]) caused decreased condition and reproductive output, and resulted in limited population

recovery (Rose and O'Driscoll 2002). Significant decreases in Fulton's condition factor were similarly observed in northern GoM Tilefish and correlated to the declines in stored lipid. Lastly, a small sample ($n = 46$) of GoM Tilefish ovaries collected in 2017 were analyzed via two extraction methods (modified Folch and traditional accelerated solvent extraction) and lipid levels quantified were extremely low (< 2% wet wt.) in the eggs from spawning capable (F4) and spawning (F5) stage ovaries. Typical total lipid contents in teleost eggs are 10-30% dry weight (Parma et al. 2015; Tocher 2003; V'Uorela, Kaitaranta, and Linko 1979). Using a general conversion factor of 3.5 obtained from V'Uorela, Kaitaranta, and Linko (1979), the total lipid content of Tilefish eggs is still substantially lower than reported values for other teleosts.

If research on GoM Tilefish were to be continued I recommend the following, with priority on north central GoM Tilefish: 1) further monitoring of PAH exposure and accumulation, Fulton's condition factor, hepatic energy stores, and abundance, 2) full lipid and fatty acid profiles in tissues (e.g. liver, muscle, ovaries), 3) stable isotope analysis in tissues (e.g. eye lens, liver, muscle) to investigate potential diet and trophic shifts, and 4) quantification of persistent organic pollutants, contaminants of emerging concern, and mercury in archived tissues (which my program has stored) to fully define exposure history.

In addition to the numerous characteristics that result in Tilefish being vulnerable to environmental disturbances (habitat-restricted, burrow-forming, dense aggregation, non-migratory, long-lived, slow-growing, late-maturing, hermaphroditic), continued commercial and recreational exploitation in addition to potentially looming health effects from chronic PAH exposure potentially puts the north central population at risk for stock decline. Particularly when the GoM Tilefish population is harvested with limited biological information informing commercial catch limits (Lombardi-Carlson 2012). In addition to commercial importance,

Tilefish are regarded as ecosystem engineers with their large funnel-shaped burrows altering the seafloor landscape and providing habitat for many other species of teleosts and benthic invertebrates. Reduction in Tilefish abundance would not only impact its fishery, but also the populations of other species that depend upon Tilefish habitat. Due to their economic and ecological value, and signs of chronic PAH exposure and looming impact, the GoM Tilefish population, particularly individuals from north central Gulf, should be closely monitored.

Scientific Needs for Improved Preparedness in the Gulf of Mexico

As a nation we were fortunate that the known environmental effects of the *DWH* oil spill were limited at the population and ecosystem levels. This has been attributed to numerous factors that obscured and dampened population-level signals, and life history characteristics of many Gulf species that distribute risk across space and time. As a Gulf coast community we should take steps moving forward to be better prepared for the next large GoM oil spill, including: 1) establishing a long-term monitoring program informed by GoMRI research, 2) closing the gap between observed individual-level effects of oil exposure and lack of negative effects observed at the population level, and 3) creating an improved regulatory framework that balances economic drivers and marine conservation in the GoM.

The GoM would benefit from the establishment of a long-term monitoring program of contamination and health indices informed by the results of GoMRI research. This program could collect periodic broad-scale baseline data, evaluate location-specific baselines and risk assessments prior to lease sales, and monitor certain species, communities, and locations at regular time points, with a focus on those determined to be vulnerable or affected post-*DWH*,

139

iconic species of the GoM, commercially important species, protected marine mammals, and endangered wildlife. The National Oceanic and Atmospheric Administration's Mussel Watch program monitors contaminants in inshore sediments and filter-feeding invertebrates in coastal waters; however, no parallel long-term contaminant monitoring program exists offshore. A newly established monitoring program for the offshore should concentrate on continental shelf and deep-water environments. Offshore benthic and deep-sea communities are critical to continue monitoring post-*DWH* and post-GoMRI as they were undoubtedly affected by *DWH*, and are more fragile and less reliant due to species life history strategies, aggregated habitat, and lower species richness and diversity (Murawski et al. 2018; Koslow et al. 2000). It is largely unknown how anthropogenic alterations effect deep-sea and connected communities, therefore, endangering these communities by increasingly deeper offshore drilling has an extremely high potential cost ecosystem-wide (Koslow et al. 2000; Sutton et al. 2020). A long-term monitoring program would build on our scientific understanding of these communities and aid in advocating for their conservation.

Monitoring contaminants and their effects across biological scales is not a trivial task. The current regulatory toxicology framework is under scrutiny for relying on standard endpoints (e.g. LC50, EC50) that are determined for individual chemicals over extremely short time scales, and which have limited ecological relevance based on conditions in nature (e.g. chronic exposure, complex pollutant mixtures, co-occurring stressors, sublethal effects). Specifically, sediment quality standards for PAHs are commonly set based on toxicity endpoints in benthic invertebrates, critical body burdens in fish, or BSAFs, instead of well-established biomarkers of exposure such as biliary PAH metabolites and dietary exposures in resident fish (Collier et al. 2014). Reviews by Connon et al. (2019) and Collier et al. (2014) provide excellent suggestions

for improvements on environmental monitoring and aquatic toxicology research including: 1) establishing comprehensive monitoring systems in coordination with hypothesis-driven research, 2) measuring environmentally relevant complex mixtures and the interactions between components, 3) performing sublethal health effect assessments and understand their mechanisms and linkages across biological scales, 4) gaining insight into the synergistic effects of multiple stressors (e.g. temperature, salinity, pathogens), 5) beginning research on emerging novel contaminants (e.g. microplastics, synthetic fibers), 6) increasing spatial and temporal coverage of monitoring, 7) emphasizing data analysis, modeling, and synthesis of results via a dedicated research program, 8) improving collaboration among researchers, government monitoring programs, and legislators, and 9) and building an adaptive management framework that can quickly incorporate new relevant information into assessments and actions.

Research following both *DWH* and EVOS acknowledged a gap between toxic effects observed at the individual-level from oil exposure, both in the laboratory and in the field, and a lack of observed effects at the population-level in the field. This uncertainty has led to an ongoing call for understanding toxicological effects across all levels of biological organization, not only in the oil spill community but the broader field of Ecotoxicology. In order to close this gap, research at both low (e.g. molecular, organ, individual) and high (e.g. population, community, ecosystem) levels of biological organization needs to be performed, ideally in parallel, with all studies accurately characterizing exposure in addition to effect (Pasparakis et al. 2019). The coordinated research efforts funded by GoMRI post-*DWH* have jumpstarted the oil spill research community towards closing this gap for crude oil and PAHs. For example, the RECOVER consortium has been researching the mechanisms of oil toxicity on fishes from the cellular to organism-level with carefully chosen endpoints that have implications for fitness. It is

this type of coordinated research effort that will successfully further our understanding of mechanisms of oil toxicity and how those mechanisms scale up to population-level effects.

Lastly, U.S. environmental policy needs to shift towards enacting proactive rather than reactive response measures. This applies for both long-term environmental monitoring and oil spill scenarios, neither of which has kept pace with advancements in their respective fields (Connon et al. 2019; Wallace, Gilbert, and Reynolds 2019). Environmental monitoring should be aided by more extensive testing of new chemicals before they enter the market and inevitably the aquatic environment, shifting the burden to the industry or the government to ensure the new chemical is safe for production. In the case of oil spills, the burden also needs to be shifted to the industry to establish acceptable risk of their actions, instead of the current practice of relying on costly post-crisis response and restoration when risks result in spills (Wallace, Gilbert, and Reynolds 2019). Specifically, new regulations need to be enacted to focus on the environmental risks of ultradeep oil development, especially since deep-water communities have been established as vulnerable, and impacted post-*DWH*. Wallace, Gilbert, and Reynolds (2019) calls for a policy paradigm shift away from favoring oil and gas development, and towards valuing conservation of a GoM system under increasing pressure. In the GoM where the high density of the offshore oil and gas industry is moving increasingly deeper and compounding risk, meaningful action towards improved regulation is needed in a vulnerable post-*DWH* system, where another comparable spill could tip the scales towards substantial ecological and economic losses.

References

Collier, T. K., B. F. Anulacion, M. R. Arkoosh, J.P. Dietrich, J. P. Incardona, L. L. Johnson, G. M. Ylitalo, and M. S. Myers. 2014. 'Effects on fish of polycyclic aromatic hydrocarbons (PAHS) and naphthenic acid exposures.' in K. B. Tierney, A. P. Farrell and C.L. Brauner (eds.), *Fish Physiology: Organic Chemical Toxicology of Fishes* (Elsevier Inc.).

Connon, Richard E., Simone Hasenbein, Susanne M. Brander, Helen C. Poynton, Erika B. Holland, Daniel Schlenk, James Orlando, Michelle Hladik, Tracy K. Collier, Nathaniel L. Scholz, John P. Incardona, Nancy D. Denslow, Amro Hamdoun, Sascha Nicklisch, Natalia Garcia-Reyero, Edward J. Perkins, Evan P. Gallagher, Xin Deng, Dan Wang, Stephanie Fong, Richard S. Breuer, Mehrdad Hajibabei, James B. Brown, John K. Colbourne, Thomas M. Young, Gary Cherr, Andrew Whitehead, and Anne E. Todgham. 2019. 'Review of and recommendations for monitoring contaminants and their effects in the San Francisco Bay−Delta', *San Francisco Estuary and Watershed Science*, 17.

De Pedro, N., A. I. Guijarro, M. J. Delgado, M. A. Lopez-Patino, M. L. Pinillos, and M. Alonso-Bedate. 2001. 'Influence of dietary composition on growth and energy reserves in tench (Tinca tinca)', *Journal of Applied Ichthyology-Zeitschrift Fur Angewandte Ichthyologie*, 17: 25-29.

Enes, P., S. Panserat, S. Kaushik, and A. Oliva-Teles. 2009. 'Nutritional regulation of hepatic glucose metabolism in fish', *Fish Physiology and Biochemistry*, 35: 519-39.

Furuita, H., H. Tanaka, T. Yamamoto, N. Suzuki, and T. Takeuchi. 2002. 'Effects of high levels of n-3 HUFA in broodstock diet on egg quality and egg fatty acid composition of Japanese flounder, Paralichthys olivaceus', *Aquaculture*, 210: 323-33.

Helmueller, G.J. 2019. 'Population demographics of Golen Tilefish (Lopholatilus chamaeleonticepts) in the Gulf of Mexico', University of South Florida.

Hinton, D.E., H. Segner, and T. Braunbeck. 2001. 'Toxic responses of the liver.' in D. Schlenk and W.H. Benson (eds.), *Target Organ Toxicity in Marine and Freshwater Teleosts* (Taylor & Francis).

Koslow, J. A., G. W. Boehlert, J. D. M. Gordon, R. L. Haedrich, P. Lorance, and N. Parin. 2000. 'Continental slope and deep-sea fisheries: implications for a fragile ecosystem', *Ices Journal of Marine Science*, 57: 548-57.

Lombardi-Carlson, L.A. 2012. 'Life history, population dynamics, and fishery management of the Golden Tilefish, *Lopholatilus chamaeleonticeps*, from the Southest Atlantic and Gulf of Mexico', University of Florida.

Marshall, C. T., and K. T. Frank. 1999. 'The effect of interannual variation in growth and condition on haddock recruitment', *Canadian Journal of Fisheries and Aquatic Sciences*, 56: 347-55.

Murawski, S. A., E. B. Peebles, A. Gracia, J. W. Tunnell, and M. Armenteros. 2018. 'Comparative Abundance, Species Composition, and Demographics of Continental Shelf Fish Assemblages throughout the Gulf of Mexico', *Marine and Coastal Fisheries*, 10: 325-46.

Parma, L., A. Bonaldo, M. Pirini, C. Viroli, A. Parmeggiani, E. Bonvini, and P. P. Gatta. 2015. 'Fatty Acid Composition of Eggs and its Relationships to Egg and Larval Viability from Domesticated Common Sole (Solea solea) Breeders', *Reproduction in Domestic Animals*, 50: 186-94.

Pasparakis, Christina, Andrew J. Esbaugh, Warren Burggren, and Martin Grosell. 2019. 'Physiological impacts of Deepwater Horizon oil on fish', *Comparative Biochemistry and Physiology Part C: Toxicology & Pharmacology*, 224: 108558.

Rose, G. A., and R. L. O'Driscoll. 2002. 'Capelin are good for cod: can the northern stock rebuild without them?', *Ices Journal of Marine Science*, 59: 1018-26.

Song, X. R., L. Marandel, M. Dupont-Nivet, E. Quillet, I. Geurden, and S. Panserat. 2018. 'Hepatic glucose metabolic responses to digestible dietary carbohydrates in two isogenic lines of rainbow trout', *Biology Open*, 7.

Sutton, T.T., T. Frank, H. Judkins, and I.C. Romero. 2020. 'As Gulf oil extraction goes deeper, who is at risk? Community structure, distribution, and connectivity of the deep-pelagic fauna.' in S.A. Murawski, C.H. Ainsworth, S. Gilbert, D.J. Hollander, C.B. Paris, M. Schluter and D.L. Wetzel (eds.), *Scenarios and responses to future deep oil spills: Fighting the next war* (Springer Nature Switzerland AG: Cham, Switzerland).

Tocher, D. R. 2003. 'Metabolism and functions of lipids and fatty acids in teleost fish', *Reviews in Fisheries Science*, 11: 107-84.

———. 2010. 'Fatty acid requirements in ontogeny of marine and freshwater fish', *Aquaculture Research*, 41: 717-32.

Trustees, Deepwater Horizon Natural Resource Damage Assesssment. 2016. "Deepwater Horizon Oil Spill: Final Programmatic Damage Assessment and Restoration Plan and Final Programmatic Environmental Impact Statement." In. Silver Spring, MD: National Oceanic and Atmospheric Administration.

V'Uorela, R., J. Kaitaranta, and R. R. Linko. 1979. 'Proximate Composition of Fish Roe in Relation to Maturity', *Canadian Institute of Food Science and Technology Journal*, 12: 186-88.

Wallace, R.L., S. Gilbert, and J.E. III Reynolds. 2019. 'Improving the Integration of Restoration and Conservation in Marine and Coastal Ecosystems: Lessons from the Deepwater Horizon Disaster', *Bioscience*, 69: 920-27.

Appendix A
Institutional Animal Care and Use Committee (IACUC) Approval Letter for
CIMAGE Demersal Fish Sampling

USF | UNIVERSITY OF SOUTH FLORIDA

RESEARCH INTEGRITY AND COMPLIANCE
INSTITUTIONAL ANIMAL CARE & USE COMMITTEE

MEMORANDUM

TO: Steven Murawski,

FROM:

Farah Moulvi, MSPH, IACUC Coordinator
Institutional Animal Care & Use Committee
Research Integrity & Compliance

DATE: 2/6/2017

PROJECT TITLE: Center for Integrated Modeling and Analysis of Gulf Ecosystems-CIMAGE III

FUNDING SOURCE: Non-Profit (Private Foundations, H. Lee Moffitt Cancer Center, etc.), For Profit (Industry Sponsored) or Other
                             Gulf of Mexico Research Initiative

IACUC PROTOCOL #:   W IS00003388

PROTOCOL STATUS: **APPROVED**

The Institutional Animal Care and Use Committee (IACUC) reviewed your application
requesting the use of animals in research for the above-entitled study. The IACUC **APPROVED**
your request to use the following animals in your **protocol for a one-year period beginning
2/6/2017:**

---

up to 150 species of marine fishes in the Gulf
of 5500 Mexico, with focus on snappers,
groupers, tilefishes, and other species of
commercial and recreational interest (adult and

sub adult specimens from 40 cm to 150 cm
long and up to 25 kg)

Please take note of the following:

• **IACUC approval is granted for a one-year period at the end of which, an annual renewal form must be submitted for years two (2) and three (3) of the protocol through the eIACUC system.** After three years, all continuing studies must be completely re-described in a new electronic application and submitted to IACUC for review.

• **All modifications to the IACUC-Approved Protocol must be approved by the IACUC prior to initiating the modification.** Modifications can be submitted to the IACUC for review and approval as an Amendment or Procedural Change through the eIACUC system. These changes must be within the scope of the original research hypothesis, involve the original species and justified in writing. Any change in the IACUC-approved protocol that does not meet the latter definition is considered a major protocol change and requires the submission of a new application.

• **All costs invoiced to a grant account must be allocable to the purpose of the grant.** Costs allocable to one protocol may not be shifted to another in order to meet deficiencies caused by overruns, or for other reasons convenience. Rotation of charges among protocols by month without establishing that the rotation schedule credibly reflects the relative benefit to each protocol is unacceptable.

• **The PI must assist the IACUC with tracking wild animal field research activities.** The PI must report episodes of wild animal use, the approximate range of taxa, and the approximate numbers of animals encountered or used at intervals appropriate to the study but at least once a year.

RESEARCH & INNOVATION • RESEARCH INTEGRITY AND COMPLIANCE
INSTITUTIONAL ANIMAL CARE AND USE COMMITTEE
PHS No. A4100-01, AAALAC No. 000434, USDA No. 58-R-0015
University of South Florida • 12901 Bruce B. Downs Blvd., MDC35 • Tampa, FL 33612-4799
(813) 974-7106 • FAX (813) 974-7091

146

Table B1. GC-MS/MS operating parameters for analysis of PAHs and alkylated homologs in liver tissue.

GC carrier gas	Ultra-high purity helium, 1mL/min
Oven program	Initial temp: 60°C, 3 min hold
	12°C/min increase to 120°C
	8°C/min increase to 300°C
	15°C/min increase to 320°C, 4 min hold
Inlet temperature	295°C
Transfer line temperature	320°C
EI source temperature	300°C
Quadrupole temperature	150°C
Collision gas	Ultra-high purity nitrogen, 1.5mL/min
Quench gas	Ultra-high purity helium, 2.25mL/min

Table B2. Mass spectrometry acquisition method parameters for identification and quantification of analytes (pre- and post-extraction internal standards, parent PAHs and alkylated homologs) in standards and liver tissue extracts.

Analyte	Reference to standard	Quantification transition ions	CE[1]	Qualifier transition ions	CE[1]
p-Terphenyl-d14 (post-ext. IS)		$244 \rightarrow 237.3$	25	$244 \rightarrow 159.3$	50
Naphthalene-d8 (I-1)		$136 \rightarrow 108$	25	$136 \rightarrow 134$	10
Naphthalene (NPH)	I-1	$128 \rightarrow 102$	25	$128 \rightarrow 127$	20
C1 NPH	I-1	$142 \rightarrow 141$	20	$142 \rightarrow 115$	25
C2 NPH	I-1	$156 \rightarrow 141$	20	$156 \rightarrow 115$	30
C3 NPH	I-1	$170 \rightarrow 155$	20	$170 \rightarrow 127$	30
C4 NPH	I-1	$184 \rightarrow 169$	30	$184 \rightarrow 154$	40
Acenaphthylene-d8 (I-2)		$160 \rightarrow 158$	30	$160 \rightarrow 132$	30
Acenaphthylene	I-2	$152 \rightarrow 151$	15	$152 \rightarrow 150$	20
Acenaphthene-d10 (I-3)		$164 \rightarrow 162.1$	20	$164 \rightarrow 160.1$	40
Acenaphthene	I-3	$154 \rightarrow 153$	15	$154 \rightarrow 152$	30
Fluorene-d10 (I-4)		$176 \rightarrow 174$	40	$176 \rightarrow 146$	30
Fluorene (FLU)	I-4	$166 \rightarrow 165$	20	$166 \rightarrow 163$	30
C1 FLU	I-4	$180 \rightarrow 165$	25		
C2 FLU	I-4	$194 \rightarrow 179$	30		
C3 FLU	I-4	$208 \rightarrow 193$	40		

Table B2. (Continued)

C4 FLU	I-4	222 → 206	40	222 → 179	40
Dibenzothiophene-d8 (I-5)		192 → 160.1	40	192 → 146	40
Dibenzothiophene (DBT)	I-5	184 → 139	30		
C1 DBT	I-5	198 → 197	20	198 → 165	30
C2 DBT	I-5	212 → 197	40		
C3 DBT	I-5	226 → 211	40		
C4 DBT	I-5	240 → 211	40		
Phenanthrene-d10 (I-6)		188 → 160.1	30	188 → 184.1	10
Phenanthrene (PHN)	I-6	178 → 176	30	178 → 152	30
Anthracene-d10 (I-7)		188 → 160.1	30	188 → 184.1	10
Anthracene (ANT)	I-7	178 → 176	30	178 → 152	30
C1 PHN/ANT	I-7	192 → 191	20	192 → 189	40
C2 PHN/ANT	I-7	206 → 191	20	206 → 189	40
C3 PHN/ANT	I-7	220 → 205	30	220 → 189	40
C4 PHN/ANT	I-7	234 → 219	50	234 → 204	20
C5 PHN/ANT	I-7	248 → 247	20	248 → 246	40
Fluoranthene-d10 (I-8)		212 → 208.1	50	212 → 184.1	40
Fluoranthene (FLA)	I-8	202 → 201	30	202 → 200	40
Pyrene-d10 (I-9)		212 → 208.1	50	212 → 184.1	20
Pyrene (PYR)	I-9	202 → 201	30	202 → 200	40
C1 FLA/PYR	I-9	216 → 215	30	216 → 213	40
C2 FLA/PYR	I-9	230 → 229	40	230 → 215	20
C3 FLA/PYR	I-9	244 → 229	40	244 → 228	40
C4 FLA/PYR	I-9	258 → 243	20	258 → 228	40
C5 FLA/PYR	I-9	272 → 271	10	272 → 257	40
Benzo[a]anthracene-d12 (I-10)		240 → 236.1	50	240 → 212.1	40
Benzo[a]anthracene (BaA)	I-10	228 → 226	40	228 → 202	30
Chrysene-d12 (I-11)		240 → 236.1	50	240 → 212.1	40
Chrysene (CHR)	I-11	228 → 226	40	228 → 202	30
C1 BaA/CHR	I-11	242 → 241	40	242 → 239	40
C2 BaA/CHR	I-11	256 → 255	20	256 → 239	40
C3 BaA/CHR	I-11	270 → 255	20	270 → 239	50
C4 BaA/CHR	I-11	284 → 282	50	284 → 269	50
C5 BaA/CHR	I-11	298 → 296	50	298 → 283	50
Benzo[b]fluoranthene-d12 (I-12)		264 → 260.1	50	264 → 236	40
Benzo[b]fluoranthene	I-12	252 → 250.1	40	252 → 224	35
Benzo[k]fluoranthene-d12 (I-13)		264 → 260.1	50	264 → 236	40
Benzo[k]fluoranthene	I-13	252 → 250.1	40	252 → 224	35
Benzo[e]pyrene-d12 (I-14)		264 → 260.1	50	264 → 236	40
Benzo[e]pyrene	I-14	252 → 250.1	40	252 → 226	40
Benzo[a]pyrene d12 (I-15)		264 → 260.1	50	264 → 236	40

Table B2. (Continued)

Benzo[*a*]pyrene	I-15	252 → 250.1	40	252 → 224	35
Perylene-d12 (I-16)		264 → 260.1	50	264 → 236	40
Perylene	I-16	252 → 250.1	40	252 → 224	35
Indeno[1,2,3,-*cd*]pyrene-d12 (I-17)		288 → 284.1	50	288 → 255.9	50
Indeno[1,2,3,-*cd*]pyrene	I-17	276 → 274	50	276 → 203	40
Dibenzo[*a,h*]anthracene-d14 (I-18)		292 → 288.3	50	292 → 105	40
Dibenzo[*a,h*]anthracene	I-18	278 → 276.1	40	278 → 252	50
Benzo[*g,h,i*]perylene-d12 (I-19)		288 → 284.1	50	288 → 256.1	50
Benzo[*g,h,i*]perylene	I-19	276 → 274	50	276 → 248.2	50

[1]CE = collision energy
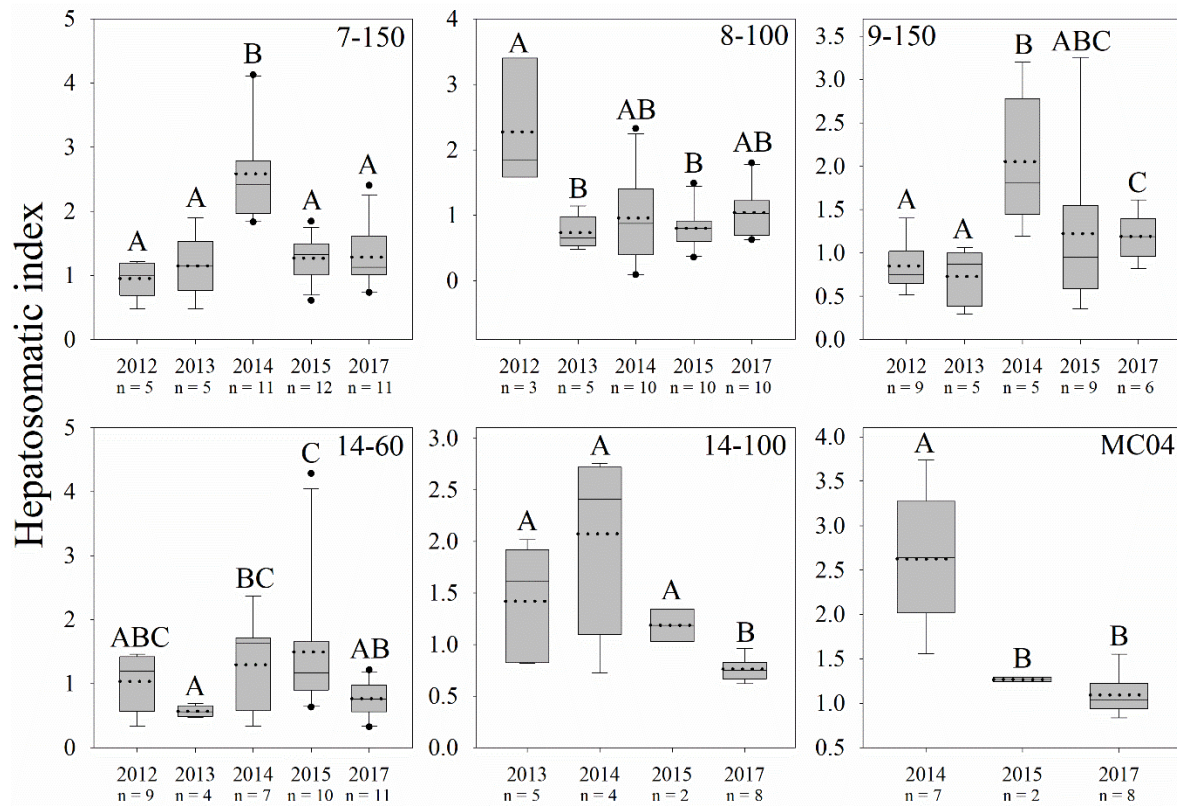
Figure B1. Hepatosomatic index (HSI) over time for Tilefish sampled at individual stations (station number designated on plot) in the northern Gulf of Mexico. Sample size (n) noted by year. Letters (ABC) denote significantly different years. Solid line = median; dotted line = mean.

149

Appendix C
Supplementary Information for Chapter 3

Table C1. Detection frequency of high molecular weight (HMW) PAHs, mean, and range of the ΣHMW PAHs in liver tissue of Tilefish from the six geographic regions.

Region	Detection frequency	Mean ΣHMW PAHs (ng g^{-1} w.w.)[1]	Range ΣHMW PAHs (ng g^{-1} w.w.)
North central	9.52%	8.10 ± 5.76	4.13 – 19.4
Northwest	3.33%	14.89 ± 16.7	3.05 – 26.7
Southwest	3.03%	1.51	1.51 – 1.51
Bay of Campeche	12.8%	9.95 ± 8.62	4.39 – 26.8
Yucatán shelf	6.25%	1.91 ± 0.580	1.50 – 2.32
Northwest Atlantic	62.9%	13.39 ± 31.5	0.5 - 199
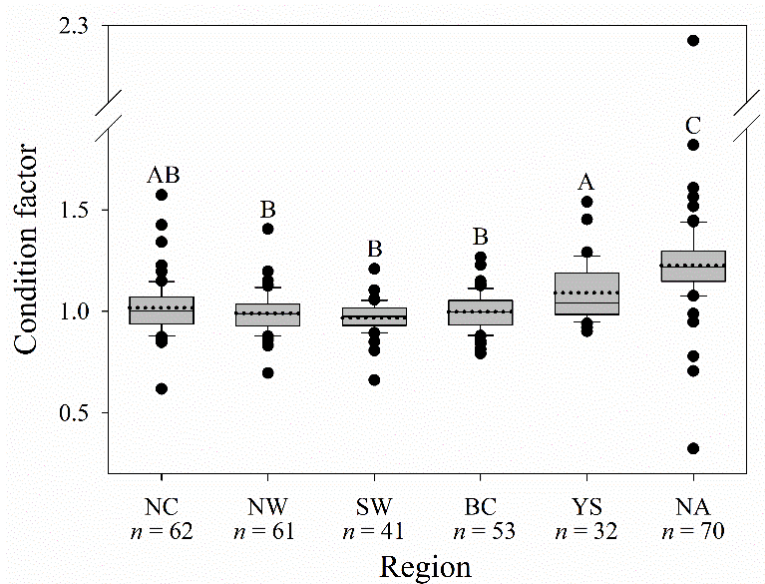
Figure C1. Fulton's condition factor (K) for Tilefish by region (NC = north central; NW = northwest; SW = southwest; BC = Bay of Campeche; YS = Yucatán Shelf; NA = north Atlantic). Sample size (*n*) noted by region. Letters (ABC) denote significantly different regions at α = 0.05. Solid line = median; dotted line = mean.
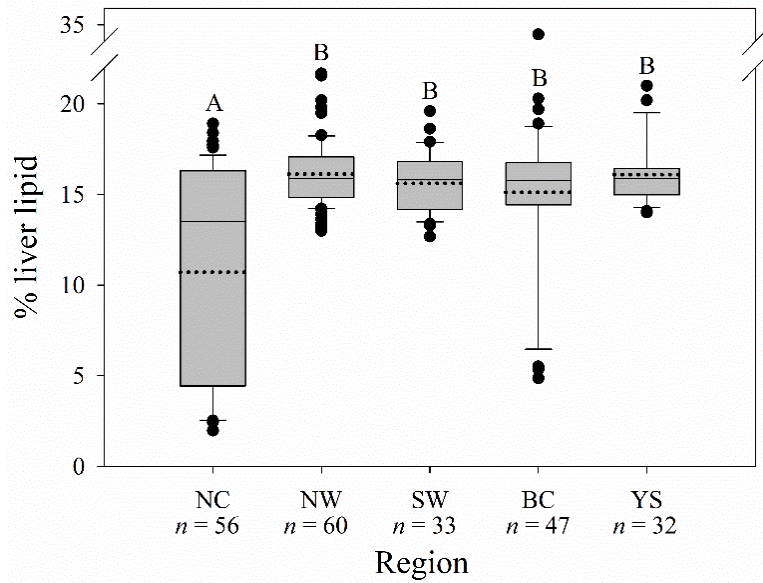
Figure C2. Percent liver lipid for Gulf of Mexico Tilefish sampled 2015 and 2016 by region (NC = north central; NW = northwest; SW = southwest; BC = Bay of Campeche; YS = Yucatán Shelf). Sample size (*n*) noted by region. Letters (ABC) denote significantly different regions at α = 0.05. Solid line = median; dotted line = mean.
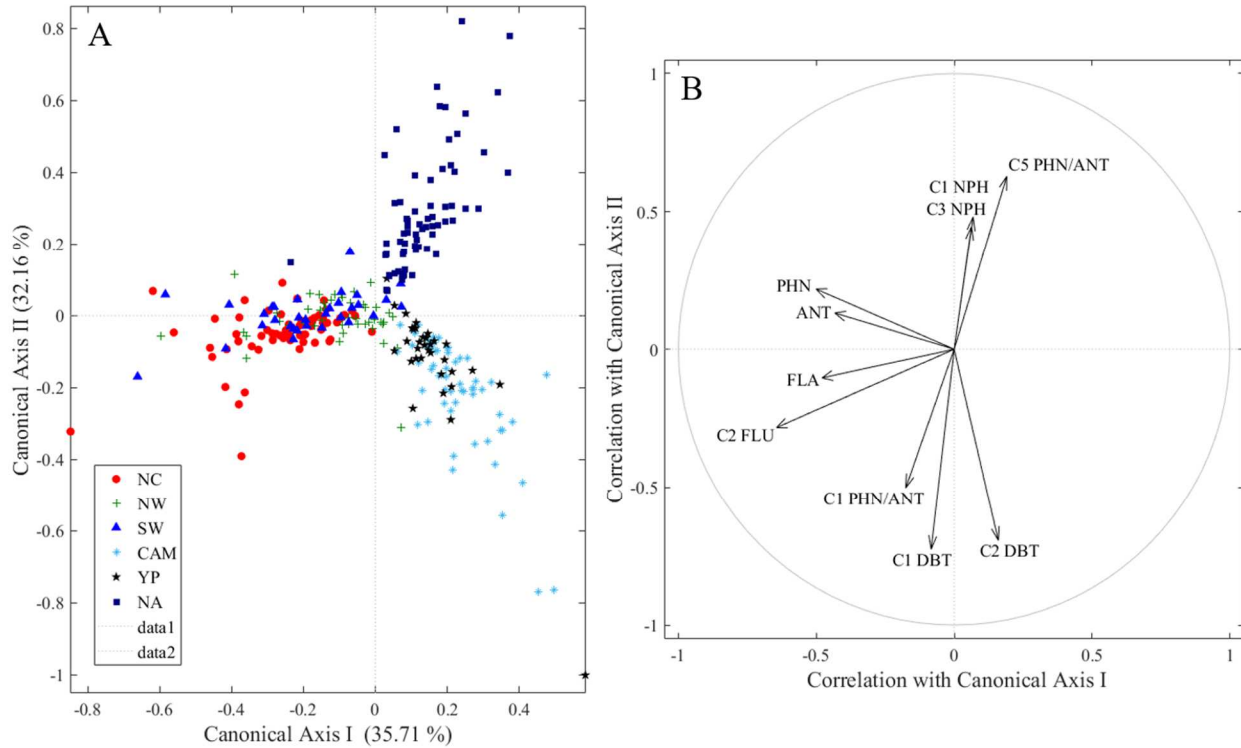
Figure C3. Canonical analysis of principal coordinates ordination (A) of Tilefish liver PAH composition by region (NC = north central; NW = northwest; SW = southwest; CAM = Bay of Campeche; YP = Yucatán Shelf; NA = north Atlantic), and the top ten biplot vectors explaining separation of groups (B; PHN = phenanthrene; ANT = anthracene; NPH = naphthalene; FLA = fluoranthene; FLU = fluorene; DBT = dibenzothiophene).
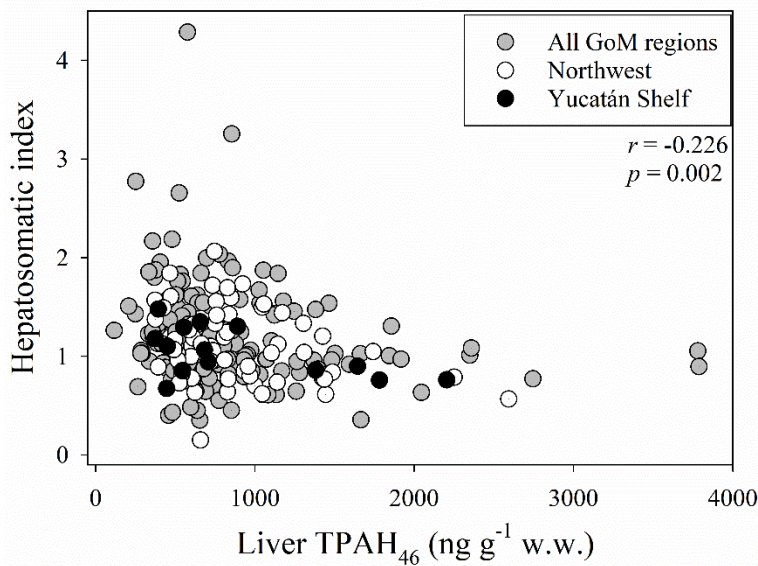
Figure C4. Hepatosomatic index verses liver total PAH (TPAH$_{46}$) concentration for Gulf of Mexico Tilefish sampled 2015 to 2016. Correlations are significant at $\alpha = 0.05$.
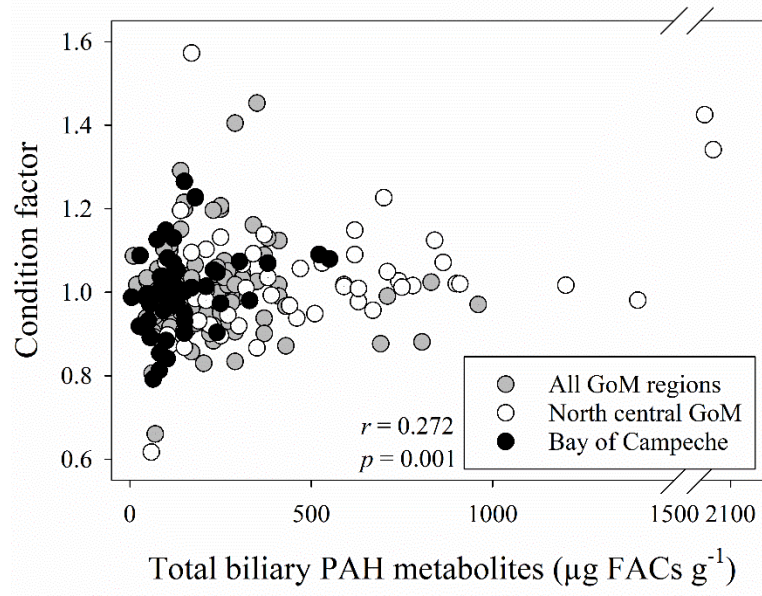
Figure C5. Fulton's condition factor versus total biliary PAH metabolite equivalents for Gulf of Mexico Tilefish sampled 2015 to 2016. Correlations are significant at $\alpha = 0.05$.
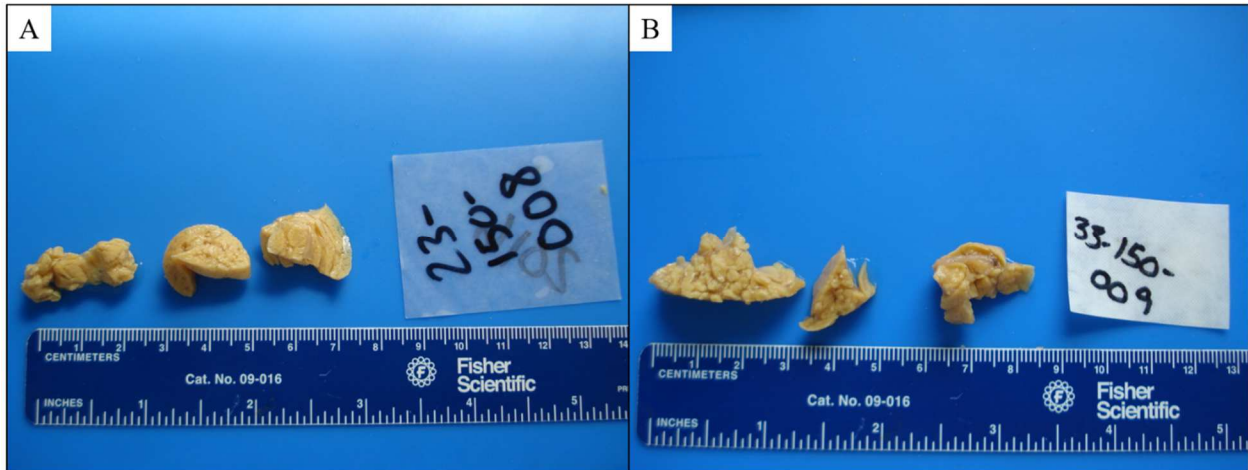
Figure D1. Variation in lobulation in Tilefish liver. Note the prominent vasculature/ducts throughout the parenchyma.
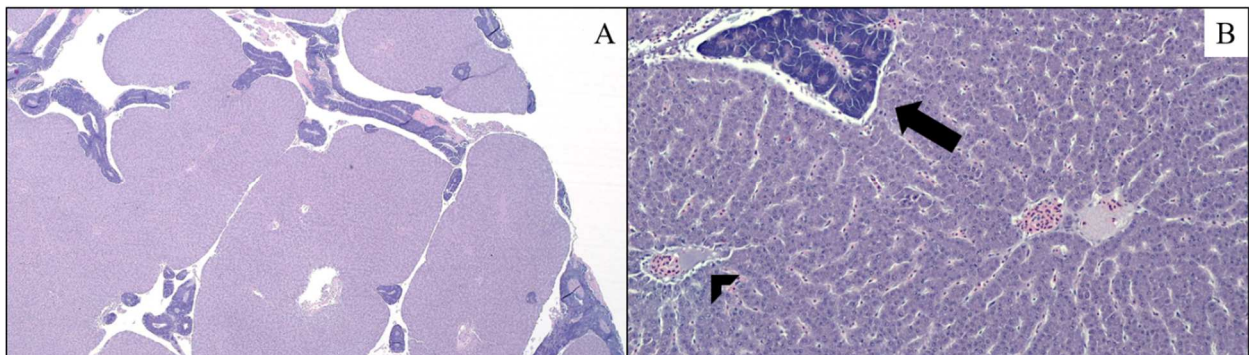
Figure D2. Photomicrograph of normal liver with lobular arrangement (A; H&E; 20x). Photomicrograph of normal liver with hepatic cords, exocrine pancreas (arrow), and central veins (arrowhead; B; H&E; 100x).
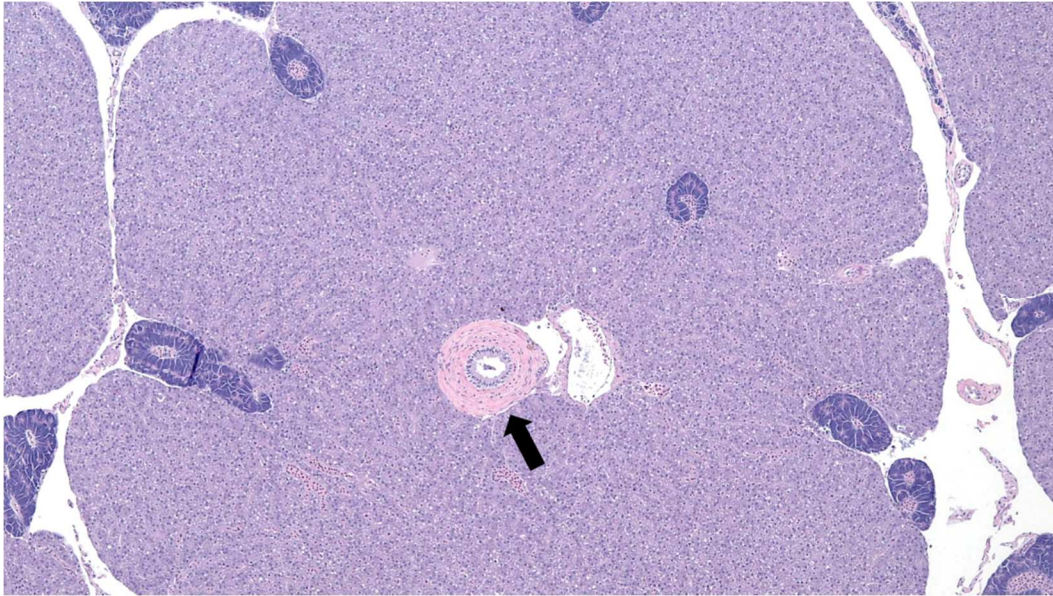
Figure D3. Photomicrograph of bile duct lined by cuboidal epithelial cells supported by concentric layers of peribiliary fibrous connective tissue (arrow; H&E; 100X).
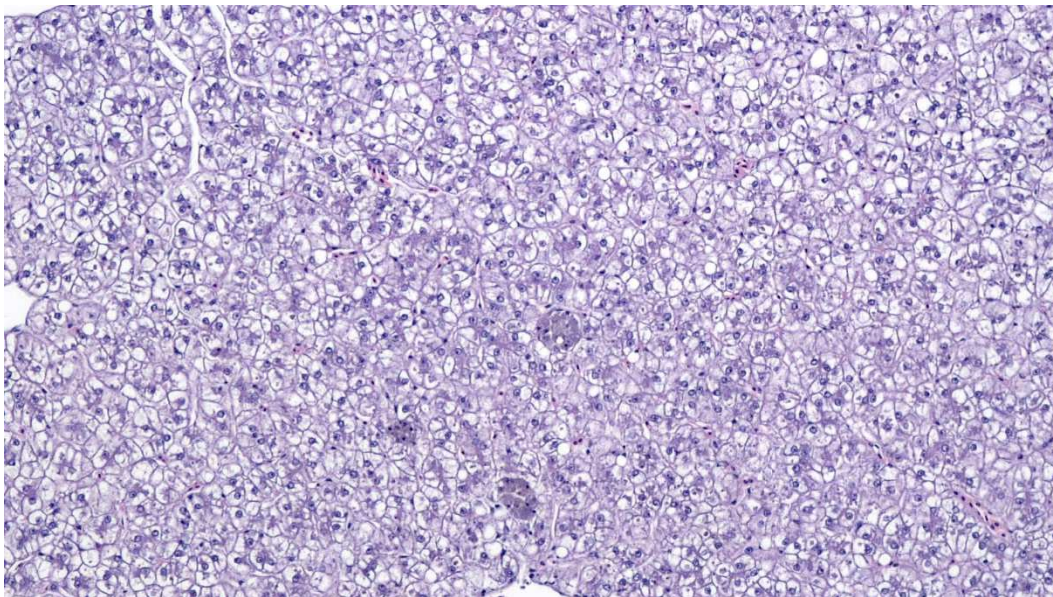
Figure D4. Photomicrograph of hepatocytes moderately expanded by glycogen-type vacuolization (H&E; 100x).
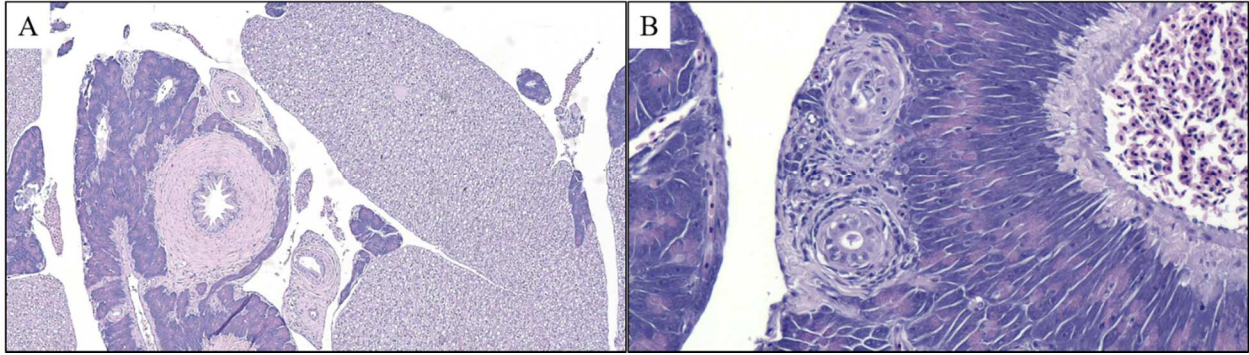
Figure D5. Photomicrograph of moderate to severe bile duct fibrosis and duplication (A; H&E; 40x). Photomicrograph of bile duct duplication (B; H&E; 100x).
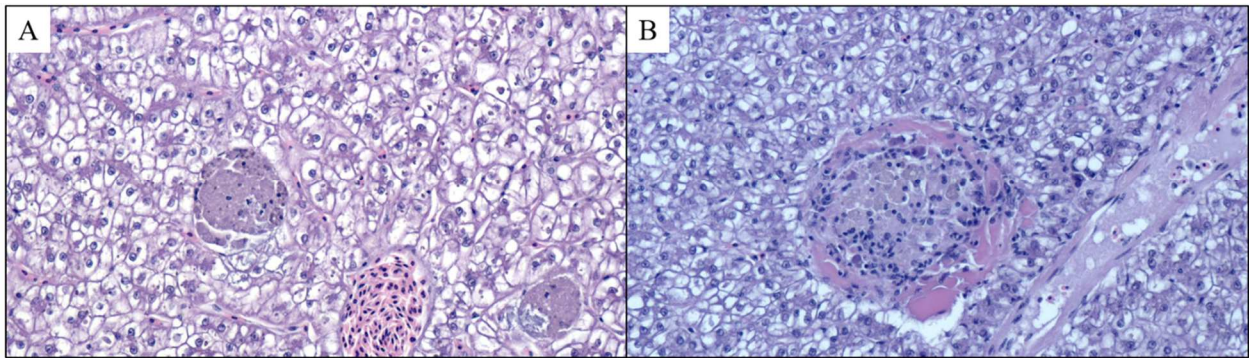
Figure D6. Photomicrograph of section with mild to moderately increased pigmented macrophage aggregates and severe glycogen-type vacuolization (A; H&E; 100x). Photomicrograph of mildly increased pigmented macrophage aggregates with fibrin (B; H&E; 200x).
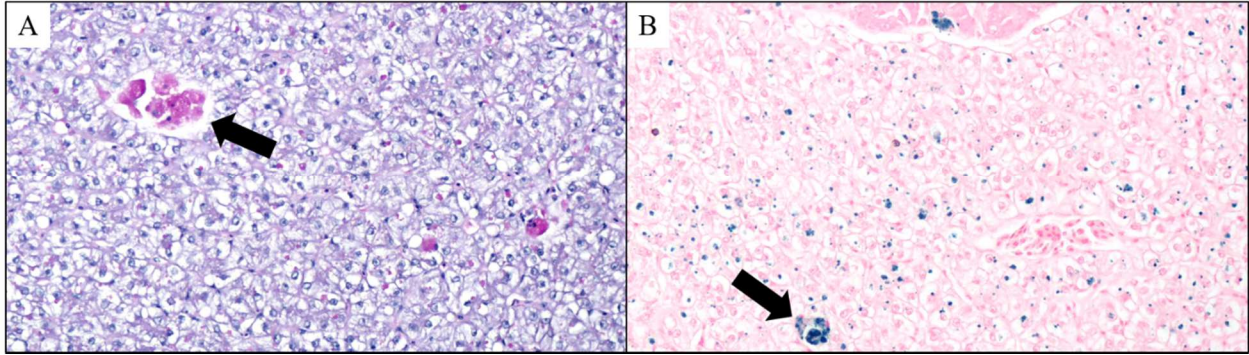
Figure D7. Photomicrograph of pigmented macrophage aggregates and intracellular pigment staining positive for Periodic Acid Schiff with diastase (A; arrow; 200x). Periodic Acid Schiff positive material is also present within hepatocytes (A). Photomicrograph of pigmented macrophage aggregates and intracellular pigment staining positive (blue) for Perl's iron (B; arrow; 200x).
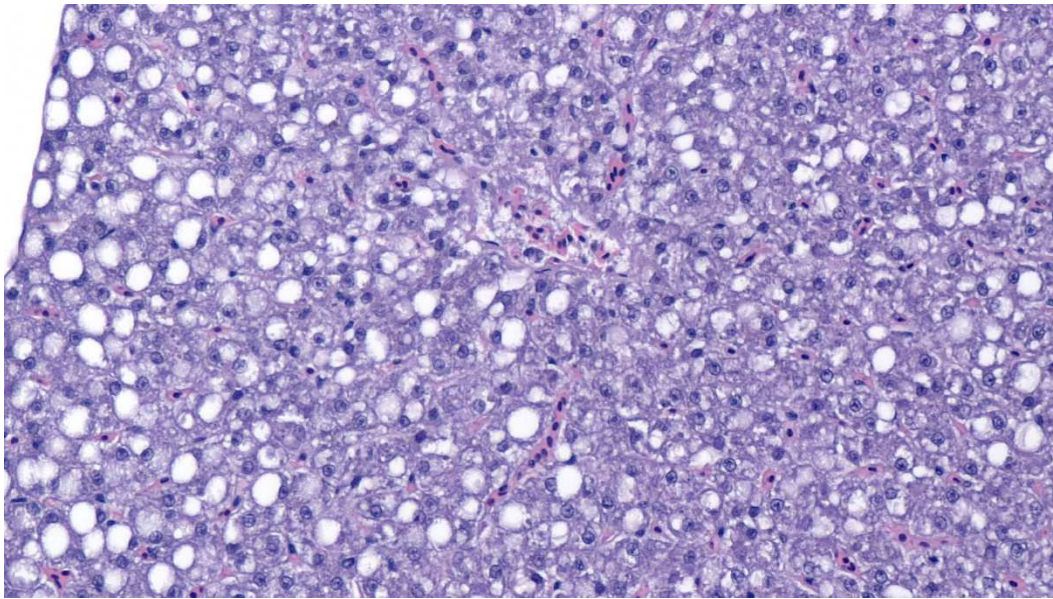
Figure D8. Photomicrograph of hepatocytes with mild to moderate cytoplasmic expansion by lipid-type vacuolization (H&E; 200x).
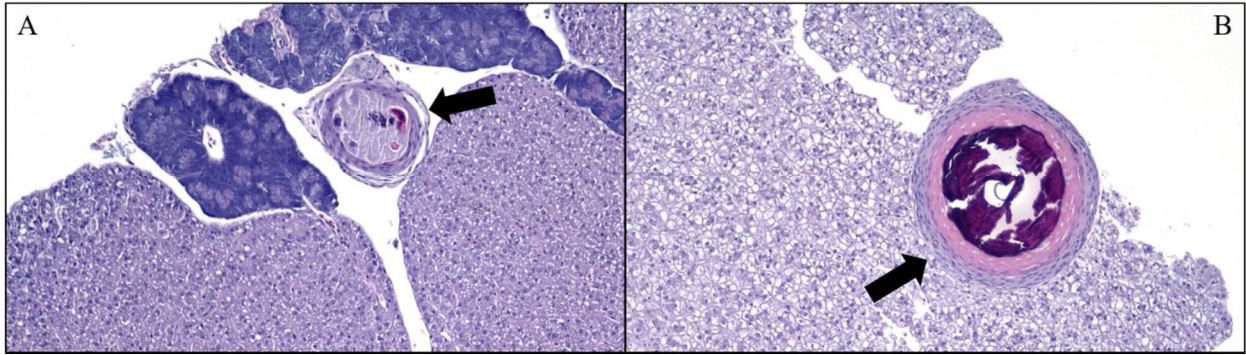
Figure D9. Photomicrograph of granulomas associated with the pancreatic lobules and in the hepatic parenchyma (arrows; H&E; 200x).
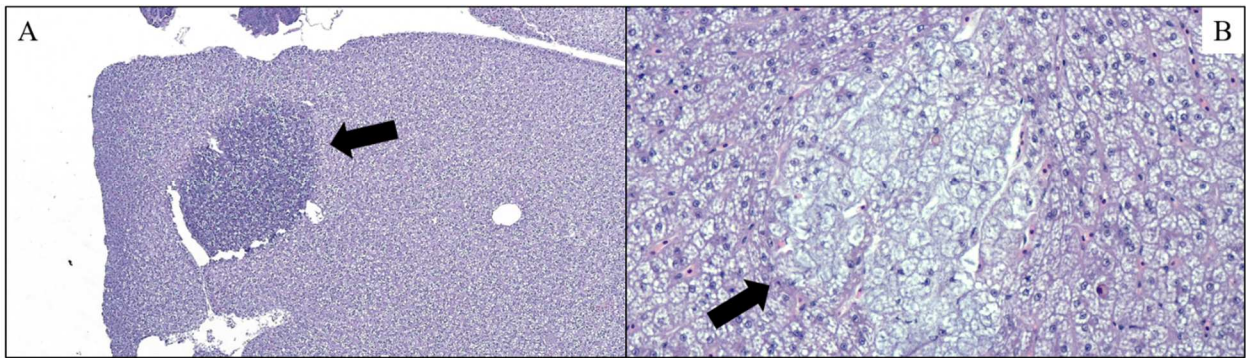
Figure D10. Photomicrograph of a hepatocellular basophilic focus (A; H&E; 40x) and a hepatocellular clear-cell focus (B; H&E; 100x).
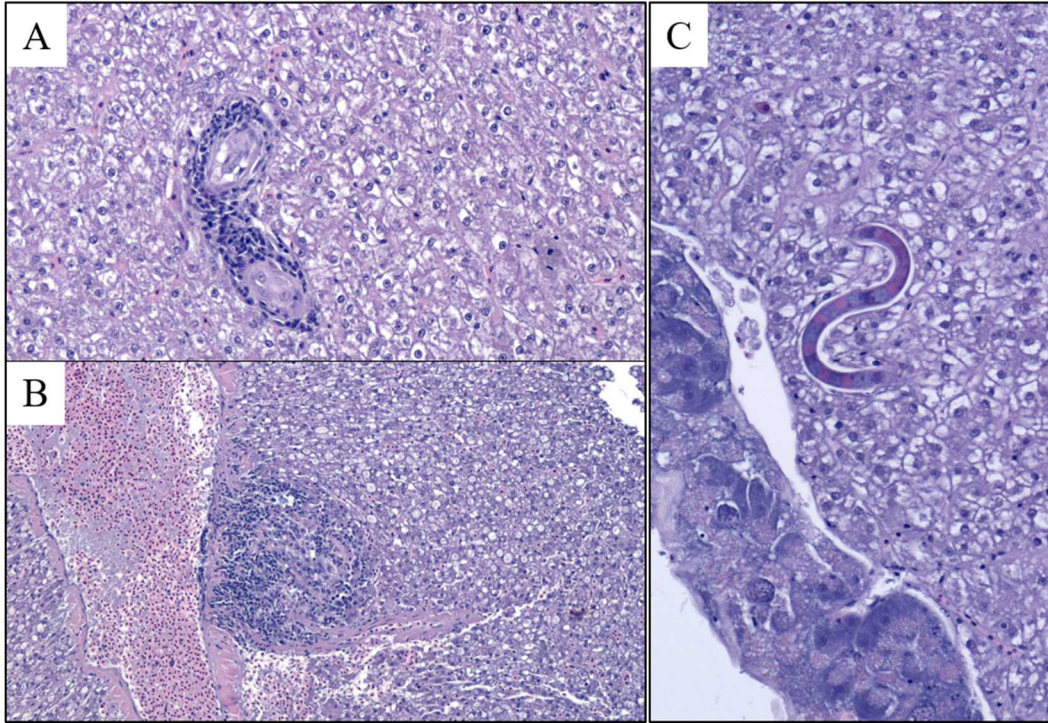
Figure D11. Photomicrographs of inflammation and associated larvae (A; H&E; 200x), lymphocytic inflammation (B; H&E; 100x), and a migrating nematode (C; H&E; 200x).
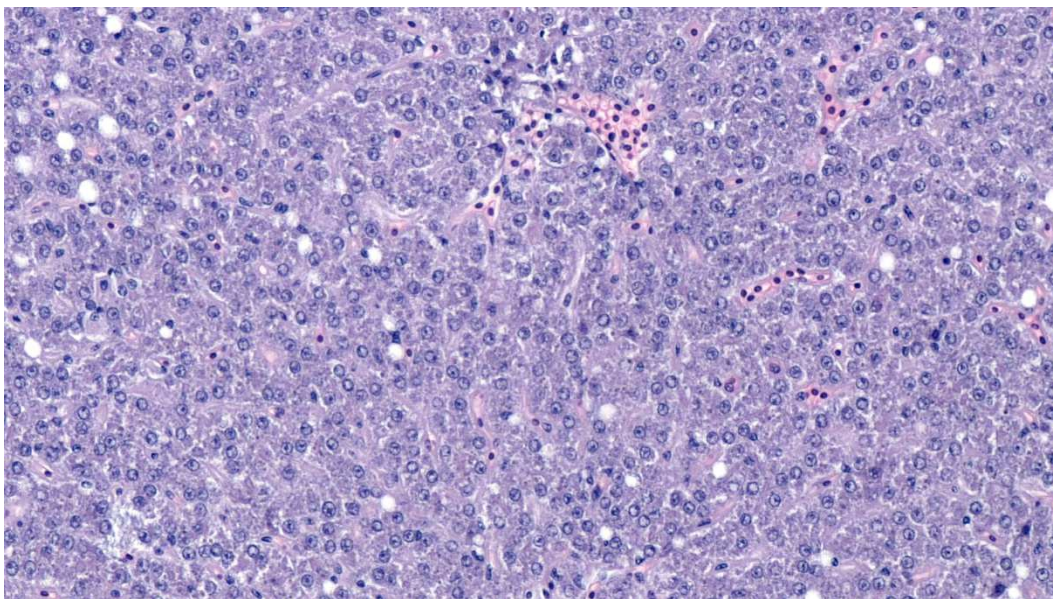
Figure D12. Photomicrograph of hepatocellular atrophy (H&E; 200x).
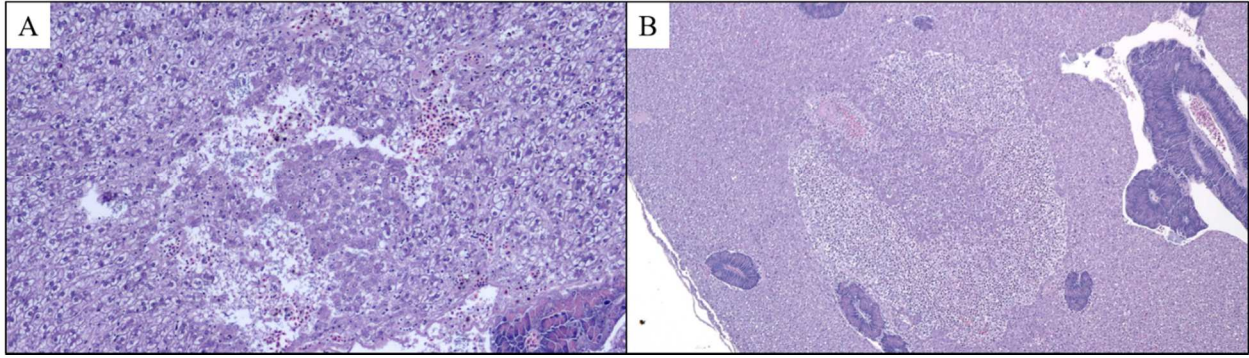
Figure D13. Photomicrograph of foci of hepatocellular necrosis (A; H&E; 100x). Photomicrograph of large foci of hepatocellular necrosis centered on a thrombosed vessel (B; H&E; 40x).
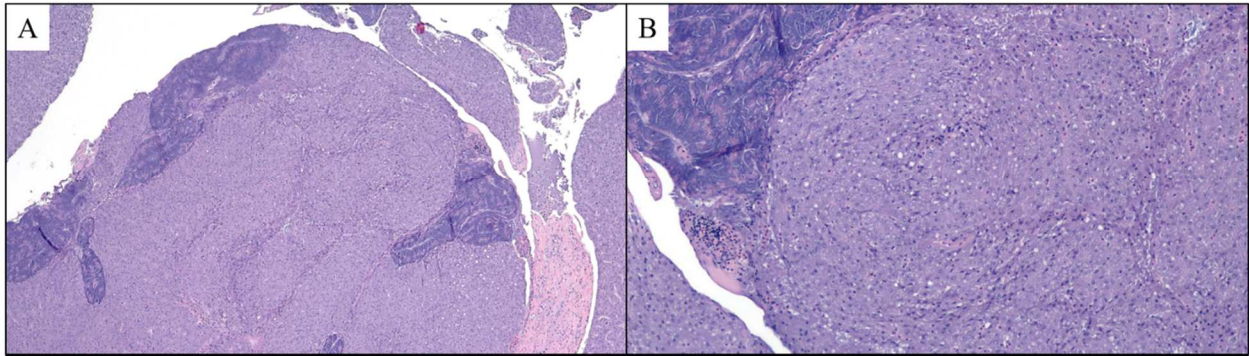
Figure D14. Photomicrographs of hepatocellular adenoma (H&E; A40x; B100x).
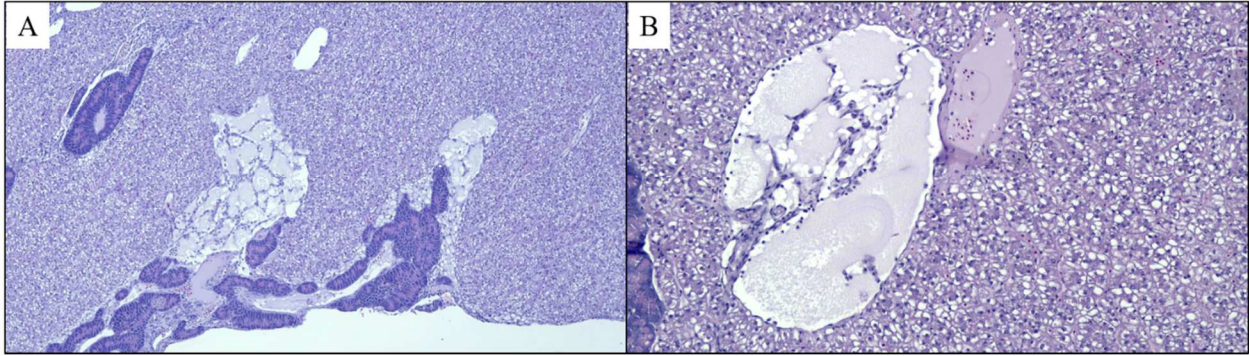
Figure D15. Photomicrographs of cystic spaces (A; H&E; 40x) and pseudocystic spaces (B; H&E; 100x).
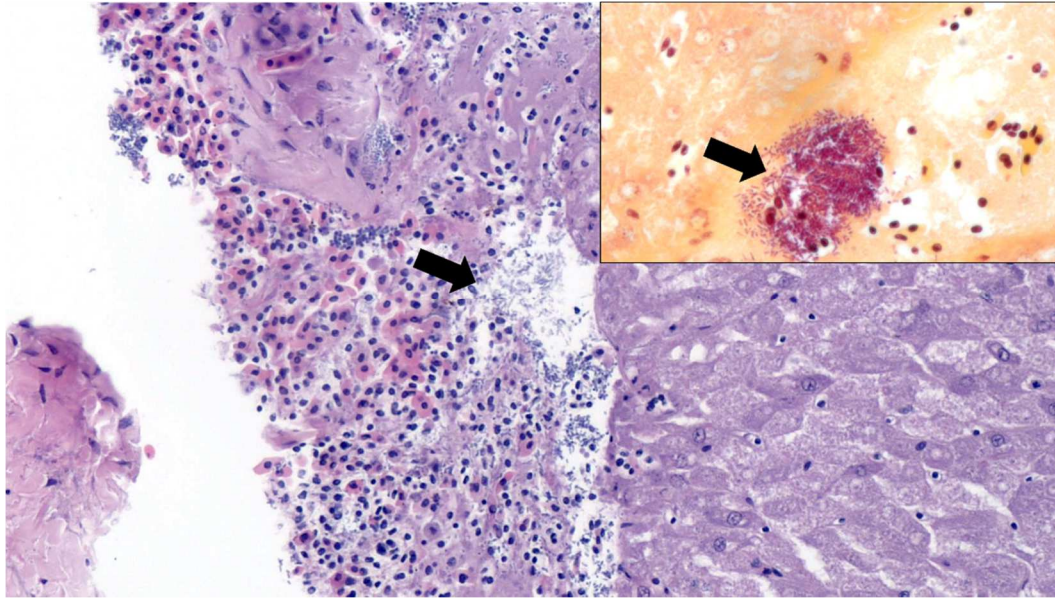
Figure D16. Photomicrograph of hepatic vessels with bacteria (H&E; 200x). Note hepatocytes are moderately autolyzed. The inset is a photomicrograph with gram-staining of bacteria identifying Gram-negative rods (600x).
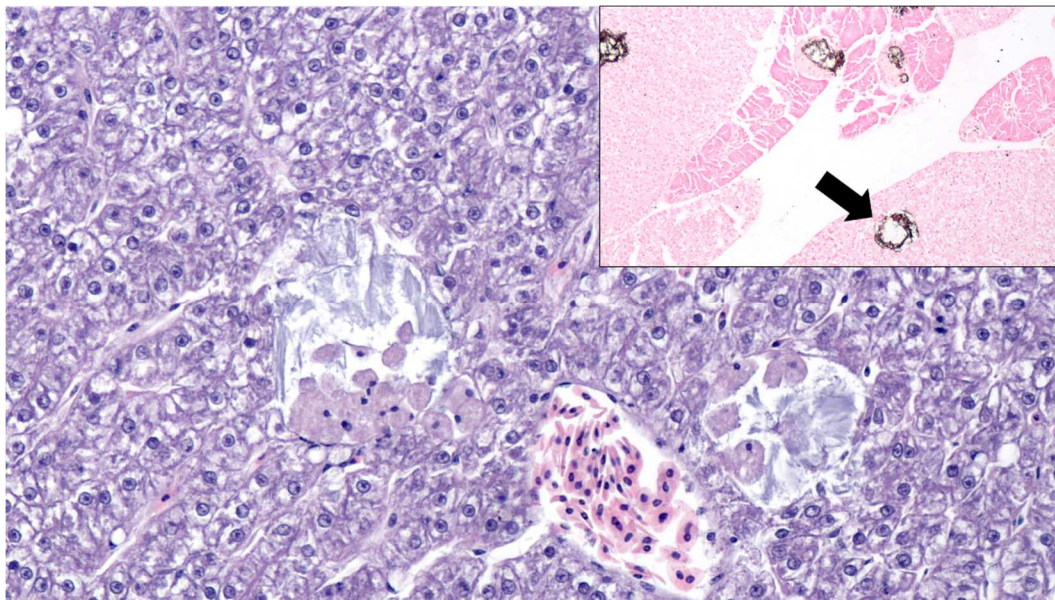
Figure D17. Photomicrograph of radiating basophilic material within hepatic cords (H&E; 100x). The inset is a photomicrograph of positive Von Kossa staining of the material (100x)

Table E1. Raw data for Tilefish collected via these studies, including the unique fish ID (station-number), year of collection, sex, total length, weights (total weight, liver weight, gastrointestinal tract (GIT) weight, gonad weight), total liver PAH concentration (TPAH46), total biliary PAH metabolite concentration, and liver lipid.

Fish ID	Year	Sex	Total length (cm)	Weights (kg)				Liver TPAH46 (ng/g w.w.)	Total Biliary PAH Metabolites (ug FACs/g)	Liver lipid (%)
				Total	Liver	GIT	Gonad			
14-60-005	2012	F	47	1.724	0.018	0.044		671	180	5.42
14-60-006	2012	F	53	1.674	0.02	0.038	0.018	456	270	17.16
14-60-008	2012	M	67	4	0.056	0.058		569	160	11.00
14-60-010	2012	F	50	1.51	0.022	0.04	0.018	608	180	11.27
14-60-011	2012	F	52	1.8	0.006	0.054	0.016	531	340	13.04
14-60-012	2012	F	79	6.8	0.098	0.189	0.002	568	320	16.92
14-60-013	2012	F	64	3.2	0.042	0.076	0.016	624		10.40
14-60-014	2012	U	58	2.2	0.01	0.05		497	150	6.22
14-60-016	2012	F	75	6.2	0.042	0.172		1009	220	10.73
7-150-001	2012	F	79	5.6	0.05	0.21	0.006	1370	230	6.31
7-150-006	2012	F	49	1.248	0.006	0.046	0.006	8110	220	
7-150-012	2012	F	79	5.748	0.07	0.244	0.01	1034	230	7.80
7-150-015	2012	F	89	6.125	0.072	0.202	0.006	925	250	
7-150-021	2012	F	82	7.46	0.074	0.224	0.002	918	300	6.97
7-150-023	2012	F	80	7.08					76	
8-100-002	2012	F	56	2.4	0.038	0.056		1201	300	
8-100-004	2012	U	50	1.47	0.05	0.074			210	
8-100-011	2012	U	57	2.5	0.046	0.048		795	230	15.50
9-150-007	2012	U	56	2.2	0.02	0.05		509	190	20.92

Table E1. (Continued)

9-150-010	2012	F	81	7	0.068	0.204	0.002	476	160	22.17
9-150-011	2012	F	89	10	0.052	0.273		1041	300	15.87
9-150-012	2012	F	81	7.6	0.056	0.192	0.002	590	110	16.34
9-150-014	2012	F	75	6	0.034	0.12		969	330	
9-150-016	2012	U	59	2.4	0.018	0.058		436	260	12.75
9-150-018	2012	F	45	1	0.014	0.022	0.004		170	
9-150-025	2012	F	83	6	0.044	0.104		790		12.50
9-150-028	2012	F	92	9	0.096	0.338		607	280	17.16
9-80-021	2013		73	4.4	0.023	0.134	0.048	1076	210	4.95
9-80-022	2013	F	66	3.328	0.019	0.098	0.023	1129	130	5.31
9-80-023	2013	F	70	3.97					270	
9-80-024	2013	M	68	3.786	0.027	0.0198		560	69	3.96
9-80-027	2013	M	92	9.4	0.051	0.314		1520		2.88
9-80-028	2013	U	66	3.468	0.038	0.092		567	250	3.05
9-80-033	2013	F	62	3.396	0.029	0.107		472	120	6.06
9-80-034	2013	F	46	1.413					250	
9-80-035	2013	F	45	1.049					130	
14-60-001	2013	M	80	5.206					140	
14-60-002	2013	M	93	9.8	0.046	0.218	0.003	2401	170	9.13
14-60-003	2013	F	60	2.11					220	
14-60-004	2013	F	62	2.81					350	
14-60-008	2013	F	89	9.2	0.063	0.238	0.007	1242	200	7.39
14-60-010	2013	F	58	1.967					220	
14-60-012	2013	U	61	2.414					170	
14-60-015	2013	F	79	5.17				1205	280	6.22
14-60-022	2013	U	63	2.642					180	
14-60-027	2013	F	40	0.98					110	
14-60-034	2013	F	61	2.6					260	
14-60-035	2013	U	77	5.8	0.032	0.147		1399	270	5.47
14-60-047	2013	F	62	2.64					57	

Table E1. (Continued)

14-60-048	2013	F	56	1.87					240	
14-60-059	2013	M	92	10.2	0.058	0.256	0.011	1380	270	4.83
14-60-067	2013	F	59	2.458					110	
14-60-068	2013	F	53	1.624					68	
5-100-014	2013	F	49	1.312	0.018	0.042		564	240	7.43
5-100-015	2013	F	50	1.394	0.018	0.038		763	360	4.43
5-200-015	2013	F	51	1.714	0.032	0.264	0.014	523	250	4.37
5-200-020	2013	F	61	2.466	0.037	0.11		767	260	5.05
7-150-005	2013	F	51	1.44					450	
7-150-008	2013	F	48	1.14	0.012	0.04	0.01	695		
7-150-017	2013	F	48	0.946	0.018	0.044	0.014	1570		
7-150-018	2013	F	55	1.896	0.022	0.074	0.012	563		7.39
7-150-020	2013	F	59	2.1	0.01	0.068		616		6.93
7-150-023	2013	F	52	1.226	0.014	0.042	0.012	748	430	6.40
8-100-002	2013	U	52	1.856				640	240	
8-100-005	2013	M	75	4.728	0.054	0.132		476	320	16.18
8-100-006	2013	U	78	4.53	0.037	0.126		989	22	15.50
8-100-010	2013	U	70	3.306	0.016	0.104		914	480	13.24
8-100-011	2013	F	56	2.49					400	
8-100-018	2013	M	71	4.146	0.027	0.127		971	370	17.24
8-100-020	2013	M	82	7				731	460	16.18
8-100-023	2013	U	74	5.504	0.032	0.161		576	340	18.37
8-100-024	2013	M	70	4.034					380	
8-100-026	2013	U	43	0.945					320	
8-100-029	2013	U	51	1.493					420	
8-100-030	2013	F	56	1.854					270	
9-150-014	2013	M	72	3.904	0.034	0.142		656	220	15.84
9-150-022	2013	M	85	8	0.038	0.246		655	270	15.66
9-150-025	2013	U	72	4.71	0.014	0.22		425	170	16.67
9-150-027	2013	M	71	3.872					260	

Table E1. (Continued)

9-150-028	2013	U	50	1.617					190	
9-150-029	2013	U	70	4.482	0.042	0.202	0.04	928	230	8.16
9-150-030	2013	U	47	1.288					240	
9-150-031	2013	M	70	4.22					240	
9-150-032	2013	M	72	4.44	0.047	0.214		495	240	16.10
9-150-033	2013	F	63	2.674					270	
9-150-035	2013	M	49	1.416					130	
11-150-002	2013	F	69	3.744	0.038	0.184	0.036	1190		6.90
11-150-005	2013	M	64	3.128	0.036	0.129		867	180	3.98
11-150-008	2013	F	62	3.2	0.032	0.101		733		6.25
11-150-009	2013	F	79	5.666	0.054	0.218		958	44	3.00
11-150-012	2013	F	83	8.2	0.067	0.374		833	68	4.39
11-150-014	2013	F	75	4.888					120	
11-150-017	2013	F	66	3.672					200	
11-150-018	2013	M	68	4.054					250	
11-150-022	2013	F	44	0.966					32	
11-150-023	2013	F	60	2.367					180	
12-100-013	2013	F	90		0.165	0.33		698	44	5.39
14-100-003	2013	M	81	6	0.05	0.162		1040	230	6.34
14-100-005	2013	U							69	
14-100-006	2013	M	99	12.4	0.101	0.286		1410	110	11.59
14-100-010	2013	U	63	2.63	0.048	0.081		517	66	6.00
14-100-012	2013		63	2.974	0.06	0.104		812	66	7.18
14-100-025	2013	M	76	4.702	0.076	0.193	0.014	789	72	7.28
14-100-048	2013	U	56	2.17					200	
14-100-049	2013	U	50	1.332					54	
GP03-007	2014	F	60	2.93	0.034	0.07	0.008	454	200	10.29
MC04-002	2014	F	61	3.072	0.062	0.156	0.034	770	140	7.04
MC04-004	2014	F	53	1.818	0.068	0.052	0.01	570		
MC04-006	2014	F	66	3.86	0.102	0.128		930		

Table E1. (Continued)

MC04-009	2014	F	58	2.198	0.072	0.306	0.038		300	
MC04-011	2014	F	69	4.564	0.071	0.166	0.048	610	310	4.95
MC04-014	2014	F	64	2.86	0.082	0.21	0.056	804	330	5.45
MC04-016	2014	F	64		0.052	0.17	0.054	542	220	5.31
MC04-017	2014	M	83	8	0.182	0.226		502	1100	7.46
9-80-004	2014	U	47	0.514	0.018	0.022		883		3.98
9-80-005	2014	F	71	3.958	0.022	0.156	0.036	1840	830	6.06
9-80-007	2014	M	78	6.35	0.07	0.192		934	560	7.43
9-80-010	2014	F	51	1.598	0.03	0.042	0.002	1880	130	4.00
14-60-001	2014	M	87	8.89	0.03	0.246		1670	510	6.83
14-60-002	2014	F	63	2.676	0.044	0.112	0.052	1280		5.29
14-60-003	2014	F	58	2.126		0.05	0.004		430	
14-60-004	2014	F	62	3.068	0.05	0.108	0.014		330	
14-60-006	2014	F	60	2.36	0.056	0.124	0.046	763	250	4.35
14-60-007	2014	U	82	6.89	0.118	0.274		742	150	6.12
14-60-008	2014	F	66	3.306	0.026	0.15	0.034	1750		6.86
14-60-009	2014	F	62	2.776	0.016	0.062			310	
14-60-013	2014	F	58	2.136		0.08			450	
14-60-018	2014	F	59	2.51		0.032			410	
7-150-001	2014	F	48	1.238	0.05	0.454	0.05	1204	470	3.94
7-150-002	2014	F	84	6.33	0.116	0.268		800		6.00
7-150-004	2014	F	44	1.358	0.03	0.06	0.024	418	310	4.81
7-150-005	2014	F	49	1.29	0.036	0.054	0.032		530	
7-150-006	2014	M	55	1.932	0.038	0.08		565	230	10.05
7-150-007	2014	F	61	2.638					320	
7-150-008	2014	M	91	10.33	0.426	0.344	0.026	1390	580	6.03
7-150-009	2014	F	59	2.302	0.056	0.136	0.028	752	430	7.35
7-150-010	2014	F	54	1.692	0.046	0.084	0.03	684		9.60
7-150-011	2014	F	48	1.314	0.026	0.044	0.018	528	570	6.76
7-150-012	2014	F	58	2.09	0.04	0.092	0.026	1230	400	7.04

166

Table E1. (Continued)

7-150-013	2014	F	52	1.566	0.038	0.06	0.022	7720	640	6.09
8-100-001	2014	F	77	4.658	0.048	0.156		596	620	15.84
8-100-003	2014	M	75	5.6	0.13	0.224		596	320	16.18
8-100-004	2014	F	61	3.248	0.044	0.102		724	180	11.54
8-100-006	2014	M	85	8	0.038	0.228		2420	920	12.68
8-100-007	2014	M	84	7.4	0.112	0.252		939	550	15.50
8-100-009	2014	M	51	2.24	0.002	0.118			410	
8-100-011	2014	M	84	5.84	0.042	0.224			460	
8-100-012	2014	F	48	1.338	0.002	0.05			270	
8-100-015	2014	F	75	5.04	0.028	0.156			240	
8-100-020	2014	F	51	1.758	0.024	0.07			470	
9-150-001	2014	M	65	3.4	0.058	0.11		288	270	14.63
9-150-002	2014	F	67	3.7	0.044	0.154	0.044	681	240	16.67
9-150-003	2014	F	49	1.186	0.038	0.056		730	210	
9-150-008	2014	F	56	2.036	0.048	0.06	0.028	683	80	15.35
9-150-018	2014	F	70	3.968	0.072	0.124	0.078	762	120	15.76
9-150-059	2014	F	39	0.64					100	
11-150-002	2014	F	67	3.9	0.148	0.23	0.134	986	280	7.35
11-150-003	2014	M	78	6.3	0.064	0.26		505		12.63
11-150-005	2014	F	70	3.693	0.02	0.1		314	120	13.64
11-150-007	2014	F	54	1.816	0.024	0.062	0.006	577	160	8.37
11-150-009	2014	F	64	3.212	0.056	0.102	0.022	428	610	9.14
14-100-011	2014	M	72	3.88	0.028	0.072		1280	120	7.80
14-100-016	2014	F	40	1.208				489		7.00
14-100-021	2014	F	50	1.388					180	
14-100-022	2014	F	63	2.254	0.05	0.064	0.034	1190	230	6.06
14-100-025	2014	F	56	1.692	0.044	0.082	0.204	509	65	3.94
14-100-029	2014	F	35	0.29	0.008	0.018		446	82	3.38
GP03-012	2015	F	92	8	0.082	0.214	0.074	1660	740	8.25
GP03-022	2015	F	69	3.4	0.038	0.082		712	380	12.20

Table E1. (Continued)

MC04-002	2015	M	89	7.4	0.092	0.284		911		5.31
MC04-004	2015	F		7.495	0.07	0.328		1510	540	18.41
MC04-005	2015	M	68	3.1	0.04	0.14		536		2.87
DSH07-005	2015	F	74	4.178	0.042	0.164	0.042	1840	94	4.35
DSH07-006	2015	U	60	2.026	0.014	0.092		738	460	2.93
DSH07-007	2015	F	89	6.972	0.058	0.264	0.002	1280	170	3.94
DSH07-008	2015	F	74	3.904	0.04	0.182		890	110	1.97
DSH07-009	2015	F	99	10.576	0.1	0.436	0.004	1260	620	3.41
DSH07-010	2015	F	65	2.726	0.028	0.118	0.03	1502	390	2.51
DSH07-013	2015	F	73	3.968	0.038	0.214	0.044	1370	900	3.35
DSH07-015	2015	F	59	1.888	0.02	0.064	0.018	973	300	2.56
DSH07-016	2015	F	64	2.29	0.022	0.066	0.018	1480	110	2.51
DSH07-017	2015		47	1.022	0.01	0.03	0.004	844	180	2.51
9-80-002	2015	F	82	6.2	0.04	0.208	0.056	1260	840	6.25
14-60-001	2015	U	49	1.578	0.016	0.052		954	1900	17.59
14-60-002	2015	U	64	2.478	0.024	0.072		1070	270	16.42
14-60-003	2015	F	47	1.018	0.02	0.04	0.01	832	210	16.50
14-60-004	2015	F	59	1.926	0.03	0.074	0.026	1180		16.26
14-60-005	2015	F	59	2.2	0.032	0.086	0.034	1250	860	16.42
14-60-006	2015	F	65	2.942	0.025	0.11	0.025	1170	99	15.69
14-60-007	2015	M	95	7.9	0.05	0.275		2045	220	16.33
14-60-008	2015	U	34	0.38	0.005	0.015		592		
14-60-009	2015	U	34	0.35	0.015	0.01		576		
14-60-010	2015	F	68	2.725	0.025	0.095	0.01	1590	350	17.00
7-150-003	2015	U	49	1.196	0.016	0.044		495	1200	17.73
7-150-004	2015	F	95	8.2	0.05	0.426		1050	670	13.71
7-150-007	2015	M	83	5.2	0.08	0.172		1032	150	15.76
7-150-010	2015	F	73	3.8	0.052	0.152		581	630	6.28
7-150-012	2015	F	57	1.816	0.026	0.112	0.014	1130	1400	13.86
7-150-013	2015	M	76	4.248	0.038	0.182		871	440	14.50

Table E1. (Continued)

7-150-015	2015	F	61	2.118	0.028	0.088	0.016	577		15.84
7-150-017	2015	F	54	2.476	0.024	0.076		1072	170	17.00
7-150-018	2015	F	80	5.2	0.06	0.138	0.003	1103	780	4.57
7-150-019	2015	F	71	5.1	0.064	0.164		723	1800	15.74
7-150-023	2015	M	69	2.782	0.042	0.086		718		15.76
7-150-042	2015	F	63	2.17	0.04	0.066		661	150	14.29
8-100-004	2015	F	53	1.562	0.012	0.058	0.006	614	710	
8-100-008	2015	F	54	1.68	0.025	0.076	0.014	515	310	6.76
8-100-016	2015	U	54	1.664	0.014	0.068		484	470	
8-100-022	2015	F	53	1.71	0.018	0.048	0.01	3780	620	4.83
8-100-028	2015	F	65	2.8	0.018	0.114		691	910	17.95
8-100-031	2015	F	82	5.9	0.036	0.234		1130	530	16.83
8-100-035	2015	F	74	4.1	0.034	0.146		864	750	14.29
8-100-042	2015	F	63	2.534	0.022	0.098	0.022	1396	590	16.50
8-100-047	2015	F	66	2.9	0.016	0.092		774	630	4.41
8-100-051	2015	F	78	4.5	0.016	0.182		1670	510	18.91
9-150-004	2015	F	103	13.4	0.436	0.64	0.012	855	700	14.63
9-150-005	2015	F	67	1.856	0.024	0.1	0.036	734	59	
9-150-006	2015	U	54	1.556	0.028	0.07		369	45	
9-150-014	2015	F	74	4.586	0.042	0.152	0.058	890	250	13.30
9-150-016	2015	F	93	7.49	0.03	0.3		458	190	16.59
9-150-017	2015	F	66	3.17	0.04	0.135	0.035	817	210	14.36
9-150-019	2015	U	89	7.12	0.025	0.26	0.15	654	320	15.92
9-150-026	2015	U	52	1.262	0.012	0.046		463	104	3.52
9-150-028	2015	U	45	0.778	0.006	0.002		2750	82	
11-150-004	2015	F	53	1.78	0.008	0.054	0.012	638	140	6.80
11-150-012	2015	F	75	4.8	0.054	0.146	0.036	878	370	8.33
11-150-013	2015	F	65	3	0.03	0.1	0.024	940	340	5.58
11-150-015	2015	F	77	5	0.048	0.144		931	170	2.42
14-100-006	2015	F	62	2.134	0.022	0.068		491	250	4.48

Table E1. (Continued)

14-100-010	2015	U	58	1.934	0.026	0.052		434	98	12.44
30-100-003	2015	U	40	0.632	0.006			337	43	16.75
30-100-030	2015	M	96	9.5	0.096	0.254		2350	302	15.61
30-100-038	2015	F	57	2.086	0.034	0.094	0.022	511	75	14.15
30-150-002	2015	F	51	1.376	0.028	0.038	0.008	778	84	15.42
30-150-003	2015	F	58	1.954	0.03	0.078	0.016	1460	150	15.50
30-150-005	2015	M	84	6.4	0.062	0.25	0.01	1920	550	14.50
30-150-006	2015	F	50	1.066	0.014	0.032	0.008	632	84	15.84
30-150-007	2015	U	55	1.528	0.014	0.056		775	26	15.20
30-150-010	2015	F	52	1.254	0.012	0.04	0.01	745	56	5.50
30-150-012	2015	F	50	1.242	0.016	0.038	0.01	389	110	15.50
30-150-013	2015	U	48	0.93	0.004	0.024		482	103	33.85
31-150-001	2015	F	63	2.634	0.044	0.088	0.026	1026	230	15.92
31-150-002	2015	F	52	2.806	0.056	0.11	0.026	697	120	16.26
31-150-003	2015	F	67	2.964	0.048	0.1	0.026	638	130	18.91
31-150-004	2015	F	70	3.532	0.052	0.17	0.038	1380	92	15.50
31-150-005	2015	F	75	4.6	0.06	0.206	0.064	1860	520	17.73
31-150-006	2015	M	94	10.2	0.164	0.368	0.008	601	180	15.35
31-150-007	2015	U	80	4.982	0.068	0.176	0.002	468	250	17.82
31-150-008	2015	F	64	2.836	0.062	0.134	0.026	480	104	15.76
31-150-009	2015	U	56	1.79	0.02	0.068		661	120	16.59
31-150-010	2015	M	52	2.988	0.046	0.12		641	28	15.35
31-150-011	2015	F	54	1.808	0.048	0.06	0.012	525	99	14.43
31-150-012	2015	U	48	1.094	0.02	0.032		532	100	16.18
31-150-019	2015	U	45	0.9	0.01	0.028		741	5.1	14.29
31-150-020	2015	U	70	3.466	0.05	0.12		581	170	17.09
31-150-021	2015	F	61	2.564	0.048	0.082	0.022	1053	120	17.00
33-100-001	2015	F	53	1.638	0.032	0.056	0.01	405	110	15.92
33-100-015	2015	U	67	3.2	0.06	0.112		377	301	15.50
33-150-001	2015	F	65	3.292	0.058	0.242	0.004	544	250	15.98

Table E1. (Continued)

33-150-002	2015	F	65	3.292	0.058	0.242	0.004	515	150	15.84
33-150-004	2015	F	82	6.7	0.074	0.236	0.002	804	150	15.42
33-150-006	2015	F	51	1.442	0.012	0.052	0.008	558	10	16.75
33-150-008	2015	M	69	3.814	0.054	0.132		1120	340	20.20
33-150-009	2015	M	88	9.9	0.156	0.306	0.004	906	350	14.85
33-150-010	2015	U	83	6.9	0.042	0.212		1081	250	15.42
33-150-011	2015	F	69	4.028	0.036	0.142	0.046	3790	180	15.92
33-150-012	2015	M	89	9.1	0.074	0.28	0.012	1031	140	14.65
33-150-013	2015	F	57	1.74	0.032	0.072	0.02	1140	160	16.08
33-150-014	2015	F	51	1.356	0.022	0.054	0.012	504	93	15.38
34-100-003	2015	F	69	3.434	0.032	0.116		425	310	15.69
34-100-006	2015	U	68	3.5	0.05	0.132		249	110	14.01
34-100-007	2015	F	51	1.428	0.018	0.048	0.01	116		17.82
34-150-002	2015	F	59	2.308	0.064	0.062	0.016	252		15.98
20-100-007	2016	M	64	2.668	0.004	0.074		658	410	15.50
20-100-008	2016	F	39	0.638	0.01	0.026		373		13.20
20-100-009	2016	U	51	1.31	0.018	0.046		374		15.42
20-100-010	2016	U	65	2.718	0.03	0.1		604	300	20.20
20-100-011	2016	U	73	3.528	0.026	0.106		1140	220	14.29
20-100-012	2016	M	61	2.472	0.02	0.068		1440	370	16.59
20-100-013	2016	U	47	0.948	0.006	0.03		623	160	13.37
20-100-014	2016	F	44	0.804	0.008	0.026		599		16.84
20-100-015	2016	F	60	1.882	0.012	0.054		827	430	16.00
20-100-016	2016	U	55	1.426	0.01	0.044		999	170	16.34
20-150-001	2016	F	57	1.288	0.01	0.148	0.006	604		15.42
20-150-002	2016	F	47	0.91	0.012	0.024	0.006	611	690	14.63
20-150-003	2016	F	49	0.976	0.01	0.026	0.006	514	204	16.34
20-150-004	2016	U	53	1.352	0.016	0.04		613	290	16.16
20-150-005	2016	F	64	2.684	0.032	0.078	0.026	806	170	15.84
20-150-007	2016	F	56	1.802	0.014	0.06	0.012	1420	350	17.59

171

Table E1. (Continued)

20-150-008	2016	U	56	1.738	0.026	0.074		1050		16.83
20-150-010	2016	M	82	5.086	0.04	0.268		2250		16.75
20-150-012	2016	M	82	4.598	0.026	0.248		2590	290	14.22
20-150-013	2016	M	75	3.818	0.032	0.128		1490	290	16.42
21-100-002	2016	U	56	1.826	0.026	0.05		836	150	15.61
21-100-003	2016	M	87	7.575	0.096	0.262		586	140	21.56
21-100-004	2016	F	54	1.612	0.02	0.05	0.1	826		21.67
21-100-008	2016	M	95	9.635	0.108	0.198	0.004	1140	410	15.35
21-100-010	2016	F	60	2.164	0.026	0.084	0.016	1430	98	17.95
21-100-016	2016	M	94	8.505	0.052	0.234		1440	830	17.68
21-100-017	2016	F	58	2.078	0.036	0.072	0.018	922	180	15.27
21-100-018	2016	M	60	2.584	0.022	0.11		933	230	14.50
21-100-021	2016	M	93	8.38	0.128	0.292		1056	270	14.71
21-100-022	2016	M	88	7.325	0.126	0.25		734	260	14.93
21-150-017	2016	U	37	0.514	0.006	0.018		497	120	14.93
21-150-021	2016	F	57	2.084	0.03	0.07	0.016	1170		16.42
21-150-022	2016	F	45	0.872	0.014	0.028	0.006	472	180	15.42
21-150-023	2016	U	57	1.636	0.018	0.054		720	230	16.50
21-150-024	2016	F	53	1.454	0.03	0.05	0.012	746	120	15.20
21-150-025	2016	F	55	1.654	0.022	0.066	0.018	751	120	17.73
21-150-026	2016		51	1.304	0.01	0.058	0.006	1440	130	14.36
21-150-031	2016	F	66	2.674	0.028	0.1	0.018	1740	90	17.44
21-150-032	2016	M	60	2	0.016	0.072		968	63	17.73
21-150-033	2016	F	57	1.802	0.024	0.016	0.01	1310	203	17.82
21-150-040	2016	F	75	3.716					805	
22-150-001	2016	F	51	1.326	0.014	0.04	0.006	736	220	19.80
22-150-004	2016	F	50	1.412	0.026	0.056	0.012	466	380	19.50
22-150-006	2016	U	63	2.344	0.018	0.076		832	370	15.27
22-150-008	2016	M	74	3.884	0.024	0.162		1045	170	15.23
22-150-012	2016	F	50	1.756	0.028	0.64	0.012	849	290	15.12

Table E1. (Continued)

22-150-016	2016	F	50	1.156	0.018	0.046	0.012	757	180	17.16
22-150-017	2016	F	54	1.55	0.016	0.07	0.012	1103		17.17
22-150-020	2016	F	55	1.652	0.028	0.056	0.014	828	280	16.16
22-150-021	2016	M	85	6.365	0.066	0.326		1310		15.92
22-150-022	2016	M	79	5.088	0.072	0.168		760	310	16.02
23-150-001	2016	M	90	6.93	0.078	0.272		663	240	14.50
23-150-002	2016	F	53	1.458	0.014	0.06	0.012	516	110	13.93
23-150-003	2016	F	53	1.48	0.014	0.07	0.022	724	280	15.69
23-150-004	2016	F	57	1.874	0.018	0.092	0.004	810	250	14.71
23-150-005	2016	M	78	4.494	0.04	0.202		393	210	16.67
23-150-006	2016	F	63	2.452	0.022	0.152	0.024	957	210	13.00
23-150-007	2016	M	94	8.625	0.092	0.32		492	270	14.80
23-150-008	2016	M	83	5.615	0.046	0.194		541	230	18.27
23-150-009	2016	M	63	2.47	0.018	0.112		525		13.64
23-150-010	2016	M	94	8.73	0.13	0.3		425	270	14.71
24-100-002	2016	F	64	2.668	0.036	0.08	0.026	519	19	19.60
24-100-004	2016	F	66	2.982	0.042	0.108	0.024	543	140	17.17
24-100-005	2016	F	79	4.802	0.038	0.152	0.04	931	270	17.24
24-100-008	2016	F	75	3.925	0.038	0.102	0.034	830	270	14.08
24-100-015	2016	M	79	4.685	0.05	0.156		581	250	13.73
24-100-016	2016	U	52	1.288	0.014	0.05		461	78	14.63
24-100-017	2016	U	65	2.484	0.022	0.07		436	64	15.76
24-100-018	2016	U	62	2.264	0.03	0.072		391	103	14.22
24-100-019	2016	M	64	2.522	0.038	0.094		207	170	14.07
24-100-020	2016	F	69	2.648	0.028	0.144		287	61	16.02
24-100-026	2016	F	46	1	0.014	0.028	0.006		48	
24-100-027	2016	F	48	1.01	0.012	0.028	0.006		130	
24-100-028	2016	U	54	1.466	0.012	0.042			120	
24-150-004	2016	M	67	2.832	0.022	0.084		713	68	16.24
24-150-005	2016	F	59	2.034	0.032	0.068	0.008	452	410	14.15

173

Table E1. (Continued)

24-150-006	2016	F	47	0.98	0.012		0.04	332		15.69
24-150-012	2016	F	74	3.44	0.038	0.124	0.016	704		16.18
24-150-022	2016	F	57	1.894	0.026	0.066	0.01	463		15.82
24-150-023	2016	F	56	2.122	0.046	0.106	0.01	358		16.75
24-150-024	2016	M	81	4.955	0.042	0.112		981	51	15.20
24-150-025	2016	M	77	4.48	0.048	0.132		706	70	13.30
24-150-026	2016	M	81	5.304	0.052	0.182		679	240	14.63
24-150-027	2016	U	68	3.184	0.038	0.11		580	140	15.84
24-150-041	2016	F	57	1.872	0.028	0.062	0.016		110	
24-150-042	2016	U	47	1.03	0.018	0.03			48	
24-150-043	2016	M	70	3.636	0.012	0.142			240	
24-150-044	2016	F	71	3.28	0.038	0.118	0.03		110	
24-150-045	2016	M	63	2.382	0.028	0.086			140	
24-150-046	2016		60	1.946	0.02	0.06			220	
25-150-001	2016	U	71	3.78	0.05	0.18		583	77	17.82
25-150-002	2016	U		1.822	0.018	0.062		964	95	16.00
25-150-003	2016	F	59	2.034	0.022	0.114	0.02	2360	710	18.63
25-150-019	2016	U	52	1.34	0.014	0.034		650	66	14.36
25-150-023	2016	F	56	1.16	0.022	0.058	0.014	859	70	14.78
25-150-026	2016	M	64	2.666	0.02	0.08		556	270	15.92
25-150-037	2016	F	56	1.742	0.012	0.056		266	53	15.84
25-150-042	2016	U	49	1.05	0.016	0.03		396	67	17.91
26-150-001	2016	M	84	6.18	0.074	0.208	0.002	716	240	13.37
26-150-002	2016	U	50	1.242	0.008	0.05		630	130	13.66
26-150-010	2016	F	52	1.416	0.016	0.042	0.014	388	71	16.92
26-150-011	2016	U	55	1.836	0.016	0.044		634	94	17.16
26-150-015	2016	F	48	1.038	0.016	0.026	0.004	676	46	12.68
27-100-004	2016	F	49	1.184	0.014	0.03	0.006	363	84	17.00
27-100-005	2016	U	59	2.082	0.026	0.054		357	210	12.69
27-100-007	2016	M	66	2.89	0.022	0.066		475	140	18.72

Table E1. (Continued)

27-150-001	2016	F	52	1.4	0.012	0.032		523	87	15.98
27-150-006	2016	U	40	0.596	0.006	0.014		687	51	4.85
27-150-014	2016	F	58	1.586	0.02	0.044		859	81	18.41
27-150-016	2016	F	45	0.885	0.004	0.028	0.002	852	55	5.34
27-150-017	2016	F	47	0.938	0.08	0.03		489	240	7.66
27-150-018	2016	F	50	1.242	0.006	0.018		597	64	5.50
27-150-024	2016	U	50	1.244	0.012	0.038		657	47	6.70
27-150-028	2016	M	82	5.776	0.072	0.222	0.008	504	240	15.20
27-150-030	2016	U	61	2.198	0.018	0.06		833	120	13.13
27-150-033	2016	M	97	11.548	0.214	0.322		334	150	19.70
27-150-041	2016	F	47	0.822	0.006	0.022			64	
27-150-042	2016	F	52	1.268	0.012	0.034			150	
27-150-043	2016	F	50	1.298	0.016	0.04			89	
27-150-044	2016	U	40	0.642	0.01	0.022			120	
27-150-046	2016	F	49	1.04	0.012	0.032			100	
27-150-047	2016	F	36	0.428	0.002	0.01			31	
28-100-002	2016	F	60	1.988	0.018	0.052	0.014	594	40	15.84
28-100-003	2016	M	88	6.68	0.062	0.212		583	330	20.29
28-100-004	2016	F	61	2.112	0.018	0.056		549	150	16.16
28-150-004	2016	U	59	1.952	0.022	0.058		414	150	15.20
28-150-005	2016	M	82	5.268	0.046	0.164		680	92	12.20
28-150-006	2016	F	51	1.166	0.012	0.038		293		15.84
28-150-007	2016	F	68	3.308	0.034	0.114		284	130	16.16
28-150-008	2016	F	72	3.992	0.036	0.126	0.034	535	380	16.00
36-100-037	2016	U	52	1.454	0.016	0.034		450	170	15.84
36-100-038	2016	F	66	2.976	0.02	0.074		446	260	16.50
36-100-041	2016	F	89	7.175	0.106	0.196		394	290	16.24
36-100-043	2016	M	81	5.16	0.044	0.128		544	260	14.29
36-100-046	2016	M	54	1.528	0.018	0.04		374	960	14.29
36-150-006	2016	M	72	3.788	0.034	0.102	0.002	1640	99	14.08

Table E1. (Continued)

36-150-008	2016	F	68	2.892	0.022	0.092	0.028	2204	230	21.00
36-150-009	2016	F	54	1.628	0.014	0.008	0.016	1380	47	14.50
36-150-012	2016	F	54	1.536	0.02	0.034	0.01	891	280	14.36
36-150-013	2016	M		9.682	0.138		0.008	566	380	16.18
36-150-014	2016	F	73	3.96	0.03	0.214	0.048	1780	590	15.74
36-150-018	2016	U	63	2.446	0.026	0.0866		683		16.24
36-150-022	2016	M	74	6.235	0.084			656		20.19
36-150-025	2016	F	76	4.242	0.04	0.122		706	430	17.95
36-150-027	2016	F	60	2.166	0.028	0.074		553	210	16.58
36-150-040	2016	F	66	2.59	0.01	0.052	0.018		370	
GP03-016	2017	M	54	1.484	0.012	0.034		620	340	4.04
GP03-021	2017	F	54	1.645	0.014	0.036	0.006	488	350	5.45
MC04-006	2017	F	54	1.288	0.02	0.012	0.01	639		4.67
MC04-010	2017	F	81	4.8	0.048	0.188	0.006	800	180	6.43
MC04-011	2017	F	57	1.742	0.016	0.06	0.02	941	740	4.22
MC04-012	2017	F	65	2.6	0.028	0.074	0.004	698	1100	6.76
MC04-013	2017	F	57	1.768	0.018	0.06	0.018	1110	220	5.04
MC04-014	2017	F	89	6.8	0.072	0.182	0.008	878	140	10.29
MC04-015	2017	F	58	1.914	0.016	0.07	0.002	569	540	5.18
MC04-016	2017	F	53	1.602	0.0204	0.054		453	780	6.95
9-80-002	2017	F	66	2.762	0.02	0.216	0.118	972	240	4.84
9-80-004	2017	M	62	2.576	0.02	0.084		567	530	4.97
9-80-005	2017	F	71	3.958	0.022	0.156	0.036	1430	830	6.06
9-80-007	2017	M	94	9	0.048	0.264		1197	660	8.68
1-150-004	2017	M	110	14.8	0.122	0.466	0.074	1797	350	
14-60-001	2017	F	85	5.6	0.018	0.192		1224	390	6.00
14-60-002	2017	U	49	1.026	0.01	0.036		923	1600	3.80
14-60-003	2017	U	48	1.018	0.004	0.032		963	720	5.35
14-60-005	2017	F	57	1.71	0.014	0.052	0.012	1078	1600	3.96
14-60-006	2017	U	48	1.076	0.006	0.032		1310	890	4.63

Table E1. (Continued)

14-60-007	2017	F	50	1.298	0.012	0.1	0.006	470		7.36
14-60-008	2017	U	48	1.056	0.008	0.032		455	990	6.19
14-60-009	2017	U	44	0.826	0.01	0.03		338	970	5.56
14-60-010	2017	U	46	0.954	0.01	0.028		954	380	5.51
14-60-011	2017	F	94	8.4	0.064	0.332	0.004	1300	1400	4.38
14-60-018	2017	F	47	0.94	0.006	0.034	0.004	1410	570	4.26
7-150-001	2017	F	48	1.244	0.014	0.014	0.01	662	200	4.39
7-150-002	2017	F	44	0.854	0.012	0.026	0.004	392	280	6.86
7-150-003	2017	F	70	3.37	0.034	0.13		936	280	5.67
7-150-004	2017	U	41	0.666	0.016	0.03		410	502	7.92
7-150-005	2017	F	56	1.724	0.028	0.134	0.01	777	640	3.98
7-150-006	2017	F	68	3.212	0.052	0.152	0.016	474	370	4.48
7-150-007	2017	F	72	3.234	0.026	0.106	0.004	1080	690	8.82
7-150-008	2017	F	71	3.28	0.024	0.126	0.006	1360	440	5.53
7-150-010	2017	F	56	1.786	0.022	0.051	0.014	811	1600	6.73
7-150-011	2017	F	64	2.416	0.026	0.068	0.004	618	170	10.68
7-150-013	2017	F	61	1.994	0.022	0.06	0.022	1440	580	5.31
7-150-050	2017	F	49	1.114					1200	
8-100-003	2017	F	63	2.23	0.014	0.11		1470	1200	5.50
8-100-004	2017	F	90	7	0.05	0.268	0.012	1820	1200	4.85
8-100-005	2017	F	57	1.67	0.03	0.068	0.016	840		9.64
8-100-007	2017	F	61	2.244	0.014	0.152	0.018	1310	700	7.18
8-100-008	2017	F	59	1.858	0.018	0.072	0.018	1170	180	6.86
8-100-009	2017	M	57	1.68	0.014	0.052		740	520	4.98
8-100-010	2017	F	47	0.922	0.01	0.038	0.004	560	420	4.85
8-100-011	2017	F	46	0.886	0.014	0.03	0.004	391	700	4.06
8-100-012	2017	F	48	1.09	0.012	0.034	0.008	583	430	3.98
8-100-013	2017	F	51	1.274	0.014	0.0452	0.012	560	290	5.67
9-150-002	2017	U	58	1.88	0.024	0.078		505	440	4.88
9-150-003	2017	F	62	2.182	0.024	0.082	0.002	539	130	5.50

Table E1. (Continued)

9-150-004	2017	F	67	2.852	0.046	0.094		534	220	5.56
9-150-005	2017	F	68	3.328	0.044	0.16	0.012	628	560	6.53
9-150-006	2017	U	74	3.908	0.032	0.188		778	1200	4.33
9-150-010	2017	F	78	5.34	0.054	0.296	0.088	1072	1100	4.43
11-150-001	2017	F	65	2.9	0.036	0.08	0.022	1180	660	4.32
11-150-006	2017	M	93	9.8	0.07	0.31	0.006	1595	310	4.16
11-150-007	2017	F	51	1.376	0.01	0.03		608	240	5.14
11-150-010	2017	F	66	3.068	0.014	0.106	0.038	1260	580	4.40
11-150-011	2017	F	45	0.944	0.016	0.026	0.002	322	570	9.42
11-150-012	2017	F	57	2.082	0.018	0.05	0.008	422	440	10.71
11-150-013	2017	F	71	4.006	0.04	0.14	0.024	1380	490	5.22
11-150-014	2017	F	69	3.348	0.03	0.16	0.024	1120		13.40
11-150-015	2017	F	55	1.708	0.018	0.048	0.004	613	140	8.62
11-150-016	2017	M	83	7.682	0.056	0.23		676	610	22.55
14-100-002	2017	U	63	2.258	0.014	0.078		650		3.53
14-100-003	2017	F	57	1.656	0.012	0.048	0.01	425		3.61
14-100-004	2017	U	61	2.066	0.016	0.062		660	450	4.71
14-100-005	2017	F	71	3.138	0.026	0.086	0.022	705	840	2.40
14-100-006	2017	U	57	1.705	0.014	0.064		503	820	4.48
14-100-008	2017	F	94	8	0.052	0.212	0.004	1270		5.06
14-100-013	2017	F	64	2.696	0.026	0.01		449	330	1.99
14-100-015	2017	F	73	4.244	0.03	0.128	0.05	1480	1800	4.49
16-150-011	2017	F	39	0.63	0.006	0.02	0.002	1350	230	4.41
NA-58-385	2017	M	49	0.38				873		
NA-67-324	2017	F	48	0.78				2370		
NA-73-298	2017	M	48	0.86				290		
NA-73-299	2017	M	48	0.86				1203		
NA-192-28	2017	M	110	12.6				422		
NA-96-250	2017	F	37	0.5				196		
NA-96-254	2017	M	38	0.59				1240		

Table E1. (Continued)

NA-93-503	2017	F	52.5	1.56	812
NA-67-316	2017	F	41	0.76	464
NA-58-374	2017	F	44	0.94	1250
NA-93-514	2017	M	58	2.17	3410
NA-126-193	2017	M	52.2	1.6	595
NA-162-79	2017	F	38	0.62	2850
NA-96-251	2017	F	38.5	0.65	1130
NA-58-375	2017	F	45	1.04	1495
NA-96-253	2017	M	37	0.58	234
NA-97-484	2017	M	47	1.19	750
NA-58-371	2017	F	41.5	0.82	665
NA-187-2-30	2017	F	46	1.12	2240
NA-58-388	2017	M	51	1.54	201
NA-73-300	2017	U	39	0.7	84.9
NA-73-301	2017	U	39	0.7	215
NA-126-182	2017	M	39.5	0.73	759
NA-93-500	2017	F	35.5	0.53	303
NA-58-370	2017	F	41	0.82	695
NA-126-175	2017	F	49	1.4	320
NA-96-249	2017	F	36.5	0.58	3440
NA-97-483	2017	F	54	1.88	1660
NA-112-148	2017	M	43	0.95	658
NA-93-501	2017	F	49	1.41	2062
NA-126-194	2017	M	55	2	437
NA-58-387	2017	M	51	1.6	672
NA-159-91	2017	U	45	1.1	191
NA-93-511	2017	M	52	1.7	609
NA-187-2-31	2017	F	47	1.26	2860
NA-96-252	2017	U	36	0.57	585
NA-93-502	2017	F	49	1.44	683

179

Table E1. (Continued)

NA-93-513	2017	M	55	2.04	1130
NA-67-320	2017	F	42	0.91	496
NA-187-2-63	2017	U	45	1.12	1340
NA-126-176	2017	F	49	1.45	286
NA-187-2-32	2017	M	47	1.28	669
NA-67-315	2017	F	40.5	0.82	1450
NA-194-54	2017	F	65	3.4	1601
NA-93-506	2017	M	48	1.37	657
NA-97-302	2017	F	49	1.46	760
NA-58-369	2017	F	41	0.86	679
NA-93-510	2017	M	50	1.56	323
NA-187-26	2017	U	49	1.48	265
NA-IS-335	2017	F	101	13	4720
NA-126-180	2017	M	39	0.75	621
NA-67-317	2017	F	42	0.95	1020
NA-159-88	2017	F	64	3.39	581
NA-159-87	2017	F	50	1.63	195
NA-67-311	2017	F	39	0.78	6180
NA-112-147	2017	F	45	1.2	862
NA-159-90	2017	M	68	4.2	1740
NA-126-178	2017	F	70	4.6	669
NA-126-195	2017	M	76	5.9	458
NA-67-325	2017	U	42	1.02	1280
NA-112-149	2017	M	84	8.2	594
NA-67-321	2017	F	44	1.18	556
NA-58-389	2017	M	73	5.5	249
NA-146-92	2017	M	88	9.82	340
NA-126-174	2017	F	48.5	1.65	98.8
NA-96-248	2017	F	35	0.65	222
NA-159-89	2017	M	67	4.7	496

Table E1. (Continued)

NA-187-2-62	2017	M	77	7.34		424
NA-192-27	2017	F	77	8.3		496
NA-126-171	2017	F	37	1.16		722